

UNCLASSIFIED

AD NUMBER

AD469154

NEW LIMITATION CHANGE

TO

**Approved for public release, distribution
unlimited**

FROM

**Distribution authorized to U.S. Gov't.
agencies and their contractors; Critical
Technology; JUN 1965. Other requests shall
be referred to Air Force Materials
Laboratory, Wright-Patterson AFB, OH
45433.**

AUTHORITY

AFML ltr dtd 1 Aug 1969

THIS PAGE IS UNCLASSIFIED

AFML-TR-65-171

45154
15154
15154
15154

15154
15154
15154
15154

AEROSPACE CERAMICS - CHARACTERISTICS

AND DESIGN PRINCIPLES

Paul Boland and J. D. Walton, Jr.
Georgia Institute of Technology
Engineering Experiment Station

TECHNICAL REPORT AFML-TR-65-171

June 1965

Air Force Materials Laboratory
Research and Technology Division
Air Force Systems Command
Wright-Patterson Air Force Base, Ohio

DDC
RECEIVED
SLP 8 1965
GOLITZ
TISIA 5

DISCLAIMER NOTICE

**THIS DOCUMENT IS BEST QUALITY
PRACTICABLE. THE COPY FURNISHED
TO DTIC CONTAINED A SIGNIFICANT
NUMBER OF PAGES WHICH DO NOT
REPRODUCE LEGIBLY.**

SECURITY

MARKING

The classified or limited status of this report applies to each page, unless otherwise marked.
Separate page printouts MUST be marked accordingly.

THIS DOCUMENT CONTAINS INFORMATION AFFECTING THE NATIONAL DEFENSE OF THE UNITED STATES WITHIN THE MEANING OF THE ESPIONAGE LAWS, TITLE 18, U.S.C., SECTIONS 793 AND 794. THE TRANSMISSION OR THE REVELATION OF ITS CONTENTS IN ANY MANNER TO AN UNAUTHORIZED PERSON IS PROHIBITED BY LAW.

NOTICE: When government or other drawings, specifications or other data are used for any purpose other than in connection with a definitely related government procurement operation, the U. S. Government thereby incurs no responsibility, nor any obligation whatsoever; and the fact that the Government may have formulated, furnished, or in any way supplied the said drawings, specifications, or other data is not to be regarded by implication or otherwise as in any manner licensing the holder or any other person or corporation, or conveying any rights or permission to manufacture, use or sell any patented invention that may in any way be related thereto.

NOTICES

When Government drawings, specifications, or other data are used for any purpose other than in connection with a definitely related Government procurement operation, the United States Government thereby incurs no responsibility nor any obligation whatsoever; and the fact that the Government may have formulated, furnished, or in any way supplied the said drawing, specifications, or other data, is not to be regarded by implication or otherwise as in any manner licensing the holder or any other person or corporation, or conveying any rights or permission to manufacture, use, or sell any patented invention that may in any way be related thereto.

Qualified requesters may obtain copies of this report from the Defense Documentation Center (DDC), Cameron Station, Bldg. 5, 5010 Duke Street, Alexandria, Virginia, 22314. The distribution of this report is limited because the report contains technology identifiable with items on the strategic embargo lists excluded from export or re-export under U. S. Export Control Act of 1949 (63 STAT. 7), as amended (50 U. S. C. App. 2020.2031), as implemented by AFR 400-1C.

Copies of this report should not be returned to the Research and Technology Division, Wright-Patterson Air Force Base, Ohio, unless return is required by security considerations, contractual obligations, or notice on a specific document.

AEROSPACE CERAMICS - CHARACTERISTICS
AND DESIGN PRINCIPLES

Paul Boland and J. D. Walton, Jr.
Georgia Institute of Technology
Engineering Experiment Station

FOREWORD

The report was prepared by the Engineering Experiment Station of the Georgia Institute of Technology, Atlanta, Georgia for the United States Air Force on Contract No. AF 33(615)-1308. This contract was initiated under Project No. 7381, "Materials Application," Task No. 738105, "Ceramic and Graphite Technical Information." The work was administered under the direction of the Materials Information Branch, Materials Applications Division, Air Force Materials Laboratory, Research and Technology Division, at Wright Patterson Air Force Base, Ohio, with Mr. B. R. Emrich serving as project engineer.

This report in conjunction with RTD-TDR-63-4102 "Refractory Ceramics of Interest In Aerospace Structural Applications - A Materials Selection Handbook" provides the designer with the most reliable means of using aerospace ceramics for structural applications. RTD-TDR-63-4102 consists of properties data useful in the preliminary selection of materials applicable for specific requirements. This report complements RTD-TDR-63-4102 by explaining the factors which the designer must consider to use ceramics more efficiently. This report also explains, by example, the need for closer working relationships between the materials engineer and the design engineer.

This report covers work conducted from January 1964 to April 1965.

Georgia Tech personnel directly concerned with this effort include Messrs. Paul Boland, J. D. Walton, Jr., L. R. Johnson, W. M. Linstrom, and C. A. Burrows, with Paul Boland serving as project director.

The authors wish to acknowledge the many specialists who have contributed significantly to this manual. Special thanks go to the 125 hosts at 55 research organizations who participated in private discussions and volunteered information on the behavior of brittle materials under thermal and mechanical loads.

Manuscript released by authors on 30 June 1965 for publication as an RTD Technical Documentary Report.

This technical documentary report has been reviewed and is approved.

D. A. Shinn
D. A. SHINN
Chief, Materials Information Branch
Materials Applications Division
AF Materials Laboratory

ABSTRACT

The purpose of this research was to compile into a single volume present knowledge which will be useful to a designer applying ceramic materials in aerospace structural applications. All efforts were directed toward the collection of information to acquaint designers with the properties, fundamental principles, characteristics, limitations, utilization and performance of high-temperature, load-bearing ceramic products and with the characteristics, limitations and utilization of ceramic processes. The information provided in this manual was obtained by means of intensive literature surveys and through contacts with various government agencies, industrial concerns, and academic institutions. The case-history approach was used for the compilation of information on the behavior of ceramic products and material systems subjected to thermal loads to provide the background for a possible correlation between known thermal shock theories and brittle materials behavior.

TABLE OF CONTENTS

	Page
I. THE PROBLEM OF DESIGNING WITH CERAMIC MATERIALS	1
1.1 <u>Background</u>	1
1.2 <u>Complexity of the Problem</u>	2
1.3 <u>The Materials Problem</u>	2
1.4 <u>The Environment Problem</u>	6
1.5 <u>The Design Engineer</u>	8
1.6 <u>The Testing Problem</u>	12
1.7 <u>Problems of Mechanical Testing</u>	13
1.8 <u>Ceramic Systems</u>	17
1.9 <u>Conclusions</u>	17
II. SCOPE OF THE REPORT	19
III. SUMMARY	20
IV. USE OF CERAMIC MATERIALS IN AEROSPACE STRUCTURAL APPLICATIONS - GENERAL LIMITATIONS	24
V. BRITTLE BEHAVIOR	26
5.1 <u>Brittle Nature of Ceramic Materials</u>	26
5.2 <u>Ductile Ceramics - A Distant Future Possibility</u>	28
5.3 <u>Statistical Approach to Brittle Fracture</u>	29
5.3.1 The statistical concept-material flaws	29
5.3.2 Weibull distribution function	30
5.3.3 Evaluation of Weibull parameters	30
5.3.4 Critique	33
5.4 <u>General References on Brittle Behavior</u>	34
VI. CERAMIC FORMING PROCESSES	35
6.1 <u>Cold Forming</u>	35
6.1.1 Slip-casting	35
6.1.2 Dry pressing	35
6.1.3 Isostatic pressing	35
6.1.4 Vibratory compaction	36
6.1.5 Extrusion	36
6.2 <u>Hot Forming</u>	37
6.2.1 Uniaxial hot pressing	37
6.2.2 Biaxial hot pressing	37
6.2.3 Hot isostatic pressing	37
6.2.4 Hot extrusion	38
6.3 <u>Other Forming Methods</u>	38
6.3.1 Nucleation	38
6.3.2 Melt spraying	38
6.3.3 Foamed ceramics	38
6.3.4 Molding	38

(Continued)

TABLE OF CONTENTS (Continued)

	Page
6.4 <u>Machining and Grinding</u>	39
6.4.1 Abrasive grinding	39
6.4.2 Ultrasonic machining.	39
6.5 <u>General References on Ceramic Forming Processes</u>	39
 VII. PROPERTIES OF CERAMIC MATERIALS	 40
7.1 <u>Physical Properties</u>	40
7.1.1 Refractoriness.	40
7.1.2 Hardness.	40
7.2 <u>Elastic Properties</u>	42
7.2.1 Elastic modulus	42
7.2.2 Shear modulus	45
7.2.3 Bulk modulus.	47
7.2.4 Poisson's ratio	48
7.3 <u>Strength</u>	49
7.3.1 Tensile strength.	49
7.3.2 Flexural strength	49
7.3.3 Compressive strength.	50
7.3.4 Impact strength	51
7.3.5 Porosity and grain size effects	51
7.4 <u>Notch Sensitivity</u>	53
7.5 <u>Thermal Properties</u>	54
7.5.1 Thermal expansion	54
7.5.2 Thermal conductivity.	55
7.6 <u>Fatigue</u>	60
7.6.1 Cyclic fatigue.	60
7.6.2 Static fatigue.	60
7.7 <u>Creep</u>	60
7.8 <u>Thermal Shock Resistance</u>	61
7.8.1 Definitions	61
7.8.2 Test methods.	61
7.8.3 Factors affecting thermal shock resistance.	64
7.8.4 Thermal shock parameters.	64
7.9 <u>General References on the Properties of Ceramic Materials</u>	70
 VIII. HIGH-TEMPERATURE STRUCTURAL MATERIALS	 71
8.1 <u>Oxides</u>	71
8.1.1 Alumina	71
8.1.2 Beryllia.	71
8.1.3 Ceria	72
8.1.4 Chromia	73
8.1.5 Hafnia.	73
8.1.6 Magnesia.	73
8.1.7 Silica.	73
8.1.8 Thoria.	74
8.1.9 Yttria.	74
8.1.10 Zirconia.	75

(Continued)

TABLE OF CONTENTS (Continued)

	Page
8.2 <u>Carbides</u>	75
8.2.1 Boron carbide	76
8.2.2 Hafnium carbide	77
8.2.3 Silicon carbide (self-bonded)	77
8.2.4 Tantalum carbide.	77
8.2.5 Titanium carbide.	77
8.2.6 Tungsten carbides	77
8.2.7 Zirconium carbide	78
8.3 <u>Borides</u>	78
8.3.1 Chromium diboride	78
8.3.2 Hafnium diboride.	78
8.3.3 Niobium diboride.	79
8.3.4 Tantalum diboride	79
8.3.5 Titanium diboride	79
8.3.6 Vanadium diboride	79
8.3.7 Zirconium diboride.	79
8.3.8 Mixed borides	80
8.4 <u>Nitrides</u>	80
8.4.1 Aluminum nitride.	80
8.4.2 Beryllium nitride	81
8.4.3 Boron nitride	81
8.4.4 Silicon nitride	81
8.5 <u>Intermetallic Compounds</u>	82
8.5.1 Aluminides.	82
8.5.2 Beryllides.	82
8.5.3 Silicides	82
8.6 <u>Composites</u>	83
8.6.1 Fiber composites.	83
8.6.2 Flake composites.	84
8.6.3 Cermets	84
8.6.4 Filled composites	86
8.6.5 Laminar composites.	87
8.7 <u>General References on High-Temperature Structural Materials</u>	87
IX. <u>REFRACTORY STRUCTURAL COMPONENTS - THERMAL SHOCK BEHAVIOR</u>	88
9.1 <u>Effect of Pores</u>	89
9.2 <u>Foamed Ceramics</u>	91
9.3 <u>Effect of Particle Size</u>	93
9.4 <u>Effect of Crystalline Inversions</u>	95
9.5 <u>Effect of Notches</u>	97
9.6 <u>Effect of the Temperature Dependence of Material Properties</u>	97
9.7 <u>Effect of Impurities</u>	98
9.8 <u>Effect of Low Modulus Additions</u>	99
9.9 <u>Cermets</u>	100
9.10 <u>Skeleton-Skeleton Structures</u>	101
9.11 <u>Metal Fiber-Reinforced Ceramics</u>	102

(Continued)

TABLE OF CONTENTS (Concluded)

	Page
9.12 <u>Use of Metal-Ceramic Layer</u>	104
9.13 <u>Metal Wire-Reinforced Ceramics</u>	106
9.14 <u>Honeycomb Structures</u>	107
9.15 <u>Radomes</u>	108
9.16 <u>Leading Edges</u>	111
9.17 <u>Frestressed Ceramic Structures</u>	113
9.18 <u>Thermal Stress Testing</u>	114
9.19 <u>Selected References on the Thermal Shock Behavior of Refractory Structural Components</u>	116
X. DESIGN WITH BRITTLE MATERIALS	117
10.1 <u>Design Guides</u>	117
10.2 <u>General References on the Design of Brittle Materials</u>	119
REFERENCES	120
APPENDIX I. EXTENDED ABSTRACTS OF SELECTED ARTICLES	135
APPENDIX II. AN EXAMPLE OF A THERMO-STRUCTURAL ANALYSIS	171

LIST OF ILLUSTRATIONS

	Page
1. Strength-Temperature-Grain-Size Surface for Dense Pure Hot-Pressed Alumina.	3
2. Strength-Temperature-Grain-Size Surface for Dense Pure Hot-Pressed Magnesia	4
3. Relative Thermal Shock Resistance of Al_2O_3 and BeO as Function of Thermal Shock Environment (ah).	9
4. Relative Thermal Shock Resistance of Candidate Reentry Radome Materials as a Function of Thermal Shock Environment (ah).	10
5. Inside Wall of Aluminum Oxide Shapes Immersed in Molten Babbitt.	14
6. Temperature Distribution for Radome Immersed in Molten Babbitt	15
7. Thermal Gradient in the Wall of Radome Injected into Hot Gas Stream	16
8. Special Graph Paper.	32
9. Melting or Decomposition Temperatures of Selected Refractory Ceramics	41
10. Theoretical Mach Number Histories Used in Thermal Stress Analysis.	182
11. Temperature Gradients at Stagnation Point for Pyroceram® Radome.	183
12. Tensile Thermal Stress at Stagnation Point Versus Flight Time for Pyroceram® Radome.	184
13. Temperature Gradients at Stagnation Point for Alumina Radome	185
14. Tensile Thermal Stress at Stagnation Point Versus Flight Time for Alumina Radome	186

SYMBOLS

Symbol

A	a constant, area
a	empirical constant, half thickness of plate or wall, inner radius
α	thermal diffusivity
B	working parameter
b	empirical constant, outer radius
c	distance
c	specific heat
C_p	specific heat at constant pressure
C_v	specific heat at constant volume
D	diameter
\bar{D}	working parameter
E	elastic modulus
F	probability of fracture, Fourier number
G	shear modulus, grain size
h	heat transfer coefficient
I	moment of inertia
K	bulk modulus
k	thermal conductivity
L	linear dimension
M	moment, merit index, Mach number
m	flaw density
N	Nusselt number
P	volume fraction of pores, pressure
P_r	Prandtl number
p	safety factor
Q	quantity of heat
q	heat flux
r, θ, z	cylindrical coördinates
R	thermal shock resistance parameter
R_e	Reynolds number
r	relative density

(Continued)

SYMBOLS (Continued)

Symbol

r_a	middle radius
S	strength, surface area
t	temperature
t_r	recovery temperature
u	velocity
V	volume, loading rate
V_o	working parameter
v	volume fraction
x	distance from stagnation point measured along surface
x, y, z	cartesian coördinates
z	a constant
z'	a constant
α	coefficient of thermal expansion
β	Biot's modulus
γ	geometrical pore factor, ratio of specific heats
ΔT	temperature difference
ϵ	emissivity
λ	mean free path, working parameter
μ	Poisson's ratio
$\bar{\mu}$	viscosity
η	angle between stream and tangent to surface
ρ	density
ρ, θ, ϕ	spherical coördinates
σ	stress
$\sigma_r, \sigma_\theta, \sigma_z$	normal stress components in cylindrical coördinates
$\sigma_p, \sigma_\theta, \sigma_\phi$	normal stress components in spherical coördinates
σ_μ	zero strength
σ_o	scaling factor
σ_s	Stephan's radiation constant

(Continued)

SYMBOLS (Concluded)

Symbol

θ	time
v	mean velocity

SUBSCRIPTS

bc	circular cylinder subjected to pure bending
br	rectangular cylinder subjected to pure bending
c	closed pores
d	dispersed phase
i	initial conditions
m	matrix, metal
P	Pores
0	zero porosity
o	open pores
r	radome
s	surface conditions
t	cylinder subjected to tension
x	cross sectional
y	longitudinal
δ	local conditions at outer edge of boundary layer
δ_s	stagnation conditions behind normal shock wave
\approx	conditions in undisturbed flow

I. THE PROBLEM OF DESIGNING WITH CERAMIC MATERIALS

1.1 Background

Ceramic materials have been used throughout the history of civilization. Historically the use of these materials has required only nominal physical and mechanical properties. The coming of the space age, however, found the designer's problems more serious than ever before. He needed to use ceramics in high stress applications. The materials engineer was of little help. He offered materials which were only slightly improved over those of recent history. Communications between the designer and the materials engineer began to break down. The designer wanted to design with ceramics as he had learned to do with metals and plastics. The materials engineer felt that his materials were adequate for space age structural requirements and that all the designer needed to do was to design shapes without sharp corners and use ceramics in compression. Neither side had the answer to the problem. Neither understood the complexity of the problem.

The criteria for selecting brittle materials for hyperthermal applications depend upon design considerations, environment and materials properties.

First, it is important to keep the weight of all flight hardware at a minimum. Therefore, strength-to-weight relationships are much more meaningful than strength values alone.

Second, the design strength is not simple to define, and should always be considered in light of the application and the material properties. For example, suppose that aluminum oxide were being considered for use as a Mach 3-4 sea level radome application. Analysis would probably show that the strength requirements from the standpoint of thermal shock considerations would be an order of magnitude greater than those required from the standpoint of aerodynamics or other mechanical considerations. Typical transverse strength requirements might be 20,000 to 40,000 psi for thermal stress and 2,000 to 4,000 psi for mechanical stress. Since the strength requirement for thermal stress is so much higher than for mechanical stress, the designer would probably neglect the latter. If, in the course of the program, it were found necessary to consider alternate materials, the relationship of material strength-to-application requirement might be forgotten. In this case the designer would find himself searching materials property tables for materials with transverse strengths above 20,000 psi. What is so easy to overlook in this situation is the fact that a material with a very low coefficient of thermal expansion and/or low modulus of elasticity will require less strength to withstand thermal stress. If this strength were found to be well below the requirement for mechanical load, the designer might be able to use a material with a transverse strength of the order of 4,000 to 5,000 psi. Therefore, in this case the materials screening program should have considered a strength-modulus of elasticity-coefficient of thermal expansion relationship, rather than just strength alone.

1.2 Complexity of the Problem

In order for brittle materials such as ceramics to be efficiently used in the severe thermal environments associated with rocket nozzles, leading edges, nose cones, radomes, etc. the ultimate in performance is required. All aspects of materials and design technology must be developed to a level never before attempted. Not just one, but at least three branches of technology must contribute vital information to describe the complex interaction between the desired piece of hardware and its environment before significant progress can be made towards predicting its behavior. These branches of technology involve the materials engineer, the design engineer, and the aero-thermodynamics engineer. In other words, the performance of a material in a severe thermal environment depends upon the properties of the material, the design (shape, size, etc.) of the piece, and the thermal environment. The performance is dependent upon the interaction of all three. Because of this, it is necessary that each of these contributory factors be completely characterized. If even one parameter of any one factor is not known then the design is compromised.

1.3 The Materials Problem

In order to appreciate the magnitude of the problem, each factor will be dealt with separately, remembering the interdependency of all three. First consider material properties. Aluminum oxide will be used as an example since it represents a single oxide ceramic which has been studied extensively during the past twenty years. The literature is filled with data on this material.

The properties which are most critical to the engineer who is designing for a hyperthermal (thermal shock) environment are as follows: 1) strength, 2) thermal conductivity, 3) thermal expansion, 4) emittance, 5) modulus of elasticity, 6) specific heat, 7) density.

What is the strength of aluminum oxide? First, it must be decided what type of aluminum oxide is desired. Assuming it will be a polycrystalline material, will it be hot pressed, pressed and sintered, or slip-cast? What purity? What porosity? All are related to the fabrication technique used, maturation parameters, raw material, etc. Certain techniques are suitable for scale up to large shapes, others are limited. Any one selected will require compromises at some stage in the design. Assuming that the designer wants a strong material with a high density (90 - 100%) a range of room temperature modulus of rupture values between 20 and 40,000 psi was reported by Hague et al (Ref. 1). Two years later in Supplement 2 Lynch (Ref. 2) reported values between 18,000 and 66,000 psi for hot pressed aluminum oxide of 98% density. The only variable was grain size, which ranged from 1-2 μ for the highest strength to 150-250 μ for the lowest strength. Mitchell, Spriggs and Vasilos (Ref. 3) have presented these data graphically as a function of temperature as shown in Figure 1. Figure 2 shows similar data for magnesium oxide.

These strength data offer enough confusion to the designer without further complication. However, the designer must be aware of the fact that the actual

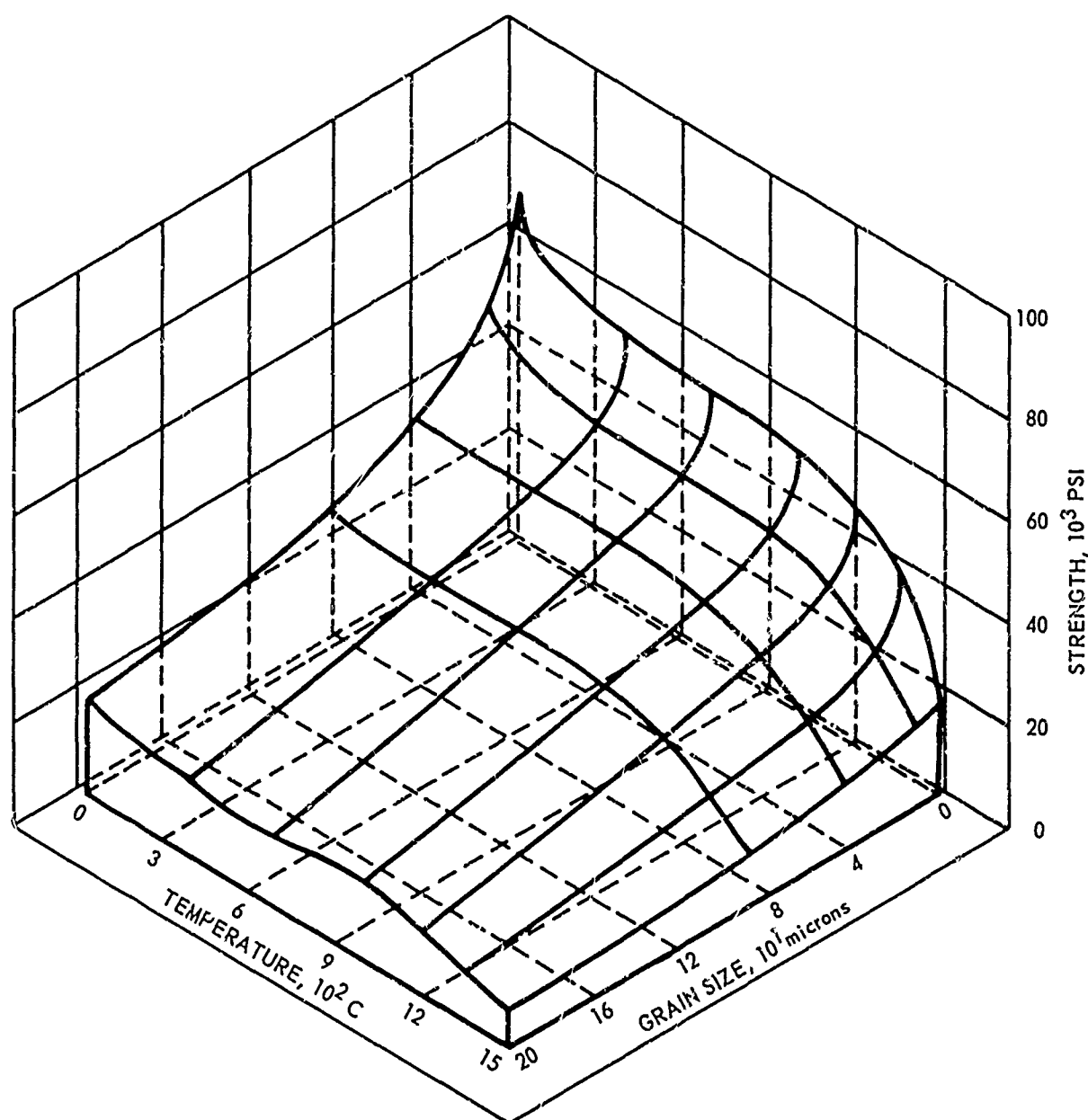


Figure 1. Strength-Temperature-Grain-Size Surface for Dense Pure Hot-Pressed Alumina.

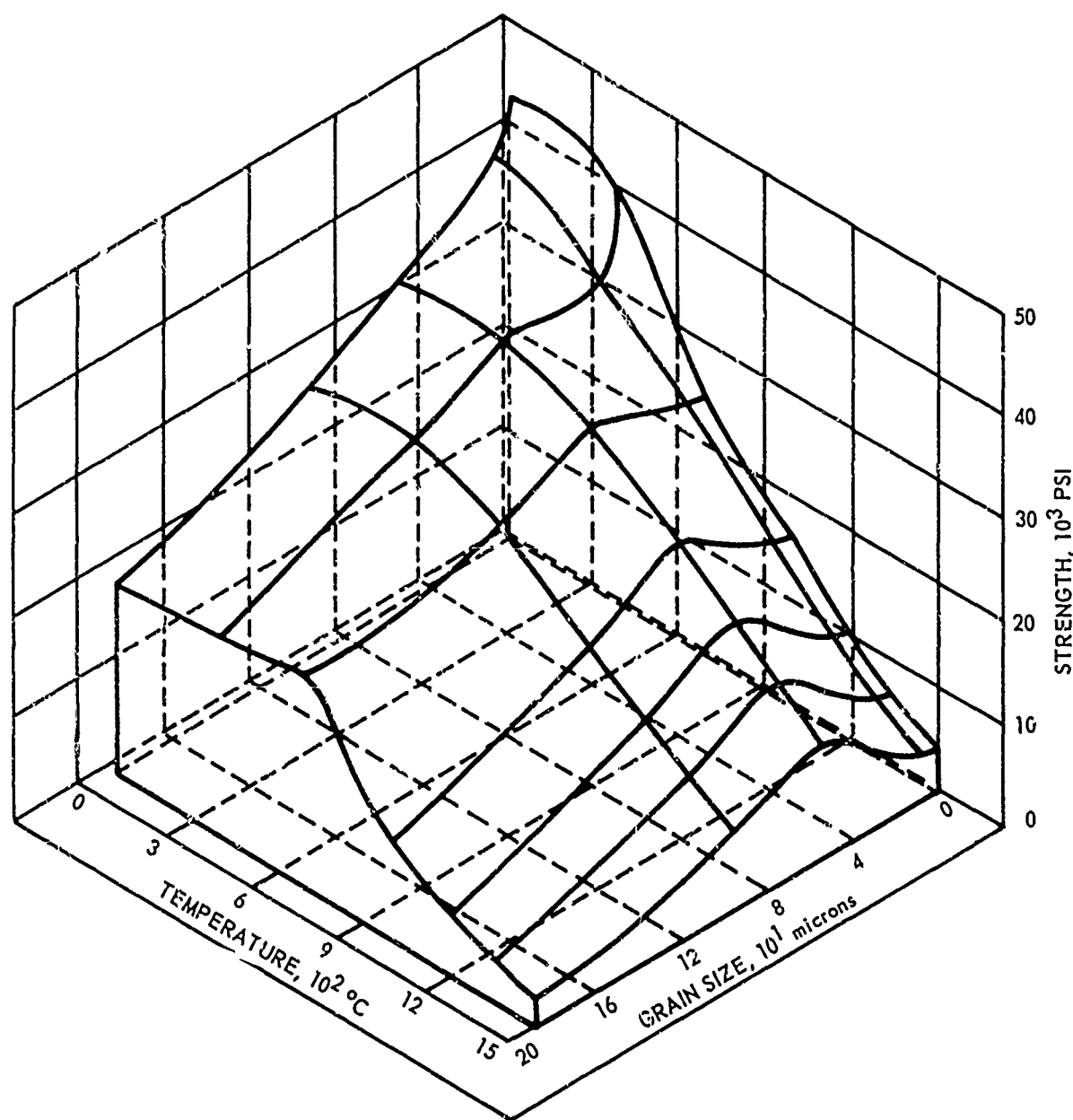


Figure 2. Strength-Temperature-Grain-Size Surface for Dense Pure Hot-Pressed Magnesia.

value obtained for any particular grain size is dependent upon specimen size, surface finish, loading rate, breaking span to thickness ratio, method of loading (4-point or 3-point) etc. To properly design with a given material it is important that the stress field in the test specimen simulate the stress field resulting from thermo-mechanical loading in service. He must know if the behavior of the material in a specific application depends upon the properties of the bulk material or whether the surface condition of the specimen is the limiting factor.

An additional confounding factor is one of size. First there is the problem of relating the strength behavior of a large specimen to data obtained on a small specimen, assuming the character of both specimens is identical. The practical problem is compounded by the fact that the character of the two specimens is very unlikely to be the same, and that this difference is not consistent. A large specimen usually tends to vary through the cross section, particularly as it becomes thick. This problem varies with the fabrication technique used and maturation parameters.

In order to provide the designer with meaningful strength data it is necessary to test enough specimens so that such data will have statistical significance. This creates an additional problem. Since ceramics are brittle they are unable to deform under load and adjust in such a way as to assure uniform stress distribution over the test area. Therefore, test data tend to vary over a relatively wide range. This is due primarily to two factors. First, there is the problem of non-uniform loading resulting from specimen misalignment or poor testing procedures. Second, there is the problem of material variability, particularly from the standpoint of flaws or defects in the material itself and surface defects on the specimen. This last problem is the one which may well cause the designer to become so suspicious of ceramic materials that he will use them only as a last resort and then penalize them to the point that service performance is essentially independent of the improved properties that the materials engineer worked so hard to develop.

Thermal conductivity, emittance and modulus of elasticity may vary in a manner similar to strength. Thermal conductivity and emittance may be varied over a wide range depending upon density. A very porous body will have a low thermal conductivity and high emittance relative to a dense body. Although the thermal shock resistance of a body would be expected to decrease with decreasing thermal conductivity it has been reported that certain aluminum oxide bodies increase in thermal shock resistant with increasing porosity. In this case the thermal shock resistance would appear to be increasing as the strength and thermal conductivity decrease, further contradicting thermal shock theory.

Other properties such as thermal expansion and specific heat are related to the physical nature of the oxide and are relatively insensitive to the fabrication and maturation techniques. However, they may be affected by impurities.

In hyperthermal environments where heat transfer is primarily by convection and the body is free to radiate to space, as in the case of a nose

cone, leading edge, or radome, emittance is of critical importance. A high emittance material may provide a surface temperature many hundreds of degrees cooler than a low emittance material in the same environment. It is not always appreciated that the surface finish of a material greatly affects its emittance. For example, a very porous foam structure may approach an emittance of 1, while the emittance of a polished surface of the same material might be 0.5 or lower. In a high temperature environment which would heat the low emittance material to 4000° F, the high emittance form of the same material could assume a temperature 500° F lower. This would have the effect of making the porous form of the material appear 500° F more refractory than the dense low emittance form of the same material. Emittance is of little importance for applications where the material is not free to radiate to a cooler environment, as in the case of rocket nozzles.

It should be clear from this discussion that the use of tabular, handbook data for ceramic materials is dangerous unless the material and test conditions are completely characterized and are consistent with the design criteria for which the material is being considered. It is easy to see that the variations available in a single oxide material such as aluminum oxide may be greater than between similar physical forms of two different materials. This situation may be even more critical with other materials. A classic example is the thermal conductivity of fused silica. The thermal conductivity of clear fused silica at high temperatures is sufficiently high for it to be used as the glass envelope in quartz lamp heaters. At the high temperatures generated by the tungsten filament the heat transfer is largely by radiation, and the clear fused silica is essentially transparent to radiant energy. On the other hand, slip-cast fused silica (a sintered, polyparticulate form of fused silica) has a very low thermal conductivity up to its melting point. In the range of 2000° to 3000° F there are several orders of magnitude difference in the thermal conductivity between clear and slip-cast fused silica. However, in the physical and chemical sense the materials are identical. They differ only in particle size and method of fabrication. Therefore, if the designer were to seek the thermal conductivity of fused silica, it would be imperative that he know the type of fused silica, or the value could be in error by orders of magnitude. In fact, this very difference in thermal conductivity has resulted in one application where slip-cast fused silica was used as a thermal insulator and reflector for quartz lamp (clear fused silica) heaters. The same material was serving two functions which required extremes in thermal conductivity.

1.4 The Environment Problem

The importance of characterizing the thermal environment in which ceramic systems are to function cannot be overemphasized. Unfortunately many materials engineers and many designers have not appreciated the importance of this factor. This is illustrated by the fact that a relative thermal shock resistance merit index is often included in material property data tables. Such indexes suggest that thermal shock resistance is simply a materials property. The expression:

$$M = \frac{Ks}{E\alpha} \quad (1)$$

where

M = merit index
k = thermal conductivity
S = tensile strength
E = elastic modulus
 α = coefficient of thermal expansion

is usually used to give this index. What is overlooked in using this expression is that this relationship holds only for conditions of mild thermal shock. Most engineers appreciate the fact that the thermal shock resistance of a given material depends upon the severity of the environment. However, this idea usually goes no further than considering the severity of the environment as dependent upon the temperature range through which the thermal shock operation (test) is carried out. Temperature is only one of the parameters involved in this process. The primary factor is the net heat transfer rate to the specimen. This may be altered by orders of magnitude without changing the temperature of the environment. Design engineers have only recently recognized the fact that even the relative thermal shock resistance between two different materials may be reversed depending upon the severity of the thermal shock environment. Manson (Ref. 4) and Kingery (Ref. 5) have developed expressions which take into account the thermal shock environment. These expressions relate the maximum temperature from which a material can be quenched (to room temperature) to the severity of the quench. The term ah has been used to denote this severity, where

a = half thickness of the plate
h = heat transfer coefficient

If the term t_{max} is the maximum temperature from which the material can be quenched, then

$$t_{max} \propto \frac{ks}{E\alpha} \quad (2)$$

but for severe conditions (high values of ah)

$$t_{max} \propto \frac{S}{E\alpha} \quad (3)$$

These expressions emphasize the fact that a material may have satisfactory thermal shock resistance under mild thermal shock conditions by possessing a high thermal conductivity. However, it will receive essentially no benefit from this property under very severe conditions. Manson determined the

maximum temperature from which Al_2O_3 and BeO could be quenched as a function of the thermal shock environment. The data are shown in Figure 3. According to these data, BeO should be superior to Al_2O_3 in a mild thermal shock environment while the reverse should be true under more severe thermal shock conditions. Also in Figure 1 are experimental data showing the maximum temperature from which BeO and Al_2O_3 withstood quenching into room temperature air and water. The air represented a mild thermal shock environment and water a severe environment. The predicted reversal in the order of merit of these materials was observed experimentally.

As missile speeds increase above Mach 3, particularly as they reach Mach 5 and higher at sea level, a critical ceramic materials problem develops. These systems must function over a relatively wide range of heat fluxes for varying periods of time depending upon the mission. In order to illustrate the dependency of the thermal shock resistance of candidate radome materials on the thermal shock environment, Walton (Ref.6) presented the data shown in Figure 4. The thermo-mechanical properties used to calculate these data are shown in Table I. The data shown in Figure 4 are based on room temperature properties; and, with the exception of slip-cast fused silica and boron nitride, poorer performance data would have been presented had the effect of temperature on property values been taken into account.

Although constant property values were used, it can be seen that the thermal shock resistance order of merit among these materials is almost entirely dependent upon the severity of the thermal shock environment. For example, BeO should have the highest thermal shock resistance under mild thermal shock conditions, but will be next to the poorest under severe conditions. It is interesting to note that the maximum quench temperature for slip-cast fused silica is above its melting point for all conditions of thermal shock.

This brief review of one aspect of the interaction between the environment and the material and its effect on the performance of the material should serve to illustrate the complexity of the problem under discussion. It should not be difficult to predict the performance of a ceramic material under thermal shock conditions if both the material and the environment are completely characterized.

1.5 The Design Engineer

The design engineer adds further restrictions to the problem of designing with brittle materials. Since he requires a particular piece of hardware to serve a specific function, the shape and size of the piece must be within certain limits. A nose cone, leading edge, radome or other exterior flight hardware item must be aerodynamically acceptable, and the heat transfer rate to the material and the resultant thermal shock environment will be a function of the actual shape. For example, the heat transfer rate at the stagnation point increases as the shapes become more slender and pointed. On the other hand, the performance of a given material may be extended if a large radius is used and/or the thickness of the section is reduced. If the design is thus altered to accommodate a given material, it is possible that the performance of

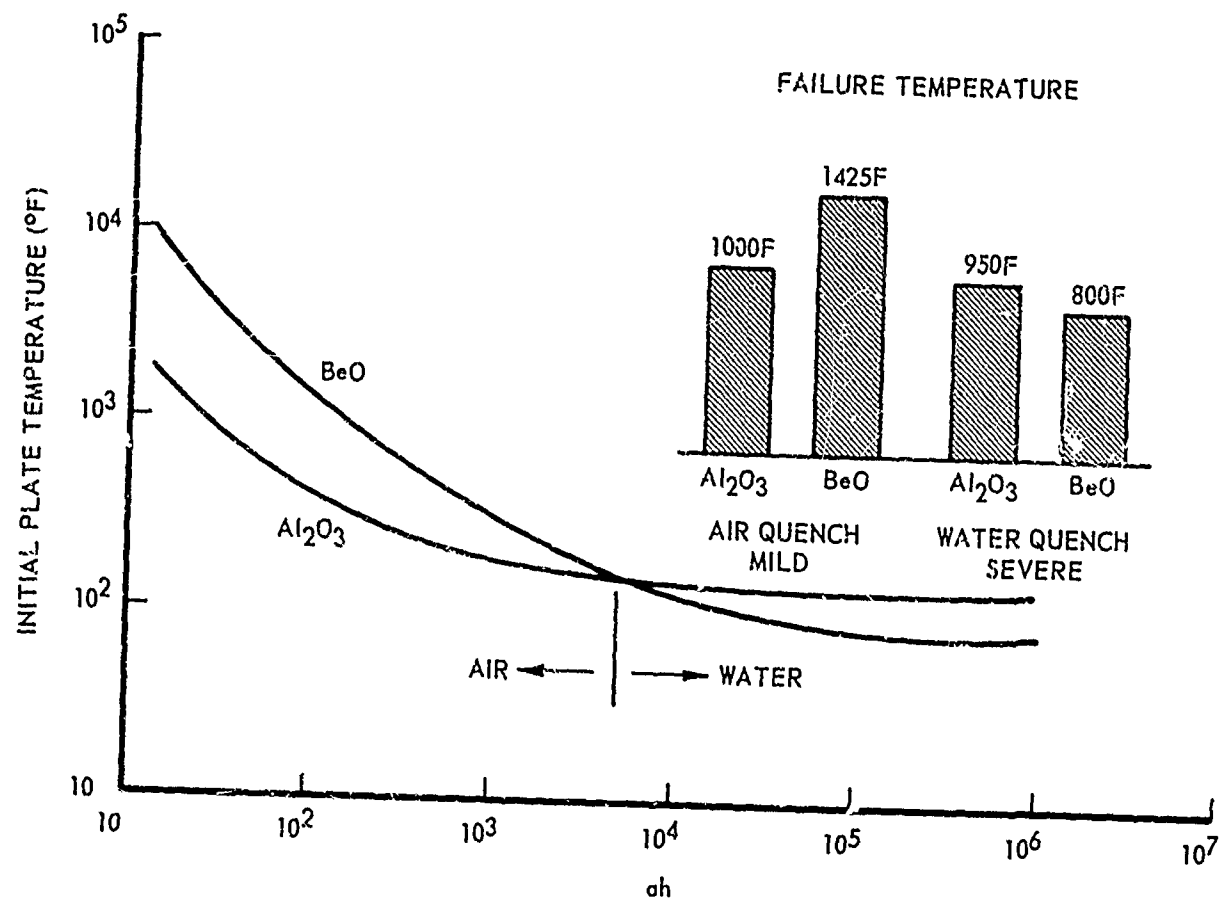


Figure 3. Relative Thermal Shock Resistance of Al_2O_3 and BeO as Function of Thermal Shock Environment (ah).

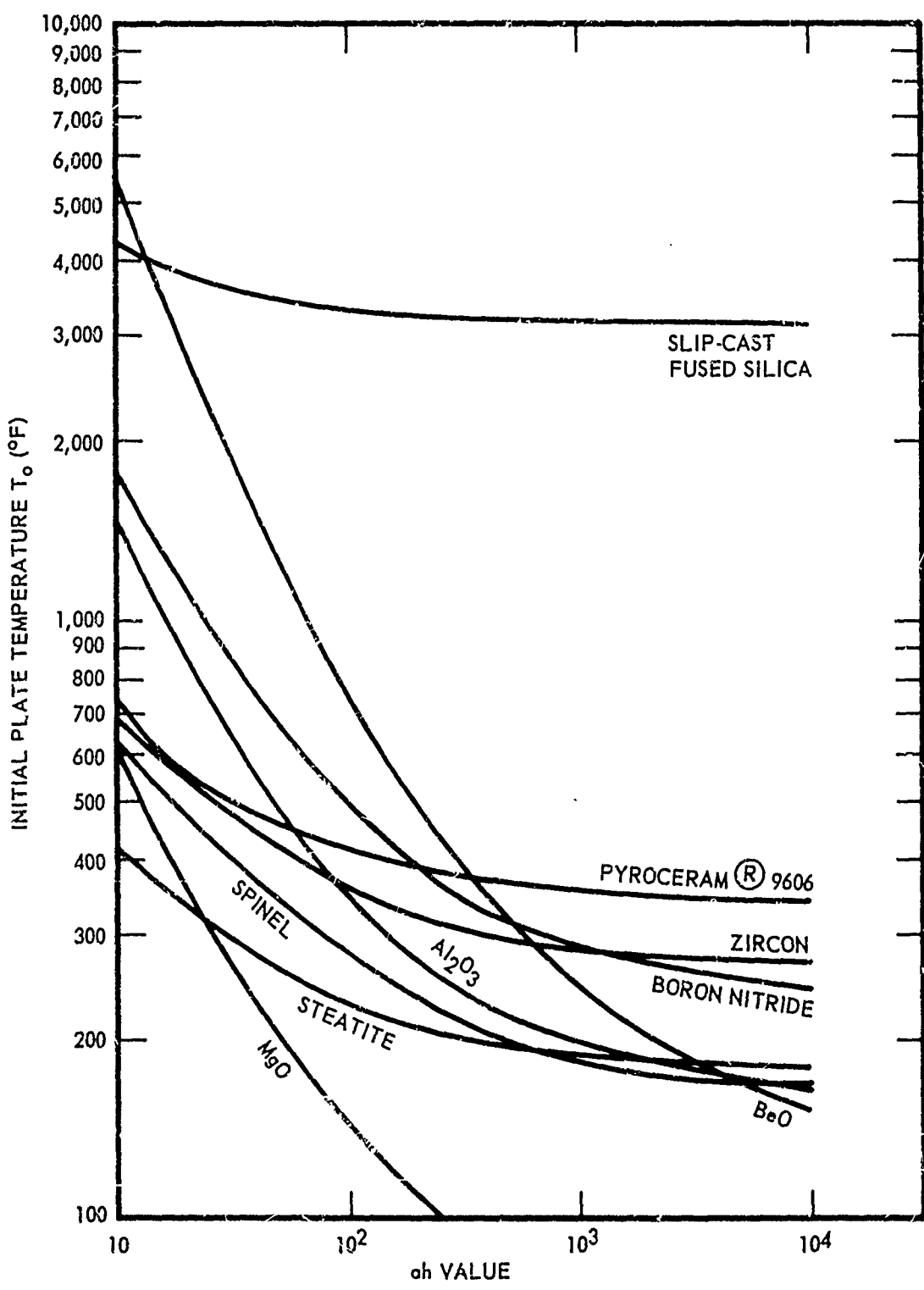


Figure 4. Relative Thermal Shock Resistance of Candidate Reentry Radome Materials as a Function of Thermal Shock Environment (ah).

TABLE I

MECHANICAL AND THERMAL PROPERTIES OF CERAMIC RADOME MATERIALS

	Thermal Conductivity (BTU/hr-ft-°F)	Transverse Strength (psi x 10 ³)	Young's Modulus (psi x 10 ⁶)	Thermal Expansion (α x 10 ⁻⁶ /°F)
Aluminum Oxide	20	47	52.4	4.35
Beryllium Oxide	125	35	42.8	5.1
Boron Nitride	18	15.9	12.4	4.2
Forsterite	1.94	20		5.4
Magnesium Oxide	27	23	40.0	7.7
Pyroceram® 9606	2.1	20	17.3	2.7
Slip-Cast Fused Silica	0.4	4.5	3.8	0.3
Spinel	6.8	24.1	31.7	3.6
Steatite	2.5	15	14.5	4.6
Zircon	3.15	22	24	2.7

the vehicle will be compromised. Such designs generally increase drag. This could be particularly critical in the case of defensive missiles where speed and range must be optimized.

Additional requirements may further compound the design problem. In the case of radomes, the wall thickness is critical and is determined by the dielectric properties of the material, the frequency of the radar and the impingement angle of the radar signal on the surface of the radome. Conventional ceramic radomes are usually designed as a one-half wave wall. This is of the order of 1/4-inch for aluminum oxide, 5/16-inch for Pyroceram® and 3/8-inch for slip-cast fused silica.

One of the attractive features of ceramic radomes is their resistance to rain erosion at high velocity. Aluminum oxide excels all other materials in this respect. This results from the extreme hardness and high strength of alumina. However, as flight velocities exceed Mach 3, the thermal shock resistance of aluminum oxide radomes becomes critical. One way to increase the thermal shock resistance of such radomes would be to reduce the wall thickness (reduce a_h). Electrical requirements dictate that if the wall thickness is less than half wave (≈ 0.25 inches) it must be reduced to at least one-tenth wave (0.050 inches) or preferably one-twentieth wave (0.025 inches) in order to maintain acceptable radar transmission properties. This reduction in thickness might allow the radome to survive the thermal shock environment associated with Mach 4 or possibly Mach 5 flight. However, the structural and mechanical capabilities have been so compromised that only very small radomes (12 to 18 inches long) would be practical, and such radomes fail catastrophically from rain impact at Mach 3. Therefore, design restrictions for this particular application have defined a very narrow corridor of applicability for one of our most completely characterized ceramics.

1.6 The Testing Problem

From an analytical standpoint, the test environment, particularly for thermal shock testing, is probably the most difficult factor to characterize. Also, judging from the great volume of test data reported in the literature, it is the least understood and least appreciated factor in the problem of designing with brittle materials. Essentially every laboratory engaged in high temperature materials work has its own pet thermal shock test geared to what it believes to best suit its test needs. Oxy-acetylene and plasma torches, and quartz lamp heaters are used in great profusion. Probably no two torches operate under the same conditions of gas flow, power setting, exit velocity, gas temperature and enthalpy, heat flux, etc. In many instances these parameters are not even known. Because of these problems and the almost impossible task of determining the actual interaction between the hot gas (conditions unknown) and the material (properties unknown) such devices are used for empirical studies. These are usually restricted to oxidation tests of coated refractory metals and ablation tests for ablative plastics and resin filled ceramic foams.

The problem of developing thermal shock test facilities which can simulate actual in flight environmental conditions for any sustained period of time is a serious one. At the present time the engineer must be satisfied with a test which can simulate the net heat transfer which he predicts will be encountered in flight. Such devices as large plasma jet wind tunnels, rocket motors, and ram jet engines have been used for this purpose. The results of such tests are subject to all of the variables previously discussed plus the added variables associated with the test itself. Conclusions drawn from such tests must be considered in the light of the problems previously discussed. For example, a poorly designed holding fixture and attachment system might cause the failure of a radome being tested in a ram jet engine (Ref. 7). Such attachments are usually designed only for the test and present problems in their own right which are not encountered in the actual flight situation.

Other types of tests are used to obtain thermal shock data and to evaluate materials for hyperthermal flight applications. However, the tests are usually designed to generate a thermal gradient in the material and to determine the material's behavior in the presence of the resultant thermal stresses. Such devices as hot-flue gases, hot salt baths, and hot metal baths have been used for this purpose. When a hot bath system is used, the investigator must recognize that the bath simulates the flight environment at best only in terms of heat transfer rate, and he must be aware of any chemical reaction which might take place between the material and the bath. For example, it was reported that slip-cast fused silica could not withstand the thermal shock associated with repeated immersions in a hot salt bath (Ref. 8). On closer examination it was learned that the molten salt was reacting with the fused silica causing it to devitrify or change phase. Therefore, after several cycles the material being tested was no longer fused silica but cristobalite. This material would not be expected to withstand the thermal shock. This problem would not be expected in actual service, unless it was required to fly in a hot salt bath.

In a similar manner a nose cap shape of aluminum oxide was shocked by immersion in molten babbitt at 800° F (Ref. 9). The temperature of the inside of the wall was measured with a thermocouple, Figure 5. It was assumed by the investigator that the outside wall rapidly reached the temperature of babbitt. An analysis (Ref. 10) later showed that there was a large thermal drop in the babbitt at the surface of the nose cap since the molten babbitt was not in motion. From the analysis the outside wall temperature was calculated and it was found that the maximum thermal gradient in the wall was of the order of 50° F, Figure 6. The investigator had assumed it to be several hundred degrees. Also an aluminum oxide radome was injected into a 3000° F gas stream without failure (Ref. 9). From the performance of the radome it was assumed that the radome would function satisfactorily in any flight environment up to 3000° F. Heat transfer rate was ignored. Analysis (Ref. 9) based on inside wall temperature measurements indicated that the maximum thermal gradient in the wall was of the order of 100° F (Figure 7) and that the heat transfer rate was less than would be expected during flight, even at much lower temperatures.

It is significant to note that although the type of data discussed here cannot be related to particular systems, theory of aerodynamic heating, or design with brittle materials in particular, it is serving to awaken the ceramic community to the problems that face the design engineer. The tests are generating data which can improve a designer's understanding of the problems involved in evaluating ceramic materials for future applications.

1.7 Problems of Mechanical Testing

In the area of mechanical testing valuable data are being generated. Many investigators are studying the effect of stressing ceramics by various methods, and these investigations should improve our understanding of brittle materials. As test methods are devised which reduce the scatter of data, the designer should attempt to incorporate the methods in the design and use

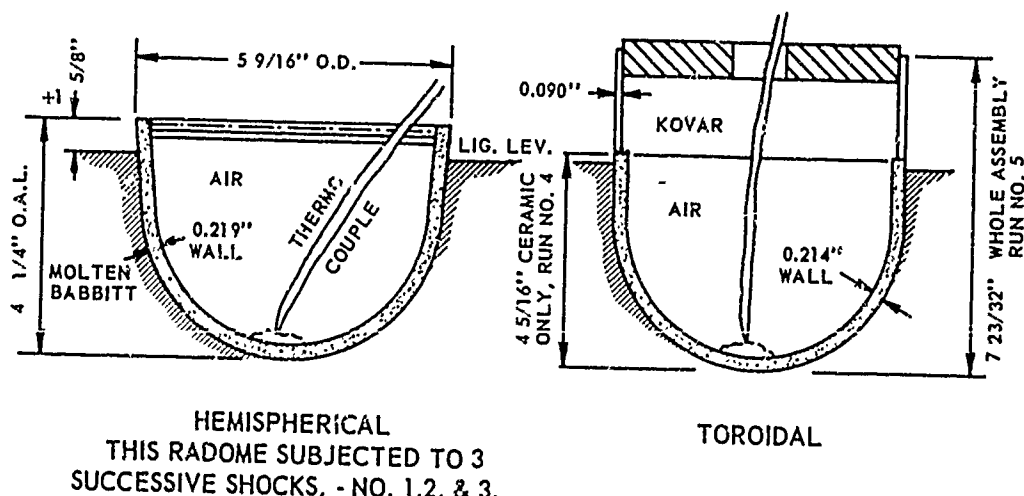
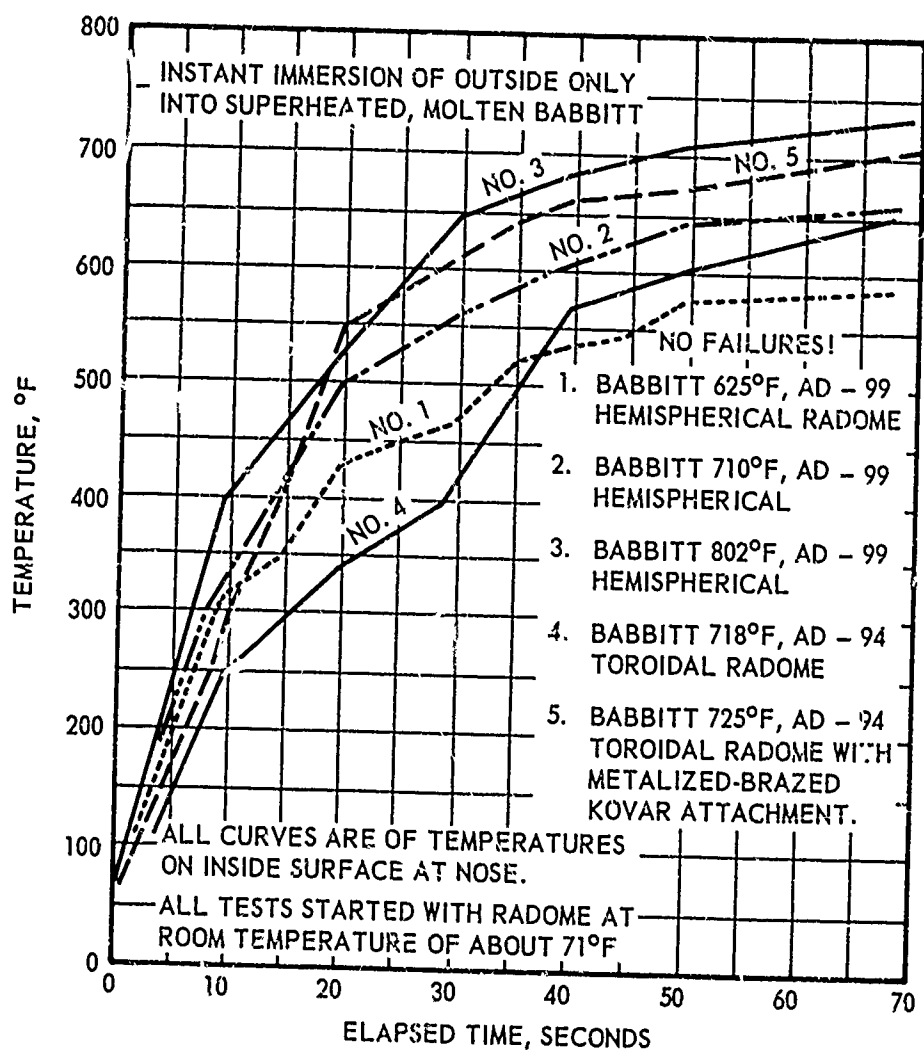


Figure 5. Inside Wall of Aluminum Oxide Shapes Immersed in Molten Babbitt.

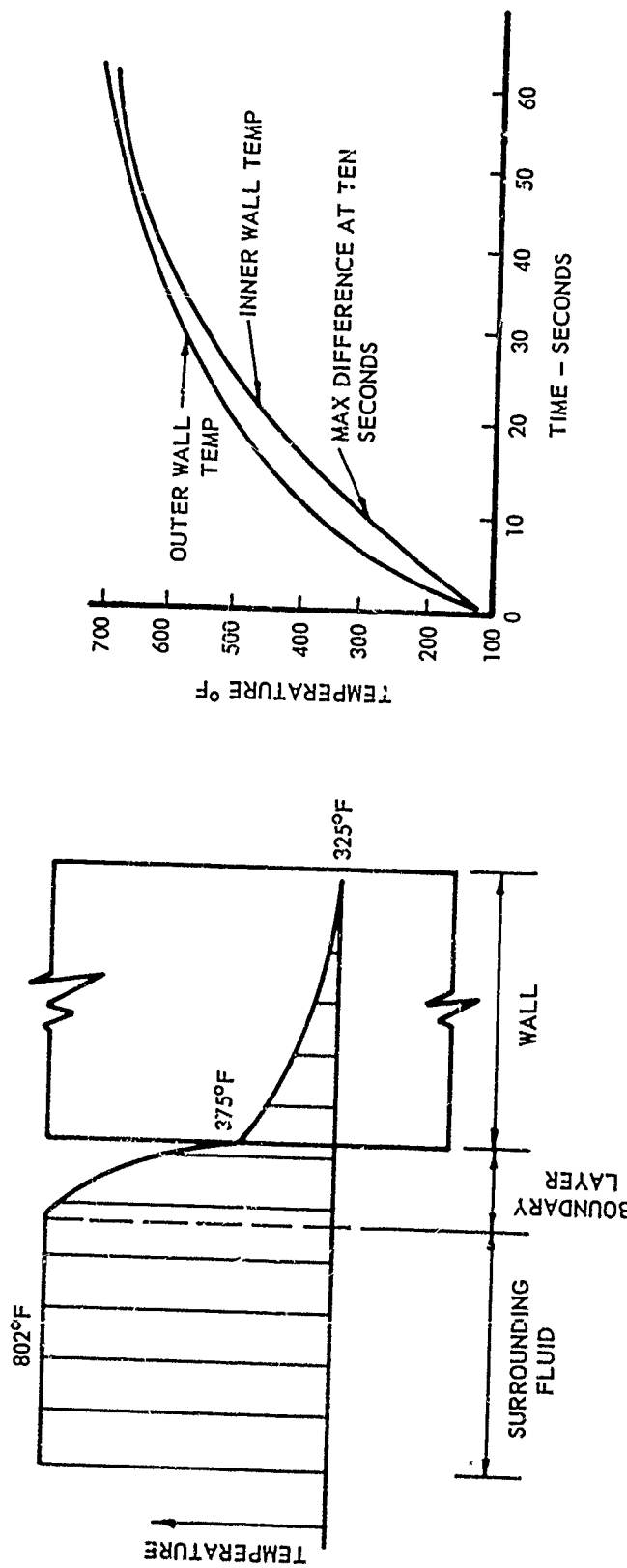


Figure 6. Temperature Distribution for Radome Immersed in Molten Babbitt.

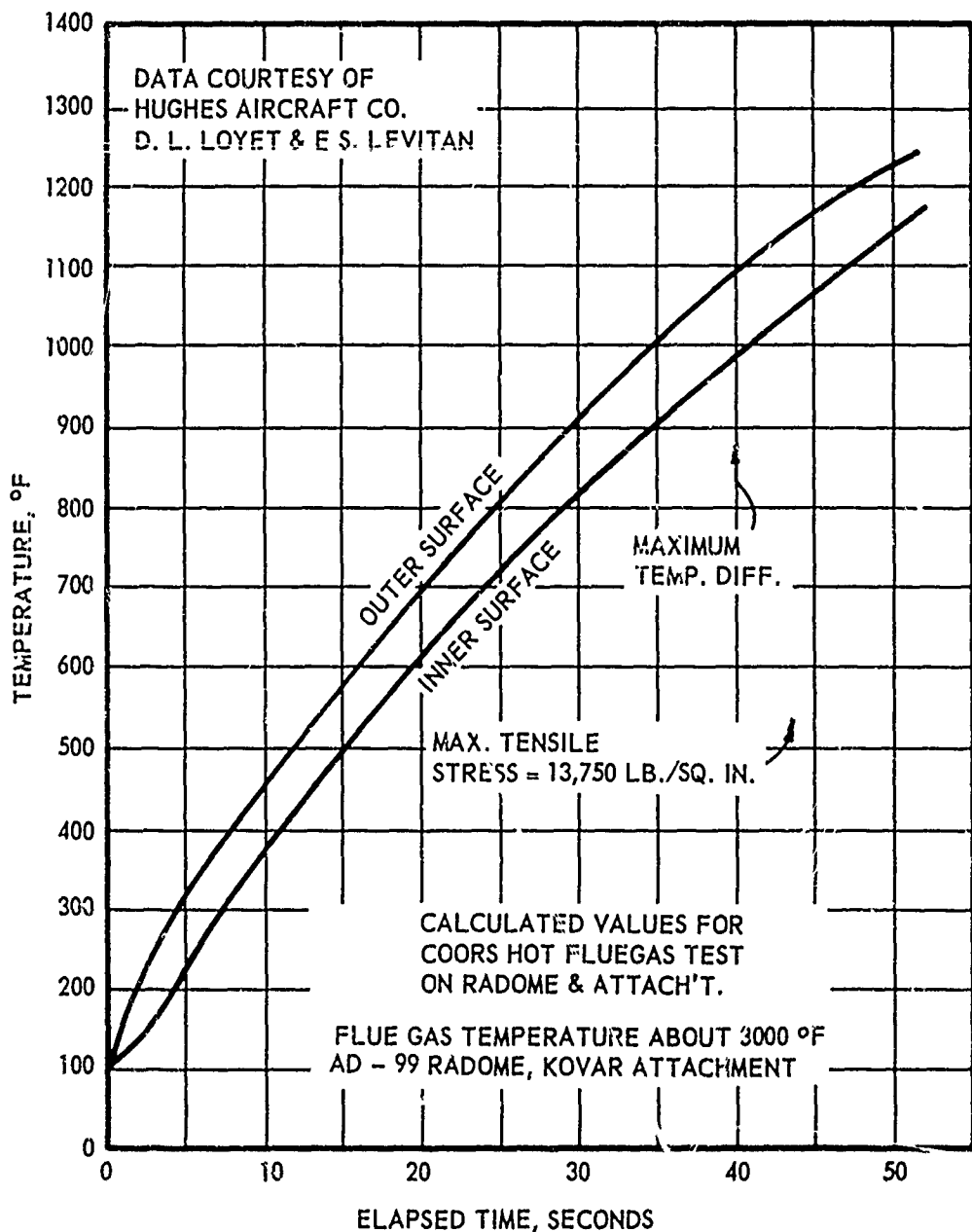


Figure 7. Thermal Gradient in the Wall of Radome Injected into Hot Gas Stream.

of ceramic materials in flight applications. Conversely, if the designer is restricted to a particular method of attaching, supporting, or loading a piece of hardware, he should see that the materials being evaluated for his program are tested in such a manner that stress fields are similar to those encountered in service. To use data obtained under near ideal conditions for an application in which the material will be used in a very non-ideal situation would almost guarantee failure.

As mentioned previously, specimen conditions of microstructure, surface finish, size factor, etc. must all be taken into account in order to properly characterize mechanical test data and make them meaningful to the designer.

1.8 Ceramic Systems

The information thus presented would suggest that it would be essentially impossible to design with brittle materials for hyperthermal applications. If this statement were qualified to say, "design for maximum efficiency with monolithic brittle materials," it would be correct. Materials systems for current applications are overdesigned, modified, and compromised to such a degree that a precise knowledge of properties, design, and environment are not necessary for their use. Also, empirical testing of such systems provides all of the necessary information to determine it's suitability for a particular job.

The nose cap development work on the X-20 program is a good example of a combined empirical-analytical approach (Ref. 11). The ceramic material was used as small tiles, which covered a graphite support shell. By keeping the size of the tile small enough so that each section could withstand the thermal shock environment, it was possible to construct a nose cap which would be capable of survival. A second approach utilized zirconium oxide reinforced with platinum-rhodium wire. The outer surface was interrupted by a hexagonal void pattern to a depth of 0.5 inches. The end result was the same as for the tile. It was concluded that the techniques developed in the X-20 nose cap program "--- provide an excellent analytical starting point for future design studies on advanced vehicles."

1.9 Conclusions

From this review it is evident that the current state-of-the-art of designing with brittle materials does not provide the designer with specific data which will allow him to design an optimum system. It should also be evident that the results of thermal shock tests or actual flight tests would be of little value to the designer in those cases where the material and environment were not at least partially characterized. In fact they could be very misleading. Therefore, in this manual case histories dealing with thermal shock testing are limited to cases where some method of analysis was employed and where, hopefully, meaningful material property data were available and at least some attempt was made to characterize the environment. Such conditions were met in only a few cases.

At the present time it appears that the radome designers have progressed the furthest in developing analyses to relate the material, design, and

environment to the performance of a monolithic ceramic structure. This results from the fact that the radome designer has been limited to the use of such structures without the design freedom that is enjoyed by nose cone and leading edge designers.

It is hoped that this report will mark a turning point in the design with brittle material. Indications are that the design engineer, materials engineer, and aero-thermodynamic engineer are responding to the seriousness of the problem. Each is becoming increasingly aware of the other's problem and attempting to provide all of the information needed from his field of specialization. The successful implementation of this approach should provide the information needed to efficiently design with brittle materials. Therefore, this report will have served one of its major objectives if it helps to promote more cooperation between the design, materials, and aero-thermodynamics engineer.

II. SCOPE OF THE REPORT

This report deals with the existing information which can be used to improve a designer's understanding of ceramic products and processes. The general assets and limitations of ceramic materials are detailed, and the critical gaps that must be filled to promote the successful and efficient utilization of ceramics in aerospace structures are considered. The brittle nature of ceramics, ceramic forming processes, and ceramic materials properties are discussed in detail. Attention is focused on the oxides, carbides, borides, nitrides, and intermetallic compounds and on composite systems. A case-history approach is used to present information on the behavior of ceramic products and material systems subjected to thermal loads and to provide a background for the correlation between known thermal shock theories and brittle materials behavior. Past and current research efforts to predict the behavior of ceramic materials and to minimize their undesirable characteristics are described in detail. Hopefully, this background of information will place the designer in a better position to cope with the problems associated with the use of ceramic materials in aerospace structural applications.

The information provided in this report was obtained by means of intensive literature surveys and through contacts with various government agencies, industrial concerns, and academic institutions. No experimental work was performed. Both unclassified and classified source material was explored. The literature search included a state-of-the-art survey on brittle materials in East and West Europe conducted under a sub-contract by the Kreidl, K. G., the Vienna affiliate of Clyde Williams and Company, under the direction of Dr. Theodor Chvatal.

III. SUMMARY

Ceramic materials tend to favor extremes. Their melting points are high, their densities and their thermal expansion coefficients are relatively low, they are highly resistant to corrosion at most temperatures, and they offer the advantages of high-temperature strength and high resistance to creep. Because of these reasons, because there is an abundant supply and a wide occurrence of ceramic raw materials, and because many ceramics have unique electrical and optical properties and resist oxidation, ceramic materials offer many exciting possibilities for modern technology.

One of the most exciting possibilities for ceramics is their use in aerospace structures. Unfortunately, however, ceramics are quite brittle at ordinary temperatures and, as such, are highly susceptible to catastrophic failure. While this shortcoming has been tolerated in conventional ceramics for many years, the threat of brittle failure has limited the use of ceramic materials in aerospace structures to areas where the conventional materials have had insurmountable deficiencies.

It appears that the following rules describing the general nature of ceramic materials result in part, either directly or indirectly, from their brittle character:

1. The apparent strength differs from the strength calculated on the basis of molecular structure.
2. A high degree of scatter is associated with mechanical property data on ceramics, and ceramics are less reliable than metals for structural applications.
3. Ceramics are stronger in compression than in tension.
4. The average strength of a ceramic specimen decreases with an increase in the size of the specimen.
5. The apparent strength of a ceramic material is influenced by the features of the stress field within the material.
6. The strength of some ceramic materials increases with an increase in temperature.
7. Most ceramic materials are sensitive to thermal and mechanical shock.

Clearly, brittleness represents the most striking feature of ceramic materials and must be a major consideration in their use. In most metals, stored strain energy can be converted into heat through plastic flow, and the materials undergo considerable deformation before breaking. However, in a brittle material stored strain energy can only be converted into surface energy and kinetic energy of broken pieces. As a result, when a brittle component fails, stored energy is usually released in an uncontrollable fashion, and shattering occurs. Thus, the design approach used for the

conventional ductile materials cannot be directly applied to ceramics. A completely new design philosophy may not be required for brittle materials, but there are certainly many gaps that must be bridged in the present philosophy before it can be successfully extended to brittle state members.

Much attention has been focused on the possibilities of devising ductile ceramics, but the problem of obtaining ductile ceramics that are practical is vast. To date, only a few ceramic materials have been known to exhibit appreciable ductility at low or moderate temperatures, and these have been limited to single crystals with a particular type of structure. As a result, many investigators have concluded that ductile ceramics will become a reality only when they can be produced as crack-free bodies in which dislocations are prevented from collecting together to produce stress concentrations at barriers.

There seems to be little agreement among scientists as to the prospects of obtaining polycrystalline ceramics in a ductile state. Preliminary studies on such materials have failed to show ductility, but many believe that ductility can be achieved in these materials by altering their microstructures. However, some fear that ductility will be obtained only at the expense of losing high temperature strength, and it is a combination of strength and ductility that is really needed. In any event, further studies in this direction are warranted since most ceramic materials have a low coefficient of thermal expansion, and a small increase in ductility can be expected to produce a rather large increase in the thermal shock resistance of a ceramic material.

While progress toward the obtainment of ductile ceramics moves slowly, there have been some particularly noteworthy successes in the area of improved thermal shock resistance for ceramics. Major improvements have been realized through:

1. The control of microstructure.
2. The modification of material properties.
3. Good design practice.

There is good evidence that the thermal shock resistance of a ceramic can be improved when a coarse pore system is present. Apparently, the pores serve as crack arresters if the cracks are relatively small and if the strain energy is diffuse, as in the case of high temperature spalling. The behavior seems to be associated with the reduction of stress concentration through the blunting of crack tips.

There is also good evidence that the thermal shock resistance of a ceramic article can be significantly improved through the careful control of the particle size distribution. The thermal resistance increases with increasing particle size at least up to a certain limit, which suggests that thermal shock cracks are generally formed between the particles in a ceramic body and not within them. The use of a wide range of particle sizes is also favorable.

Apparently, the latter provides a structure with a heterogeneous character in which crack propagation can be limited to small distances and still provide adequate stress relief under certain thermal shock conditions.

Chemically bonded ceramics seem to be particularly well suited for use under thermal shock conditions. Apparently, their outstanding thermal shock behavior derives from relatively weak particle-to-particle bonding which limits crack propagation to microscopic distances when temperature intensities are localized. When these relatively soft materials are subjected to a sudden temperature change, they fail locally at the exposed surfaces, but retain their strength. Since the chemically bonded materials cannot be sintered at high temperatures without sacrificing thermal shock resistance, metal reinforcement may be essential to their successful use. Fortunately, the chemically bonded materials can be cured in place and metal reinforcement is easily achieved.

The thermal shock resistance of a ceramic can also be improved by the presence of a metal phase or a low elastic modulus phase such as graphite. The improvement appears to stem from an increase in critical strain and/or a decrease in the amount of elastic energy released during fracture, which reduces the tendency toward catastrophic failure. Metal reinforcement is particularly attractive since it offers the potential of allowing a practical prestressed system of the reinforced concrete type where the brittle phase is held in compression.

Good design practices which have led to an improvement in the thermal shock behavior of ceramic components include:

1. The use of metal reinforcement.
2. The use of ceramics in compression.
3. The cushioning of ceramic components to minimize the intensities of localized stresses.
4. Careful machining of ceramic and adjacent components to close tolerances to prevent mechanical mismatch.
5. Careful thermal analysis and materials selection to prevent thermal mismatch.
6. The use of ceramics prestressed compressively.
7. The elimination of mechanical restraints on ceramic parts.
8. The avoidance of sharp corners, thick sections, and sudden changes of section.
9. The use of generous radii at angles and edges.
10. The use of emissive coatings.
11. The use of ceramics in the form of small individual elements.

It is gratifying indeed that the thermal shock behavior of a ceramic material can often be significantly improved. However, it must be understood that the thermal shock resistance of a material is not an intrinsic material property, but depends on complex interactions between the material properties and the environment. As a result, the thermal shock resistance of a material has not been clearly defined and there is no hope for the establishment of a meaningful standardized thermal shock test. There is hope for the establishment of a meaningful thermal shock test for a specific application. At the present state-of-the-art, most workers use a particular thermal shock test simulating the intended use conditions for their product. To date, the degree of success has varied markedly according to the degree of simulation.

During the conduct of the program, it became apparent that there was no source of principles available that would enable the immediate efficient use of refractory structural ceramics. Ceramic materials are very complicated and few details are known concerning their basic nature. In addition, there is a general lack of data on ceramic materials, and much of the available data is confined to areas of specific interests. The unfortunate consequence of the situation has been a heavy dependence upon an empirical approach to high temperature structural design, which has significantly increased the cost of many aerospace programs.

While the current state-of-the-art of designing with brittle materials does not provide the designer with specific data which will allow him to design an optimum high-temperature structure, indications are that the design engineer, materials scientist, and aerodynamist are responding favorably to the seriousness of the problem, and the past few years have witnessed a considerable amount of research, which should at least provide a guide line to the eventual solution of the brittle design problem.

IV. USE OF CERAMIC MATERIALS IN AEROSPACE STRUCTURAL APPLICATIONS GENERAL LIMITATIONS

In order to promote the successful and efficient utilization of ceramic materials in aerospace structural applications, a number of critical gaps must be filled. Six gaps appear to be outstanding, namely:

1. Many engineers are unfamiliar with ceramics.
2. No source of principles that would enable the immediate use of refractory structural ceramics is available.
3. The existing data on the property values of ceramic materials are widely scattered.
4. Many inconsistencies are found in the published data on ceramics, and there is a lack of sufficient data for the intelligent use of most high temperature brittle materials.
5. There is a dire need for improvement in the ductility and shock resistance of ceramic materials and material systems containing ceramics.
6. The new technologies associated with the aerospace field have placed demands on high-temperature materials which cannot be met with existing techniques.

Each of the above points warrants further consideration. First, it is important that the designer who is unfamiliar with ceramics realizes the problems and principles associated with their use. Most metals undergo considerable deformation by plastic flow before breaking, while ceramics are brittle and usually fail suddenly. As a result, the design approach used for the conventional ductile materials is not applicable.

Second, ceramics are quite complicated. Little knowledge is available on the behavior of ceramics at the molecular level, and, as a result, few details are known concerning their basic nature. In addition, the ceramic industry is highly product-oriented so that much of the available data on ceramics is confined to areas of specific interests. An unfortunate consequence of this situation has been a heavy dependence upon an empirical approach to high temperature structural design, an approach that has significantly increased the cost of many aerospace programs.

Third, available data on the properties of ceramic materials are widely scattered. For example, Chemical Abstracts lists over 400 references on the properties of the carbides covering the period January 1947 to June 1964, and many of these refer to a specific property of a particular carbide over a limited temperature range. Of course, the designer must have data on the properties of ceramic materials, but it is important that these data are made available in readily useable form.

Fourth, most ceramic components contain a wide variety of defects or flaws. Because of these flaws, a high degree of scatter is associated with mechanical property determinations. In addition, small amounts of impurities introduced by preparation techniques may change the constitution of a ceramic system (Ref. 12, 13), and the size and shape of the grain dictated to a large extent by consolidation techniques can have a striking effect on many of the properties of a ceramic part. Because of these reasons, because of a lack of specifications for available ceramic materials, and because of a lack of standardized test methods for determining thermo-physical properties, many inconsistencies are found in the published data on ceramics. In addition, the intelligent use of brittle materials in aerospace structures will most likely require more property data than are generally available at this time.

Fifth, since ceramics are brittle and usually fail suddenly, ceramic materials are less favorable than the conventional ductile materials for structural applications. There is a dire need to improve the ductility of ceramics, but the problem is vast. Progress towards the obtainment of ductile ceramics moves slowly, and there is little agreement among scientists as to the prospects of obtaining ductile ceramics that are practical.

Sixth, because of the severe environments encountered by aerospace systems, great demands have been made for more sophisticated structural materials. With attention focused on ultra-high operating temperatures, extreme corrosive conditions, and unusual optical criteria, many designers are turning to ceramic materials and to elaborate material systems containing one or more ceramic materials (Ref. 14, 15), but in many cases the knowledge that would allow immediate technological progress to be made is not available. The requirements of the aerospace designer cannot be met with the existing technology and processing limitations.

The traditional ceramics technology has utilized the basic capabilities of materials quite well, and major advances must, in general, come from new and different materials, or from materials radically changed by improved fabrication methods (Ref. 16).

For an excellent summary on the problems associated with the use of ceramic materials in aerospace structural applications, the reader is referred to References 16 to 27.

V. BRITTLE BEHAVIOR

5.1. Brittle Nature of Ceramic Materials

Modern technology in many branches of science and engineering has approached the point where the environments encountered greatly exceed the limitations of the refractory metals, and, in many respects, ceramic materials appear to fulfill the requirements of a number of new applications. One of the most exciting possibilities for ceramics is their use in aerospace structures. Unfortunately, however, ceramics are quite brittle at ordinary temperatures and, as such, are highly susceptible to catastrophic failure. While this shortcoming has been tolerated in conventional ceramics for many years, the threat of brittle failure has limited the use of ceramic materials in aerospace structures to areas where the conventional materials have had insurmountable deficiencies.

Clearly, brittleness represents the most striking feature of ceramic materials and must be a major consideration in their use.

The term brittleness has been clearly defined by no one; however, it has been described in a number of ways:

1. An absence of appreciable plastic deformation (before fracture) (Ref. 28).
2. A material condition under which the shearing stress to cause slip is high relative to the tensile stress to cause failure (Ref. 29).
3. A lack of plastic deformation to accommodate stress redistribution (Ref. 30).
4. A material condition when the flow strength is very high in relation to the rupture strength (Ref. 31).
5. A tendency for low-energy fracture accompanied by little or no plastic deformation (Ref. 32).
6. A tendency for failure as the result of a purely elastic interaction (Ref. 33).
7. A tendency to exhibit relatively small deformation prior to fracture (Ref. 34).
8. Accurately following Hooke's Law up to the point of fracture with no plastic deformation (Ref. 35).
9. An absence or partial absence of the shear-stress mechanism transferring stress from one strained portion to those around it at energy levels safely below the bonding energy (Ref. 36).

A few (Ref. 28, 37) have attempted to classify brittle materials, and in regard to ceramics the most interesting classes are:

1. Those brittle under all conditions.
2. Those brittle at room temperature, but ductile at elevated temperatures.

For all practical purposes, all structural materials are included in these two classes since all materials may exhibit brittle behavior under certain conditions of temperature and stress. For example, under low temperature and under high rates of stress even the conventional metals will exhibit brittle fracture if there is insufficient time to dissipate stress by relaxation. In addition, in a body under a hydrostatic pressure or hydrostatic tension no shearing stresses occur, and even the most ductile metals must then fail in brittle fashion (Ref. 29). Most non-metallic materials fall within the second class and deform plastically only at higher temperatures under ordinary stress states. Unfortunately, only a few ceramic materials have been found to undergo appreciable plastic deformation at moderate temperature, and these have been restricted to single crystals with the rock salt structure.

The behavior of brittle materials is far from being fully understood. However, the problem is in the description stage, and a few general observations can be made:

1. Brittleness is a characteristic of materials with strong, directional bonds which are not easily re-formed once they are broken.
2. Less symmetrical structures correspond to greater brittleness to the extent that the only likely modes of deformation in an amorphous material are fracture and viscous flow.
3. There are indications that brittleness might be reduced by close control of impurities, particle size distribution and morphology, and pore structure (i.e., by decreasing grain size and porosity); however, a systematic study of these effects has not been made.
4. Environmental effects can play a major role in brittleness. The decrease in elastic energy caused by a fracture can be no smaller than the increase in surface energy due to new surfaces which are created so that any factor that modifies the surface energy of a material will also modify its tendency toward brittle behavior.

It appears that the following rules describing the general nature of ceramic materials result in part, either directly or indirectly, from their brittle character:

1. The apparent strength differs from the strength calculated on the basis of molecular structure.
2. A high degree of scatter is associated with mechanical property data on ceramics, and ceramics are less reliable than metals for structural applications.

3. Ceramics are stronger in compression than in tension.
4. The average strength of a ceramic specimen decreases with an increase in the size of the specimen.
5. The apparent strength of a ceramic material is influenced by the features of the stress field within the material.
6. The strength of some ceramic materials increases with an increase in temperature.
7. Most ceramic components exhibit a high degree of notch sensitivity.
8. Most ceramic materials are sensitive to thermal and mechanical shock.

During the conduct of this program, it became painfully evident that few details are known concerning the behavior of ceramic materials. The experience with metallic structures subject to brittle behavior, while significant, has not added vastly to the knowledge. The reason is that the tendency toward brittle behavior is not equally shared (Ref. 28). For example, the ductility of cast iron, which is considered brittle among the metals, is an order of magnitude greater than that of ceramic materials (Ref. 35). Thus, the aerospace designer finds himself in an awkward position. He must turn to ceramic materials for critical structural applications, and the basic knowledge (of these materials) that would allow immediate technological progress to be made is not available.

5.2 Ductile Ceramics - A Distant Future Possibility

Much attention has been focused on the possibilities of devising ductile ceramics, but progress toward obtaining such materials moves slowly. Of course, this is not surprising since an improvement in the ductility of a ceramic can only follow a change in the basic nature of the material itself.

To date, only a few ceramic materials have been known to exhibit appreciable ductility, and these have been limited to single crystals with a particular type of structure. As a result, some have concluded that ductile ceramics will become a reality only when they can be produced as crack-free bodies in which dislocations are prevented from collecting together to produce stress concentrations at barriers (Ref. 38).

There seems to be little agreement among scientists as to the prospects of obtaining polycrystalline ceramics in a ductile state. Preliminary studies on such materials have failed to show ductility, but many believe that ductility can be achieved in these materials by altering their microstructures. However, some fear that ductility will be obtained only at the expense of losing high temperature strength, and it is a combination of strength and ductility that is really needed.

The problem of obtaining ductile ceramics that are practical is indeed sizeable. However, further studies in this direction are warranted since

most ceramic materials have a low coefficient of thermal expansion, and a small increase in ductility can be expected to produce a rather large increase in the thermal shock resistance of a ceramic material.

5.3 Statistical Approach to Brittle Fracture

Since recent publications are available which list the present knowledge on the statistics of brittle materials, this section is by no means intended to portray an extensive survey on the subject.

5.3.1 The statistical concept - material flaws

For ductile materials, the scatter of mechanical property determinations is small, and structural designs can be based on the average strength of a group of test samples. However, this is not generally true for ceramic materials (Ref. 35). A high degree of scatter is usually associated with the strength measurements on ceramic specimens, and the designer must use a distribution curve(s) of the properties being considered so that he can select the design criteria corresponding to a given probability of failure (Ref. 34). In addition, the strength determinations on ceramic samples do not, in general, conform to a normal (Gaussian) distribution, and the use of the average (arithmetic) strength can be misleading (Ref. 35).

It is widely accepted that the dispersion of mechanical property determinations on ceramics is attributed to the presence of defects or flaws already existing either in the interior or on the surface of the material. According to the famous theory of Griffith (Ref. 39), such flaws, or microcracks, are present in most materials, and in the absence of plastic flow the cracks act as stress raisers with maximum stress and maximum elastic strain energy occurring at the tip of the crack. By equating the elastic energy and the energy to propagate the crack, Griffith was able to derive an expression relating the applied tensile stress to cause failure as a function of the surface energy and elastic modulus of the material and the length of an incipient crack (Ref. 29). For an atomically sharp crack, Griffith's theory predicts crack propagation at stress levels normally observed for incipient cracks approximately one micron in length (Ref. 40).

Thus, the notion that a brittle material contains a number of defects or flaws is based on sound reasoning and some experimental evidence. Immediate corollaries to the notion are:

1. The strength of a brittle material is a statistical quantity determined by the chance occurrence of a flaw large enough to cause failure at a given stress level.
2. The expected strength of a large specimen is lower than that of a small specimen since there is a greater chance for a large flaw to be found in the larger specimen.
3. A group of large specimens will exhibit less scatter of strength measurements than a group of small specimens since a large specimen contains more flaws than a small specimen.

5.3.2 Weibull distribution function

Several investigators have proposed distribution functions in an attempt to quantify the statistical nature of brittle fracture. The most widely accepted distribution function was proposed by Weibull (Ref. 41). Weibull assumed that flaws of random size distributed throughout a ceramic material caused the scatter observed in its mechanical properties, and, on the basis of the weakest-link concept of failure, devised a distribution function of the form:

$$F(\sigma) = 1 - \exp \left[-V \left(\frac{\sigma - \sigma_{\mu}}{\sigma_0} \right)^m \right] \quad (4)$$

where

F = probability of failure

V = volume subjected to stress

σ = stress

σ_{μ} = zero strength; that is, the strength below which fracture will not (cannot) occur

σ_0 = a scaling factor

m = flaw density

5.3.3 Evaluation of Weibull parameters

The subject is only considered briefly in this section. For a more extensive coverage, the reader is referred to the recent and excellent survey conducted by W. B. Shock at Ohio State (Ref. 42).

Equation 4 can be expressed in the form

$$F(\sigma) = 1 - \exp \left[- \left(\frac{\sigma - \sigma_{\mu}}{B} \right)^m \right] \quad (5)$$

where $B = \sigma_0 V^{-1/m}$ can be viewed as a working parameter. The equation

suggests that a plot of:

$$\log \left\{ \ln \frac{1}{1 - F(\sigma)} \right\} \text{ versus } \log (\sigma - \sigma_{\mu})$$

should result in a straight line with slope m . To facilitate making such a plot, it is desirable to devise a special graph paper such as that shown in Figure 8. The instructions for the use of this graph paper follow.

1. Let N represent the number of strength determinations made using N nominally identical specimens subjected to nominally identical loads.
2. Number the strength determinations from $n = 1$ to $n = N$ in the order of increasing strength. That is, the lowest strength value will be associated with the number $n = 1$, the next lowest with $n = 2$, and so on, until the highest strength value has been assigned the number $n = N$.
3. Plot $\frac{n}{N+1} \times 100$ versus $(\sigma - \sigma_{\mu})$ for various trial values of σ_{μ} . The quantity $\frac{n}{N+1}$ is used as an approximation to $F(\sigma)$. If only a limited number of specimens are used (say 50 or less), the use of median ranks (instead of the numbers $\frac{n}{N+1}$) is highly recommended. For a discussion of median ranks, the reader is referred to Reference 43.
4. The parameters are estimated as follows:
 - a. σ_{μ} is that trial value which produces a straight line in Step 3 above.
 - b. m is the slope of the resultant straight line $\times 1.71$. The need for scaling the slope results from the fact that arbitrary scales were used when devising the special graph paper.
 - c. B is the abscissa of the point of intersection of the resultant straight line and the horizontal dash line.
5. The abscissa is on a logarithmic scale so that any constant multiple of the numbers displayed along the abscissa may be used.

Example:

For the locus of points shown in Figure 8 and for a constant abscissa multiple of 1000 psi:

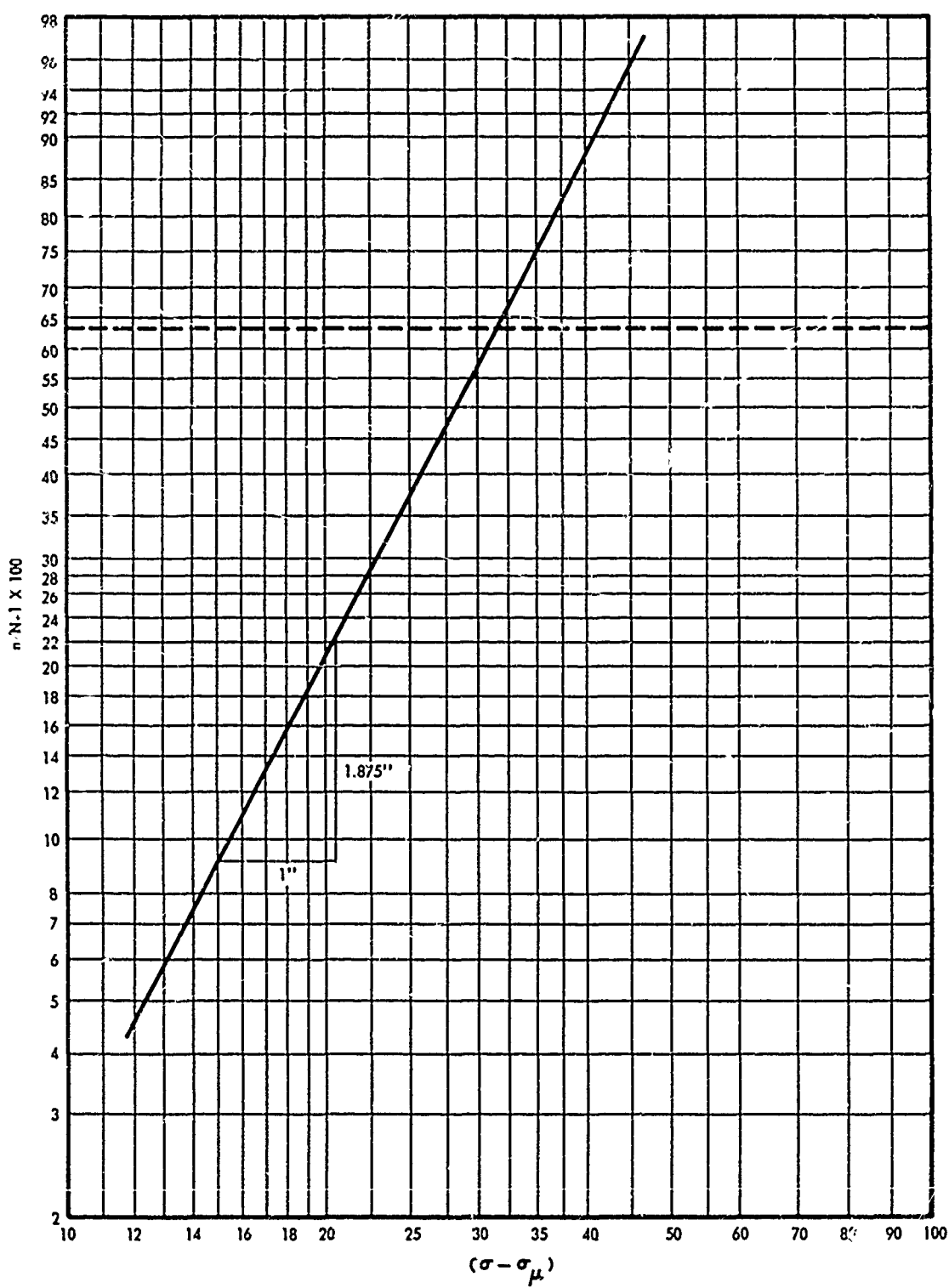


Figure 8. Special Graph Paper.

1. The scale factor $B = \sigma_0 V^{-\frac{1}{m}}$ was estimated to be 31,300 psi.
2. The slope was estimated to be 1.875 giving the estimation $m = 1.875 \times 1.71 \doteq 3.2$.
3. Assuming that the volume of the test specimen under critical stress was 10 cubic units (for example, if a volume of 10 cubic units of material had been loaded in pure tension), the following estimate was obtained

$$\sigma_0 = B V^{\frac{1}{m}} \doteq 31,300 (10)^{0.312} \doteq 64,000 \text{ psi.}$$

5.3.4 Critique

Weibull's theory is based on the assumption that flaws of random size exist in a ceramic component and that fracture of the single most severe flaw results in the failure of the entire component. That is, it is based on the so-called weakest-link concept. One of the most noteworthy advantages of Weibull's theory is that, like most weakest-link theories, it is not mathematically complex. Under the additional assumptions of the tensile-stress-criterion for failure and a uniform dispersion of flaws throughout a ceramic material, the Weibull distribution function has given reasonable correlation with experimental data. As a result, Weibull's theory and its associated assumptions have been rather widely accepted. However, a number of investigators have questioned the general applicability of the theory, or at least questioned it in its present state-of-the-art.

Because ceramics are often highly sensitive to surface effects, a number of investigators believe that the most serious flaws in a ceramic material exist either on or near the surface*. They contend that a surface layer, with properties different from the bulk material, must be considered and that both the surface layer and the bulk material must be characterized either by single strength values or by statistical techniques. In the case of single strength values the behavior of a component would depend on the geometry and on the thickness of the surface layer. In the case requiring statistical descriptions the problem would be confounded if the thickness of the surface layer varied from component to component.

Another contention holds to the classical concept that a single strength value characterizes even a brittle material and that the variability observed is attributed to uncontrolled factors in raw materials, processing and testing

* In a recent study at the Lawrence Radiation Laboratory more flaws initiating fracture were found near the surface of fractured bend-specimens than were predicted by the Weibull theory, and flaws appeared to be especially heavily concentrated at sharp corners of test samples (Ref. 44).

and to differences in internal stresses in different components. While such a concept implies the potential of a simple design guide, it has met little favor to date.

There are also a number of researchers who would replace the weakest-link or series model with a parallel model. This contention allows the fracture of a single flaw to result simply in a redistribution of stresses. Total fracture would occur only if the undamaged portion of the material was incapable of supporting the redistributed load. While the parallel model has not found wide acceptance, many feel that a combination of the series and parallel models may hold the key to the successful design of brittle structures. Unfortunately, however, the mathematics associated with the combined model are abominable.

Finally, Weibull's distribution function does not lend itself readily to the bimodal distributions of strength which are frequently observed, none of the statistical theories lend themselves to a description of internal stresses, and none describe the differences in the processing of small and large specimens.

5.4 General References on Brittle Behavior

A number of recent publications by the Armour Research Foundation provide an excellent summary of the present knowledge on the statistics of brittle materials (Ref. 45-47). Earlier work in the area of statistical failure concepts is reported by Battelle Memorial Institute (Ref. 48-50). For recent publications which deal with the general concept of brittle behavior the reader is referred to References 19, 23, 24, 28, 51, 52, and 53.

VI. CERAMIC FORMING PROCESSES

The following sections deal with the advantages, limitations and possibilities of various forming processes. Processes currently being used to produce ceramic structural elements are considered.

6.1 Cold Forming

6.1.1 Slip-casting

The method of slip-casting offers the potential of allowing the fabrication of large and intricate shapes, of making the production of short-run parts economically feasible, and of giving a fabricated part which is isotropic (Ref. 54). These basic advantages are not offered by conventional hot or cold pressing because of the complex tooling requirements and because of the non-uniform pressure distribution in a pressed powder arising from the inability of solid powders to transmit pressure uniformly. In addition, since powder particles are not deformed or worked during slip-casting, little or no nucleation should occur in a slip-cast part, and continuous grain growth should be favored during sintering; (Ref. 55).

The basic advantages of the slip-casting techniques have prompted a number of workers to consider the extension of slip-casting to areas previously confined to powder metallurgy, and techniques have been presented for the slip-casting of cermets, oxides, carbides, borides, and silicides (Ref. 56, 57).

Unfortunately, until very recently, little attention has been given to the mechanisms involved in slip-casting, with the result that most investigators regard slip-casting as being difficult to control, affording poor tolerances, and giving low densities. However, with sufficient development, slip-casting systems can be refined to the point of not suffering from these disadvantages (Ref. 58, 59).

Slip-casting systems generally are capable of producing green densities only up to about 70 per cent of theoretical. As a result, sintering of the cast compacts to acceptable densities causes large amounts of shrinkage. The fused silica slip studied at Georgia Tech is a notable exception, giving green densities of about 83 per cent of theoretical (Ref. 6).

The microstructure and mechanical properties of a slip-cast body may depend on the orientation of particles during casting (Ref. 60). In addition, slip-casting like other wet processing methods encounters problems during drying. Large sections require close drying control over a long period of time to prevent cracking.

The limitations on the size of a slip-cast component must be related to the total processing rather than to the casting operation alone. The properties of a green shape may limit its size. For example, the green compressive strength must be high enough for the shape to support its own weight. In addition, many ceramic materials lose strength during the early stages of heat treatment, and handling problems are then increased.

Another limitation on size is the availability of large heat treating equipment. In the production of a 4 foot fused silica radome at Georgia Tech, a special furnace had to be devised to meet the requirements for maturation (Ref. 61). The problem of the large furnace would have been confounded if a high temperature or a controlled atmosphere had been required.

6.1.2 Dry pressing

The dry pressing method provides an economical technique for the production of small, precision parts. Once the die has been made and the pressing conditions established, uniform and consistently accurate parts can be produced without machining.

Dry pressing is accomplished with the aid of binders which provide strength during the early stages of heat treatment. Moisture contents generally vary from 2 to 5 per cent. Sintered densities range from 80 to 90 per cent of theoretical, and maximum strengths are therefore not possible. Attempts to improve the strength by higher firing or by the introduction of impurities usually, if not always, result in substantial grain growth.

The heavy equipment requirements for dry pressing have precluded the production of large shapes. Finished shapes to date have been limited in cross section to about one square foot and in thickness to about 4 inches.

6.1.3 Isostatic pressing

The isostatic process allows the production of large and complex shapes with highly uniform texture. Small additions of binder are used, but moisture is not required. Sintered densities range from about 80 to 95 per cent of theoretical, and shrinkage is uniform, preferred orientation is minimal, and die costs are low.

At the present state-of-the-art, the process seems to be limited only by the lack of experience and ingenuity of the tooling designer. The dimensional accuracy of surfaces pressed against rubber are on the order of a few per cent, but surfaces pressed against metal usually require no machining. However, the use of rigid members causes departures from a true isostatic state (Ref. 62).

6.1.4 Vibratory compaction

In this process, the particles are agitated under a slight restraint to promote close packing. Compaction is accomplished without the use of binders, and densities of 90 per cent of theoretical have been obtained (Ref. 63). However, particle size distribution has a considerable influence on the density (Ref. 64).

6.1.5 Extrusion

This process is limited to shapes of regular cross section. Diameters have been limited to a few inches for non-clay ceramics, and the need

for plasticizers in non-clay ceramic powders leads to final compositions that are invariably complex.

6.2 Hot Forming

Hot forming methods have, in general, been generated by the application of heat to cold forming counterparts: they involve the simultaneous application of heat and pressure to densify and shape ceramic compacts. Their major benefit is to offer a closer approach to theoretical density and to allow a closer control over microstructure. The methods are unique in that they allow many powders to be formed into high density shapes without prior particle treatment and without extensive experimental study. Oxides, borides, nitrides, and carbides have been successfully hot pressed.

6.2.1 Uniaxial hot pressing

Graphite is the most common die material used and is operative up to 4500° F and 10,000 psi. Induction heating is usually employed because of the high temperature obtainable; however, this technique does not allow close control over heating and cooling rates and does not provide temperature uniformity. Below 3900° F, graphite must be used in an inert atmosphere or vacuum. Above 3900° F, an inert atmosphere must be used. With oxide dies and in some cases, with graphite dies, radiated heat from resistance heating elements has been used. Heating by radiation has allowed closer temperature control, but has limited the operating temperature to about 3200° F. Carbides, borides, and alloys have also been used as die materials.

Density variations are found in materials formed by uniaxial hot pressing as the result of pressure gradients that exist in the material during the pressing operation. As the size of the shape is increased, the problem of pressure gradients is expected to become more important. To minimize the effects of pressure gradients, length-to-diameter ratios are usually held below 4 to 1. Uniformity has not been thoroughly studied, but grain size is known to have varied from 10 microns at the center to about 100 microns at the edge in one large shape. Pressed shapes have been limited to about one foot in diameter and one foot in length.

6.2.2 Biaxial hot pressing

Biaxial hot pressing has been attempted, but has not provided any real gain over its uniaxial counterpart.

6.2.3 Hot isostatic pressing

Hot isostatic pressing offers the potential of allowing the fabrication of large and complex shapes with uniform texture, closely controlled microstructure, and high density. Hence, it provides one of the most exciting areas for future research. Current interest is in using a solid or a gas as the transmissive medium. The method has been applied to ceramics and to composite systems containing ceramics.

6.2.4 Hot extrusion

Hot extrusion has been greatly limited by a lack of suitable high temperature dies and by an inadequate control of the rheology.

6.3 Other Forming Methods

6.3.1 Nucleation

The controlled crystallization in glass materials has led to the obtainment of extremely fine polycrystalline materials, the so-called glass-ceramics. These materials have been found to be relatively insensitive to surface damage and to exhibit high strength with good reproducibility. In addition, the fine microstructure in these materials is capable of tolerating the anisotropic thermal expansion typical of low expansion crystals and thus allows low thermal expansion ceramics to be achieved. Unfortunately, available glass-ceramics soften below 2000° F and are limited in long-term use to about 1500° F. Close tolerances can be obtained with glass-ceramics without machining.

6.3.2 Melt spraying

Melt spraying has been successfully used to coat various materials and to produce free standing ceramic shapes. While coating thickness is limited, shapes of almost any configuration can be coated. Edges and corners, however, continue to be a problem. Free standing forms have been limited to thin-walled shapes with axial symmetry.

Particles less than 5 microns in size are difficult to feed into an arc or flame so that a grain size smaller than 5 microns is not easily obtained. The grains are usually flat. Residence times are not, in general, long enough for phase changes to occur, and the particles and the substrate (or the particles alone in the case of a multicomponent feed) are seldom given the opportunity to react. Typical densities range from 83 to 99 per cent of theoretical, and deposition efficiencies vary between 15 and 95 per cent.

6.3.3 Foamed ceramics

The major techniques that have been used to produce light weight ceramics include: burnout of additives, chemical reaction, chemical decomposition, sublimation, air incorporation by agitation, bloating, and cementation of preformed spheres. Materials which have been produced as foams include: silicon carbide, alumina, zirconia, fused silica, and Pyroceram[®] (Ref. 65). Size limitations depend to a large extent on the foaming method employed. Massive blocks are commercially available in a few cases, and the blocks can be machined to most any shape desired. However, the foams are friable, and special machining techniques might be required if tolerances are close (Ref. 66).

6.3.4 Molding

A wide variety of sizes and shapes can be produced by the bulk

placement of material. Large structures may be possible if the material is placed in sections to avoid thermal rupture during the cure.

6.4 Machining and Grinding

Machining and grinding are generally used to produce dimensional accuracy, complex designs, or specific surface textures which cannot be provided by any other forming technique. Whenever possible, machining and grinding operations are carried out before final heat treatment.

6.4.1 Abrasive grinding

The usual choice for an abrasive is silicon carbide. However, diamond abrasives are required for very hard ceramics. The removal of ceramic material is generally slow and expensive. The removal of more than 0.015-inch of material in a single pass is unusual. The presence of phases with different degrees of hardness and the occurrence of pores can prevent the obtainment of a good finish. Exterior surfaces present no serious problems, but the grinding of internal surfaces is difficult if the length-to-area of cross section ratio is large.

6.4.2 Ultrasonic machining

Ultrasonic machining is usually employed when abrasive grinding is unsuitable. Basically, the technique uses a tool which is simply the reverse image of the impression desired. The tool is lightly pressed against the ceramic with an alternating motion while an abrasive slurry is circulated between the tool and the ceramic. The machined part is always slightly oversize relative to the tool. Dimensions can be held to about 0.002-inch with 200 mesh abrasive grain. However, tolerances as close as 0.0005-inch have been met by using finer abrasives.

6.5 General References on Ceramic Forming Processes

The most recent publication which permits a broad concept of the present state-of-the-art is Technical Documentary Report No. RTD-TDR-63-4069, "Critical Compilation of Ceramic Forming Methods," (Ref. 67). References 54, 65, 68, and 69 also contain extensive information on ceramic forming methods. For recent foreign publications in the area of ceramic forming, the reader is referred to Extended Abstracts 1 and 2 of Appendix I.

VII. PROPERTIES OF CERAMIC MATERIALS

The properties of ceramic materials tend to favor extremes. Their melting points are high, their densities and their thermal expansion coefficients are relatively low, they are highly resistant to corrosion at most temperatures, and they offer the advantage of high-temperature strength and high resistance to creep. Because of these reasons, because there is an abundant supply and a wide occurrence of ceramic raw materials, and because many ceramics have unique electrical properties and resist oxidation, ceramic materials offer many exciting possibilities for aerospace structures.

The properties of ceramic materials are briefly discussed in the sections which follow. Properties of interest to the aerospace engineer are considered, and the discussion is limited to areas where significant design data are available. In some cases, methods used to predict property values are cited. Such methods allow estimates of the properties of a materials system to be made on the basis of the properties of the individual constituents in the system. However, the methods are generally based on simple models and should be used only in the absence of experimental data.

7.1 Physical Properties

7.1.1 Refractoriness

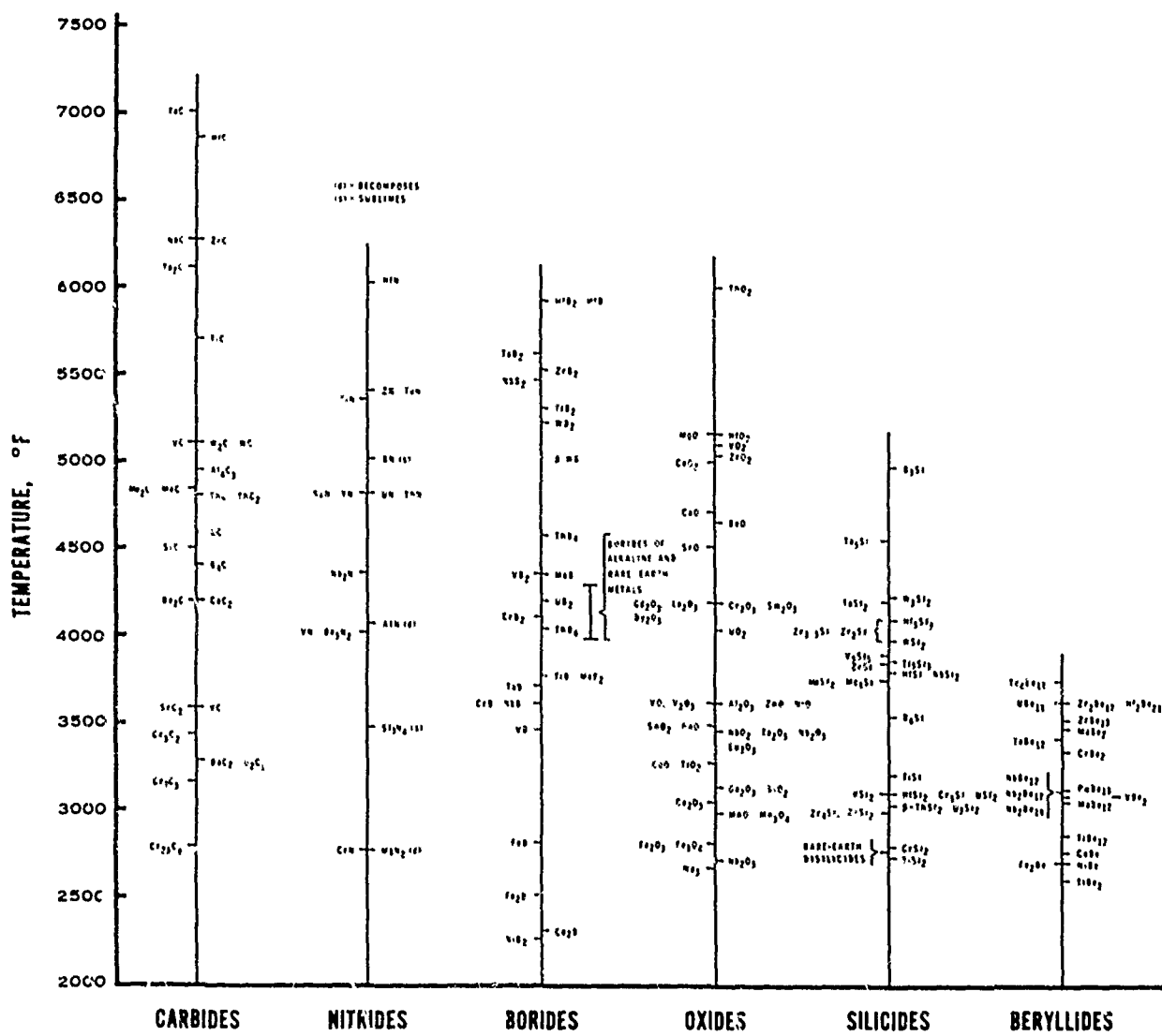
The melting or decomposition temperatures of selected refractory ceramics are given in Figure 9. The refractory ceramics start to melt at a temperature above 3000° F. The highest melting point reported is 7090° F for the complex carbide 4TaC:Hfc (Ref. 70).

While the melting point of a ceramic material serves as a index of the material's usefulness at high temperatures, it can be very misleading. Many ceramics become unstable at temperatures below their melting point, and their selection must be based on their maximum use temperature in a specified medium. Conversely, certain materials may be used for short times at temperatures well above the melting or decomposition point. Ablative plastics and fused silica are examples. For load-bearing applications the strength of the material at specified temperature levels must also be considered (Ref. 20).

7.1.2 Hardness

Because of its empirical nature, hardness information can seldom be correlated to service use. However, hardness measurements can serve as a guide in materials selection.

Most hardness tests for ceramics measure the resistance to wear or indentation. Although scratch tests are seldom used, it has been observed that most ceramics fall between 7 to 9-1/2 on the Mohs hardness scale. The Rockwell and Brinell tests cannot be used because large indenters under high loads cause ceramic materials to fracture in tension near the point of contact. However, a microhardness test using a small diamond indenter under a light



REFERENCE INDIVIDUAL BAR CHARTS OBTAINED FROM RTD-TDR-63-4102
 REFRACTORY CERAMICS OF INTEREST IN AEROSPACE STRUCTURAL APPLICATIONS - A MATERIALS SELECTION
 HANDBOOK, OCTOBER 1963

COMPILED AND PREPARED BY B R EMRICH, MATERIALS INFORMATION BRANCH, (MAAM), A.F. MATERIALS
 LABORATORY, WPAFB, OHIO 45433

Figure 9. Melting or Decomposition Temperatures of Selected Refractory Ceramics.

load is quite satisfactory, and loads in the range of 25 to 500 grams give permanent impressions from 10 to 100 microns in diameter without causing fracture. The 136° diamond pyramid (Vickers indenter) or the Knoop indenter are the usual choice, and results are expressed in terms of load divided by the area of the indentation. Commercial microhardness instruments are available (Ref. 35).

7.2 Elastic Properties

7.2.1 Elastic modulus

For ceramic materials, the modulus of elasticity or Young's modulus ranges from about 3×10^6 to 60×10^6 psi at room temperature and remains essentially constant for a given material up to about 1600° F.* In this temperature range ceramic materials generally obey Hooke's law up to the point of fracture. At elevated temperature (often beginning at a temperature equal to about two-thirds of the melting point), plastic flow becomes appreciable.

Elastic moduli are measured either statically or dynamically. The measurement under static conditions gives values for the isothermal moduli, while adiabatic moduli are obtained by the sonic or ultrasonic techniques. Indications are that the adiabatic and isothermal values do not differ by more than a few per cent. However, at sonic frequencies and above, there is not enough time between cycles to allow relaxation by creep, and the sonic measurements give an unrelaxed value which always exceeds the static or relaxed value (Ref. 71).

7.2.1.1 Effect of porosity: Spriggs (Ref. 72) suggested an empirical expression for the effect of porosity on the elastic modulus of polycrystalline refractory materials of the form:

$$E = E_0 e^{-b P} \quad (6)$$

where

E = elastic modulus of porous material

E_0 = elastic modulus of nonporous material

b = an empirical constant

P = volume fraction of pores.

*This is not true however for a number of amorphous materials which show a steady increase in modulus with increasing temperature.

Data on alumina from various investigations showed that b varied from 2.4 to 4.4 with an average value of about 4.0 (Ref. 72,73).

Spriggs (Ref. 74) later proposed that the combined effect of open and closed pores could be taken into account by a modification of the equation originally presented:

$$E = E_0 e^{-b_o P_o - b_c P_c} \quad (7)$$

where

b_o, b_c = empirical constants

P_o = volume fraction of open pores

P_c = volume fraction of closed pores.

Data on alumina with induced porosity suggested that slightly better fits could be obtained with the modified equation.

Hasselman (Ref. 75) noted that Spriggs' original expression (Equation 6) did not satisfy the boundary condition: $E = 0$ for $P = 1$. To remove this discrepancy, Hasselman proposed an equation of a different form based on a general equation given by Hashin (Ref. 76):

$$E = E_0 \left[1 - \frac{AP}{1 + (A-1)P} \right] \quad (8)$$

where

A = a constant.

Hasselman's equation for the assessment of both open and closed pores (Ref. 77) becomes:

$$E = E_0 \left[1 - \frac{A_o P_o}{1 + (A_o - 1)P} - \frac{A_c P_c}{1 + (A_c - 1)P} \right] \quad (9)$$

Hasselman and Fulrath (Ref. 78) fitted experimental data on glass containing small fractions of spherical pores with an expression of the form:

$$E = E_0 (1 - bP) \quad (10)$$

In this case the theoretical value of b could be calculated from the equation:

$$b = \frac{3(9 + 5\mu_0)(1 - \mu_0)}{2(7 - 5\mu_0)} \quad (11)$$

where

μ_0 = Poisson's ratio of nonporous material

The experimental value b (2.06 ± 0.06) compared favorably with the theoretical value of 2.00 for $\mu_0 = 0.20$.

Fryxell and Chandler (Ref. 59) fitted dynamic elasticity data on two grades of extruded MgO with expressions of the form given in Equations 6, 8, and 10. The porosity of the test specimens ranged from about 2 to 17 per cent. In this range the experimental data did not really distinguish among the three forms. It appeared that the linear equation would describe data well enough for most practical purposes up to a porosity of about 17 per cent and that Equation 6 and Equation 8 would give essentially identical results up to a porosity of nearly 40 per cent.

A recent investigation at the Cornell Aeronautical Laboratory (Ref. 71) has indicated that Young's modulus may be predicted with small error for composite bodies which remain continuous solids by a method developed by Kerner (Ref. 80). For porous media, based on Kerner's expressions Young's modulus is given by the equation:

$$E = \frac{G_0 (1-P)}{\frac{G_0}{E_0} + \frac{2P}{3} - \frac{P}{4}} \quad (12)$$

where

G_0 = shear modulus of nonporous material

Z = a constant

The constant Z can be evaluated for spherical pores as follows:

$$Z = \frac{5(3K_0 + 4G_0)}{(9K_0 + 8G_0)} \quad (13)$$

where

K_0 = bulk modulus of nonporous material.

The value of Z has been found to be approximately two for many ceramic materials.

7.2.1.2 Heterogeneous materials: Generally, equations are developed for predicting the shear and bulk moduli. Young's modulus is then calculated from the relation.

$$\frac{3}{E} = \frac{1}{3K} + \frac{1}{G} \quad (14)$$

where

G = shear modulus

K = bulk modulus

The assumptions inherent in Equation 14 are that the material is isotropic and that no phase changes occur.

7.2.2 Shear modulus

The shear modulus or modulus of rigidity of a ceramic is measured by subjecting specimens of circular cross section to a twisting moment and

observing the angular twist or by using dynamic techniques. Torsional resonance methods are easily adapted to high-temperature work, but few results have been reported.

7.2.2.1 Effect of porosity: Spriggs and Brissette (Ref. 81) suggested that the shear modulus of a refractory oxide could be related to the porosity by a simple exponential equation of the type:

$$G = G_0 e^{-bP} \quad (15)$$

Good fits to an equation of this form have been obtained with data on alumina (Ref. 81) and magnesia (Ref. 82).

Mackenzie (Ref. 83) derived an expression for the shear modulus of a solid containing isolated, spherical pores:

$$G = G_0 (1 - ZP) \quad (16)$$

where Z is given by Equation 13. Reasonable experimental verification of Mackenzie's formula has been provided by Hasselman and Fulrath (Ref. 78).

Coble and Kingery (Ref. 84) have suggested that Mackenzie's expression be extended to:

$$G = G_0 (1 - ZP + Z' P^2) \quad (17)$$

where the constant Z' may be evaluated by setting $G = 0$ when $P = 1$.

7.2.2.2 Heterogeneous materials: Kerner (Ref. 80) derived the following expression for the shear modulus of a heterogeneous material:

$$G = G_1 \left[\frac{\sum_{i=2} \frac{G_i v_i}{(7 - 5\mu_i) G_1 + (8 - 10\mu_i) G_i} + \frac{v_1}{15(1-\mu_1)}}{\sum_{i=2} \frac{G_i v_i}{(7 - 5\mu_i) + (8 - 10\mu_i) G_i} + \frac{v_1}{15(1-\mu_1)}} \right] \quad (18)$$

where the subscript 1 refers to the matrix material and v_i is the volume fraction of the i th phase. The expression has been applied to ceramic bodies in a recent study at the Cornell Aeronautical Laboratory (Ref. 71).

Hashin (Ref. 76) developed bounds for the elastic moduli of nonhomogeneous systems based on a concentric-spheres model. An approximation for the shear modulus was presented in the form:

$$\frac{G}{G_m} = 1 + \frac{15(1 - \mu_m)}{7 - 5\mu_m + 2(4 - 5\mu_m)} \frac{\left(\frac{G_d}{G_m} - 1\right) v_d}{\left[\frac{G_d}{G_m} - \left(\frac{G_d}{G_m} - 1\right) v_d\right]} \quad (19)$$

where the subscript m refers to the matrix, d refers to the dispersed phase, and v_d is the volume fraction of the dispersed phase. Hashin also developed approximate bounds for the shear modulus, but a discussion of these is beyond the scope of this report.

Hashin's method has been applied in at least one recent study. Hasselman and Shaffer (Ref. 84) used the method in an attempt to determine the effect of graphite inclusions on the properties of zirconium carbide. A good correlation was obtained using Hashin's lower bound.

7.2.3 Bulk modulus

The difficulties associated with the observation of volume contraction have generally prohibited the generation of direct experimental data. Indirect experimental data are usually obtained using Equation 14 or the following equation which is strictly valid only for isotropic materials.

$$K = \frac{E}{2(1-2\mu)} \quad (20)$$

7.2.3.1 Effect of porosity: While the bulk modulus is difficult to measure experimentally, it is amiable to theoretical studies. Mackenzie's expression (Ref. 83) for the bulk modulus for solids with spherical isolated pores is of the form:

$$K = \frac{4K_0 G_0 (1 - P)}{4G_0 + 3K_0 P} \quad (21)$$

7.2.3.2 Heterogeneous materials: Hashin's approximation (Ref. 76) for the bulk modulus of a two phase nonhomogeneous material is of the form:

$$K = K_m + (K_d - K_m) \frac{(4 G_m + 3 K_m) v_d}{4 G_m + 3 K_d + 3 (K_m - K_d) v_d} \quad (22)$$

Kerner's formula for bulk modulus (Ref. 80) has been extended to the case of porous multiple-phase ceramic bodies (Ref. 71). The extension led to an equation of the form:

$$K = \frac{\frac{K_m v_m}{3 K_m + 4 G_m} + \frac{K_d v_d}{3 K_d + 4 G_m}}{\frac{v_m}{3 K_m + 4 G_m} + \frac{v_d}{3 K_d + 4 G_m} + \frac{v_p}{4 G_m}} \quad (23)$$

7.2.4 Poisson's ratio

Poisson's ratio is measured at room and moderate temperatures using strain gages. However, considerable difficulty is encountered because at these temperatures ceramics will tolerate only a small amount of strain. Resonance methods can often be used at higher temperatures, but iterative techniques are required.

Although the data on Poisson's ratio is limited, it has been observed that Poisson's ratio ranges from 0.10 to 0.30 for many ceramic materials. One would expect Poisson's ratio to remain relatively constant up to about 1600° F. As the temperature is increased above the point where plastic deformation occurs, Poisson's ratio should gradually increase approaching 0.5 at the melting point.

Poisson's ratio is often calculated using the equation:

$$\mu = \frac{E}{2G} - 1 \quad (24)$$

However, it is obvious from the form of the equation that rather precise modulus data are required for a good estimation. While the equation applies to only isotropic bodies, reasonable estimates are expected if anisotropy is confined to small crystals randomly oriented (Ref. 79).

The dependence of Poisson's ratio on porosity can be predicted with the aid of Equation 24. For example, Spriggs and Brissette (Ref. 81) used the relationship given by Equation 24 and simple exponential expressions for the elastic and shear moduli (Equations 6 and 15) to derive an approximation of the type:

$$\mu = \mu_0 - bP \quad (25)$$

An excellent fit was obtained for a set of data on cold-pressed and sintered alumina.

7.3 Strength

7.3.1 Tensile strength

The tensile test is not usually carried out on ceramic materials because of the extreme care that is required to insure true axial loading. Uncontrolled eccentricity resulting from slight misalignment or from unsymmetrical specimen dimensions can lead to large extraneous stresses during the test. Recent developments, however, indicate that the use of a gas bearing support system can lead to significant improvements. One gas bearing facility has produced tensile strength data which were at least 1.3 times higher than those previously reported for the same materials (Ref. 85).

Recognition of the problems associated with the "uniaxial" tensile test has led to the development of a number of indirect methods which minimize restraint and multiaxial stress. Two of these are the internally pressurized ring test used at the Stanford Research Institute (Ref. 86) and the diametral-compression test (Ref. 87).

In the studies at the Stanford Research Institute the tensile strength of a commercial, high alumina body was investigated by using hydraulically expanded cylindrical test specimens. The values of the ultimate tensile strength obtained were higher than tensile strength values previously reported in the literature and approached flexural values. The most important aspect of the data, however, was that a low scatter of results was observed. The maximum (coefficient of) variation of strengths within single groups of specimens was less than 7.6 per cent. This value compares favorably with the value of 10 or more normally associated with flexural strength data.

The diametral-compression test is gaining increasing favor because it provides an experimentally simple method for measuring tensile strengths. An important feature of the test is that it allows the maximum tensile stresses to be produced within the body of a material, rather than at the surface.

7.3.2 Flexural strength

The flexural strength is usually determined by bending a bar or rod of simple shape to the point of fracture. The maximum tensile stress at

fracture is computed from the fracture loads, and this maximum stress is referred to as the flexural strength or the modulus of rupture. The specimen is laid across two supports and a concentrated load is applied at the center, or two concentrated loads are symmetrically placed between the supports, to cause fracture. It is assumed that the material is homogenous and obeys Hooke's law up to the point of fracture, and the calculations are based on the equation for pure bending:

$$\sigma = \frac{Mc}{I} \quad (26)$$

where

σ = maximum tensile stress

c = distance from the neutral axis of the specimen to the fiber under maximum tensile stress

M = bending moment at the point of fracture

I = moment of inertia of the cross section about the neutral axis

When corrections are made for wedging (Ref. 42) center-point loading data and four-point loading data can be compared and different thickness-to-span ratios can be taken into account. For large thickness-to-span ratios the data should be corrected for frictional restraint.

Because of its simplicity, the bend test has been the most widely used method for determining the strength of ceramic materials, and a number of authorities consider it to be the most reliable test for obtaining design stresses. However, surface conditions must be closely controlled, and care must be taken to prevent torsional loading.

7.3.3 Compressive strength

It is not possible to obtain the true compressive strength of a ceramic material by the usual method of applying a unidirectional compressive load to a portion of a test specimen. Failure will occur as the result of tensile stresses which are induced in the material during the test. It has been predicted that tensile stresses reach a maximum of one-eighth the applied pressure at the tip of microcracks oriented 30° to the direction of the compression (Ref. 31).

Data on the compressive strength of ceramic materials is limited. However, ceramics are invariably stronger in compression than in tension. The compressive strengths are often higher than the tensile strengths reported for same material by a factor of 6 to 10, although factors ranging from 4 to 5 are reported for some amorphous materials.

7.3.4 Impact strength

Impact strength has not been precisely defined, but, generally speaking, it is the resistance to fracture under a dynamic load which is suddenly applied. While most impact tests were developed to simulate service conditions, there have been few attempts if any to correlate the measured impact strength of a ceramic material with its performance in service.

A number of investigators have suggested that a close relationship exists between the impact strength and the flexural strength of a ceramic material. Kliman (Ref. 88) investigated the effects of fiber content on alumina fiber-ceramic composites and found that the variation of impact strength was similar to that for transverse rupture strength. On the premise that most ceramics fail at a strain between 0.10 and 0.15 per cent Dinsdale, et al, predicted an approximate linear relationship between the impact strength and the modulus of rupture (Ref. 89). Phillips and DiVita (Ref. 90) reported that accumulated data on commercial ceramics indicate that materials such as alumina, steatite, zircon, wollastonite, and borosilicate glass behave very similarly in respect to impact strength in spite of their differences in composition and structure.

In the work discussed by Phillips and DiVita, polycrystalline ceramics and glass were impact tested by the incremental drop method using specimens in the form of cylindrical rods 6 in. long and 1/2-in. in diameter. The flexural strength of the cylindrical rods was measured using three-point loading, a 4-in. span, and a stressing rate of 10,000 psi per minute. The average value for the impact strength-to-flexural strength ratio for 9 materials was 1.81 ± 0.09 .

7.3.5 Porosity and grain size effects

7.3.5.1 Porosity effects: An empirical expression which has met considerable success in fitting strength-porosity data has the form:

$$S = S_0 e^{-bP} \quad (27)$$

where

S = strength of porous material

S_0 = strength of nonporous material

However, not all of the available data are in agreement. In some instances a linear relationship provides a better fit.

Wilcox (Ref. 91) considered the strength-porosity data of ceramic materials during the initial stage of sintering and found that the data fit a semi theoretical expression of the type:

$$S = \frac{P_i - P}{A(1-P)} \quad (28)$$

where

P_i = porosity prior to any densification due to sintering

A = a constant

Hasselman (Ref. 92) considered polycrystalline materials for which the porosity effect on strength and Young's modulus could be closely approximated using linear expressions:

$$S = S_0(1 - bAP) \quad (29)$$

$$E = E_0(1 - AP) \quad (30)$$

Hasselman predicted that the value of the constant b would be unity for pores in the form of long circular cylinders parallel to the applied stress, approximately 1.28 for long cylinders perpendicular to the applied stress, and approximately 1.5 for pores with an average shape approximately spherical. A comparison of the modulus of rupture and Young's modulus for several materials showed that the value of b ranged from 1.4 to 1.5. The same procedure applied to data on alumina expressed in exponential form produced values from 1.5 to 1.6.

7.3.5.2 Grain size effects: The exponential relation given by Knudsen (Ref. 93) is the most widely used expression for predicting the effect of grain size on the strength of a ceramic material:

$$S = AG^{-n} \quad (31)$$

where

G = grain size

A, a = empirical constants

A value of $a = 1/2$ is predicted by Griffith's equation (Ref. 39) if the most severe microcrack is equal to the grain size. However, a value of $1/3$ has been reported for alumina and magnesia, a value of 0.4 for thoria, and a value of 0.55 for chromium carbide (Ref. 32).

In a recent study by Spriggs, Mitchell, and Vasilos (Ref. 94) the elastic modulus and modulus of rupture of pure, dense alumina were determined as a function of grain size (1 to 250 microns) over the temperature range 86° to 2732° F. The room temperature modulus of rupture data agreed closely with Knudsen's equation for $a = 1/3$. The strength of the fine-grain material continued to be substantially higher than that of the coarse-grain material up to 2732° F. However, the grain-size dependence was significantly lessened above 1832° F. Other noteworthy observations were that the 1 to 2 micron material exhibited considerable yielding and nonlinear load-deflection behavior above 1832° F and that grain size appeared to have no effect on Young's modulus over the entire temperature range studied.

7.3.5.3 Combined effects: Knudsen's equation (Ref. 93) is generally used to predict the combined effects of porosity and grain size:

$$S = A G^{-a} e^{-bP} \quad (32)$$

Fryxell and Chandler (Ref. 79) analyzed modulus of rupture data on beryllia and magnesia in terms of Knudsen's equation. The grain size ranged from 10 to 100 microns, the porosity ranged from 1 to 15 per cent, and the temperature range 78° to 2192° F was investigated. The dependence on grain size decreased as the temperature increased ($a = 0.35$ to $a = 0.11$ for magnesia, and $a = 0.50$ to $a = 0.03$ for beryllia). The porosity coefficients remained fairly constant ($b \approx 2.5$ for both materials), but there was considerable scatter.

7.4 Notch Sensitivity

Most researchers view ceramic materials as being highly sensitive to notches. The usual argument given in support of this view is that ceramics are brittle, and plastic deformation does not take place in a brittle material, and stress concentrations at the tip of a notch can not be relieved in the absence of plastic flow. While the argument seems plausible, it is apparently based on little experimental evidence because few data are available on the notch sensitivity of refractory ceramic materials. It is known that glasses are highly sensitive to surface scratches, and perhaps the knowledge of this fact has influenced the opinion of some.

A few investigators have presented data which support the opposite view. For example, in a recent study at the Stanford Research Institute (Ref. 95) it was found that the introduction of notches in a dense magnesia body caused no appreciable change in its behavior under thermal stress conditions. In another recent study, at Syracuse University (Ref. 96), external notches artificially introduced in alumina and in glass-bonded mica had a rather mild effect on the notch strength. In the latter study it was suggested that ceramics should be relatively insensitive to notches because they already contain stress raisers, some of which are of the order of magnitude of those that can be artificially induced.

It appears, then, that the notch sensitivity of a brittle material will depend upon the size of the flaws that already exist in the material. The introduction of a notch no "larger" than the material flaws already present would not be expected to influence the material's performance. However, the possibility of interactions between notches or between a notch and the material flaws should not be overlooked. While a single scratch might be detrimental to a polished surface, a great number of scratches might have little effect and may even serve to relieve stress or to distribute it more uniformly.

7.5 Thermal Properties

7.5.1 Thermal expansion

While the thermal expansion of refractory ceramic materials is relatively low, it varies considerably from one ceramic material to another, and it exerts the most important influence on the thermal shock behavior. For example, the expansion coefficient of fused silica is so low that it is essentially incapable of failure under pure thermal shock in spite of its low strength. On the other hand alumina has been known to fracture under a pure thermal shock of less than 200° F in spite of its high mechanical strength.

The thermal expansion of a ceramic can be measured with a fair degree reliability. The expansion is not noticeably effected by small amounts of impurity or by changes in grain size or fabrication techniques, but may be affected by the atmosphere in which the expansion test is conducted (Ref. 97).

A crude approximation for the thermal expansion of a mixture is obtained by volume-averaging the thermal expansion of each phase present. The method should only be used as a last resort.

An extensive investigation of the aspects of the thermal expansion of ceramic materials was conducted at the Cornell Aeronautical Laboratory (Ref. 71). A brief report on the knowledge gained in that investigation follows.

A reliable estimate of the thermal expansion of a mixture requires a knowledge of the elastic properties of the end members. The elastic moduli which should be used are those for the fully-dense polycrystalline material. A greater validity of Kerner's method over Turner's method has been demonstrated.

Turner's Method:

$$\alpha = \frac{\sum_{i \geq 1} \alpha_i E_i v_i}{\sum_{i \geq 1} E_i v_i} \quad (33)$$

Kerner's Method:

$$\alpha = \left(\frac{4G_0}{K_0} + 3 \right) \sum_{i \geq 2} \frac{\alpha_i v_i}{\frac{4G_0}{K_1} + 3} \quad (34)$$

$$G_0 = G_1 \left[\frac{\sum_{i=2} \frac{G_1 v_i}{(7 - 5\mu_1) G_1 + (8 - 10\mu_1) G_1} + \frac{v_1}{15(1-\mu_1)}}{\sum_{i=2} \frac{G_1 v_i}{(7 - 5\mu_1) G_1 + (8 - 10\mu_1) G_1} + \frac{v_1}{15(1-\mu_1)}} \right] \quad (35)$$

$$K_0 = \frac{\sum_{i=1} \frac{K_1 v_i}{3K_1 + 4G_1}}{\sum_{i=1} \frac{v_i}{3K_1 + 4G_1}} \quad (36)$$

where

α = linear thermal expansion coefficient.

7.5.2 Thermal conductivity

The thermal conductivity is the property capable of the largest variation in ceramic materials. The thermal conductivity exhibits a two-order-

of-magnitude variation between different materials or between different forms of a single material. When sizeable temperature variations are to be encountered in service, the designer should carefully consider the temperature dependence of this property.

The factors which may influence the thermal conductivity of a ceramic material include: the molecular structure of each phase, the total amount of each phase present, the distribution of the phases, impurities, the size and shape of pores and grain, the amount of porosity, the temperature, anisotropy and directional effects, and the emissivities of the grains.

At temperatures above the Debye temperature, phonon-phonon interaction by lattice vibration is the principal process for the conduction of heat in ceramics, and this is governed by the equation (Ref. 98):

$$k = 1/3 c v \lambda \quad (37)$$

where

k = thermal conductivity

c = specific heat

v = mean velocity or elastic wave velocity

λ = mean free path between interactions.

Any reduction in the mean free path of the phonons will cause an increase in the resistance and thereby lower the conductivity. For example, impurities which do not go into solid solution serve as centers for phonon scattering, and herein lies the reason that small amounts of impurities often greatly reduce the conductivity of polycrystalline materials. Since the mean path due to lattice scattering decreases with temperature, the effect of impurities is greatest at low temperatures (Ref. 99).

Since the mean velocity and specific heat are relatively independent of temperature while the mean path due to lattice scattering varies inversely with temperature, the thermal conductivity would be expected to vary inversely with temperature. The conductivity of polycrystalline ceramics usually varies in the following fashion:

$$k = \frac{a}{t} + b \quad (38)$$

where

t = temperature

a, b = constants

Above about 2200° F the inverse relationship can not be applied since radiant effects become important. The conductivity will take on a minimum value in the vicinity of 2700° F and then rise again at higher temperature (Ref. 98).

In amorphous materials the mean free path of the phonons is similar to the interatomic dimensions and cannot decrease as the temperature increases. In these materials the conductivity varies with temperature according to the variation in the specific heat. Thus for amorphous ceramics, the conductivity is low and may increase gradually with temperature up to the point where radiation effects become important. At low temperatures the variation can often be described by a linear relationship:

$$k = a t + b \quad (39)$$

Impurities which go into solid solution have a smaller effect on the conductivity than those which do not go into solid solution. However, if the amount of solute is increased to the point where it approaches the magnitude of the lattice dimensions, the conductivity will reach a minimum value of approximately $0.7 \text{ Btu/hr}\cdot\text{ft.}^{\circ}\text{F}$. This value, which is the approximate value of the conductivity for glasses at room temperature, should be the lower limit for the conductivity of any nonporous solid (Ref. 98).

7.5.2.1 Effect of grain size: Few investigations have generated dependable data on the grain size effects at or above room temperature. Indications are, however, that grain size will not affect the thermal conductivity of ceramics with an average grain size larger than 10 microns (Ref. 100).

In the study conducted at Alfred University (Ref. 100), the conductivity of a dense alumina was investigated in the temperature range 212° F to 1832° F as the average grain size was varied from 10 to 4 to 2 microns. At 212° F the conductivity was eight per cent higher for the 10 micron material than it was for the 2 micron material. This difference decreased slightly as the temperature was increased to 1832° F. At 212° F the relative conductivity closely followed a volume effect of the grain boundaries.

7.5.2.2 Heterogeneous materials, including pores: A number of investigators have considered the thermal conductivity of multiphase materials. The recent presentation by Brailsford and Major (Ref. 101) was favored during the preparation of the present section.

The electrical analogy rule can be used to develop expressions for the thermal conductivity of a laminate:

$$\frac{1}{k} = \frac{1 - v_1}{k_1} + \frac{v_1}{k_2} \quad (40)$$

$$k = (1 - v_1) k_2 + v_1 k_1 \quad (41)$$

These equations represent the thermal conductivity for laminae perpendicular to the flow of heat and laminae parallel to the flow of heat, respectively. Reasonable verification of the relationships has been obtained experimentally (Ref. 102). These expressions place a lower bound and an upper bound on the thermal conductivity of any two-phase system.

For mixtures, the expressions are usually based on the assumption of spherical inclusions in a continuous phase. For example, the thermal conductivity of a three-phase mixture would be:

$$k = \frac{\frac{k_m v_m + k_1 v_1}{(2 k_m + k_1)} + \frac{3 k_m}{(2 k_m + k_2)} v_2}{\frac{v_m + v_1}{(2 k_m + k_1)} + \frac{3 k_m}{(2 k_m + k_2)} v_2}$$

where the subscript m refers to the continuous phase and $v_m + v_1 + v_2 = 1$.

An expression for a random two-phase assembly can be obtained by setting $k_m = k$ in Equation 42 and solving for k (i.e., by assuming the continuous phase has a conductivity equal to the value of the conductivity of the two-phase assembly being considered):

$$k = (3v_1 - 1)k_1 + (3v_2 - 1)k_2 + \left[\left\{ (3v_1 - 1)k_1 + (3v_2 - 1)k_2 \right\}^2 + 8k_1 k_2 \right]^{1/2} \quad (43)$$

where $v_1 + v_2 = 1$.

7.5.2.3 Effect of particle (or pore) shape: Hamilton and Crosser (Ref. 103) proposed a semi theoretical expression for the thermal conductivity of a continuous phase containing particles of arbitrary shape:

$$k = k_m \left[\frac{k_d + (n-1) k_m - (n-1) v_d (k_m - k_d)}{k_d + (n-1) k_m + v_d (k_m - k_d)} \right] \quad (44)$$

For the case of spherical particles, a good fit was obtained by setting $n = 3$ as expected.

Expressions for particles in the shape of rods, platelets, or ellipsoids can be found in Reference 98.

7.5.2.4 Radiant effects: For dense, polycrystalline ceramics, radiant effects are found to be significant at temperatures above 2700° F. For translucent materials, radiant heat transfer begins at lower temperatures.

For porous materials, the effect of radiation across the pores can be taken into account using an equation developed by Loeb (Ref. 104,105):

$$k = k_0 (1 - p_x) + \frac{p_x}{\frac{p_y k_0}{4 \bar{\sigma} \epsilon \gamma t^3} + (1 - p_y)} \quad (45)$$

where

k_0 = thermal conductivity of nonporous material

p_x = cross-sectional pore fraction

p_y = longitudinal pore fraction

$\bar{\sigma}$ = Stephan's radiation constant

ϵ = total emissivity of solid surface

γ = geometrical pore factor (2/3 for spherical pores)

t = mean temperature

The radiation effect is not significant for pores smaller than 0.1 mm in diameter or for temperatures below 900° F. For pores larger than 1 mm in diameter, the radiation effect is considerable above 900° F and is greatly affected by the emissivity.

7.6 Fatigue

7.6.1 Cyclic fatigue

Very little work has been done on cyclic fatigue studies of ceramic materials. Williams (Ref. 106) found that the fatigue survival stress was approximately 0.57 of the single stroke bend strength for a commercial alumina. The fatigue survival stress for the alumina did not change significantly at temperatures up to 1650° F. Mizushima and Knapp (Ref. 107) studied the behavior of a whiteware ceramic under cyclic loading and found that its fatigue survival stress was about 0.80 of the single-stroke value.

7.6.2 Static fatigue

It is often observed that the measured strength of ceramics depend on the rate of stress application. Slower loading rates generally reduce the resistance to failure. However, the effect is very small, if not absent, at cryogenic temperatures, in high vacuum, or in inert atmospheres. The effect is most generally attributed to the presence of water vapor. Factors known to have an influence on the delayed fracture of ceramic materials include the temperature, atmosphere, surface condition, strain rate, and prior thermal history.

7.7 Creep

For applications involving high temperatures, the time-dependent deformation and failure characteristics of a ceramic must be known. At temperatures of about two-thirds of the melting point, some plastic flow sets in and deformation under load becomes an important factor. In addition, anisotropy, nonhomogeneity, and pores and other defects, which persist at all temperatures, often cause a loss in the creep strength at temperatures as low as one-half of the melting point. Thus there is no relationship between the creep characteristics and composition alone, and structural influences must be investigated.

Unfortunately, little creep data exist for refractory ceramic materials. Progress has been seriously hampered by the need for sophisticated test equipment. Attempts to adapt tensile creep testing techniques to brittle materials evaluation have met only limited success. However, flexural tests conducted at elevated temperatures should provide useful information on the creep properties of these materials.

7.8 Thermal Shock Resistance

With the call for ceramic materials in high performance vehicles and reentry situations, the problem of designing an effective ceramic structure has taken on a new dimension. In the past, ceramic structures were subjected to only moderate heat fluxes, and thermal shock effects were of a secondary nature. Today's aerospace systems encounter dreadful heat fluxes which impose severe thermal shock conditions on ceramic members. While the failures induced by these conditions appear to be simple in nature, the thermal-shock resistance of a ceramic is probably the most difficult property to measure and assess.

7.8.1 Definitions

7.8.1.1 Thermal stress: A thermal stress is generally defined as a stress which arises as the result of a temperature gradient or a temperature change. Thermal stresses are attributed to the thermal expansions of various parts of a body in which free expansion of each volume element cannot take place (Ref. 5). Thermal stresses in the absence of temperature gradients result from external restraints, differences in expansion between various phases, nonisotropic expansion of crystal grains, or from volume changes due to polymorphic transitions, devitrification processes, and chemical reactions.

7.8.1.2 Thermal stress resistance: Thermal stress resistance is the ability to withstand thermal stresses.

7.8.1.3 Thermal shock: A body is said to be subjected to thermal shock when transient temperature gradients are induced in it. Thus the occurrence of a thermal shock implies the existence of a temperature gradient, but the occurrence of a thermal stress does not. It seems likely that thermal stresses set up by temperature changes alone have contributed to the damage reported in many cases as thermal shock failure (Ref. 29).

7.8.1.4 Thermal shock resistance: The thermal shock resistance of a body is its resistance to deterioration or failure when subjected to thermal shock.

7.8.1.5 Thermal spalling: Thermal spalling is the breaking away of pieces of a shape or structure as the result of thermal stresses.

7.8.2 Test methods

There are perhaps as many thermal shock tests as those who have used them. In most tests a simple shape or a prototype design is subjected to a severe thermal environment which is selected on the basis of convenience or on the basis of anticipated service conditions. Thermal shock tests generally involve a rapid cooling technique, although rapid heating techniques are also used. In an effort to simulate service conditions, the following systems have been used (Ref. 42,108).

1. A hot gas test in which a gas stream is directed onto a specimen while the gas feed and distance are varied.
 - Natural gas-air
 - Natural gas-oxygen
 - Propane-oxygen
 - Acetylene-oxygen
 - Hydrogen-oxygen
2. A plasma arc test programmed to follow a desired time-temperature profile by control of the gas feed, power supply, and distance.
3. An arc-imaging furnace with variable focus, intensity, and distance.
4. A rocket motor test in which the distance and specimen orientation are varied to evaluate materials under severe thermal shock conditions.
5. A quartz lamps test to simulate aerodynamic heating on a desired configuration by variation of electrical power supply, distance, and surface reflectivity.
6. A furnace test programmed to follow a limited time-temperature profile by control of the amount and distribution of gas feed and residence time using a belt furnace, rotary furnace, or similar device.

When a rather crude screening test is desired, a specimen is often simply immersed in a hot or cold fluid or a hot or cold fluidized bed.

The thermal shock resistance of a material is usually determined by measuring the time required for fissures to form during a test cycle or by measuring the extent of damage or deterioration after one or more cycles. Measurements which have been made during a test cycle include:

1. Visual observations
2. Electrical resistance measurements on a conductive coating or on the test specimen itself.

Measurements which have been made on specimens before and after one or more cycles include:

1. Visual observations
2. Penetrant dye tests or fluorescent particle inspection
3. Permeability, specific weight, water uptake, and porosity
4. Strength

5. Modulus of elasticity, either by sonic methods, ultrasonic methods, or static methods.

Indications are that the sonic modulus test is superior to the strength test. The sonic modulus test is more sensitive to thermal shock damage and has provided the more reproducible data. The use of surface area measuring techniques to determine the effect of thermal shock has been suggested (Ref. 109). Such techniques should provide a sensitive method for determining the extent of damage in thermal-shock-tested or proof-tested ceramic bodies.

Recently, a number of research organizations have addressed themselves to the task of developing new methods for simulating the severe heat fluxes encountered in aerospace situations. Two of these are Space Technology Laboratories (Ref. 110) and General Dynamics/Pomona (Ref. 111).

At Space Technology Laboratories, a specimen in the form of a hollow right circular cylinder is used, and heating is accomplished using an electron beam heat source capable of delivering heat fluxes in excess of 10,000 Btu/ft²-sec. The major disadvantage of electron-beam heating appears to be its inability to cope with extraneous gases, and surgical cleanliness and high vacuum technology are required. Present experiments are designed to provide severe thermal transient environments which are realistic yet amiable to analysis.

At General Dynamics/Pomona hot metal baths are being used to simulate the aerodynamic heating associated with radome applications, or at least to simulate the thermal stresses involved in aerodynamic heating. The primary features of the testing facility consist of a test chamber, a cylinder of liquid metal, and a driving piston which forces liquid metal out of the cylinder and into the test chamber around a radome. The speed of the driving piston controls the liquid metal feed, and the local velocities are established by the chamber design. Heat transfer rates on the order of 350 to 700 Btu/ft²/sec. have been obtained using molten lead-bismuth baths. The baths can be operated over a temperature range of about 450° to 1400° F, and the lead-bismuth system remains a liquid up to about 3000° F. The disadvantages to the hot metal baths are:

1. Bath temperature determination is difficult.
2. The molten metal bath is a very corrosive environment.
3. There is a health hazard and a safety hazard.
4. There is more data scatter when the molten metal bath is used than there is when a hot salt bath is used.
5. It is difficult to tailor the system so that the desired heat flux will be obtained at various stations on the radome.

7.8.3 Factors affecting thermal shock resistance

The assessment of the thermal shock resistance of a brittle material entails three basic considerations: the temperature distribution in the material, the resultant stresses, and the strength of the materials. The temperature distribution depends on the thermal properties of the material, on the size and shape of the specimen, and on the net heat transfer between the specimen and its surroundings. The stresses resulting from a given temperature distribution depend on the thermal expansion and elastic properties of the material. The strength of a brittle material may depend on a multitude of factors, including the size of the specimen, the distribution of stress, the type of stress, and the rate of loading.

Thus the thermal shock resistance of a material is not an intrinsic material property but depends on complex interactions between the material properties and the environment. As a result, the thermal shock resistance of a material is not clearly defined and there is little hope for the establishment of a meaningful standardized thermal shock test. A number of investigators have attempted to circumvent this difficulty by rating a material relative to a given environment, but many deficiencies persist:

1. Experimental results are affected by subjective influences. The application should dictate whether or not a material has failed during a thermal shock test, yet this decision is generally left up to the investigator.
2. Test results depend on the method used to manufacture the specimen. For example, internal stresses induced during maturation can lead to a high scatter of thermal shock resistance values.
3. The material properties of interest usually vary appreciably with temperature, and exact analytical treatment is difficult if not impossible.

7.8.4 Thermal shock parameters

Because of the complexity of the thermal shock problem, a general solution is impossible. Each problem, however, need not require a completely independent treatment since similarities exist in thermal shock situations. Because of these similarities, a number of investigators have attempted to group material properties and environmental descriptors so that general principles could be applied.

The thermal shock behavior of a ceramic material in the form of a simple shape can be predicted under certain boundary conditions. Generally, these predictions are made under the assumptions that failure results from the effect of tensile stresses alone, that Hooke's law is obeyed up to the point of fracture, that the materials are isotropic and homogeneous, and that the material properties are independent of temperature.

Based on the assumptions listed above, theoretical considerations have led to an extended use of a number of thermal shock parameters. While these parameters cannot be applied with high reliability, several indications in the parameters are borne out by experience. Thus a parameter may serve as a screening method when the theoretical model resembles the actual service situation.

The five thermal shock parameters most frequently used are:

$$R^{(1)} = \frac{S}{E\alpha} \quad (46)$$

$$R^{(2)} = \frac{S(1-\mu)}{E\alpha} \quad (47)$$

$$R^{(3)} = \frac{Sk}{E\alpha} \quad (48)$$

$$R^{(4)} = \frac{Sk(1-\mu)}{E\alpha} \quad (49)$$

$$R^{(5)} = \frac{Sa(1-\mu)}{E\alpha} \quad (50)$$

where

R = thermal shock resistance index

S = strength

E = Young's modulus

α = linear thermal expansion coefficient

μ = Poisson's ratio

k = thermal conductivity

α = thermal diffusivity

and

$$\alpha = \frac{k}{\rho c} \quad (51)$$

where

c = specific heat.

The parameters $R^{(1)}$ and $R^{(2)}$ with dimensions of temperature have quantitative physical significance. The use of $R^{(1)}$ is suggested in the extreme case of heating a surface by an intensive point-source. Spot heating may occur to some extent in other thermal shock situations because of the non-homogeneity of ceramic materials (Ref. 112). The index $R^{(2)}$ is similar to $R^{(1)}$ but applies in the case where a large portion of the surface is rapidly heated or where a ceramic is completely restrained from expanding due to the design of a part. The index $R^{(2)}$ represents the maximum temperature variation which a material can tolerate without cracking, whatever the intensity of the thermal shock.

There are indications that the nonaxial heat flow per unit length required to fracture a hollow ceramic cylinder can be represented by the product of the index $R^{(3)}$ and a separate factor characterizing the shape of the cylinder (Ref. 113,114).

The parameters $R^{(2)}$, $R^{(4)}$, and $R^{(5)}$ were considered by Kingery (Ref. 5). For the steady-state case of a hollow right circular cylinder with infinite length and an interior heat source, the maximum temperature difference was expressed as the product of the index $R^{(2)}$ and a size factor, and the maximum allowable heat flow rate was represented by the product of $R^{(4)}$ and a size factor. For a plane slab heated or cooled in such a manner that its surface temperature changed at a constant rate, Kingery suggested that the maximum rate of temperature change without fracture could be represented by the product of $R^{(5)}$ and a size factor.

Manson (Ref. 4) considered the problem of a flat plate, initially at uniform temperature, suddenly immersed in a medium of lower temperature. Manson found that the theoretical response pattern could be closely fitted over the entire range of heat transfer coefficients using an equation of simple form:

$$\Delta T_{\max} \approx R^{(2)} (1.5 + 3.25 \frac{1}{\beta} - 0.5 e^{-16/\beta}) \quad (52)$$

where

ΔT = initial temperature of the plate less the temperature of the medium in which it is immersed.

β = Biot's modulus

and

$$\beta = \frac{ah}{k} \quad (53)$$

where

a = half thickness of the plate

h = heat transfer coefficient

k = thermal conductivity

Manson's expression provides a means of determining thermal shock parameters under various conditions. For thick plates or large heat transfer coefficients, the thermal conductivity has little influence and ΔT_{\max} is approximately equal to $R^{(2)}$. Thus, in the case of a large body or a rapid transfer of heat the surface of the body responds far more rapidly than the interior of the body, and there is almost complete restraint. For thin plates or low rates of heat transfer, thermal conductivity has a considerable influence and the tolerance varies directly as $R^{(4)}$. Thus a material with inherently poor thermal shock characteristics might tolerate severe thermal shock conditions if it is formed into a thin shape, or if it has a high thermal conductivity.

The major advantage to Manson's expression is that it provides a means of analysis for intermediate values of Biot's modulus. It also suggests that test conditions should closely simulate in-service conditions. This applies to the size and shape of the test piece and to the heat transfer rate. It is significant that Manson correctly predicted a reversal of merit index for alumina and teryllia when quenched in air and when quenched in water.

Because of its high thermal conductivity, beryllia was superior to alumina for mild quenching. However, with severe quenching alumina was superior because of its high strength.

Buessem (Ref. 115) extended the curve-fitting technique to a number of elementary shapes, initially at uniform temperature, suddenly subjected to a medium of a different temperature:

For a plate, with symmetrical cooling:

$$\Delta T_{\max} = R^{(2)} (1.5 + 3.25 \frac{1}{\beta}) \quad (54)$$

For a plate, with symmetrical heating:

$$\Delta T_{\max} = R^{(2)} (3.33 + 6 \frac{1}{\beta}) \quad (55)$$

For a plate, with asymmetrical cooling:

$$\Delta T_{\max} = R^{(2)} (1.5 + 9.6 \frac{1}{\beta}) \quad (56)$$

For a right circular cylinder, heating and cooling:

$$\Delta T_{\max} = R^{(2)} (2.0 + 4.3 \frac{1}{\beta}) \quad (57)$$

For a sphere, heating and cooling:

$$\Delta T_{\max} = R^{(2)} (2.5 + 5 \frac{1}{\beta}) \quad (58)$$

Buessem also listed the materials best suited for thermal-shock applications. For high heat-transfer rates, materials with a large $R^{(2)}$ value should be selected. For low heat-transfer rates, materials with a large $R^{(4)}$ value should be used.

The parameters $R^{(1)}$, $R^{(2)}$, $R^{(3)}$, $R^{(4)}$, and $R^{(5)}$ have a number of glaring deficiencies. They furnish only an approximate idea of the thermal shock

resistance of a material, they relate only to the appearance of fissures, and they cannot be applied to the problem of failure caused by repeated thermal shock cycles. However, these gaps have been partially bridged by the recent efforts of Hasselman and Shaffer (Ref. 84).

Hasselman and Shaffer introduced a "thermal shock damage resistance parameter" of the form:

$$R^{(6)} = \frac{E}{S^2 (1-\mu)} \quad (59)$$

If a material has a high $R^{(6)}$ value, a relatively small amount of elastic strain energy will be stored in the material at the onset of fracture. Thus only a relatively small amount of energy would be available to activate crack nucleation or to facilitate crack propagation once cracks are formed. The tendency toward crack nucleation and propagation will also depend, of course, on the manner in which the stored strain energy is released. In most metals stored strain energy can be converted into heat through plastic flow, and insufficient elastic energy remains for catastrophic fracture to occur. Thus the incorporation of metal fibers in a ceramic should lead to improved thermal shock resistance.

In a ceramic material essentially all stored strain energy is converted to surface energy and kinetic energy of broken pieces. Thus a ceramic material will have less tendency to fracture catastrophically if its effective surface energy is high. For ceramic materials the effective surface energy does not differ greatly from one material to the next. It follows, then, that $R^{(6)}$ should be an effective measure of the thermal shock damage resistance of a ceramic material. It is significant that the value of $R^{(6)}$ increases as the porosity is increased in a ceramic material. It is also significant that Hasselman and Shaffer correctly predicted that the presence of a graphite dispersion would affect the thermal-shock fracture behavior of zirconium carbide.

Hasselman and Shaffer investigated the thermal shock failure of zirconium carbide containing 0, 10, 20, 30, 40, and 50 volume per cent graphite. The index $R^{(6)}$ took on a decisive maximum value at a graphite content of approximately 30 per cent. When subjected to 3632° F, a sphere of zirconium carbide alone fractured catastrophically, while spheres of the other compositions appeared unharmed. Close examination revealed the presence of cracks on the surface of the sphere which contained 10 per cent graphite, and internal cracks were found in all spheres with graphite additions.

Another deficiency of the thermal shock parameters remains to be discussed. A high degree of scatter is associated with thermal shock resistance measurements. Of course, this is to be expected since the resistance to thermal shock depends on the strength of the material. One approach to this problem is to

assume that the same statistics that apply to the strength of a material also apply to the thermal shock resistance of the material. Such an approach was taken by Manson and Smith (Ref. 116) more than a decade ago.

Manson and Smith formulated a theory of thermal shock resistance based on Weibull's statistical theory for strength. The statistical theory and the maximum tensile-stress theory were compared, and the following indications evolved from the study:

1. Weibull's homogeneity parameter m should be listed as a thermal shock parameter.
2. If m is high, the theory of maximum stress will give adequate results. However, for the range of values of m for ceramic materials, the parameter should always be considered when high rates of heating or cooling are encountered.
3. The probability of failure is likely to reach a maximum not when the maximum point-wise stress is reached but when the general stress level is high.

It is significant that Manson and Smith were able to deduce from thermal shock tests a value of m for steatite which was in good agreement with the value determined from bending strength data.

7.9 General References on the Properties of Ceramic Materials

For a recent and critical review of the testing techniques for ceramics the reader may refer to Reference 42. For recent reports which constitute an extensive compilation of data on refractory ceramic materials the reader is referred to References 2 and 3 and to Extended Abstracts 3 to 7 in Appendix I. Extended Abstracts 8 to 33 in Appendix I refer to recent foreign publications which deal with ceramic material properties.

VIII. HIGH-TEMPERATURE STRUCTURAL MATERIALS

8.1 Oxides

Although the oxides are exceeded in high-temperature strength by a number of other materials, they constitute an important class of non-metallic refractory materials. They are characterized by outstanding chemical resistance over a wide range of temperatures, relatively low density, moderately high melting point, brittleness at low temperatures, and low to moderate cost. Their fracture strength compares favorably with that of the high-temperature metals on a strength-per-unit weight basis, and they are unexcelled in resistance to oxidation. They are also usually highly stable in reducing atmospheres.

At temperatures above 2700° F, all of the oxides have low mechanical properties, and variations in these properties due to differences in porosity and grain size are considerable. An increase in porosity of 10 per cent can lower the strength by as much as 50 per cent. In addition, small amounts of impurities often have an appreciable effect on the creep strength and thermal conductivity of a polycrystalline oxide body.

The use of refractory oxides has been limited by the lack of high-temperature strength, by the lack of impact strength, and, with the single exception of silica, by the lack of thermal shock resistance. As a result, most of the refractory oxides have been used in aerospace structures only to protect other less stable materials.

Some of the refractory oxides are expensive because they are scarce, or because they are difficult to recover in pure form. These include yttria, hafnia, ceria, and thoria. The refractory oxides which are available in abundance include alumina, silica, magnesia, zirconia, and beryllia.

8.1.1 Alumina

Aluminum oxide, Al_2O_3 , is one of the most widely used refractory compounds because of its low cost, high mechanical strength up to about 2200° F, availability in a number of forms, and because of a vast background of information regarding its use. Aluminum oxide melts at 3720° F and is chemically one of the most stable oxides. It can be used above 3100° F in a strongly reducing atmosphere and up to about 3500° F under oxidizing conditions.

Alumina ware can be formed by slip casting, extrusion, cold or hot pressing, or injection molding. The first ceramic radomes were obtained by casting an alumina slip or by isostatically pressing an alumina suspension on a core. In 1955, a prestressed ceramic wing was tested at the University of California (Ref. 117). The wing segments were formed from alumina by slip casting.

8.1.2 Beryllia

Beryllium oxide, BeO , has a melting point of 4660° F and a specific gravity of only 3.03. It is the most resistant of all the oxides to reduction

by carbon at elevated temperatures and is stable in air, hydrogen, carbon monoxide, argon, nitrogen, or vacuum to 3100° F. It is not stable, however, in halogen or sulfurous atmospheres. The thermal conductivity of beryllia at low temperatures is outstanding, surpassing even a number of the metals. At high temperature, the conductivity is much lower. While the low temperature conductivity is greatly affected by small amounts of certain impurities, commercial beryllia ceramics are now available with reproducible ($\pm 7\%$) thermal conductivity at a level of 105-110 BTU/hr./ft./° F for dense material. The electrical conductivity is very low.

Beryllia has the highest specific heat of all the refractory oxides. Its high heat capacity and thermal conductivity and its uniform thermal expansion make it fairly resistant to thermal shock.

In the past, beryllia ceramics were relatively weak at low temperatures. However, with the application of modern processing methods and careful quality control during all phases of product fabrication, uniform batch to batch and firing to firing bend strengths of 25,000 to 35,000 psi have been achieved. More importantly, when the kinds and amounts of impurities are carefully controlled, and when great care is taken to minimize internal stresses by proper die loading and uniform firing in the temperature range where maximum shrinkage occurs, beryllia exhibits less dispersion in mechanical strength than most other ceramic materials. One company is presently supplying 16 in. by 16 in. by 2 in. beryllia windows machined from blocks showing an average modulus of rupture of at least 30,000 psi on each of the four edges with no value falling below 25,000 psi (Ref. 118). The mechanical properties remain fairly constant with temperature up to about 2900° F, and at this temperature beryllia is one of the strongest oxides in compression.

Beryllia is chemically stable in contact with metals at high temperature. It shows no tendency toward reduction in hydrogen up to 4250° F and is stable in a vacuum to at least 3600° F. However, above 3000° F, beryllia reacts with water to form a volatile hydroxide. Beryllia is toxic, but it is only dangerous when small particles are inhaled so that the hazard is easily eliminated by reasonable hooding.

Objects made from beryllia can be fashioned in complicated forms, particularly by cold pressing, hot pressing, isostatic pressing, or slip casting. Extrusion is employed when small, modular units made by pressing would be unsatisfactory from a design standpoint. With extrusion, an increase in bending strength of 25 per cent can result due to orientation of needlelike grains present in the powder material; however, such preferred orientation would be expected to lower the thermal shock resistance of a part.

8.1.3 Ceria

Cerium oxide, CeO₂, is generally inert in spite of its variable oxygen content. Since it is compatible with a number of oxides, it is an ideal choice to separate incompatible materials. Ceria has been used as a coating for zirconia in contact with magnesia and as an additive to stabilize zirconia. Ceria can be readily flame-sprayed to form a dense coating.

8.1.4 Chromia

Chromic oxide, Cr_2O_3 , melts at about 4100° F and has a vapor pressure about twice that of alumina around 3100° F . Chromic oxide has found some use as a refractory when it is combined with alumina and magnesium. Small additions of chromia have been found to effect an increase in the emittance of at least two other oxides.

8.1.5 Hafnia

Hafnium oxide, HfO_2 , melts at 5090° F and has attractive refractory properties. Pure hafnia is scarce because it is difficult to separate from the zirconium minerals with which it is generally found. However, it forms a solid solution with zirconium oxide, and its properties are not seriously impaired by small amounts of the zirconia. Hafnia with zirconia as an impurity is easily flame- or plasma-sprayed, and it has the same degree of stability and chemical inertness as zirconia. Pure hafnia would be preferred in most applications if cost were not a factor. Hafnia undergoes inversions similar to that in zirconia, but the inversion from the monoclinic form of hafnia occurs at a much higher temperature (about 3100° F) so that, in hafnia, the conversion should not present a severe thermal shock problem.

8.1.6 Magnesia

Magnesium oxide, MgO , melts at 5070° F and shows no conversions up to the melting point. It has better high-temperature oxidation resistance than alumina and is stable in contact with carbon up to about 3300° F . However, it is less stable than alumina in contact with most metals, it is limited to about 3100° F in reducing atmospheres or in a vacuum, and its mechanical strength is low due to its distinct cubic cleavage.

While magnesia shows little tendency to hydrate in the densely sintered condition, finely divided particles hydrate rapidly, and it is more difficult to slip-cast magnesia than it is to slip-cast alumina or beryllia. Magnesia can also be fabricated by extrusion, pressing, or even by fusion. Sintering begins at temperatures as low as 1600° F .

Magnesia has a high thermal expansion and, as a result, is highly susceptible to thermal shock in spite of its high thermal conductivity.

8.1.7 Silica

Silicon dioxide, SiO_2 , melts at 3110° F ; however, the melt is so viscous that it acts essentially like a solid material up to about 4500° F . At 4500° F , the silica volatilizes rapidly.

The most useful form of silica for structural applications is the amorphous form, fused silica. It exhibits practically no thermal expansion so its thermal shock resistance is superb. Unfortunately, the fused material devitrifies in the approximate temperature range 2000° to 3000° F .

When fused silica is maintained above a temperature of 2000° F , β - crist-

balite forms. Upon subsequent cooling below about 500° F, the β - cristobalite is transformed to α - cristobalite, and microcracks usually develop in the cristobalite regions. Usually, these microcracks can be traced to cooling stresses that result from the difference between the thermal expansion of the cristobalite and that of the fused silica and from the decrease in volume associated with the transformation from the β to the α cristobalite. In air under one atmosphere of pressure, a critical cristobalite content is reached in slip-cast fused silica* at the end of two days at 2100° F, at the end of five hours at 2200° F, and at the end of one and one-half hours at 2300° F. Under higher partial pressures of oxygen or in the presence of water vapor, the devitrification rate is higher. In a reducing atmosphere, in an inert atmosphere, or in a vacuum, the devitrification is retarded. For the times associated with reentry and most other hypersonic flight applications, fused silica would not be expected to devitrify. In addition, devitrification is only a problem when the silica must be cooled below 500° F.

The slip-cast and sintered fused silica has a room-temperature flexural strength of only 4000 psi. The strength increases with temperature in a nearly linear fashion to a value of about 8000 psi at 2200° F. The slip-cast material shows only 1.3 per cent linear shrinkage measured from the green state to the fully matured state. Thus large, intricate shapes can be economically formed to fairly close tolerances. Slip-cast fused silica is presently a leading candidate for use in radomes and nose cones. The material is unique in that it can function as a thermal shock resistant ceramic to 4000° F for periods up to five minutes with very little ablation and can also function as an efficient ablator above 4000° F (Ref. 6, 119).

Silica is an excellent insulator, both thermally and electrically, and the specific gravity of fused silica is only 2.2.

8.1.8 Thoria

Thorium oxide, ThO_2 , has the highest melting point of all the oxides, 5800° F. It has a very low vapor pressure at high temperatures and is chemically the most stable oxide. The major deterrents to its use include its high specific gravity of 9.9, high cost, and slight radioactivity. In addition, its high thermal expansion and its low thermal conductivity make it highly sensitive to thermal shock.

Thoria bodies can be formed by pressing, tamping, and slip casting.

Thorium oxide occurs as cubic crystals, show no inversions upon heating, and ablates without melting.

8.1.9 Yttria

Yttrium oxide, Y_2O_3 , melts at 4370° F, has a cubic structure, and shows no inversions. Its high cost and slight tendency to hydrate and form

*Glasrock Products, Inc.

a carbonate at low temperature limit its use. In respect to thermal expansion and thermal shock resistance, yttria is similar to alumina.

8.1.10 Zirconia

Zirconium oxide, ZrO_2 , melts at $4870^{\circ} F$, and has relatively high mechanical strength, unusually low thermal conductivity, and excellent chemical stability. It can be used at higher temperatures than alumina, but is more expensive.

Zirconium oxide is normally monoclinic to $2160^{\circ} F$ with a specific gravity of 5.56 and tetragonal above $2160^{\circ} F$ with a specific gravity of 6.10. The transition temperature shifts downward with added impurity. The disruptive transition can be eliminated or modified by the addition of 3 to 15 per cent CaO , CeO_2 , Y_2O_3 , or MnO with only a slight loss in refractoriness. These compounds form a solid solution of cubic structure with the zirconium oxide. The cubic structure is stable at high temperatures and metastable below 1470° to $2000^{\circ} F$.

Completely stabilized zirconia can be achieved, but it is desirable to retain approximately 15 per cent monoclinic zirconia to lower the total thermal expansion and improve the thermal shock characteristics. Partially stabilized zirconia is used as a substitute for thoria in high-temperature corrosive situations if thoria is unsuitable because of its poor thermal shock response.

Zirconia is normally associated with 2 to 7 per cent hafnia with which it is found in nature. Usually the hafnia is not removed during processing since it forms a solid solution with zirconia and is not detrimental to the properties of the zirconia.

Bodies of stabilized zirconia may be fabricated by ramming, dry pressing, extrusion, and slip casting. However, because of the high specific gravity, more care should be taken in selecting and controlling the particle sizes than is usually taken with the lighter oxides.

Zirconia is reported to be stable in a vacuum, in hydrogen, or in contact with carbon up to $4170^{\circ} F$ and to be stable in contact with molybdenum up to $3600^{\circ} F$.

8.2 Carbides

The highest melting temperatures known today belong to the carbides. For example, hafnium carbide melts at $7030^{\circ} F$, tantalum carbide at $7020^{\circ} F$, the complex $4TaC:HfC$ at $7690^{\circ} F$, and the complex $4TaC:ZrC$ at $7970^{\circ} F$. The carbides are also characterized by good strength at elevated temperatures, high hardness, good abrasion resistance, excellent chemical stability toward other materials, low electrical resistivity, high thermal conductivity, and a lack of ductility.

None of the carbides occurs naturally to an appreciable extent. However, most metals and their oxides react with carbonaceous materials to form carbides, and undecomposed carbides of many of the metals can be produced at

relatively low temperatures. Carbides with only 0.3 per cent impurity, including free carbon, have been prepared (Ref. 120).

While the hardness, abrasion resistance and refractoriness of the carbides are assets in the finished articles, these properties act as handicaps during fabrication. However, methods used to form carbide shapes have improved to the point where reasonably high densities can be obtained in simple geometrical shapes. More complicated shapes can be obtained by pre-compaction and sintering under protective atmospheres, but here final density, strength, and corrosion resistance are sacrificed.

The limiting characteristics of the carbides include high cost, lack of ductility, instability in oxidizing atmospheres, and poor thermal shock resistance. With the exception of silicon carbide, none of the carbides can be used at temperatures above 1830° F for long periods of time when oxygen is present. However, most of the carbides are more resistant to oxidation than graphite, and some are more resistant than metals having comparable melting points. The carbides are fairly stable toward nitrogen, they can withstand temperatures of 3900° to 4500° F in a reducing atmosphere, and they volatilize very slowly in vacuum at temperatures approaching their melting points.

Again with the exception of silicon carbide, none of the carbides can be classified as having good thermal shock resistance, in spite of their high strength and high thermal conductivity. Thermal shock resistant bodies, however, have been fabricated by embedding a low-modulus dispersed graphite phase in a high-modulus continuous carbide matrix (Ref. 84). The technique has been used to increase the thermal shock resistance of zirconium carbide and silicon carbide. The increase in resistance has been attributed to a decrease in the elastic strain energy stored at fracture and, to a lesser extent, to an increase in the thermal conductivity and thermal diffusivity.

Coefficients of thermal expansion range from $2.7 \times 10^{-6}/^{\circ}\text{F}$ to about $7.0 \times 10^{-6}/^{\circ}\text{F}$ for the carbides, specific heats range between 0.04 and 0.5 BTU/lb-° F, and, for the temperature range 1000° to 3000° F, thermal conductivities generally fall between 10 and 30 BTU/ft · hr · ° F. At room temperature, tensile strengths range from 5,000 to 50,000 psi, compressive strengths from 60,000 to 350,000 psi, and bend strengths from 10,000 to 120,000 psi with variations as high as 85 per cent of the mean for any particular carbide. In general, values of the elastic modulus of carbides at room temperature are about 50×10^6 psi, but for carbides of tungsten a significantly higher modulus is reported.

8.2.1 Boron carbide

Boron carbide, B_4C , has a compressive strength above 400,000 psi at room temperature and a hardness superior to that of silicon carbide. It melts at 4440° F and can be readily self-bonded by hot pressing. Although resistant to air up to 1800° F, boron carbide degrades rapidly in oxidizing gases at higher temperatures. The specific gravity of boron carbide is 2.51.

8.2.2 Hafnium carbide

Hafnium carbide, HfC , has the highest reported melting point of all simple compounds, 7030° F . However, hafnium carbide has found little usage because of its high cost and high specific gravity, 12.7. Some use in experimental nozzles, however, has been reported.

8.2.3 Silicon carbide (self-bonded)

Silicon carbide, SiC , has a cubic structure with a specific gravity of 3.21 at low temperatures and a hexagonal structure with a specific gravity of 3.208 above temperatures in the range 3800° to 4500° F . The material does not melt but undergoes complete dissociation to silicon and carbon at temperatures ranging from 3720° to 5710° F .

The self-bonded material is far superior to any of the other available varieties. It has a high thermal conductivity, moderate thermal expansion, low density, high hardness, moderately high strength, excellent creep resistance, and good resistance to corrosion, abrasion, and thermal shock. In addition, it is chemically inert in a large number of systems, and it can be used at temperatures as high as 2900° F under oxidizing conditions owing to the formation of an excellent self-healing film of silica glass on the surface of the material.

At present, silicon carbide is by far the most attractive carbide for high-temperature structural usage.

8.2.4 Tantalum carbide

Tantalum carbide, TaC , melts at 7020° F and is unaffected by nitrogen up to 5400° F provided there is no hydrogen present. However, its use has been limited because of its high specific gravity, 14.4.

8.2.5 Titanium carbide

Titanium carbide, TiC , melts at 5880° F and has been reported in nitrogen at 4500° F . Because of its low specific gravity, 5.9, and its moderate thermal shock resistance, it has been of considerable interest as a potentially useful structural material. However, fabricated parts are expensive, and no compositions have been found to exhibit outstanding oxidation resistance.

8.2.6 Tungsten carbides

The tungsten carbides, WC and W_2C , are both stable at low temperatures, and WC decomposes to W_2C at 4710° F . The melting point of tungsten carbide has been reported to be in the range 4710° to 5220° F . The high density of tungsten carbide and its instability in oxygen above 1000° F have limited its use. The commercial value of the carbide lies in its hardness and toughness when bonded with certain metals.

8.2.7 Zirconium carbide

Zirconium carbide, ZrC , melts at about $6000^{\circ} F$, has a specific gravity of 6.8, and has a sufficiently low vapor pressure for use in vacuum to $4000^{\circ} F$. Although the thermal shock resistance of the carbide has been improved by the incorporation of a dispersed graphite phase, little usage of the carbide is reported.

8.3 Borides

The borides are a highly refractory class of ceramic materials characterized by extreme hardness, a high electrical conductivity, and a positive temperature coefficient of electrical resistance. All borides have a metallic appearance, and some are better conductors of electricity than the parent metals. The borides of most interest for high-temperature structural applications are the diborides of chromium, hafnium, niobium, tantalum, titanium, vanadium, and zirconium.

The technical importance of the diborides emanates from their low density, chemical stability, intermediate thermal expansion, relatively good thermal shock resistance, moderate thermal conductivity, oxidation resistance, and high strength. The major disadvantage of the diborides is a lack of room temperature toughness, and they are probably not ductile at any useful temperature.

The borides are chemically stable to very high temperatures. They are inert to most oxides, and some are stable in contact with tungsten, molybdenum, and graphite. Because of their compatibility with other materials, the borides are leading candidates for use in composite structures.

The oxidation resistance of the borides is good, but not exceptional. However, there is evidence that better oxidation resistance can be obtained with the addition of boron which oxidizes to a glass-forming oxide.

A few diboride powders and simple shapes are available commercially, but most of the diborides are experimental materials. Parts can be fabricated by slip-casting, cold pressing, or hot pressing, and coatings can be prepared by flame spraying. Because of their high strength and hardness, fabricated shapes can be machined and finished only by diamond grinding.

8.3.1 Chromium diboride

Chromium diboride, CrB_2 , has a specific gravity of 5.6 and melts at $3660^{\circ} F$. It has high strength and can be used in air up to about $1800^{\circ} F$.

8.3.2 Hafnium diboride

Hafnium diboride, HfB_2 , melts at $5880^{\circ} F$ and has a high thermal conductivity. It has the disadvantage of a high specific gravity, 11.2.

8.3.3 Niobium diboride

Niobium diboride, NbB_2 , has a specific gravity of 7.1 and melts at 5430° F . A vitreous, semiprotective oxide film is formed on the material at low temperatures, but the material oxidizes readily at about 2000° F . However, niobium diboride should be stable under neutral or reducing conditions above 3600° F .

8.3.4 Tantalum diboride

Tantalum diboride, TaB_2 , has a specific gravity of 12.6 and melts at 5610° F . It is similar to niobium diboride in its behavior towards oxidizing, neutral, and reducing environments.

8.3.5 Titanium diboride

Titanium diboride, TiB_2 , is one of the most stable borides. It is compatible with tungsten, molybdenum, and graphite, and it can be used in an oxidizing atmosphere to 2550° F for an extended period of time. The material melts at 5320° F and has a specific gravity of only 4.5. A titanium diboride body, 98 to 99 per cent purity, has been reported to have a room-temperature and 3600° F flexural strength of 35,000 psi, and a strength-to-weight ratio that is not exceeded by any other bulk material in the temperature range 2900° to 3600° F .

8.3.6 Vanadium diboride

Vanadium diboride, VB_2 , has a specific gravity of 5.2 and melts at 4350° F . It has high strength, but oxidizes readily in air at a temperature of about 2000° F .

8.3.7 Zirconium diboride

Zirconium diboride, ZrB_2 , has a specific gravity of 6.1 and melts at 5500° F . It is stable in contact with tungsten, molybdenum, and graphite, and it resists oxidation to 2370° F for extended periods of time. The oxidation resistance has been improved through a 10 per cent addition of molybdenum disilicide which promotes the formation of a self-healing protective film on the surface of the boride (Ref. 121). In this way, oxidation resistance can be achieved up to 3600° F . Interestingly, a 90 per cent ZrB_2 , 10 per cent MoSi_2 body showed a 50 per cent increase in strength following 30 cycles from room temperature to 2460° F with air-stream cooling.

Zirconium diboride has found use in cermets and rocket nozzles, and an experimental leading edge has been made from zirconium diboride by hot pressing.

Zirconium diboride exhibits high strength which is not significantly decreased by increasing temperatures from room temperature to 2730° F .

8.3.8 Mixed borides

While a number of the diborides are potentially qualified for high-temperature structural applications, it is believed that mixed borides may be the only materials capable of supporting substantial loads for extended periods of time at 4000° F.

Recent studies have been encouraging. It has been demonstrated that "alloys" of two diborides can be prepared by simultaneously reducing and boriding mixtures of the metal oxides and that the composition of the products can be closely controlled without difficulty. The projection of experimental data has indicated that the diborides (Ti, Ta) B₂, (Ti, V) B₂, and (Ti, Nb) B₂ will have rather low rates of oxidation if fabricated to near theoretical density (Ref. 122). The compositions Ti_{0.67} Cr_{0.33} B₂ and Ti_{0.5} Cr_{0.5} B₂ have been found to exhibit superior oxidation resistance (Ref. 123).

On the basis of recent findings at the Norris Metallurgy Research Laboratory (Ref. 124), it appears that mixed borides may exhibit outstanding thermal shock resistance. At the Norris Laboratory, specimens are subjected to a thermal shock condition during thermal emf determinations. One end of a sintered 4-inch bar is heated to about 1500° F in about four minutes, while the other end is submerged in an ice bath. The thermal gradient is very sharp at the heated end. Bars of different porosities from nine compositions in the system (Ti, Cr) B₂ were subjected to the test, and no thermal shock failures were observed. Bars from five compositions in the system (Ta, Cr) B₂ were also subjected to the test, and the incident of thermal shock failure was approximately 50 per cent. However, when bars of TaB₂ alone were subjected to test, failure occurred in every case, regardless of the heating rate. In addition, Pt-Rh thermocouples have been resistance-welded to TiCrB₄ compositions without breakage.

8.4 Nitrides

While a number of the nitrides have high melting points, their usefulness is generally limited because of their relatively high dissociation pressures. The covalent nitrides of aluminum, beryllium, boron, and silicon are refractory, but only silicon nitride can be recommended for extended use in air above 2000° F.

8.4.1 Aluminum nitride

Aluminum nitride, AlN, has a specific gravity of about 3.2. The material starts to vaporize around 4100° F and is completely vaporized at about 4500° F. It can be obtained in amorphous or crystalline forms, and it can be formed into dense objects of high purity through pyrolytic deposition. A hot-pressed aluminum nitride ceramic is reported to have a flexural strength of 38,000 psi at room temperature and 18,000 psi at 2550° F. The material has a low thermal expansion, a high thermal conductivity, and good thermal shock resistance. However, it is readily oxidized above 1800° F.

8.4.2 Beryllium nitride

Beryllium nitride, Be_3N_2 , dissociates near its melting point, 4000° F . It can be obtained in amorphous or crystalline forms, but requires a temperature close to the melting point for crystallization. While its oxidation product, BeO , should provide oxidation resistance for the dense material, beryllium nitride has been reported to be stable in air only to about 1800° F . Beryllium nitride decomposes slowly in boiling water.

8.4.3 Boron nitride

Boron nitride, BN , is considered to be the most attractive nitride for high-temperature structural applications. It crystallizes in the same crystal systems as carbon, and the usual hexagonal form is often called "white graphite" in analogy to carbon. The material offers the advantages of low density, low dielectric constant and low loss tangent, good corrosion resistance, exceptional machinability, excellent thermal shock resistance, high thermal conductivity, and high electrical resistance at high and low temperatures. The material is very inert chemically, is surprisingly stable toward oxidation, and is not wetted by many molten metals and salts. Like graphite, the material has mechanical and thermal properties which vary widely depending on the orientation of the particles.

Pure boron nitride has been hot pressed to good density and strength levels, and data have been developed on a body containing 2.4 per cent boron oxide made by hot pressing*. A 97 per cent pure and 93 per cent dense compact showed a weight loss of 0.235 mg/cm^2 after a 60-hour exposure to air at 1300° F . At 1800° F , the loss was 10 mg/cm^2 . The material was stronger mechanically than graphite at room temperature. The bend strength dropped to 1000 to 2000 psi in the temperature range 1800° to 2700° F , but increased to values near those found at room temperature when 4350° F was reached. Apparently, the rather odd strength-temperature behavior is closely associated with the oxide binder.

A disadvantage of boron nitride has been its tendency to hydrolyze. A number of investigators have reported that compacts of the material "exploded" during rapid heating. Apparently, the failures resulted from moisture which could not escape fast enough from within the compacts. The problem was eliminated by heating the compacts to 660° F before they were put into service. A new grade of boron nitride is reported to have outstanding resistance to moisture absorption**.

8.4.4 Silicon nitride

Silicon nitride, Si_3N_4 , exists in two hexagonal forms which differ slightly in lattice dimensions. The low-temperature form, with specific

*The Carborundum Company.

**Union Carbide Corporation.

gravity 3.44, undergoes transformation when heated above 2820° F. The material sublimes at 3450° F. The material is of interest because it is quite resistant to oxidizing conditions and thermal shock, and because it can be produced in intricate shapes to close tolerances. The material is very inert chemically and has a low thermal expansion and a low modulus of elasticity. Reported flexural-strength values for silicon nitride range from 10,000 to 25,000 psi at temperatures between 80° and 2500° F.

8.5 Intermetallic Compounds

The intermetallic compounds are the inorganic nonmetallic materials generally considered as having the greatest potential for achieving low-temperature ductility. The aluminides, beryllides, and silicides show the most promise for aerospace applications. They are hard and brittle in polycrystalline form at room temperature, but can be deformed plastically at elevated temperatures.

8.5.1 Aluminides

The aluminides have a lower use temperature than the refractory beryllides and silicides. None of the aluminides melt above 4000° F, and three melt above 3000° F. Nickel aluminide, NiAl, which has been investigated more extensively than any other aluminide, shows good oxidation resistance and strength only up to 2000° F. Titanium aluminide, TiAl, exhibits good strength and fair oxidation resistance up to about 1800° F. Metallic additions have been used to improve the strength of nickel aluminide. A flexural strength close to 150,000 psi was achieved through a 4 per cent titanium addition. The aluminides NiAl₃ and TiAl₃ were reported to have excellent oxidation resistance at 2300° F, but only marginal resistance at 2500° F for 190 hours of exposure.

8.5.2 Beryllides

The most promising beryllides appear to be those of hafnium, molybdenum, niobium, tantalum, and zirconium. An outstanding feature of these and other beryllides is their resistance to oxidation up to 2500° F due to the formation of a tenacious beryllium oxide film. Indications are that the more oxidation resistant compounds are the higher beryllides.

The beryllides are an attractive class of materials for structural applications to 3000° F. In addition to excellent oxidation resistance, they have low density, good thermal shock resistance, and exceptional strength to 2900° F. Flexural strengths range from 20,000 to 80,000 psi with peak values occurring around 2200° F. Higher strengths can be obtained through mixtures of beryllides in a given reactive metal system.

Beryllide compacts with densities ranging from 97 to nearly 100 per cent of theoretical have been achieved by hot pressing with pressures of 2000 psi at temperatures of 2800° to 3000° F.

8.5.3 Silicides

The melting temperatures of the silicides are much lower than those

of the borides and carbides, and they are not as hard. However, a number of the disilicides are highly resistant to oxidation and retain their strength at elevated temperatures. The compounds of interest for structural use above 2500° F are the disilicides of chromium, molybdenum, niobium, tantalum, titanium, tungsten, vanadium, and zirconium.

Although the silicides are thermodynamically unstable in oxidizing atmospheres, they have exceptional resistance to oxidation as a result of the formation of a self-healing film of silica. The disilicides of chromium, titanium, and tungsten can be used for extended periods of time in air to about 2500° F. Molybdenum disilicide is not attacked by oxygen at 3100° F. The disilicides of tantalum and tungsten retain high flexural-strength values up to 2750° F.

The silicides possess high thermal conductivity, good resistance to chemical attack, and excellent thermal shock resistance. The major disadvantages of some of the silicides are poor resistance to oxidation at low temperatures, excessive creep at high temperatures, and low-temperature brittleness.

8.6 Composites

The increasing severity of performance requirements in the aerospace field has taxed many of the conventional single-phase materials to the limit. Improvements in the high-temperature properties of a monolithic material are often won only after long and intensive study, and in many cases only a small degree of improvement can be expected. As a result, many engineers are turning to composites in the belief that a properly designed composite will exhibit the favorable properties of each of its constituents.

There are five general classes of composites based on the form of the structural constituents: fiber, flake, particulate, filled, and laminar. The characteristics and properties of these composites are determined by a large number of factors including: the basic materials used, the size and shape of the constituent elements, the distribution and arrangement of the elements, and the interactions between the elements. These many factors give composite systems a great versatility, but also make analysis, fabrication and prediction of performance difficult.

8.6.1 Fiber composites

The inclusion of fibers in a matrix has evoked great interest among engineers concerned with structural applications. Only rather recently, however, has the use of metal and ceramic fibers in a ceramic matrix been explored. Most of these fiber composites are still in the experimental stage.

The inclusion of fine metal fibers in a refractory ceramic is almost certain to improve the strength and shock resistance of the ceramic. The technique offers the potential of allowing practical prestressed - ceramic - structures to be developed. Such structures could have very high strength-to-weight ratios and could be very efficient in aerospace situations.

A number of monocrystalline ceramic fibers have been developed recently, and they exhibit a mechanical resistance greatly superior to that of many ordinary metals. They are often hundreds of times more resistant than crystals in bulk form, and their strength approaches the theoretical limit of atomic cohesion. Because of their low density, refractoriness, high strength, and good stiffness, the ceramic whiskers offer the exciting possibility of increased allowable loads for space vehicles and engines. A few ceramic whiskers are now available commercially*, but their cost is in the neighborhood 25 to 100 dollars per gram.

8.6.2 Flake composites

The use of metal or ceramic flakes in a ceramic matrix is also only at the experimental level. However, it is clear that flakes would offer a number of special properties to be obtained because of their two-dimensional character. Being flat, they can be packed close together to provide a high percentage of reinforcing material for a given cross-sectional area. With a high degree of overlap, they form a series of barriers that can reduce the danger of mechanical damage by penetration.

Flakes offer a number of advantages over fibers. They can provide uniform mechanical properties in a plane, they have a higher modulus of elasticity than fibers, and they can be very closely packed. Flakes are less expensive than fibers, they can be handled in large batches, and they can easily be incorporated into composite systems. However, it is not easy to make effective flakes or to control their arrangement in a composite, and the mechanical properties are greatly affected by the surface conditions of the flakes.

The strength of a flake composite improves as the flake thickness is decreased, but variations in the flake diameter seem to have little effect. For optimum mechanical properties, parallel arrangement is required.

8.6.3 Cermets

Cermets have a structure composed of ceramic grains in a metal matrix. They are generally fabricated using powder-metallurgy techniques with a sintering operation at a temperature near the melting point of the metal component. When the percentage of the metallic phase is high, machining can be accomplished using conventional methods. With low metal contents, machining can be accomplished by sparking and by diamond tips, but this limits their use in precision mechanics.

While cermets were developed with the intention of joining the ductility and thermal shock resistance of metals with the oxidation resistance and refractoriness of ceramics, they have only partially accomplished the task. At the present state-of-the-art, they fill the gap between the high-temperature alloys and the ceramics. In the temperature range 1800° to 2200° F, a number

*Thermokinetic Fibers, Inc.

of cermets have adequate properties for short-time applications, and a few exhibit adequate long-time strength.

In the more successful cermets, bonding between the metal and ceramic results from a small amount of mutual solubility. In some cases, good bonding can be achieved through an addition which is partially soluble in both the metal and the ceramic.

8.6.3.1 Carbide-base cermets: The three major families of carbide cermets are based on chromium carbide, titanium carbide, and tungsten carbide.

Cermets based on chromium carbide have exhibited excellent corrosion resistance and exceptional oxidation resistance. Chromium carbide has a relatively low density, but it also has the lowest melting point of the stable carbides, and the chromium carbide cermets have not shown the combination of high-temperature strength and impact resistance which would allow them to compete successfully with the titanium carbide compositions in high-temperature applications.

Cermets based on titanium carbide have good thermal shock resistance, high elastic modulus, and good oxidation resistance when nickel is used as the binder. They provide a significant increase in strength over the conventional high-temperature alloys, especially on a unit-weight basis. While the hardness of these cermets decreases with increasing binder content, the impact strength shows a substantial increase when a higher binder content is used. The material fractures with little elongation even when a high binder content or a long-time test is used.

Cermets based on tungsten carbide are of interest for structural applications because of their high strength, hardness, and toughness. However, they lack sufficient oxidation resistance for high-temperature use.

8.6.3.2 Oxide-base cermets: In the oxide-base cermets, either the metal or the ceramic can serve as the matrix constituent. Thus, a wide range of properties can be obtained with these compositions. Alumina bonded with chromium or chromium-base alloys has shown the greatest promise. A composition containing 70 weight per cent chromium has excellent oxidation resistance to 2200° F and reasonable thermal shock resistance, but its strength falls far below that of the titanium carbide cermets. If the binder content is reduced to 30 weight per cent, improved strength and creep-rupture properties can be achieved to 2200° F, but thermal and mechanical shock resistance are sacrificed.

8.6.3.3 Boride-base cermets: Chromium-boride and zirconium-boride cermets have sufficient strength and oxidation resistance for extended use to about 2000° F, but their mechanical and thermal shock resistance is not exceptional. However, boride cermets have performed well in applications involving short-time cycles at very high temperatures. For example, beryllium oxide has been combined with metallic beryllium to produce a cermet which can be used for a very short time at a temperature far surpassing the melting point of beryllium without visible deterioration or loss of metal.

8.3.3.4 Graded refractories: Graded cermets have been constructed to improve the thermal gradient of a material and reduce its tendency to fail under thermal shock conditions. The graded cermets can be designed to combine the ductility of a metal at one extremity and the oxidation resistance of a refractory ceramic at the other. These materials should be considered for aerospace applications such as leading edges and nose cones.

8.6.4 Filled composites

Two types of filled composites are of current interest to the aerospace field. These are the solid structure consisting of two intertwining skeletons of different properties and the filled honeycomb structure.

A major problem associated with the skeleton - skeleton approach is that of finding a structure which will lend itself to complete impregnation so that optimum properties can be obtained. In addition, considerable care must be taken in selecting the skeletal materials. The materials should not react in any way that would adversely affect their inherent properties.

The skeleton - skeleton technique is being considered for the production of composites for aerospace systems required to perform under conditions of high temperature and high mechanical and/or thermal loads. At the Union Carbide Research Institute (Ref. 120), for example, carbide samples are being hot-formed using high temperatures, low pressures, and short exposures. Samples with a porosity of 15 to 20 per cent show a network of continuous, if perhaps somewhat oriented, pores which are highly conducive to metal impregnation. It appears that the ceramic could be placed in compression with the pre-stress decreasing with increased temperature. It also appears that the size, shape, and distribution of the pores can be controlled to a considerable extent by varying the particle size distribution of the starting material and the hot-forming factors, time, temperature, and pressure.

The filled-honeycomb approach is useful because it confines ceramic materials to small shapes. This is important because ceramic materials tend to have poor thermal shock resistance when they are used in bulk form. If the ceramic is in the form of separate segments, it can withstand the thermal shocks that would cause a large monolithic structure to fail.

Ceramic materials can be incorporated into a honeycomb structure by such methods as slip-casting, foaming, cold pressing, isostatic pressing, hot forming, spraying, tamping, etc. The honeycomb approach has the important advantage of allowing extremely large components to be made. In addition, many different materials in a wide variety of shapes and forms can be brought together by the filled-honeycomb approach giving the engineer a wide latitude of design possibilities.

The major problems encountered in the filled-composite approach are those associated with the processing of materials into small shapes, the joining of vastly dissimilar materials, and the fabrication and fastening of the overall composite.

8.6.5 Laminar composites

Since laminar composites are made up of films or sheets, they are relatively easy to design, produce, standardize, and control. They are generally designed to protect against corrosion, to afford high temperature oxidation resistance, to provide impermeability, to reduce cost, to improve appearance, to reduce the weight of a structural component, to overcome size limitations, and to modify thermal, mechanical, and electrical properties.

The use of sandwich structures to reduce weight penalties is of prime importance to the aerospace designer. The combination of high density facings and cellular cores provides the highest possible strength-to-weight ratio for a given set of materials. Special applications for such structures include wings, trailing edges, stabilizers, radomes, rudders, and leading edges.

The major problems encountered in the design of sandwich structures and other laminar composites are those associated with the joining and attachment of materials. The adhesive bonding agents available at the present time appear to be limited to about 1000° F.

Exotic laminar-composites have been used for high-temperature heat shields and for the walls of large missile nozzles. One of the more sophisticated heat shields is being evaluated by the Aeronca Manufacturing Corporation (Ref. 125). Aeronca has developed an inconel honeycomb coated with an alumina base powder. The coated inconel honeycomb is filled with mineral wool and alumina foam and covered with a dense zirconia. Both the alumina and the zirconia are darkened. Samples, 20 inches by 30 inches, have already been successfully tested using oxy-propane equipment and a jet motor.

8.7 General References on High-Temperature Structural Materials

Extensive information on high-temperature structural materials is contained in References 1, 2, 6, 20, 21, 30, 52, 70, 119, and 126-31. Two foreign articles were translated for the review on high-temperature structural materials, and the abstracts for the two articles appear in Appendix I as Extended Abstracts 34 and 35. For other recent foreign publications in the general area of structural materials, the reader is referred to Extended Abstracts 36 to 42 in Appendix I.

IX. REFRACTORY STRUCTURAL COMPONENTS - THERMAL SHOCK BEHAVIOR

There are many indications that the thermal shock resistance of ceramic materials can be greatly increased. Major improvements have already been realized in a number of cases. Particularly noteworthy successes have derived from:

1. The control of microstructure.
2. The modification of material properties.
3. Good design practices.

Each of these points warrants further consideration before specific cases are mentioned. First, at the present state-of-the-art, ceramic articles are highly structure-dependent. Such factors as degree of calcine, fabrication technique, annealing, firing schedule, impurities, etc., can have a considerable influence on the thermal shock behavior of a ceramic part. Because of this influence, the results of thermal shock tests frequently appear conflicting. For example, a particular material may have a high resistance to thermal rupture when incorporated in a thermal insulator, but a low resistance to thermal rupture when used in a dense body. Buckley and Cocke (Ref. 132) recently tested five zirconia products, a single type of thoria, one type of magnesia, and one type of alumina to determine their ability to withstand severe thermal shock without cracking and found that the variation was as great between the various zirconia products as between the different types of materials. The zirconia products differed primarily in the type and amount of additive used to promote crystalline stability. While it is disconcerting that ceramic articles are so highly structure-sensitive, such behavior implies that the thermal shock resistance of ceramics can be significantly improved if the microstructure is properly controlled.

Second, the thermal shock resistance of a ceramic can be modified to some extent by regulating the properties of the material, and the manner in which this can be accomplished is understood at least to a small degree. The thermal conductivity and specific heat should be as high as possible to minimize thermal gradients. The coefficient of thermal expansion should be as small as possible to minimize thermal strains. The elastic modulus should be low to limit the stresses induced by the thermal strains. And finally, the material should be mechanically strong so that the stresses can be tolerated.

Third, if a system is carefully designed, it should be possible to take advantage of the outstanding features of ceramics, while minimizing the effects of their deficiencies. For example, ceramics should be used in compression whenever possible, and they should be cushioned to guard against brittle effects.

When considering the specific case histories which follow, it is important to realize that the environment is a confounding parameter superimposed on the

material property parameters in any thermal shock situation. The thermal shock behavior of a material will generally depend markedly on the severity of the environment, and a change of environment may change a material's rating relative to another material or to another form of the same material. Refer to Section 7.8.3 Factors Affecting Thermal Shock Resistance and to Section 7.8.4 Thermal Shock Parameters.

9.1 Effects of Pores

Pores have been reported to have a beneficial effect on the thermal shock characteristics of ceramic materials under certain conditions. For example, Blome and Kummer (Ref. 133) examined small test specimens and components heated with an air arc plasma or an oxy-acetylene torch and found that coarse grained porous ceramic bodies provided the best resistance to thermal shock. Glenny and Taylor (Ref. 134) heated test specimens to a temperature just sufficient to cause their failure when subjected to a bed of fluidized solids maintained at 68° F and found that low-density grades of silicon nitride invariably failed by cracking, while high-density grades failed by fracture. The benefit of pores, however, is not always available. Coble and Kingery (Ref. 135) prepared samples of sintered alumina with porosities ranging from 4 to 50 per cent by incorporating naphthalene flakes in a casting slip. When hollow cylinders of the alumina were subjected to steady-state radial heat flow, the thermal stress resistance was found to decrease with increasing porosity. The decrease was attributed in part to a decrease in the strength-to-elastic modulus ratio and to a decrease in the thermal conductivity.

It is not easy to see how pores can have a favorable influence on the thermal shock characteristics of a ceramic body. Clearly, pores in the form of open cracks would be harmful. Large color differences are often observed across even very small cracks during heating or cooling. And there should be some ill effects even in the case of well-rounded pores. Goodier and Florence (Ref. 136) considered the uniform heat flow parallel to the edge of a semi-infinite plate on a theoretical basis and found that the heat flow was disturbed when an insulated hole was introduced, and the local intensification of temperature gave rise to thermal stress. Nevertheless, there is good evidence that the thermal shock resistance is improved when a coarse pore system is present. Apparently the pores serve as crack arresters if the cracks are relatively small and if the strain energy is diffuse as in the case of high temperature spalling. The behavior seems to be associated with the reduction of stress concentration through the blunting of crack tips (Ref. 28).

The effect of porosity on the thermal shock resistance of brittle state bodies has been studied quantitatively by Huang (Ref. 137). A parallel model was used and it was assumed that the same statistics that applied to the "probability of failure" of test bars also applied to the "percentage of damage" within a given test bar. This led to the equation

$$F(\sigma) = 0, \quad \text{for } \sigma \leq \sigma_i [1 - F_i(\sigma_i)]$$

$$F(\sigma) = \frac{F_i \left(\frac{\sigma}{1 - F_i(\sigma_i)} \right) - F_i(\sigma_i)}{1 - F_i(\sigma_i)}, \text{ for } \sigma > \sigma_i [1 - F_i(\sigma_i)] \quad (60)$$

where: F_i = probability of failure for the original material

σ = stress

σ_i = stress level during a proof-test

F = probability of failure of proof-tested material on subsequent loading

The experimental work was performed using alumina foam samples of density 0.202, 0.494, and 0.623 compared to 1.00 for a zero-porosity sample. A failure curve:

$$F = 1 - \exp \left[\int \int \int a \sigma^m r^{b-m} dV \right] \quad (61)$$

was assumed, where:

r = relative density

a, b, m = materials constants

V = volume of test specimen

The proof-test consisted of a thermal shock treatment in which

1. one face of the bar was exposed to radiant heat while the remaining faces were insulated.
2. the heat source was removed.

Temperatures were monitored during heating and cooling using thermocouples at the hot face, at the cold face, and at three intermediate stations between the hot and cold faces. The experimental degradation factors (ratio of strength of exposed material to that of original material) were found to be 0, 92.2 per cent, and 100 per cent going from the lowest to the highest density material. The theoretical values were 0, 95 per cent, and 100 per cent.

9.2 Foamed Ceramics

Four case histories on the use of foamed ceramics are cited in this section.

At the Goddard Space Flight Center (Ref. 138) a foam material has been used to protect and support small solid-state devices arranged on a "card." A phosphate-bonded alumina foam was formed in place and cured at 185° F. Test cubes, one inch on a side, were shocked from 932° F, 1832° F, and 2732° F by dropping them in water. A cube shocked from 2732° F showed rounded corners and edges and showed cracks which appeared to terminate at voids in the material (the voids were relatively large and nearly spherical). The cubes shocked from 932° F or 1832° F showed slightly rounded corners and the same type of cracks described previously.

Strauss (Ref. 139) investigated phenolic-base resins and thermoplastics such as nylon, polyethylene, and polypropylene as impregnants for porous ceramics. Impregnated alumina, zirconia, silica, and silicon carbide foams were tested to determine their thermal shock resistance, and full-size nose caps were fabricated and tested to establish the feasibility of constructing hardware of resin-impregnated porous ceramics.

Strauss found that open-celled foams of 85 to 90 per cent porosity made of a high purity, self-bonded ceramic were suitable for resin-impregnation. Impregnation with phenolic or phenyl-silane resins produced sound composites. Thermoplastic impregnants tended to damage the cell structure during heating due to swelling or to rapid gas liberation, but the deficiency was circumvented by using a mixture of thermoplastic and thermosetting resins. The density of the resin-impregnated material ranged from about 60 to 90 lb/ft³. Impregnated silica was found to be a better thermal insulator than the impregnated zirconia or alumina.

Strauss tested four phenolic-impregnated samples, 4-inch diameter and 1-1/4-inch thick, in a 7-inch diameter hot gas facility under moderate heating, high thermal shock, high mass flow, a 150 decibel noise level, and a stagnation pressure of 370 lb/ft². Two samples contained an alumina matrix, and two contained zirconia. One sample of each material was made from a single piece of foam, but the others were constructed of five individual modules separated by wedge-shaped gaps which were filled with a resin-silica fiber-ceramic powder mix. When subjected to a rectangular heating pulse to a backside temperature of about 500° F, the zirconia samples suffered structural failures, but the alumina samples were not appreciably damaged. The single-piece sample of zirconia exhibited spalling soon after the beginning of the test, but the segmented sample of zirconia survived 13 minutes without failure.

Strauss also tested two full-scale phenolic-impregnated nose caps, 13 and 15-1/2-inch chord diameters, in a 14-inch diameter hot gas facility under conditions similar to those previously described. The caps were constructed using 19 to 21 modules which were 1-1/4-inch in thickness. One nose cap contained a silicon carbide matrix, the other contained alumina.

The gaps between the modules were filled with a resin-ceramic fiber-oxide powder mix, and the silicon carbide foam was treated with zirconia to a depth of 1/4-inch before impregnation to provide oxidation resistance. The silicon carbide nose cap reached 3090° F, and there was no incident up to 12 minutes of exposure. The test was terminated after the bond between the ceramic and understructure failed, but the modules which were recovered intact revealed no sign of structural damage. The alumina nose cap reached 3440° F during a 15 minute test and exhibited surface spalling and discrete surface erosion after 10 minutes. The failure was attributed to the decomposition of the impregnant and the oxidation of the residual char which left the ceramic unprotected. However, the failure was not catastrophic.

At McDonnell Aircraft Corporation (Ref. 133) refractory ceramics of about 20 to 35 per cent of theoretical density were needed to satisfy certain density requirements in an "advanced ceramic materials development program." The low density ceramics available at the beginning of the program were found to spall or crack at heating rates of 30° to 42° F/second and were thus unacceptable. To overcome the problem attempts were made to develop light weight materials with improved thermal shock resistance and to face the low density materials using a high density component with favorable thermal shock characteristics. The impregnation approach was not considered since it did not appear suitable for multiple thermal exposures. The following improved materials are reported to have been developed:

1. Chemically bonded Al_2O_3 (density 190 or 65 lb/ft³) with excellent thermal shock resistance, slight shrinkage above 2000° F, and a surface temperature limit of 3400° F.
2. Chemically bonded ZrO_2 (density 270 or 130 lb/ft³) with excellent thermal shock resistance, slight shrinkage above 2300° F, and a surface temperature limit of 4000° F.
3. Sintered ZrO_2 (70 to 90 lb/ft³) with excellent thermal shock resistance and no shrinkage to 4000° F.
4. Chemically bonded ThO_2 (510 or 200 lb/ft³) with excellent thermal shock resistance, slight shrinkage above 2400° F and a surface temperature limit of 5000° F.
5. Sintered ThO_2 (150 lb/ft³) with fair thermal shock resistance, no shrinkage to above 4000° F, and a surface temperature limit of 5000° F.

The thermal shock resistance ratings were based on a surface heating rate of 50° F/second. The chemically bonded materials are favored because they can be cured in place and easily reinforced by metals and they require less machining. The improved materials have been incorporated in ten different ceramic-metal composite designs. The majority of the designs have been based on a coated refractory metal substructure for the support of an external lightweight ceramic insulation. Mechanical attachments have

reportedly presented few problems since the ceramic-metal interface design temperature is 2000° to 3000° F. Subscale modules have been ground tested with 8 out of 22 specimens failing the thermal exposure test.

Researchers at United Technology Center (Ref. 140) are currently evaluating phenolic impregnated ceramic foams for use as baffles in an 8000° F solid fuel - liquid oxidizer rocket chamber. Generally, the starting foams are approximately 80 per cent pores and are chemically bonded (silicate or phosphate). TiC, SiO₂, MgO, Al₂O₃, ZrO₂, ZrB₂, ZrC foams have been prepared. Densities for a number of the impregnated materials are as follows:

<u>Foam</u>	<u>Density (lb/ft³)</u>
Al ₂ O ₃	62 to 75
ZrO ₂	91, 112
ZrB ₂	87
TiC	100

The foams are all highly resistant to flame impingement, even when they have not been impregnated. Their favorable behavior has been attributed to their heterogeneous nature and their low thermal conductivity. Apparently, thermal cracks do not propagate readily through such media. However, the foams are geared for a particular application. They are highly resistant to flame impingement on one face but may not be resistant to other types of thermal shock. For example, if the foams were heated slowly in a furnace, they would sinter and shrink and lose their heterogeneous character. Successful baffles have been prepared, but only after considerable development. The pressure-temperature-time relationship had to be carefully defined and controlled during impregnation and drying. The design provided for some pre-stressing due to the shrinkage of the impregnant.

In review of the four case histories cited above, it appears that chemically bonded ceramic foams are particularly well suited for use under thermal shock conditions. Apparently, their outstanding thermal shock behavior derives from relatively weak particle-to-particle bonding which limits crack propagation to microscopic distances when temperature intensities are localized. When these relatively soft materials are subjected to a sudden temperature change, they fail locally at the exposed surfaces but retain their strength (Ref. 141). If these materials are sintered at a high temperature in an attempt to improve their strength, thermal shock resistance will be sacrificed. Thus metal reinforcement may be essential to the successful use of chemically bonded ceramics. Fortunately, these materials can be cured in place and metal reinforcement is easily achieved.

9.3 Effect of Particle Size

A number of investigators have found that the thermal shock characteristics of a ceramic article can be significantly improved through the careful control of particle size distribution.

Blome and Kummer (Ref. 133) examined small specimens and components which were heated under oxidizing conditions to a surface temperature rise of 50° F/second and found that coarse grained porous bodies provided the best resistance to thermal shock. Yavorsky (Ref. 142) found that the thermal shock characteristics of zirconia were improved by using a mixture of coarse and fine grains. Another recent development is a special oxide refractory* which is reported to have extremely good thermal shock resistance even though it has a high density. The favorable thermal shock characteristics of the oxide refractory were achieved through the careful control of the size and distribution of particles.

Logan and Niesse (Ref. 121) studied the effects of boron nitride additions on the properties of a 90 mol per cent ZrB_2 - 10 mol per cent $MoSi_2$ composition. Boron nitride was added to the base composition in three amounts (5, 10, and 20 mol per cent) and in three particle sizes (- 40 + 70 mesh, - 120 + 220 mesh, and - 325 mesh). A statistical analysis of the data showed that relatively coarse particles of boron nitride lowered the strength of the base composition but improved the heat shock resistance, while relatively fine particles of boron nitride had the opposite effect. The evaluation was based on hot pressed samples.

Vogan and Trumbull (Ref. 143) developed thoria and magnesia bodies for use in metal-ceramic composites and found that good thermal shock resistance was imparted to the bodies through the control of particle size distribution. The magnesia specimens were formed by dry pressing using a moisture content of 4 per cent and pressures from 12,000 to 16,000 psi.

The particle size distribution was found to have a great effect on the thermal shock resistance of a magnesia body. Magnesia bodies containing a wide range of particle sizes with approximately 40 per cent of the material between -14 and +65 mesh withstood heating rates far in excess of those permissible for conventional ceramic articles. Thoria bodies dry pressed at 6300 psi with 4 per cent moisture showed a thermal shock resistance comparable to zirconia when a wide range of particle sizes was used. The evaluations were based on magnesia samples and thoria samples sintered at 2800° F for 4 hours.

Bal'shin and Likhtman (Ref. 144) suggested that cracks due to thermal shock would generally be formed between the structural elements of a material and not within them. If the structural elements are very small, inter-particle cracks might be favored, and the thermal shock resistance could be low. However, if the elements are relatively large, the formation of inter-particle cracks would be more difficult, and the resistance to thermal shock could be greatly improved. If the structural elements are very large, they could fracture from within and become subdivided so that the resistance to thermal shock would increase with increasing dimensions of the structural elements only up to a certain limit. Concomitant effects might include:

* B & W CEROX, Babcock & Wilcox.

1. Preferred orientation of newly formed sub-elements.
2. Variations in bonding - the bond may be weaker between larger structural elements.
3. Variations in porosity - coarse pores might be associated with large structural elements.

Bal'shin and Likhtman also suggested that the thermal shock resistance could be improved through the use of complex structural aggregates since stronger bonding could be achieved between particles within the aggregates than could be achieved between simple particles of the same size. An investigation was made to determine the effects of granulation on the thermal shock characteristics of TiC - Cr₃C₂ - graphite hot pressed at 3992° F under a pressure of about 320 psi. Granulation of the material significantly increased the thermal shock resistance. The optimum granule size was about 160 microns when the initial particle dimensions were of the order of a few microns. As the strength of the granules increased their optimum size was increased.

In summary, the evidence now seems conclusive that the thermal shock resistance of a ceramic article can be significantly improved through the careful control of the particle size distribution. The thermal resistance increases with increasing particle size at least up to a certain limit, which suggests that thermal shock cracks are generally formed between the particles and not within them. The use of a wide range of particle sizes is also favorable. Apparently the latter provides a structure with a heterogeneous character. For example, the bond between large particles may be weaker than the bond between small particles. Thus when a wide distribution of particle sizes is used, crack propagation may be limited to microscopic distances and still provide the necessary stress relief. This heterogeneous nature may also be imparted to a body through granulation. The granulation approach could also lead to the use of lower sintering temperatures which, in turn, could enable larger parts to be fabricated.

9.4 Effect of Crystalline Inversions

Herring (Ref. 145) has studied the relative influence of quartz inversions and thermal gradients as they affect the cooling of ceramic ware. Ottawa sand, - 65 to + 200 mesh, was used in the amount of 15 weight per cent for a quartz addition to a ceramic base material. Wollastonite, also - 65 to + 200 mesh, was used in the amount of 15 weight per cent as an inert addition to the base material. Wollastonite was selected as a standard of comparison because it shows no inversion below 2192° F (quartz shows its alpha to beta inversion at 1063° F), has negligible moisture expansion, high strength, low warpage, high dimensional stability, good thermal shock resistance, low firing temperature and low shrinkage. Thermal shock tests on extruded and sintered samples showed that there was no weakening due to the quartz inversion on heating or cooling, regardless of the speed through the inversion. However, the samples lost considerable strength after two

cycles in a thermal fatigue test, and the loss was greater in the case of the quartz samples. It appears that on the first cycle localized cracks may have developed to provide stress relief, but on the second cycle the cracks acted as stress raisers and became critical. No sudden expansions were observed during the quartz inversion.

Many investigators have studied zirconia and found that its poor thermal shock resistance is caused by a crystalline inversion which occurs at about 1830° F. While the inversion has limited the use of zirconia in high-temperature structures, the shortcoming can be averted by stabilizing the material with various oxide additions. A small inversion appears to be necessary for high thermal shock resistance because the overall thermal expansion is then small and gradual, and complete elimination of the inversion leads to a high coefficient of thermal expansion (Ref. 146). It has also been suggested that a small amount of micro-cracking might aid in stress relief without causing significant degregation of the material (Ref. 142).

A nose tip utilized on ASSET (Ref. 133) contained zirconia rods at the area of maximum temperature. The zirconia was coarse grained, relatively porous, and partially stabilized with calcia and was highly micro-cracked in the "as sintered" state. The small rods have been heated at rates up to 200° F/second without catastrophic failure. The excellent thermal shock resistance was attributed to the presence of micro-cracks and to the low elastic modulus of a micro-cracked and porous structure. Thermal stress cracking may have occurred to a limited degree, but the rods were reportedly integral enough to withstand additional heating cycles in the absence of mechanical or vibrational loads. There was some evidence that the thermal shock resistance decreased with time at temperatures of approximately 4000° F.

Yavorsky (Ref. 142) used a mixture of stabilized and monoclinic phases and a mixture of coarse and fine grains to improve the thermal shock characteristics of zirconia. The material exhibited surprising thermal shock resistance in comparison to other formulations.

Seegar, Lowrance, and Rodgers (Ref. 147) used a mixture of stabilized grog and unstabilized zirconia fines to obtain a thermal shock resistant zirconia with only 1.43 per cent calcia. It is remarkable that specimens of this formulation withstood heating rates of 1300° F/second. The specimens showed a very much lower total thermal expansion at 4000° F than specimens fabricated from other stabilized grades of zirconia. However, the heterogeneous material showed numerous fissures at the boundaries of the large particle constituent. The material was recommended for rigorous cyclic temperature applications in which mechanical and vibrational loads are low.

Ohnsyty and Stetson (Ref. 148) found that the modification of hafnia with zirconia and/or yttria appeared to be capable of producing a close expansion match with 90 Ta - 10W alloy. However, yttria additions which partially stabilized the cubic form of hafnia and improved the expansion match, decreased the inversion temperature on cooling to 2000° F to 2500° F

where the probability of brittle fracture was increased. It was suggested that high purity hafnia and blends without a stabilizer may provide better thermal cycling performance because the conversion occurs above 3000° F where stress relief may occur through plastic deformation.

9.5 Effect of Notches

Few studies have been made on the effect of notches on the thermal shock resistance of ceramic shapes, and the few data available appear conflicting. McKinney and Smith (Ref. 149) tested two types of alumina and found them highly sensitive to notching. An unnotched specimen 4-inch in diameter of either alumina showed better resistance to thermal shock fracture than the same material in a specimen with a 6-inch diameter and a $1/4$ inch notch on each side. Brown (Ref. 95) evaluated the thermal stress resistance of fused alumina with a porosity of approximately 35 per cent, a high density alumina with a theoretical density of about 99 per cent, and a magnesia material with a theoretical density above 99 per cent. Notches slightly lowered the time required to fracture the porous alumina, significantly reduced the time-to-cracking for the high density alumina, but had no appreciable effect on the time required to crack the magnesia. It was noted that some magnesia specimens cracked at regions of fine porosity rather than at the notch and that a high degree of scatter was associated with the data collected on unnotched magnesia specimens.

It appears that the notch sensitivity of a ceramic material depends on the artificially induced notches, the types and positions of the inherent notches (flaws) in the material, and the interactions between the inherent notches and those artificially induced. Refer to Section 7.4 Notch Sensitivity.

9.6 Effect of the Temperature Dependence of Material Properties

Certain properties of ceramic materials depend significantly on temperature. Sometimes the dependence is drastic, and sometimes the nature of the dependency is surprising. In any event, the dependency must be carefully considered when a reasonable prediction of the thermal shock characteristics of a material is required.

At Brush Beryllium Company (Ref. 150) beryllia and beryllides were subjected to a thermal shock test designed on the basis of their expected use conditions. Specimens, 3/8-inch diameter by 3-inch length and 1/4-inch by 1/2-inch by 3-inch, were heated to 1600° F or to 2500° F in a bottom loading furnace on beryllia anvils. The samples were then lowered from the furnace and the center of the bars were subjected to an air blast until the centers were below red heat. Samples were cycled 50 to 100 times, and visual inspections were made with the aid of a dye. The beryllia showed cracks after a few cycles when it was shocked from 2500° F, but beryllia shocked from 1600° F did not develop cracks. Apparently the high thermal conductivity of the beryllia (at the lower temperatures) was beneficial. The beryllides withstood 100 cycles from 2500° F without cracking, but from 1600° F the

samples were more susceptible to thermal shock. Apparently the increased strength of the beryllides (at the higher temperatures) was beneficial.

Astarita (Extended Abstract 8, Appendix I) has demonstrated that it cannot be affirmed *a priori* if variations in the coefficient of thermal expansion and elastic modulus are favorable or unfavorable to the thermal shock resistance of a material. Stress diagrams were produced on plane surfaces, 11 cm thick, of a selected ceramic material relative to two types of thermal cycles: (1) by choosing average constant values for the coefficient of thermal expansion and modulus and (2) by taking into account their variation with temperature. For one type of thermal cycle the variation of the properties led to higher stress levels within the slab, while for the other thermal cycle the variation led to lower stress levels.

9.7 Effect of Impurities

Huffadine (Ref. 151) observed that the thermal expansion of molybdenum disilicide was essentially the same as that of alumina over the temperature range 32° to 1832° F and that the two materials would adhere strongly when simultaneously hot pressed. As a result, Huffadine was prompted to investigate the properties of bodies formed by hot pressing mixtures of alumina and the disilicide. Surprisingly the addition of 30 weight per cent alumina increased the impact resistance of the disilicide by a factor of five after the hot pressed bodies were heated in air at 2192° F for 200 hours. However, alumina additions up to 50 per cent decreased the oxidation resistance, and increasing alumina content progressively reduced the thermal shock resistance. The thermal shock resistance was considerably lowered by as little as 5 per cent alumina. It is significant that the primary creep at 1832° F of the disilicide or the disilicide-alumina was very much reduced by heat treatment at a temperature about 120° F above the hot pressing temperature.

Shaffer (Ref. 152) evaluated composite bodies of ZrB_2 with $TaSi_2$, WSi_2 , $NbSi_2$, $MoSi_2$, $ZrSi_2$, Zr_5Si_3 , (MoTa) Si_2 and (Mo, Ta₄) Si_2 . From the standpoint of oxidation resistance, high temperature strength, and thermal shock resistance, molybdenum disilicide proved to be the best. The maximum oxidation resistance was obtained using a molybdenum disilicide addition in the range 5 to 15 molar per cent. Logan and Niesse (Ref. 121) determined the optimum addition of boron nitride to the zirconium diboride-molybdenum disilicide solid solution on the basis of tests of oxidation resistance, flexural strength, and thermal shock resistance and found the optimum composition to be 86.1 weight per cent ZrB_2 , 12.8 weight per cent $MoSi_2$, and 1.1 weight per cent BN.

Arenberry, Rice, Schofield, and Handwerk (Ref. 153) studied the effect of small additions of Al_2O_3 , stabilized ZrO_2 , and MgO on the densification and thermal shock resistance of a thoria body (96.93% ThO_2 , 2.65% U_3O_8 , and 0.42% V_2O_5). The particle size distribution for the thoria was 60% - 40 + 60 mesh, 15% - 60 + 80 mesh, and 25% - 100 mesh. The alumina and stabilized zirconia were -325 mesh, and the magnesia was -200 mesh. Five weight per cent stabilized zirconia improved the thermal shock resistance, but 5 weight

per cent of the alumina or magnesia did not. Higher amounts of the zirconia (10, 20, or 40 weight per cent) were not effective.

9.8 Effect of Low Modulus Additions

Shaffer (Ref. 154) investigated the thermal shock resistance of composites consisting of a high elastic modulus continuous phase and a low elastic modulus dispersed phase. Four model systems were studied in detail: zirconium carbide-graphite, silicon carbide-graphite, zirconium diboride - boron nitride, and aluminum oxide - zirconium oxide. Results showed that low modulus dispersions reduced the elastic modulus of a composite by a factor greater than that predicted on the basis of simple volume additions. While the low modulus material lowered the strength, the critical strain was increased, and the thermal shock resistance was improved. The concept was successfully applied to a rocket nozzle insert for a solid propellant motor. While pure carbides shattered when subjected to the high mass flows and heat transfer rates associated with rocket nozzle applications, uniform composites such as silicon carbide-graphite were suitable for use in some of the less severe rocket nozzle situations.

Shaffer observed that composite bodies with a low modulus phase generally exhibited a thermal shock resistance much greater than that predicted on the basis of critical strain alone. Shaffer also observed that many bodies which had survived severe thermal shock conditions contained numerous internal cracks. The behavior appeared to be associated with the quantity of stored elastic energy that was released during fracture. An addition of 30 volume per cent of graphite to zirconium carbide lowered the stored elastic energy to one-tenth that of pure zirconium carbide. When samples of zirconium carbide-graphite and samples of the carbide alone were tested to failure under compression, the degree of shatter was noticeably greater for samples of the pure carbide than it was for the composite samples. In another test, bars of aluminum oxide-boron nitride were subjected to a cross-bending load, and the bars appeared to "bend" as a result of myriad small cracks, none of which extended through the sample.

Lepie (Ref. 155) co-deposited zirconium carbide with graphite pyrolytically and obtained a refractory which exhibited unique room temperature strength in the range 40,000 to 100,000 psi and a positive temperature coefficient of strength, in addition to exceptional thermal shock resistance. Excess carbon resulted in a second phase and, more importantly, in a marked change in the size of the carbide grains. The carbide grains were small and irregular in shape and bore little semblance to the large columnar grains normally associated with the pyrolytic carbide. The grains were very small at high carbon contents. At 80 weight per cent carbon the carbide grains were below 200 Å (i.e., the size associated with the dispersed particles in many of the best dispersion hardened metals), and the material became twice as strong as cast iron. Samples pyrolytically co-deposited from hafnium carbide and graphite were also studied, but less extensively. For a 10 volume per cent zirconium carbide dispersion in graphite, the thermal shock resistance was estimated to be two orders of magnitude higher than that for

the pure pyrolytic carbide. A hafnium carbide-graphite nozzle insert showed no ill-effects from a sudden exposure to a propellant flame temperature of 6550° F, while its dense graphite back-up fractured in many places.

Leeds, Kendall, and Ward (Ref. 156) investigated the properties of titanium carbon alloys with carbon contents in the range 18 to 30 weight per cent synthesized and fabricated by arc-melting and gravity casting techniques. The existence of a hyperstoichiometric eutectic was confirmed and established in the vicinity of 26 weight per cent carbon. The existence of free graphite platelets throughout hypereutectic specimens resulted in the improvement of their thermal shock and room temperature brittleness behavior.

9.9 Cermets

The original interest in using cermets stemmed from the hope that a dispersed metal phase would impart to a ceramic the quality of ductility without disturbing the ceramic's favorable attributes. The concept invoked a great deal of interest among engineers who sought turbine-blade materials with a low density, high melting point, and good oxidation resistance, and intensive investigations were made of the titanium carbide-cobalt, titanium carbide-nickel, and alumina-chromium systems. However, the interest in these materials has faded because of their low impact strength and poor reliability of performance and because even the most promising cermets have offered a strength advantage only in the temperature range 1800° to 2200° F. Nevertheless, it is instructive to recall the efforts which have been made to utilize cermets.

Huffadine, Longland, and Moore (Ref. 157) studied the alumina-chromium system and found that the thermal shock resistance of the cermet containing 20 per cent chromium did not differ greatly from that of a high-grade sintered alumina. However, it was possible to increase the resistance by increasing the metal content or by adding molybdenum to the chromium to give a better expansion match between the metallic and non-metallic phases. Richardson (Ref. 158) reported that the early bodies composed of cobalt or nickel-bonded titanium carbide exhibited low thermal shock resistance but that improvements could be made through the additions of alloying elements such as molybdenum, aluminum, and chromium. However, Bragdon (Ref. 159) reported that as the thermal shock resistance of the cermets was improved, more brittle failures were encountered.

Only a few cases are known where the thermal shock resistance of a ceramic material was greatly improved with the addition of only a small amount of metal. Hoffman (Ref. 160) reported that the thermal shock resistance of the composition 97.5 weight per cent zirconium diboride - 2.5 weight per cent boron compared favorably with that of the titanium carbide-cobalt and titanium carbide - nickel cermets. Vazquez and Accountis (Ref. 161) investigated the properties of anion-deficient zirconia and found that it had a considerable superiority over stoichiometric zirconia and over stabilized zirconia with respect to thermal shock resistance and stability. Zirconia specimens with small additions of copper were evaluated, and the test firing of a throat insert fabricated from an anion-deficient zirconia indicated a

thermal shock resistance equal or better to that of silicon carbide. The shock resistance was attributed to the anion deficiency. However, Voruz and Accountis indicated that the copper could act as a stress reliever and inhibit crack propagation to some extent. In one test the crack propagation in a 4 per cent copper composite was instantaneous, while it was relatively slow and could be arrested by load diminution in a 7 per cent composition.

Glenny (Ref. 162) has reviewed the design concessions that were made in an effort to utilize cermets in turbine-blade applications. The use of hollow nozzle guide vanes and a slight thickening of the trailing edge improved the thermal shock behavior to an appreciable extent. Stress concentrations at aerofoil-platform junctions were obviated by using a constant section aerofoil. Restraints on the expansions were eliminated by allowing free radial movement in the inner and outer shroud rings. Longer lives were obtained through the use of generous radii and through the use of soft-metal screens to reduce stress concentrations due to machining tolerances. Impact strength was improved by metal enrichment of the trailing edge, by the use of well-rounded ceramic particles, by cladding, and by the use of alternate cermet and metal layers. Non-destructive inspection was used in an effort to improve the reliability of performance. Surface flaw detection was accomplished using fluorescent penetrant tests. The most successful test used for internal flaw detection was one that involved electrical conductivity measurements. Proof testing of the actual components was an essential part of the inspection.

9.10 Skeleton-Skeleton Structures

Baxter (Ref. 163) reported that in general metal-ceramic composites have a higher thermal shock resistance when the two phases are continuous and interlocking than when only the ceramic phase is continuous. Williams (Ref. 163) considered infiltration to be a more favorable approach to the development of strong metal-ceramic structures than the conventional mixed-powder techniques. Williams investigated the model system alumina-silver as an example of the complete wetting of an oxide phase by a metal. The composition 50 Al₂O₃: 50 Ag was obtained by impregnating a lightly sintered alumina compact. The composition had a flexural strength above 22,000 psi at 1382° F and withstood hundreds of thermal shock cycles from temperatures up to 1760° F into a stream of cold air, even though the melting point of silver is 1760° F and its strength at 1382° F is negligible.

Baxter (Ref. 165) investigated bodies consisting of a continuous phase of alumina and a continuous phase of copper and found that they had a high level of resistance to thermal shock. Alumina blocks were impregnated with cuprous oxide by immersion in molten oxide for 1 to 2 minutes. The alumina was pre-heated to 2012° F and immersion was carried out progressively to fills of 98 to 100 per cent of the interconnected porosity. Following machining, the cuprous oxide was reduced by subjecting the samples to dry hydrogen at 1832° F for one hour. The thermal shock test consisted of exposing the end of a right cylinder, 3/4-inch diameter by 3/8-inch thick, of the material to the exhaust from a small rocket motor for 3 seconds. For the first 0.035 second the specimen was exposed to burning magnesium which produced a heat flux of 7400 BTU/ft²-sec; for the remainder of the 3 second period the heat flux

was 1850 BTU/ft²-sec. Samples containing 43 to 52 per cent alumina, 25 to 30 per cent copper and 23 to 27 per cent voids were tested. The only damage was light to moderate edge cracks (rapid shear failure) and a roughened surface.

9.11 Metal Fiber-Reinforced Ceramics

A number of investigators have designed metal-ceramic composites in which the metal phase is introduced as fibers or as whiskers, and many of the structures prepared in this manner have exhibited better thermal shock resistance than the unreinforced ceramic. Levy (Ref. 166) suggested that the use of metal fibers would offer two distinct advantages over the use of individual metal particles as far as the thermal shock behavior is concerned:

1. Fibers can transmit stress over long distances and can absorb the strains induced by thermal gradients.
2. Fibers provide a continuous ductile network which tends to hold a composite together during fabrication and service and prevent catastrophic failure.

In addition, fibers offer the potential of allowing a practical prestressed system of the reinforced concrete type where the brittle phase is held in compression (Ref. 162).

Work conducted at The Boeing Company (Ref. 143) on composites for applications at moderate temperatures has produced a phosphate-bonded alumina matrix reinforced with molybdenum fibers. The best results were obtained with 0.002-inch diameter fibers 1/4-inch long which increased the thermal shock resistance to the point where samples could withstand three quenches from 2600° F to water.

Fisher and Hodson (Ref. 167) made composite structures of tungsten fiber reinforced B₄C, SiC, TaC, HfC, TiC, and ZrC. While B₄C, SiC, and TaC reacted extensively with the metal phase and were eliminated as possible base materials, a good metallurgical bond was formed between the metal and the other carbides during hot pressing. A hot pressed tungsten reinforced titanium carbide nozzle exhibited excellent resistance to thermal shock and erosion.

At Alfred University (Ref. 168) research was devoted to the study of molybdenum fiber reinforced alumina. A review of the literature indicated that the nature of the bond between molybdenum and alumina was favorable. A chemical bond without excessive reaction was desired, and indications from the literature were that a chemical bond is formed between alumina and molybdenum at high temperatures and that the bond resulted from the formation of a small, controlled amount of reaction. The major difficulty associated with the fabrication of the system seemed to be that associated with the shrinkage of the ceramic constituent during forming and/or firing. In view of this, hot pressing was favored.

Norton 38-900 alumina was used with additions of 0, 5, 10, and 20 weight per cent molybdenum fibers which were 0.002-inch diameter x 1/8-inch long.

The fibers were cut to size from unannealed wire from Fansteel Metallurgical Corporation. Test bars, 3/8-inch x 3/8-inch x 3-inch or 4-inch length, were used. The batches were thoroughly mixed by tumbling, charged into graphite gang molds, and hot pressed at 3000 psi to produce bars with a surface free of fibers which provided some protection to oxidation during testing. The densities ranged from 91 to 93 per cent of theoretical. Heating the molds to 3000° F consumed 90 minutes, and cooling back to room temperature was accomplished in 4 hours. To aid in the production of a fiber free surface, the graphite dies were coated with a thin wash of alumina in glycol alcohol and water.

Test bars were thermal shock tested by inserting them into a furnace held at 2200° F, allowing 5 minutes for stabilization, and cooling in air. Attempts to measure the thermal shock resistance by sonic modulus measurements were unsuccessful since some bars maintained a high elastic modulus yet could be broken by hand. As a result, it was decided to break a small number of bars after every two cycles in cross bending up to 6 cycles.

The alumina bars had an initial flexural strength of about 36,000 psi, but essentially no strength after two thermal cycles. Micro-cracks were readily observable in alumina containing 10 and 20 per cent fibers as expected since the thermal expansion of alumina exceeds that of molybdenum. Nevertheless, the fibers seemed to increase the resistance of the bars to thermal endurance failure. With 10 per cent fibers, the strength remained essentially constant at about 9,000 psi through all six cycles. With 20 per cent fibers, the strength decreased from about 15,000 psi to about 11,000 psi during the six cycles. With 5 per cent fibers, the strength was about 7,000 psi after six cycles.

The impact resistance decreased appreciably with the fiber additions. However, it was felt that the use of longer fibers might lead to an increase in resistance to impact.

The thermal conductivity was increased by the fibers, and the effect was directional because of orientation.

In a later study at Alfred University (Ref. 169) two types of ceramic-metal fiber composites were considered. In one type the thermal expansion of the ceramic exceeded that of the metal, and the ceramic developed a network of microcracks while cooling from the fabrication temperature. In the other type the thermal expansion of the ceramic did not exceed that of the metal and a "noncracked system" was obtained.

As an example of a "microcracked system" an alumina-molybdenum fiber composite was examined. Norton 38-900 alumina ($E = 50 \times 10^6$ psi) and molybdenum fibers ($E = 42 \times 10^6$ psi) were thoroughly mixed by shaking and hot pressed in a graphite mold at 3000° F under 3000 to 5000 psi. The graphite mold was coated with alumina so that the composite had a fiber-free surface which gave some protection against oxidation of the molybdenum. The modulus of rupture of 2-inch x 3/8-inch x 1/4-inch bars were determined before and

after four thermal cycles, 2200° F for 10 minutes to air while resting on a thick steel plate. The strength of the composite was found to be less than that of the pure, hot-pressed alumina. However, the strength of the composite was maintained through four thermal shocks, while the alumina alone failed completely in one or two cycles. There was, of course, some sacrifice in density. The density increased from 240 to 300 lb/ft³ with the addition of 20 volume per cent molybdenum. The smaller diameter fibers gave a higher composite strength but were slightly more susceptible to oxidation.

A mullite-alumina body ($E = 34 \times 10^6$ psi) reinforced with molybdenum fibers ($E = 42 \times 10^6$ psi) was studied as an example of a noncracked system. The composite was fabricated and tested in the same manner as the alumina-molybdenum system except that the hot pressing was accomplished at 2900° F and 5000 psi. Composites were obtained with flexural strengths exceeding 30,000 psi following four thermal shock cycles, and an examination of polished sections of these composites disclosed no cracks in the ceramic phase after the thermal shock test. The flexural strength of unreinforced hot-pressed samples was 22,500 psi.

Easkin, Arenberg, and Handwerk (Ref. 170) considered thoria compacts reinforced with fibers of mild steel, stainless 430, molybdenum, niobium, Zircaloy-2, and zirconium. The compacts were hot pressed at 2732° F and 2500 psi, and very little oxidation of the fibers occurred during the hot pressing operation. Hot pressed samples were subjected to a thermal shock test which consisted of heating specimens to 1832° F and quenching with mercury. The compacts containing steel fibers and compacts of thoria alone spalled severely after a single thermal shock. However, most of the steel fibers had been forced from the compacts during hot pressing. The compacts containing zirconium and Zircaloy-2 were highly susceptible to spalling. A number of the compacts failed in the mold during cooling. Examination of the fibers of zirconium and Zircaloy-2 in the fired compacts showed that they were highly embrittled. Niobium fibers increased the resistance to spalling considerably when the fibers were not completely embrittled during hot pressing. The molybdenum fiber-reinforced thoria had a much better resistance to spalling than thoria alone, in spite of the presence of microcracks caused by the thermal mismatch. Samples containing only two and three per cent molybdenum fibers withstood two and three thermal shocks, respectively. Thin fibers were more effective than thicker ones, and the microcracks formed during fabrication served as crack suppressors and, together with the fibers, relieved stresses and prevented catastrophic failure. The compacts had a fairly characteristic number of cracks per unit volume after several shocks, depending on the percentage of fibers used.

9.12 Use of Metal-Ceramic Layers

Multilayer composites have received some study. Most of the investigations have been conducted in the area of flame-sprayed coatings.

Huminik (Ref. 171) has reviewed the design innovations that were made to produce sound coatings for high-temperature structural components. Upon

testing several single-phase coatings on stainless steel in the exhaust of a solid propellant rocket, it was found that all coatings failed within two minutes. However, it was noted that molybdenum coatings provided good erosion resistance and excellent bonding and that alumina offered good heat-insulating properties and adequate thermal shock resistance for the application. To capitalize on these properties six layers of molybdenum with an average thickness of 2 mils per layer were used alternately with five layers of alumina with a thickness of about 7 mils per layer. The multilayer coating withstood the full two minutes of the test with no spalling and only slight erosion of the top molybdenum layer. Similar coatings have been used to completely protect aluminum for two seconds of thrust burning from a rocket blast temperature of 4500° F and to completely protect a titanium alloy under the same conditions. Attempts to replace the alumina with zirconia in the multilayer system met little success, regardless of the laminating metal selected. A 50 mil alternating multilayer coating of Mo-Al₂O₃ on a 40 mil fiber glass substrate was also tested using the rocket motor facility. The composite withstood the test with no incident.

Huminik describes another test in which the multilayer Mo-Al₂O₃ coating was used to protect a "Hastelloy X" afterburner rake. The rake was exposed three times for a total of 18 minutes to severe vibration at 3000° F. While three layers were lost during each exposure, the rake was completely protected.

To provide a more resistant and better bonded coating, strips of Mo and Al₂O₃ have been sprayed alternately, using a barrier or masking screen and changing the direction of spray, to produce a complex weave or grid type of coating. On graphite, this type of coating has survived a 10 minute exposure to air at 4500° F. Suitable thick coatings have been obtained on simple tubular parts by adjusting and synchronizing two flame-spray guns and rotating the tubular part.

Finally, Huminik points out that Solar Aircraft Company has developed a series of ceramic, cermet, and metallic coating mixtures based on more than 15 years of experience and has identified a large number of coatings for use in specific environments when applied to a wide range of metal structures.

Simpson (Ref. 172) described a new type of metal-ceramic composite, referred to as a "macro-laminate composite," which was developed by The Boeing Company. Metal and ceramic powders are suspended in liquid vehicles with organic resins to form paints. The paints are then applied alternately by brushing or spraying to a substrate to build up a laminate. The laminate is stripped from the substrate and broken into particles, and the particles are warm pressed and sintered in an inert atmosphere to form a dense structural part. The use of thermoplastic binders allows large complex shapes to be fabricated. The systems niobium-yttria, tantalum-alumina, molybdenum-hafnia, and molybdenum-mullite-alumina have been evaluated. The Mo-HfO₂ system was studied rather extensively because of its superior oxidation resistance, good thermal shock resistance, and high potential use temperature. The careful control of composition and processing parameters led to the obtainment of a system with a room temperature flexural strength of about 50,000 psi,

a 3000° F flexural strength of 16,000 psi, and excellent oxidation resistance to 4000° F. Compressive elastic deformation up to 11.8 per cent and ultimate compression strength to 150,000 psi have been achieved with less than 60 volume per cent metal.

9.13 Metal Wire-Reinforced Ceramics

The use of coarse metal wires or metal strips to reinforce a structural ceramic has received some consideration. For example, in the ASSET program (Ref. 173), it was found that thoria with a density of only 70 per cent of theoretical would protect tungsten from oxidation for at least 15 minutes at temperatures above 4000° F and that thoria could be reinforced with a tungsten wire mesh to provide impact and thermal shock resistance if the reinforcement extends close to the heated surface to prevent spalling.

At Lockheed Missiles and Space Company (Ref. 174), tests were made on LMSC's "Thermo-Struct" (a composite structural system consisting of a rigid substrate, a wire or fiber reinforcing element joined to the substrate, and a coating of ceramic or other suitable composition sprayed onto the substrate reinforcement assembly) and on Marquardt W-reinforced ZrO_2 (a composite structural system consisting of a rigid substrate and a bonded zirconium oxide reinforced with a sinusoidal web of tungsten). The thermal environment was accomplished using a Giannini Plasmatron (50 kw output rating for continuous operation) and using argon, nitrogen and oxygen gases to simulate reentry conditions. The composites were not sensitive to severe thermal shock to 4800° F, and Marquardt's structure displayed resistance to prolonged and/or cyclic heating in oxidizing atmospheres up to about 4500° F. It was concluded that the composite concept (as exemplified by the structures tested) offered promise for solution of leading edge or nose cap structural components problems.

Levy (Ref. 166) has reported that an aluminum phosphate-bonded alumina reinforced with a stainless-steel corrugated strip was developed to insulate a combustion chamber and reduce its operating temperature. By substituting a molybdenum wire mesh precoated with a pack cementation coating for the stainless steel, the concept was extended to the fabrication of a wing-leading-edge configuration which successfully withstood several 20 minute exposures up to 3500° F. The concept was further extended to higher operating temperatures through the use of phosphate-bonded zirconia with the addition of chromia to improve workability and increase the emissivity. A coarse-grain zirconia with 15 weight per cent chromia was incorporated into a reinforced ceramic coating. The ceramic was applied to a 0.5 per cent Ti molybdenum alloy sheet with corrugated strips of 0.010-inch thick by 0.125-inch wide molybdenum alloy which had been resistance welded to the substrate after applying plasma flame sprayed chromium to protect the molybdenum against oxidation. The welded assembly was covered with a vitrified coating (to further enhance the oxidation resistance of the molybdenum) before the ceramic matrix was trowel-impregnated into the surface and cured at 300° F. The resultant system exhibited a 2300° F thermal drop across a 1/4-inch thickness when the ceramic surface was held at 4200° F under steady state conditions. When the surface was heated to 4400° F, held at that temperature for 2 minutes, and then dropped into water, no damage was observed after two cycles.

9.14 Honeycomb Structures

To adapt high purity ceramic bodies to severe heat transfer situations, the ceramic is often used in the form of small individual elements. This approach often alleviates the thermal shock problem. Generally, small ceramic shapes are more reliable and stronger than a large ceramic shape, and a small shape can be held to closer dimensional tolerances. When the ceramic is used in the form of small elements, it is often possible to limit in service fracture to a small local area and prevent catastrophic failure. This is especially true if a soft bond exists between the individual elements. In addition, a small ceramic part is generally easier to fabricate and, pound for pound, less expensive than a large ceramic part.

Adams and Scala (Ref. 175) studied the techniques of wire impregnation and honeycomb reinforcement and found the latter to be most successful. The thermal shock resistance and mechanical properties of magnesium oxide were considerably improved by resorting to small "pencil" shapes. A standard metallic honeycomb was filled with magnesium oxide and consolidated to a suitable density. When test bars of the composite were loaded in bending beyond the peak stress, deformation or yielding occurred rather than a complete rupture typical of monolithic brittle state materials. The honeycomb metal effectively interrupted the propagation of cracks which were formed in the ceramic. The concept was extended to the fabrication of a nose cone for an ICBM test reentry vehicle which was recovered April 8, 1959 after a 5000 mile flight down the Atlantic missile range.

Vogan and Trumbull (Ref. 143) evaluated magnesia, thoria, and zirconia for use in honeycomb structures. Inconel and platinum were selected for use as honeycomb reinforcement. Platinum proved to be the better of the two, but was not favored because of its high cost. Superalloys such as Rene' 41 were considered, but they tended to embrittle during the sintering operations. The problems associated with the sintering of Inconel were eliminated through the use of an inert atmosphere sintering cycle. Test results showed that the reinforcements served primarily to control thermal shock and to limit subsequent crack growth. Large structures, basically a chemically bonded zirconia in a noble metal honeycomb, exhibited excellent thermal shock resistance for operation at 4200° F when the proper honeycomb cell size was selected.

A nose tip utilized on ASSET (Ref. 133) consisted of small diameter zirconia rods placed side by side at the area of maximum temperature and trapped by small zirconia blocks which in turn were held by a coated molybdenum retainer ring. The blocks served to protect the retainer and to form a hexagonal boundary for the rods. The blocks, rods, and retainer were mechanically locked together at the base, and a chemically bonded zirconium oxide cement was used to fill the interstices between the rods and to form a smooth surface. The zirconia was coarse grained, relatively porous, and partially stabilized with calcia. A full size nose tip was quenched in water from 3800° F without catastrophic failure. Full size nose tips also withstood up to seven ASSET reentry thermal cycles before the ends of the zirconia rods spalled, although the rod ends spalled during the second cycle when the nose tips were subjected to intense vibration and rapid heating simultaneously.

9.15 Radomes

Bear, Gates, and Robertson (Ref. 176) evaluated small ogival radomes, approximately 6 inches in diameter by 14 inches in length, made of a 97 per cent alumina oxide ceramic by Gladding, McBean and Company and attempted to correlate thermal shock test results with calculated predictions based on the thermal stress analysis of a thin walled cylinder. Four alumina radomes were exposed to the radiant heat generated by banks of quartz tube lamps, while the temperature was monitored using thermocouples on the inner and outer surfaces at three locations on the circumference at a distance of 10 inches from the nose. Heat was applied to the radomes as rapidly as possible until a pre-selected wall temperature difference was attained. The heat input was then adjusted to maintain the difference constant, and the heating was continued until failure occurred or until the surface temperature reached 1900° F. The radomes usually broke into several pieces when failure occurred, and the fractures took place in only a fraction of a second. Test results on four alumina radomes indicated that the maximum tensile stress at failure was about 20,000 to 25,000 psi in the temperature range 800° to 1700° F. The flexural strength of the alumina was found to be 18,500 to 23,000 psi at 1000° F.

Loyet and Levitan (Ref. 177) considered three regions of a radome to be thermally critical: the forward tip where high local heat transfer rates are encountered, the transition region where complete turbulent flow first occurs, and the region of attachment. Indications were that the temperature took on an absolute maximum value at the stagnation point and a relative maximum value at the transition point, that the maximum thermal gradient occurred through the radome wall, and that the axial and circumferential thermal gradients were negligible. For the materials considered, it was also indicated that the stresses induced by the thermal gradients through a radome wall would exceed by at least an order of magnitude other stresses such as those due to aerodynamic pressure distributions. On the basis of these indications, Loyet and Levitan attempted to correlate thermal shock test results with calculated predictions based on the thermal stress analysis of a hollow spherical section for the radome tip and based on the thermal stress analysis of a thin-walled cylinder for the radome sections where the wall thickness was small compared with the inner radius. Numerical integration by trapezoidal approximations gave results within the accuracy of the available data. The basic assumptions were that:

1. Deformations were infinitesimal.
2. The material was isotropic and obeyed Hooke's law up to the point of fracture.
3. Axial and circumferential temperature gradients were negligible.

Loyet and Levitan analyzed the test results obtained in two experimental investigations. In one investigation, Coors Porcelain Company (Ref. 9) had evaluated a radome made of AD-99 alumina with a tangent ogive contour, a

5.5-inch base diameter, a 13-inch length, an X-band wall thickness, and a tip blunted to a 0.56-inch outer radius. The radome was subjected to the exhaust gas from a vertical tunnel of a periodic kiln. The temperature of the exhaust was estimated to be above 3000° F. The radome was inserted in the exhaust tunnel three times without incident:

1. For 27 seconds and then removed and allowed to reach an equilibrium temperature of 140° F.
2. For 20 seconds and then removed and allowed to cool to 100° F.
3. For 52 seconds and then removed and allowed to cool to room temperature.

Loyet and Levitan analyzed the third test, which was by far the most severe, in detail. Indications were that the maximum thermal gradient occurred after 40 seconds with the outer and inner surfaces at 1150° F and 1044° F, respectively. The calculated maximum stress level at the inner surface was 15,450 psi while the measured tensile strength of AD-99 alumina was 29,200 psi at 1044° F with a standard deviation of 4000 psi. Thus the theory predicted that the radome would survive.

The other test results analyzed were those obtained by Baer, Gates, and Robertson (Ref. 176). Two sets of test results on the alumina radomes were analyzed by Loyet and Levitan in detail. One radome failed when the calculated temperatures of the outer and inner surfaces were 807° F and 585° F, respectively. Comparable temperatures for a second radome were 1280° F and 1040° F. The calculated peak tensile stress for the first radome was 26,074 psi, the mean tensile strength was 31,500 psi, and the difference 5426 psi represented about 1.3 standard deviations. The calculated peak tensile stress for the second radome was 28,400 psi and the expected mean tensile strength at the time of failure was 29,200 psi. Thus good correlation was obtained between expected stress and strength.

Loyet and Stevens (Ref. 178) investigated the relative merits of large thin wall and half wavelength wall ogival ceramic radomes, approximately 12 inches in diameter with a fineness ratio of 2.0, on the basis of an analysis similar to that used by Loyet and Levitan. Two histories were assumed in the analysis:

Case 1. Snap-up trajectory, 43,000 to 65,000 feet altitude, Mach 2.0 launch to a peak of Mach 5.1 after 40 seconds, and a deceleration to Mach 4.5 after 60 seconds.

Case 2. Snap-down trajectory, 70,000 to 60,000 feet altitude, Mach 4.0 launch to a peak of Mach 6.9 after 6 seconds, and a deceleration to Mach 4.4 after 60 seconds.

Indications were that Pyroceram® 9606 and alumina AD-99 would exhibit similar surface temperature profiles, but that the two materials could differ significantly from the standpoint of thermal gradients. For the Case 1 history

and a half wavelength radome, the peak temperatures were 1240° F and 1205° F for the Pyroceram® and the alumina, respectively, but the thermal gradients were larger for the Pyroceram® because its thermal diffusivity was considerably lower than that of the alumina. When the wall thickness was $1/12$ of a wavelength, the thermal diffusivity had little effect, and the thermal gradients in the two materials were similar. While the thin-wall design significantly reduced the thermal gradients in the materials, it increased the operating temperatures of the radomes. The peak temperature increased from 1205° to 1510° F for the alumina and from 1240° to 1548° F for the Pyroceram® because of the reduced thermal capacity of the thinner walls. For the Case 2 history the thin wall design also significantly reduced the thermal gradients in the materials. For the Case 2 history with various launch velocities, the stress on the radomes increased as the launch velocity was increased, but the effect was much less drastic with the thin wall design.

Suess and Weckesser (Ref. 179) analyzed 21 representative trajectories, ballistic and line-of-sight, to a maximum Mach number of 4.0. The trajectory chosen as generating the maximum radome thermal stresses was the one giving the highest rate of heat input. Indications were that:

1. The line-of-sight trajectories gave higher heating rates than the ballistic trajectories.
2. The launch angle did not influence the heating rate significantly.
3. The same trajectory was thermally most severe for all wall thicknesses considered.
4. The maximum Mach number of the most severe trajectory was about 2.8, considerably below the design value of 4.0.

Two Pyroceram® radome geometries were considered: a pointed radome of a standard shape and one blunted with a 1.35-inch radius. The radome measured 13.5 inches across the base and about 28 inches in length. The extreme forward portions of the radomes were analyzed with respect to the trajectory that was found to be thermally most severe. Calculations were made using both the cylindrical and the spherical shell theories. The spherical theory gave the more conservative results. On the pointed radome the maximum temperature (855° F with the spherical theory) occurred at the stagnation point as expected. However, on the blunted radome the maximum temperature (705° F with the spherical theory) occurred at the transition point. The maximum tensile stress in the blunted radome also occurred at the transition point, and it did not differ significantly from the maximum stress that occurred at the transition point of the pointed radome. In view of these indications, it was concluded that one cannot automatically assume that nose blunting will lead to a reduction in maximum thermal stress.

Suess and Weckesser also attempted to correlate thermal shock test results with calculated predictions. Three Pyroceram® radomes were cooled to an initial temperature of $+50^{\circ}$ F or -10° F and tested at Mach 2.44, a total pressure of 215 psi, and an average total temperature of about 1350° F. Good strain gauge

data were obtained in two of the three tests. In both of these tests the maximum stress was within 2 per cent of that predicted by the cylindrical theory and within 11 per cent of that predicted by the spherical theory, and the predictions based on the spherical shell model were conservative. The experimental and theoretical stress time curves were very similar in one test, but in the other test the experimental stress peak was much sharper than that which had been predicted.

A number of investigators have considered the relative merits of various ceramic radome materials. For example, Brown (Ref. 95) determined experimentally the relative thermal stress resistance of five potential radome materials for heating conditions which simulated radome environments. In decreasing order of merit, the five materials were Pyroceram® 9608, Pyrex 7740, AD-99 alumina, MgO (greater than 99 per cent dense), and Alundum RA-3360. Walton and Bowen (Ref. 180) compared the calculated relative merit index of thermal shock resistance of slip-cast fused silica, Pyroceram®, and Al_2O_3 over a wide range of thermal shock environments and found that slip-cast fused silica was superior to both Pyroceram® and Al_2O_3 for all cases. At Hughes Aircraft Company (Ref. 181) hemispherical radomes, 2.5 inches in radius with X-band wall thickness, were subjected to cold wall heat fluxes of 50 and 75 BTU/ ft^2 -second in a quartz lamps facility. Pyroceram® 9606, aluminum oxide and aluminum oxide A-sandwich have been tested. At 75 BTU/ ft^2 -second the Pyroceram® and the aluminum oxide A-sandwich both failed at the end of about 20 seconds, while the aluminum oxide failed within a matter of a second or two. At 50 BTU/ ft^2 -second the Pyroceram® failed after 30 seconds and the alumina failed after 15 seconds. The aluminum oxide A-sandwich was not tested at the lower heat flux level.

Finally, an interesting program is presently being conducted at Whittaker Corporation, Narmco Research and Development Division under Contract AF 33(657)-10111. A mosaic radome, 9 feet high with a 30-inch base, is to be fabricated using alumina tile in two layers and a Narmco adhesive. Early results have indicated that small tile are preferred for crack arrestment, and it is contemplated that small tile will be used in the vicinity of the stagnation point (Ref. 182).

9.16 Leading Edges

There is little to report on leading edges. While a number of ceramic leading edges have been designed, few have been tested under severe conditions.

At North American Aviation, Inc. (Ref. 183) a full scale leading edge model fabricated from beryllium oxide segments supported by a silicon carbide coated graphite structure was found to be unaffected by plasma test conditions similar to those expected for a typical reentry trajectory. The design incorporated small segments of the oxide which were hot pressed to a density of about 99 per cent of theoretical. Holes were drilled in the beryllia segments with a diamond core drill, and the segments and the graphite structure were joined by beryllia pins using a simple method of attachment. The leading edge configuration had a 0.375-inch cylindrical radius and a 17 degree wedge angle. Three samples were subjected to a plasma jet test:

Sample 1. The sample was subjected to severe thermal shock conditions. The cold sample was raised into the plasma jet, the enthalpy was increased until the beryllia segments cracked at approximately 160 seconds, and the sample was removed from the jet and allowed to cool. The cracks were observed on the beryllia surface after the sample surface reached 3000° F. The segments remained intact for considerable handling after cool down. The maximum rate of temperature rise was 54° F/second.

Sample 2. The sample was preheated slowly to approximately 1600° F, heated in the plasma to a temperature of 4000° F over a period of 26 minutes, held at or near 4000° F for 16 minutes, cooled in the jet to 2200° F, and cooled from 2200° F to room temperature slowly. The maximum rate of temperature rise was 32° F/second. The sample withstood the complete test cycle with only slight surface ablation at the point of maximum temperature.

Sample 3. The sample was heated at a rate equal to or greater than that required in the simulated reentry. It was preheated slowly to 1600° F, heated in the plasma to a temperature of 4200° F over a period of 23 minutes in such a manner as to produce a time-temperature history similar to that for a reentry mission, and cooled at a rate to simulate the reentry schedule. The maximum rate of temperature rise was 80° F/second. The model cracked when the desired reentry temperature rise rate was exceeded. The beryllia segments remained intact for considerable handling after cool down. However, failure of the small beryllia attachment pins allowed the segments to fall free from the graphite support.

Anthony, Merrihew, Mistretta, and Dukes (Ref. 184) studied the aspects of leading edge design and established the design of a graphite leading edge for a hypersonic glider. A 5.0-inch diameter was established on the basis of a maximum allowable temperature of 3000° F. A lower surface length of 6.50 inches was selected so that the support structure would not exceed 2000° F and conventional super alloys could be used. The length of the upper chord was established at 4.10 inches to minimize thermal stress. The wall thickness, 3/8-inch, was dictated by fabrication consideration, and a 16-inch segment length was selected on the basis of airload considerations. The attachment design presented the major structural problem. Three graphite leading edge assemblies were tested:

Test 1. The assembly was subjected to static load at room temperature and failed at 170 per cent of the design limit load. Failure occurred not in the graphite but in a metal part. However, this precipitated fracture of the graphite leading edge at several locations.

Test 2. The assembly was subjected to the radiant energy provided by a quartz lamps facility in an attempt to simulate flight conditions. However, the maximum temperature achieved with the quartz lamp facility was 2300° F. The assembly withstood the test cycle five times with no structural failures.

Test 3. The assembly was tested under the simulated flight temperature history (up to 2300° F) in the quartz lamps facility and failed during the first cycle. The failure was attributed to insufficient clearance between members in the back structure.

Levy (Ref. 166) evaluated a leading edge comprised of an aluminum phosphate bonded alumina reinforced with a molybdenum wire mesh precoated with a pack cementation coating. The component withstood several long time exposures up to 3500° F.

5.17 Prestressed Ceramic Structures

At the University of California (Ref. 117) attempts were made to prestress ceramic wing sections through the use of pretensioned steel cables. The wing segments were formed from alumina by slip-casting, assembled in spanwise fashion, and prestressed compressively in the spanwise direction. Because of the difficulties in applying a load uniformly to a brittle structure, the program was only partially successful. A higher degree of success might have been attained through the use of rigid end plates to promote more uniform loading and/or through the use of gasketing material to reduce the intensities of localized stresses.

Warshaw (Ref. 185) reported another method of obtaining prestressed ceramics so that maximum advantage could be taken of their high compressive strength. The method consisted of forming a laminate using a ceramic material with a relatively low firing shrinkage together with another material with a relatively high firing shrinkage. During firing, the low-shrinkage ceramic phase was placed in compression as a result of the shrinkage differential.

Wenger and Knapp (Ref. 186) investigated the thermal shock behavior of a prestressed ceramic material. Eighty-three nominally identical samples of a certain ceramic composition were subjected to 10 thermal shock cycles, 500° F to an air stream. During the thermal shock tests, 27 of the samples had an external compressive load of 10,000 psi, while the remaining 56 samples had no external load. After the thermal shock test, the unstressed samples had an average compressive strength of about 15,000 psi, while the prestressed samples had an average compressive strength near 20,000 psi. The average compressive strength of 60 samples which were not subjected to thermal shock was about 22,000 psi.

The thermal shock behavior of biaxially prestressed ceramic plates is presently being investigated quantitatively at the University of California (Ref. 187). Ceramic plates are thermally shocked in a quartz lamp facility. The damage caused by thermal shock is estimated by determining the bending

strengths of thermally shocked plates. In a preliminary study, all plates tested in an unprestressed condition failed in thermal shock when a particular set of test conditions was used. Prestressed plates shocked under the same conditions in general did not fail but did exhibit some damage. The extent of the damage decreased as the prestress was increased. Indications were that moderate initial loads produced the greatest improvement and that the prestress could be increased to the point where the plates suffered little or no thermal shock damage. However, these indications are preliminary and apply only to one particular set of test conditions.

9.18 Thermal Stress Testing

At present, the most favored thermal stress test is one that involves the steady-state heating of a ring by various means from the inside. At Lawrence Radiation Laboratory (Ref. 186), however, specimens are heated from both the inside and outside. This allows the temperature gradient to be varied while the bulk temperature of the specimen is held constant, and the thermal stress resistance is determined as a function of temperature. A salient feature of the method used at Lawrence Radiation Laboratory is that the output consists of the single thermal shock parameter $\frac{Sk}{E\alpha}$, where

S = Strength

k = thermal conductivity

E = Young's modulus

α = thermal expansion coefficient

As a result only one experimental error is involved in determining the thermal stress resistance. When the parameter is computed using the four individual material properties, four experimental errors are involved. What is much more important, however, is that the method does not require a definition of the strength of the material.

Glenny and Royston (Ref. 189) compared the stress distributions in a ceramic material during mechanical testing and during thermal shock testing. The transient thermal stresses in a circular cylinder were considered, and the analysis was based on the theory of Weibull. The following relationships were developed for equal probabilities of failure:

$$\frac{\sigma}{S_t} = \left[2 (m + 1) \frac{V_t}{V_{ts}} \right]^{1/m} \quad (62)$$

$$\frac{\sigma}{S_{bc}} = \left[\frac{(m+1)}{(m+2)} \frac{(m-1)}{(m)} \frac{(m-3)}{(m-2)} \dots \frac{2}{1} \right] \frac{4}{\pi} \frac{V_{bc}}{V_{ts}} \quad (63)$$

$$\frac{\sigma}{S_{br}} = \left[\frac{V_{br}}{V_{ts}} \right]^{1/m} \quad (64)$$

where:

σ = thermal stress

S = mechanical strength

V = Volume of cylinder under stress

m = flaw density

and the subscripts apply as follows:

t = cylinder subjected to tension

bc = circular cylinder subjected to bending

br = rectangular cylinder subjected to bending

The formulas are valid when Biot's modulus* is less than two and when the material has a "zero strength" (in the sense of Weibull) of zero. Glenny and Royston used the expressions to establish the most appropriate size, shape, and loading condition for a mechanical test specimen. For example, for a cooling shock Glenny and Royston compared thermal stress values with the flexural strength of a rectangular cylinder having a volume equal to that of the thermal shock test cylinder (See Equation 64) and having the same surface area exposed to the tensile stress in the outer fibers.

After carefully establishing appropriate strength criteria for both heating and cooling shocks, Glenny and Royston compared the mechanical strength of a high alumina ceramic with its thermal stress at failure. The agreement was reasonable. However, the calculated stresses for the heating shock were higher and for the cooling shock lower than the experimental

* See Section 7.8.4 Thermal Shock Parameters.

strength values. This may have been caused by a concentration of flaws at the surface of the thermal shock test specimens. The same type of effect was observed by Crandall and Ging (Ref. 190) in their work on the rapid heating and cooling of alumina spheres.

9.19 Selected References on the Thermal Shock Behavior of Refractory Structural Components

Extended Abstracts 45 to 56 (Appendix I) refer to recent foreign publications which deal with the thermal shock characteristics of ceramic components.

X. DESIGN WITH BRITTLE MATERIALS

10.1 Design Guides

During the conduct of this program an effort was made to uncover various design hints based on the art, rather than the science, of brittle structural design. The following design rules, which deal with the problem of preventing thermal shock failure in ceramics, were collected:

1. Since ceramics are stronger in compression than in tension, they should be used in compression whenever possible. Through careful design a ceramic can be held together to the point where it continues to serve a useful function even after thermal fracture.
2. Simple shapes should be used. Sharp corners and angles should be avoided. All edges should be rounded with generous radii - in general a 1/32-inch radius is not excessive.
3. Sudden changes of section should be avoided. Thick or irregular sections should not be used. The allowable thickness depends on the thermal and mechanical properties of the material and the environment, and, in the case of a plate, cylinder, or sphere, the critical thickness can be estimated through the use of Equations 52 to 58 (Section 7.8.4 Thermal shock parameters). For a specific example illustrating the effect of thickness on the performance of a ceramic component, the reader is referred to Section 9.15 Radomes.
4. Point loading and stress concentrations should not be permitted. Holes should be kept out of tension zones, and resilient pads should be used at load bearing contact zones. Holes for attachments should not be used without special consideration. If the loads are not equally distributed over all pins, failure will most likely occur prior to the achievement of the full load carrying capacity. Under the assumption of a load uniformly distributed over all pins, the following observations have been made on the basis of experience in stress analysis (Ref. 191):
 - i. No solution exists for the case of more than two holes, but for a given unit width of material the lowest maximum stresses occur for a hole diameter to hole spacing ratio of approximately 0.4. (Thus the distance of a hole from the edge of an article should be at least 0.75 times the hole diameter.)
 - ii. Improvement in the load-carrying capacity can be effected through the use of pins which yield before the fracture load of the brittle article is reached. When the hole size is too large to accommodate a yielding solid pin, the use of a yielding hollow pin is suggested.

- iii. The stress concentrations can be reduced by using smaller holes spaced closer together or by using multiple rows of holes.
- iv. An elliptical shaped hole leads to lower stress concentration factor if the major axis of the hole is in the direction of the stress field.
- 5. Brittle structures cannot be pilled into position during assembly. Therefore this situation must be avoided by careful machining to ease tolerances. At moderate temperatures most ceramics fail at a strain between 0.10 and 0.15 per cent, and tolerances as close as 0.0005-inch may be required. The presence of phases with different degrees of hardness, the occurrence of pores and large grain limit the tolerances which can be met. (Refer to Section 6.4 Machining and Grinding.) For radomes, and other articles, mechanical mismatch is sometimes minimized by fastening the metal attachment ring and ceramic together and then match drilling the assembly to the missile body or other parts.
- 6. Noncompressive mechanical restraints should be minimized.
- 7. Advantage should be taken of the fact that the thermal expansion of a ceramic is highly reproducible. A careful analysis will help eliminate thermal mismatch. However, the designer must know the material being used. Every refractory ceramic is a special material, and the use of tabular, handbook data can be misleading. If the composition of the material is altered through the use of additives, or if the supplier changes a raw material from which his product is derived or alters a processing technique, a new product with different properties will be obtained. The designer must be aware of such changes.
- 8. In hyperthermal environments where heat transfer is primarily by convection and the body is free to radiate to space, as in the case of a nose cone, leading edge or radome, emittance is of critical importance. Consideration should be given to the use of an emissive coating and to the surface structure of the material.
- 9. For high heat transfer rates, a material with a low thermal expansion should be selected. For low heat transfer rates, a material with inherently poor thermal shock characteristics (high thermal expansion) can be used if it has a high thermal conductivity. Refer to Section 7.8.4 Thermal shock parameters.
- 10. Localized heating or cooling should be avoided.
- 11. It is desirable to confine ceramic materials to small individual cells so that destructive temperature gradients will not occur within any given cell. Refer to Section 9.14 Honeycomb Structures for specific examples.

12. Nonredundant attachments are desirable to the extent that a part can be designed with confidence when all loads are known.
13. The maximum strain criterion for failure is in some ways better than the maximum stress criterion. The critical strain is fairly constant for a wide range of ceramics.

10.2 General References on the Design of Brittle Materials

Extensive information on the design of brittle materials is contained in References 20, 23, 47, and 154 and in References 191 to 197.

REFERENCES

1. Hague, J. R., Lynch, J. F., Rudnick, A., Holden, F. C., and Duckworth, W. H., "Refractory Ceramics of Interest in Aerospace Structural Applications - A Materials Selection Handbook," RTD-TDR-63-4102 (October 1963).
2. Lynch, J. F., Bowers, D. J. and Duckworth, W. H., et al, "Refractory Ceramics of Interest in Aerospace Structural Applications - A Materials Selection Handbook," RTD-TDR-63-4102, Suppl. 2 (April 1965).
3. Mitchell, J. B., Spriggs, R. M., and Vasilos, T., "Microstructure Studies of Polycrystalline Refractory Oxides," Summary Technical Report, 12 June 1962 - 12 June 1963, Prepared U. S. Navy, Bureau of Weapons, Contract N0W 62-0648-c.
4. Manson, S. S., "Thermal Stresses," Machine Design 30, 114-120 (June 12, 1958). Ibid. "Thermal Stresses in Design," 99-103 (June 26, 1958).
5. Kingery, W. D., "Factors Affecting Thermal Stress Resistance of Ceramic Materials," J. Am. Ceram. Soc. 38, 3-15 (January 1955).
6. Walton, J. D. and Poulos, N. E., "Slip-Cast Fused Silica," ML-TDR-64-195, (October 1964).
7. Cavanaugh, J. F. and Sterry, J. P., "Heat Protective Ablative Coatings for Radomes," WADD-TR-60-507 (August 1960).
8. Burroughs, J. E., General Dynamics/Fort Worth, private communiqué.
9. Pedigo, Alan, "Resistance to Impact and Thermal Shock by Solid Alumina Radomes," a 7 page report in "Proceedings of the ASD-OSU Symposium on Electromagnetic Windows," ASD-TDR-62-676, Vol. I, AD 286552 (July 1962).
10. Fitzgerald, E. A., "Thermal Stresses in Thin Shells of Revolution for Axisymmetric Temperature Distributions," Report No. SM-42009, Missile and Space Systems Division, Douglas Aircraft Co., Inc., Santa Monica, Calif. (June 1962).
11. Stratton, W. K., et al, "Advances in the Materials Technology Resulting from the X-20 Program," AFML-TR-64-396 (March 1965).
12. Nowotny, Hans, "Crystal Structure and Stability of Refractory Phases," Advan. X-Ray Anal. 5, 13-32 (1961).
13. Lynch, C. T. and Krochmal, J. J., "Importance of Purity in Development of Ceramics," RTD Technology Briefs 1, 1-8 (October 1963).
14. Bauer, E. E. and Disotell, M. A., "New Materials in the Aerospace Industry," Industrial Research 6, 40-49 (Nov. 1964).

15. Shaffer, P. T. B., "Oxidation Resistant Boride Composition," Am. Ceram. Soc. Bull. 41, (Feb. 1962).
16. Murray, P., "The Changing Boundaries of Ceramics," J. Brit. Ceram. Soc. 1, 113-145 (1963).
17. Castelfranco, James, "What Can Ceramics Do in Missiles?," Ceram. Ind. 70, 84-89 (May 1958).
18. Castelfranco, James, "Ceramics for Supersonic Missiles," Ceramics 10, 13-18, 20 (May 1959).
19. Hahn, G. T. and Jaffee, R. I., "A Comparison of the Brittle Behavior of Metallic and Nonmetallic Materials," OTS PB 171626 (May 16, 1961).
20. Hauck, J. E., "Guide to Refractory Ceramics," Mater. Design Eng. 58, 85-96 (July 1963).
21. Kendall, E. G. and McClelland, J. D., "Nonmetallic Materials for High Temperature Structural Applications," TDR-269 (4240-10)-9 (July 22, 1964).
22. Knapp, W. J. and Shanley, F. R., "Ceramic Materials - Properties for Structural Applications," Aero/space Engineering 17 (December 1958).
23. Material Advisory Board, "National Research Council, Washington, D. C., "Report of the Ad Hoc Committee on Design for Brittle Materials," Report No. MAB-198-M (May 20, 1964).
24. Materials Advisory Board, National Research Council, Washington, D. C., "Symposium on Design with Materials that Exhibit Brittle Behavior, Volume I, December 13-14, 1960, Washington, D. C.," Report No. MAB-175-M (October 20, 1961).
25. Pellini, W. S. and Harris, W. J., Jr., "Flight in the Thermosphere: I, "Material Requirements for Thermal Protection Systems," Metal Progr. 71, 69-76 (March 1960). Ibid, "II, Materials for Nonmelting Heat Sink Systems," 113-115 (April 1960). Ibid., "III, Materials for Ablation, Sublimation and Transpiration Systems," 89-92 (May 1960). Ibid., "IV, Material Requirements for Radiative Systems," 83-93 (June 1960).
26. Kiley, M. W., "The Future for Ceramics," Materials in Design Eng. 54, 133-40 (September 1961).
27. Sterry, W. M., "Demands of Aircraft Hull Challenge at Ceramics," Ceram. Ind. 70, 155-58 (April 1958).
28. Guland, J., "The Fracture of Brittle and Quasi-brittle Materials - A Survey," OOR Report No. 2060:1 (August 1959).
29. White, J., "Some General Considerations on Thermal Shock," Trans. Brit. Ceram. Soc. 51, 591-623 (1958).

30. Ramke, W. G. and Latva, J. D., "Refractory Ceramics and Intermetallic Compounds," Aerospace Eng. 22, 76-84 (January 1963).
31. Smiley, W. D., Sobon, L. E., Hruz, F. M., Farley, E. P., Chilton, J. E., Poncelet, F. F., and Kelly, J. J., "Mechanical Property Survey of Refractory Nonmetallic Crystalline Materials and Intermetallic Compounds," WADC-TR-59-448 (January 1960).
32. Kingery, W. D. and Coble, R. L., "A Review of the Effect of Microstructure on Mechanical Behavior of Polycrystalline Ceramics," pg 103-13 of "Mechanical Behavior of Crystalline Solids: Proceeding of a Symposium April 28-29, 1962," National Bureau of Standards Monograph 59, U. S. Government Printing Office, Washington (March 25, 1963).
33. Bowman, J. C. and Bushong, R. M., "Design of a Brittle Material," pg 360-74 of "Symposium on Design with Materials that Exhibit Brittle Behavior, Volume I, December 13-14, 1960, Washington, D. C.," Materials Advisory Board, National Research Council, Washington, D. C., Report No. MAB-175-M (October 20, 1961).
34. Richardson, L. D., Sr., "An Introduction to High-Temperature Refractory Materials," pg 3-13 of "High-Temperature Technology," I. E. Campbell, ed., John Wiley and Sons, Inc. (New York 1956).
35. Parker, C. J., "Mechanical Properties of Glass and Ceramics," Glass Ind. 44, 489-94, 535-36 (September 1963).
36. Bradstreet, S. W., "Principles Affecting High Strength to Density Composites with Fibers or Flakes," ML-TDR-64-85 (May 1964).
37. Burk, J. E., "A Metallurgist Looks at Ceramics," J. Metals 11, 740-43 (November 1959).
38. Clarke, F. J. P., "Why Ceramics are Brittle," New Scientist, No. 294 (July 5, 1962).
39. Griffith, A. A., "The Phenomena of Rupture and Flow in Solids," Phil. Trans. Royal Soc. 221A, 163-98 (October 21, 1920).
40. Johnson, T. L., "Fracture Mechanisms in Crystalline Ceramics," pg 63-78 of "Mechanical Behavior of Crystalline Solids: Proceeding of a Symposium April 28-29, 1962," National Bureau of Standards Monograph 59, U. S. Government Printing Office, Washington (March 25, 1963).
41. Weibull, W., "A Statistical Theory of the Strength of Materials," Ing. Vetenskaps Akad. Handl. no. 151 (1939). Ibid, "A Statistical Distribution Function of Wide Applicability," J. Applied Mech. 18, 293-97 (September 1951).
42. Shook, W. B., "Critical Survey of Mechanical Property Test- Methods for Brittle Materials," ASD-TDR-63-491 (July 1963).

43. Johnson, L. G., "The Median Ranks of Sample Values in Their Population with an Application to Certain Fatigue Studies," Industrial Math. 2 (1951).
44. Wells, W. M., Unpublished Work, Lawrence Radiation Laboratory.
45. Weil, W. A., "Studies of the Brittle Behavior of Ceramic Materials," ASD-TR-61-628 (April 1962).
46. Armour Research Foundation, "Studies of the Brittle Behavior of Ceramic Materials," ASD-TR-61-628, Part II (April 1963).
47. Barnett, R. L., "Review of Structural Design Techniques for Brittle Components under Static Loads," ARF Report No. 8259, Phase I - Task 2 (May 1963).
48. Duckworth, W. H., Schwope, A. D., Salmassy, O. K., Carlson, R. L. and Schofield, H. Z., "Mechanical Property Tests on Ceramic Bodies," WADC-TR-52-67 (March 1952).
49. Salmassy, O. K., Duckworth, W. H. and Schwope, A. D., "Mechanical Property Tests on Ceramic Bodies," PB 119092 (March 1953).
50. Salmassy, O. K., Bodine, E. G., Duckworth, W. H. and Manning, G. K., WADC-TR-53-50 (Pt. II) (June 1955).
51. Riley, M. W., "The Future for Ceramics," Materials in Design Eng. 54, 133-40 (September 1961).
52. Materials Advisory Board, National Research Council, Washington, D. C., "Report on the Ad Hoc Committee on Refractory Inorganic Nonmetallic Structural Materials," Report No. MAB-169-M (January 1961).
53. Pisarenko, G. S. and Troshchenko, V. T., "Statistichni Teorii Mitsnosti Ta Ikh Zastosuvannya Do Metalokeramichniki Materialiv," Vidavnitstvo Akad. Nauk Ukrains, Koy RSR, Kiev (1961). English translation, "Statistical Theories of Strength and Their Application to Metalloceramic Materials/Selected Parts," FTD-TT-62-1765 (April 22, 1963).
54. Kingery, W. D., ed., Ceramic Fabrication Processes, The Technology Press of Massachusetts Institute of Technology (Cambridge 1958).
55. Hausner, H., "Slip-Casting - A New Method in Powder Metallurgy," Plansee Proceedings 1958, 49-57 (1959).
56. Rempes, P. E., Weber, B. C. and Schwartz, M. A., "Slip-Casting of Metals, Ceramics, and Cermets," Am. Ceram. Soc. Bull. 37, 334-39 (July 1958).
57. Golibersuch, E. W., General Electric Company, "Method of Making Cemented Carbide Articles and Casting Compositions Therefor," U. S. Pat. 2,698,232, (December 28, 1954).

58. Fleming, J. D. and Johnson, J. W., "Fused Silica for Reactor Applications," ORO-209, U. S. Atomic Energy Commission (December 1959).
59. Haith, W. E., Jr., "Slip-Casting of Aluminum Oxide," J. Am. Ceram. Soc. 32, 394-98 (December 1949).
60. Mehta, P. K. and Langston, R. B., "Rheology of Casting Slips in Theory and Practice," Ceram. Age 79, 49-50, 52-56 (September 1963).
61. Poulos, N. E., Walton, J. D., Murphy, C. A., Harris, J. N., Wolf, J. M. and Smith, G. W., "Design and Development of an EM Window for Air Lift Reentry Vehicles," USAF Cont. No. AF-33(657)-11504, Georgia Tech Interim Engineering Reports No. 3, No. 4, and No. 5 (January 31, April 30 and July 31, 1964).
62. Svec, J. J., ed., "Isostatic Pressing Expands Manufacturing Capabilities," Ceramic Industry 83, 55, 63, 66-67, 70 (November 1964).
63. Stoops, R. L., "98.2% Density with Vibrating Impact Presses," Ceramic Industry 82, 54-57, 66, 68 (March 1964).
64. Bell, W. C., Dillender, R. D., Lominac, H. D., Long, L. W. and Mannin, E. G., "Vibratory Compacting of Metal and Ceramic Powders," WADC-TR-13-193 (April 1954).
65. Pearl, H. A., Nowak, J. M., Conti, J. C. and Urode, R. J., "Refractory Inorganic Materials for Structural Applications," WADC-TR-59-432 (February 1960).
66. Schwartz, M. M., "Machining Foamed Ceramics," Tool and Manufacturing Engineer 51, 91-93 (October 1963).
67. Pincus, A. G., et al, "Critical Compilation of Ceramic Forming Methods," RTD-TDR-63-4069 (January 1964).
68. Emrich, B. R., "Technology of New Devitrified Ceramics - A Literature Review," ML-TDR-64-203 (September 1964).
69. Materials Advisory Board, National Academy of Sciences - National Research Council, Washington, D. C., "Ad Hoc Committee on Processing of Ceramic Materials," Report No. MAB-197-M (November 18, 1963).
70. Latva, J. D., "Selection and Fabrication of Ceramics and Intermetallics," Metal Progress 82, 139 + 7 pg (October 1962).
71. Cornell Aeronautical Laboratory, Inc., "Investigation of Theoretical and Practical Aspects of the Thermal Expansion of Ceramic Materials," AD 296188 (July 1962).
72. Spriggs, R. M., "Expression for Effect of Porosity on Elastic Modulus of Polycrystalline Refractory Materials, Particularly Aluminum Oxide," J. Am. Ceram. Soc. 44, 628-9 (December 1961).

73. Knudsen, D. P., "Effect of Porosity on Young's Modulus of Alumina," J. Am. Ceram. Soc. 45, 94-95 (February 1962).
74. Spriggs, R. M., "Effect of Open and Closed Pores on Elastic Moduli of Polycrystalline Alumina," J. Am. Ceram. Soc. 45, 454 (September 1962).
75. Hasselman, D. P. H., "Porosity Dependence of the Elastic Moduli of Polycrystalline Refractory Materials," J. Am. Ceram. Soc. 45, 452-53 (September 1962).
76. Hashin, Z., "Elastic Modulus of Heterogeneous Materials," J. Appl. Mechanics 29, 143-50 (March 1962).
77. Piatasik, R. S. and Hasselman, D. P. H., "Effect of Open and Closed Pores on Young's Modulus of Polycrystalline Ceramics," J. Am. Ceram. Soc. 47, 50-51 (January 1964).
78. Hasselman, D. P. H. and Fulrath, R. M., "Effect of Small Fraction of Spherical Porosity on Elastic Moduli of Glass," J. Am. Ceram. Soc. 47, 52-53 (January 1964).
79. Fryxell, R. E. and Chandler, B. A., "Creep, Strength, Expansion, and Elastic Moduli of Sintered BeO As a Function of Grain Size, Porosity and Grain Orientation," J. Am. Ceram. Soc. 47, 283-91 (June 1964).
80. Kerner, E. H., "Elastic and Thermoelastic Properties of Composite Media," Proc. Phys. Soc. London B69, 808-13 (August 1956).
81. Spriggs, R. M. and Brissette, L. A., "Expressions for Shear Modulus and Poisson's Ratio of Porous Refractory Oxides," J. Am. Ceram. Soc. 45, 198-99 (April 1962).
82. Spriggs, R. M., Brissette, L. A. and Vasilos, T., "Effect of Porosity on Elastic and Shear Moduli of Polycrystalline Magnesium Oxide," J. Am. Ceram. Soc. 45, 400 (August 1962).
83. Mackenzie, J. K., "The Elastic Constants of a Solid Containing Spherical Pores," Proc. Phys. Soc. London B63, 2-11 (January 1950).
84. Hasselman, D. P. H. and Shaffer, P. T. B., "Factors Affecting Thermal Shock Resistance of Polyphase Ceramic Bodies," WADD-TR-60-749 Part II (April 1962).
85. Pears, C. D., et al, "Evaluation of Tensile Data for Brittle Materials Obtained with Gas Bearing Concentricity," AD 410770 (May 1963).
86. Sedlacek, R., "Tensile Strength of Brittle Materials," ML-TDR-64-49 (March 1964).
87. Rudnick, A., Hunter, A. R. and Holden, F. C., "An Analysis of the Di-metral-Compression Test," Materials Research and Standards, 283-89 (April 1963).

88. Kliman, M. I., "Impact Strength of Alumina Fiber-Ceramic Composites," AD 291826 (November 1962). *Ibid.*, "Transverse Rupture Strength of Alumina Fiber-Ceramic Composites," AD 291883 (November 1962).
89. Dinsdale, A., Moulson, A. J. and Wilkinson, W. T., "Experiments on the Impact Testing of Cylindrical Ceramic Rods," Trans. Brit. Ceram. Soc. 61, 259-75 (1962).
90. Phillips, C. J. and DiVita, Sam, "Similarities in the Impact Behavior of Glasses and Polycrystalline Ceramics," Am. Ceram. Soc. Bull. 42, 685-87 (November 1963).
91. Wilcox, P. D., "The Strength Behavior of Some Ceramics," Thesis, PhD Ceram. Eng., University of Utah (1962).
92. Hasselman, D. P. H., "Relationship Between Effects of Porosity on Strength and on Young's Modulus of Elasticity of Polycrystalline Materials," J. Am. Ceram. Soc. 46, 564-65 (November 1963).
93. Knudsen, F. P., "Dependence on Mechanical Strength of Brittle Polycrystalline Specimens on Porosity and Grain Size," J. Am. Ceram. Soc. 42, 376-87 (August 1959).
94. Spriggs, R. M., Mitchell, J. B. and Vasilos, T., "Mechanical Properties of Pure, Dense Aluminum Oxide as a Function of Temperature and Grain Size," J. Am. Ceram. Soc. 47, 323-27 (July 1964).
95. Brown, D. A., "Evaluation of Thermal Stress Resistance in Potential Radome Materials," Final Report, Stanford Research Institute Project FMI-4538, prepared for the Naval Research Laboratory, Washington, D. C., Contract Nonr-4123(00)(X) (February 15, 1965).
96. Weiss, W., Sessler, J., Grewal, K. and Chait, R., "The Effect of Stress Concentration on the Fracture and Deformation Characteristics of Ceramics and Metals," AD 410583 (April 1963).
97. Nielsen, T. H. and Leipold, M. H., "Thermal Expansion in Air of Ceramic Oxides to 2200° C," J. Am. Ceram. Soc. 46, 381-87 (August 1963).
98. Powers, A. E., "Fundamentals of Thermal Conductivity at High Temperatures," Knolls Atomic Power Lab., Report No. KAPL-2143 (April 7, 1961).
99. Ruddlesden, S. N., "Relations Between Properties and Structure," pg 3-25 of "Special Ceramics" Popper, P., ed., Heywood and Company Ltd., London (1960).
100. Tinklepaugh, J. R., Truesdale, R. S., Swica, J. J. and Hoskyns, W. R., "Grain Size Effects on the Thermal Conductivity of Ceramic Oxides," PB 171 346 (February 1961).

101. Brailsford, A. D. and Major K. G., "The Thermal Conductivity of Aggregates of Several Phases, Including Porous Materials," Brit. J. Appl. Phys. 15, 313-19 (1964).
102. Francis, R. K., Brown, R., McNamara, E. P. and Tinklepaugh, J. R., "Metal-Ceramic Laminates," AD 205549 (November 1958).
103. Hamilton, R. L. and Crosser, O. K., "Thermal Conductivity of Heterogeneous Two-Component Systems," Ind. Engng. Chem. Fundamentals 1, 187-91 (August 1962).
104. Loeb, A. L., "Thermal Conductivity: VIII, A Theory of Thermal Conductivity of Porous Materials," J. Am. Ceram. Soc. 37, 96-99 (February 1954).
105. Franci, J. and Kingery, W. D., "Thermal Conductivity: IX, Experimental Investigation of Effect of Porosity on Thermal Conductivity," J. Am. Ceram. Soc. 37, 99-107 (February 1954).
106. Williams, L. S., "Stress-Endurance of Sintered Alumina," Trans. Brit. Ceram. Soc. 55, 287-312 (1956).
107. Mizushima, J. S. and Knapp, W. J., "Behavior of a Ceramic Under Cyclic Loading," Ceramic News 5, 26-29, 36 (December 1956).
108. Goodman, Elliot, "Testing and Evaluation of Coatings," pg 189-235 of "High-Temperature Coatings," Huminik, John, Jr., ed., Reinhold Publishing Corp., New York (1963).
109. Mueller, J. I., University of Washington, private communique.
110. Bohn, J. R., "Research on Thermal Shock Characteristics of Refractory Materials," Space Technology Laboratories, First Quarterly Progress Report, Contract AF 33(615)-1662 (October 1964).
111. Shook, R. G. and Cole, J. E., General Dynamics/Pomona, unpublished work.
112. Preist, D. H. and Talcott, Ruth, "Thermal Stresses in Ceramic Cylinders Used in Vacuum Tubes," Am. Ceram. Soc. Bull. 38, 99-105 (March 1959).
113. Baroody, E. M., Duckworth, W. H., Simons, E. M. and Schofield, H. Z., "Effect of Shape and Material on the Thermal Rupture of Ceramics," AECD-3486 (May 22, 1951).
114. Smalley, A. K., Baroody, E. M., Simons, E. M. and Duckworth, W. H., "The Thermal Fracture of Ceramic Cylinders," Battelle Memorial Institute, Report No. BMI-1102 (June 28, 1956).

115. Buessem, W. R., "Thermal Shock," pg 468-76, 482-83 of "High-Temperature Technology," Campbell, I. E., ed., John Wiley & Sons, Inc., New York (1956).
116. Manson, S. S. and Smith, R. W., "Theory of Thermal Shock Resistance of Brittle Materials Based on Weibull's Statistical Theory of Strength," J. Am. Ceram. Soc. 38, 18-27 (January 1955).
117. Shanley, F. R., Knapp, W. J. and Needham, R. A., "Prestressed Ceramic Structures," WADC-TR-54-75, Part II (January 1955).
118. Brown, R. J., Brush Beryllium Company/Elmore, private communique.
119. Fleming, J. D., "Fused Silica Manual," Georgia Institute of Technology, EES Project B-153 Final Report, Prepared for U. S. Atomic Energy Commission, Contract No. AT (40-1)-2483 (September 1, 1964).
120. Kebler, R. W., Union Carbide Institute, private communique.
121. Logan, I. M. and Niesse, J. E., "Process and Design Data on a Boride-Silicide Composition Resistant to Oxidation to 2000° C," ASD-TDR-62-1055 (November 1962).
122. Tyrrell, M. E. and Koster, J., "Preparation and Evaluation of the Diborides (Ti, V) B₂, (Ti, C) B₂ and (Ti, Ta) B₂," Bureau of Mines Report of Investigations 6407 (1964).
123. Farrior, G. M., "Corrosion Resistance of Diborides in the Pseudobinary System TiB₂ .. CrB₂," Bureau of Mines Report of Investigations 6418 (1964).
124. Farrior, G. M., Norris Metallurgy Research Laboratory, unpublished work.
125. Giemza, C. J., Aeronca Manufacturing Corp., private communique.
126. Campbell, I. E., "High-Temperature Technology," John Wiley & Sons, Inc., New York (1956).
127. Liu, Tien-Shih and Stowell, E. Z., "Parametric Studies of Metal Fiber Reinforced Ceramic Composite Materials," AD 252 916 (January 26, 1961).
128. Clauser, H. R., Hauck, J. E., Fabian, R. J., Peckner, D., Lubars, W., and Campbell, J. B., Mater. Design. Eng. 28, 79-126 (September 1963).
129. Norton, J. T., "Selecting Cermets for High-Temperature Applications," Machine Design 28, 143-48 (April 19, 1956).
130. Pentecost, J. L., "Coating Materials and Coating Systems," pg 10-109 of "High-Temperature Inorganic Coatings," Huminik, John, Jr., ed., Reinhold Publishing Corporation, New York (1963).

131. Schwarzkopf, Paul and Kieffer, Richard, "Refractory Hard Metals," The MacMillan Company, New York (1953).
132. Buckley, J. D. and Cocke, B. W., Jr., "Evaluation of Selected Refractory Oxide Materials for Use in High-Temperature Pebble-Bed Wind-Tunnel Heat Exchanges," NASA TN D-2493 (September 1964).
133. Blome, J. C. and Kummer, D. L., "Ceramic and Graphite for Glide Reentry Vehicles," Presented at the 1964 Annual Fall Meeting of the Ceramics-Metal Systems Division, American Ceramic Society.
134. Glenny, E. and Taylor, T. A., "Mechanical Strength and Thermal Fatigue Characteristics of Silicon Nitride," Powder Met. 164-95 (1961).
135. Coble, R. L. and Kingery, W. D., "Effect of Porosity on Thermal Stress Fracture," J. Am. Ceram. Soc. 38, 33-37 (January 1955).
136. Goodier, J. N. and Florence, A. L., "Thermal Stress at an Insulated Circular Hole Near the Edge of an Insulated Plate under Uniform Heat Flow," Quart. J. Mech. & Appl. Math. 16, Pt. 3, 273-82 (1963).
137. Huang, P. C., "Deterioration in Strength of Brittle-State Porous Bodies," Presented at the Annual Meeting of the American Society of Mechanical Engineers, New York, November 29 to December 4, 1964.
138. Eubanks, A. G., National Aeronautics and Space Administration, Goddard Space Flight Center, private communique.
139. Strauss, E. L., "Structural and Heat Transfer Characteristics of Resin-Impregnated Porous Ceramics," Bull. Am. Ceram. Soc. 42, 444-47 (August 1963).
140. Schwartz, M. A., United Technology Center, Division of United Aircraft Corporation, private communique.
141. Dank, M., Nelson, R. A., Sheridan, W. R. and Sutton, W. H., "Water-Stabilized Arc Tests on Nonmetallic Materials," J. Electrochemical Soc. 106, 317-21 (April 1959).
142. Yavorsky, P. J., Zirconium Corporation of America, private communique.
143. Vogan, J. W. and Trumbull, J. L., "Metal-Ceramic Structural Composite Materials," ASD-TDR-62-784 (September 1962).
144. Bal'shin, M. Yu. and Likhtman, V. I., "Certain Problems in the Theory of the Thermal Shock Resistance of Powder Metal Materials," pg 110-16 of "Izledovaniia po Zharoprotchimy Splavam" (Research on Refractory Alloys, Russian), Vol. 8, USSR Academy of Sciences Press, Moscow (1962). Translated in "Soviet Studies in Powder Metallurgy," AD 400 000 (November 20, 1962).

145. Herring, L. B., "The Limit of Cooling Schedules by the Alpha-Beta Quartz Inversion," Thesis, M. S. Ceram. Eng., Clemson Agricultural College (June 1958).
146. Curtis, C. E., "Development of Zirconia Resistant to Thermal Shock," J. Am. Ceram. Soc. 30, 180-96 (June 1947).
147. Seegar, J. W., Lowrance, D. T. and Rogers, D. C. "X-20 Nose Cap Materials Summary Report," Ling-Temco-Vought, Inc. Report No. 311.29 (15 June 1964).
148. Ohnysty, B. and Stetson, A. R., "Development of Protective Coatings for Tantalum Base Alloys," Solar Aircraft Company, Contract AF 33(657)-11259, Quarterly Progress Report 2 (December 12, 1963).
149. McKinney, K., and Smith, H. L., "Thermal Shock Studies of Ceramic Materials," U. S. Naval Research Laboratory Report 6029 (December 30, 1963).
150. Paine, R. M., Brush Beryllium Company/Cleveland, private communique.
151. Huffadine, J. E., "The Fabrication and Properties of Molybdenum Disilicide and Molybdenum Disilicide - Alumina," pg 220-36 of "Special Ceramics," Popper, P., ed., Heywood and Company Ltd., London (1960).
152. Shaffer, P. T. B., "An Oxidation Resistant Boride Composition," Am. Ceram. Soc. Bull. 41, 96-99 (February 1962).
153. Arenberg, C. A., Rice, H. H., Schofield, H. Z. and Handwerk, J. H., "Thoria Ceramics," Am. Ceram. Soc. Bull. 36, 302-306 (August 1957).
154. Shaffer, P. T. B., "Thermal Shock Resistant Refractories," Industrial Research 5, 36-40 (May 1963).
155. Lepie, M. P., "The Properties of Pyrolytic ZrC," Trans. Brit. Ceram. Soc. 63, 431-49 (August 1964).
156. Leeds, D. H., Kendall, E. G. and Ward, J. F., "Preparation and Properties of Arc-cast TiC-C Alloys," Aerospace Corporation, unpublished work.
157. Huffadine, J. B., Longland, L. and Moore, N. C., "The Fabrication and Properties of Chromium-Alumina and Molybdenum-Chromium-Alumina Cermets," Powder Met. 235-52 (1958).
158. Richardson, L. D., Sr., "Ceramics for Aircraft Propulsion Systems," Am. Ceram. Soc. Bull. 33, 135-37 (May 1954).
159. Bragdon, T. A., "Evaluation of Cermets for Jet Engine Turbine Blading," WAIC-IR-55-215, AD 76 792 (January 1955).

160. Hoffman, C. A., "Preliminary Investigation of Zirconium Boride Ceramals for Gas-turbine-blade Applications," Natl. Advisory Comm. Aeronaut. Research Memo No. E52L15a (1953). Ceram. Abs. 118j (1958).
161. Voruz, T. A. and Accountis, O. E., "Shock-Resistant Ceramics," Rocketdyne Research Report No. 64-57 (December 1964).
162. Glenny, E., "Design Considerations in the Engineering Application of Brittle Materials," Trans. Brit. Ceram. Soc. 62, 565-75 (July 1963).
163. Baxter, J. R., "Cermets," Australasian Eng. 46, 45-50 (September 7, 1955).
164. Williams, L. S., "Cermets," pg 591-93 of "Mechanical Properties of Engineering Ceramics," Kriegel, W. W. and Palmour, Hayne, III, eds. Interscience Publishers, New York (1961).
165. Baxter, J. R., "Non-linear Stress V Strain Behavior of Two Types of Cermet," Weapons Research Establishment, Australia, Technical Note CPD 65 (September 1963).
166. Levy, A. B., "Extreme High Temperature Materials," pg 45-93 of "Materials for Missiles and Spacecraft," Parker, E. R., Ed., McGraw-Hill Book Company, Inc., New York (1963).
167. Fisher, J. I. and Hodson, R. L., "Development of Metal Fiber-Ceramic Rocket Nozzles," Armour Research Foundation Report 2177-3 (August 1959).
168. Truesdale, R. S., Swica, J. J., and Tinklepaugh, J. R., "Metal Fiber Reinforced Ceramics," WADC Technical Report 58-452, ASTIA Document No. 207079 (December 1958).
169. Swica, J. J., Hoskyns, W. R., Goss, B. R., Connor, J. H., and Tinklepaugh, J. R., "Metal Fiber Reinforced Ceramics," WADC Technical Report 58-452, Pt. II (January 1960).
170. Baskin, Y., Arenburg, C. A. and Handwerk, J. H., "Thoria Reinforced by Metal Fibers," Am. Ceram. Soc. Bull. 38, 345-48 (July 1959).
171. Huminik, John, Jr., "Designing with Coatings," pg. 236-62 of "High-Temperature Inorganic Coatings," Huminik, John, Jr., ed., Reinhold Publishing Corporation, New York (1963).
172. Simpson, F. H., "Composite Material Research at the Boeing Company," Report on The Boeing Company program: "Refractory Metal-Ceramic Macro-Laminate Composites," (February 1963).
173. Licciardello, M. R., Ohnysty, E. and Stetson, A. R., "Development of Frontal Section for Super-orbital, Lifting, Re-entry Vehicle, Volume II: Materials and Composite Structural Development," FDL-TDR-64-59, Volume II (May 29, 1964).

174. Greening, T. A., Rovin, S., Lavendel, H. W. and Bruce, E., "Development and Evaluation of Refractory Coating for Missile and Spacecraft Applications," Lockheed Missiles and Space Company, Technical Report: Materials and Chemistry 6-90-62-88 (October 1962).
175. Adams, M. C. and Scala, E., "Ceramic Heat Shielding for ICBM Re-entry Vehicle," Ceramic Ind. 74, 128-33 (April 1960).
176. Baer, D. H., Gates, L. E. and Robertson, G. D., "Ceramic Radome Evaluation," pg 382-405 of "Proceedings of the OSU-WADC Radome Symposium," Fouty, Robert and Greene, W. A., WADC-TR-58-272, Volume I, AD 155831 (June 1958).
177. Loyet, D. L. and Levitan, E. S., "Programming Thermal Stress Equations on the IBM-7090 Digital Computer," a 17 page report in "Proceedings of the ASD-OSU Symposium on Electromagnetic Windows," ASD-TDR-62-676, Vol. I, AD 286552 (July 1962).
178. Loyet, D. L. and Stevens, S., "A Comparison of Thin-wall and Half-wavelength Ceramic Radomes," a 19 page report in "Proceedings of the ASD-OSU Symposium on Electromagnetic Windows," ASD-RDR-62-676, Vol. I, AD 286552 (July 1962).
179. Suess, R. P. and Weckesser, L. B., "Radome Thermal Design for a Mach 4 Missile," APL Technical Digest (July - August 1964).
180. Walton, J. D., Jr. and Bowen, M. D., "The Evaluation of Ceramic Materials Under Thermal Shock Conditions," pg 149-73 of "Mechanical Properties of Engineering Ceramics," Kriegel, W. W. and Palmour, Hayne, III, Interscience Publishers, New York (1961).
181. Loyet, D. L., Hughes Aircraft Company, private communique.
182. Jones, R. A. and Feher, Stephen, Whittaker Corporation, Narmco Research and Development Division, private communique.
183. Nixon, J., "Test of a Hypervelocity Leading Edge in a Plasma Jet," North American Aviation, Inc. Report No. NA-60-1402 (1960).
184. Anthony, F. M., Merrihew, F. A., Mistretta, A. L. and Dukes, W. H., "Investigation of Feasibility of Utilizing Available Heat-Resistant Materials, Volume I, Summary," WADC-TR-59-744 (January 1961).
185. Warshaw, S. I., "Pre-stressed Ceramics," Am. Ceram. Soc. Bull. 36, 28, 30 (January 1957).
186. Wenger, L. S. and Knapp, W. J., "Prestressing and Thermal Shock of Ceramics," Pacific Coast Ceramic News (January and February 1955).

187. Shanley, F. R. and Knapp, W. J., University of California, Unpublished preliminary data obtained under Contract No. NSG-427, for National Aeronautics and Space Administration, Office of Space Sciences, Washington, D. C.
188. Wells, W. M. and Cline, C. F., "Thermal-Stress Fracture Characteristics of BeO," Presented at the Winter Annual Meeting of the American Society of Mechanical Engineers, Philadelphia, November 17-22, 1963.
189. Glenny, E. and Royston, M. G., "Transient Thermal Stresses Promoted by the Rapid Heating and Cooling of Brittle Circular Cylinders," Trans. Brit. Ceram. Soc. 57, 645-77 (1958).
190. Crandall, W. B. and Ging, J., "Thermal Shock Analysis of Spherical Shapes," J. Am. Ceram. Soc. 38, 39-46 (January 1955).
191. Hofer, K. E., Jr., Bredzs, N., Firestone, R. and Rudy, J., "Study of Attachments for Brittle Components," IIT Research Institute Project No. 8259, Contract AF 33(657)-8339, Final Report - Phase II, (November 15, 1963).
192. Anthony, F. M. and Mistretta, A. L., "Leading Edge Design with Brittle Materials," Prepared for the Joint Meeting of the Institute of the Aeronautical Sciences and the American Rocket Society, Los Angeles, June 13-15, 1961.
193. Barnett, R. L., "Literature on Design Techniques and Analytical Methods for Brittle Materials," AD 410479 (April 1963).
194. Blizzard, J. R., "Properties and Applications of Glasses and Ceramics," Machine Design 33, 166-67 (July 6, 1961).
195. Duckworth, W. M., "Designing with Brittle Materials," Materials in Design Eng. 49, 82-85 (January 1959).
196. Nowak, J. M., "Ceramic Materials for Leading Edges of Hypersonic Aircraft," Ceram. Age 77, 109-12, 114-15 (October 1961).
197. Thurnauer, Hans, "Properties and Uses of Technical Ceramics," Materials and Methods 26, 87-92 (December 1947).
198. Bloom, M. H., et al, "Aerodynamic and Structural Analyses of Radome Shells, Volume I. Aerodynamic Analysis," WADD-TR-59-22 (February 1961).
199. Eliason, L. K. and Zellner, G. C., "A Survey of High Temperature Ceramic Materials for Radomes," ML-TDR-64-296 (September 1964).
200. van Driest, E. R., "The Problem of Aerodynamic Heating," Aeronautical Engineering Review 15, 26-41 (October 1956).

201. Stire, H. A. and Warlass, Kent, "Theoretical and Experimental Investigation of Aerodynamic-Heating and Isothermal Heat Transfer Parameters on a Hemispherical Nose with Laminar Boundary Layer at Supersonic Mach Numbers," NACA TN 3344 (December 1954).

APPENDIX I

EXTENDED ABSTRACTS OF SELECTED ARTICLES

1. Artamonov, A. Ya. and Shvedkov, E. L., "Effect of Machining on the Strength of Superhard Materials," Poroshkovaya metallurgiya (Powder Metallurgy, Soviet), no. 1 (13), 79-82 (1963).

The results of an investigation of the effect of "harsh" and "mild" electro-erosion cutting conditions on the bending strength in comparison with grinding are given for chromium carbide containing 15 per cent Ni and titanium carbide containing 30 per cent nichrome. Superhard cermets on a chromium or titanium carbide base should not be ground since thereby the strength is reduced by 40 to 60 per cent (the initial strengths being 52,700 psi for the titanium carbide cermet, and 71,300 psi for chromium carbide cermet). If the machining allowances are large, these materials should be machined by electro-erosion methods using harsh conditions which ensure a high productivity, with subsequent removal of the defective surface layer by fine electro-erosion cutting. When the machining allowances are small, machining must be carried out only under mild electro-erosion cutting conditions which increase the strength by 7 to 14 per cent.

2. Guleviv, O., "Some Ways of Speeding Up the Process of Body Formation in Casting," Szklo i ceramika (Glass and Ceramics, Polish) 14, no. 4, 111-14 (1963).

The following techniques are used for the acceleration of casting:

- (1) proper selection of materials and electrolytes;
- (2) increasing the temperature of the casting slip;
- (3) de-aeration of the slip before casting;
- (4) de-aeration of the plaster slip for molds;
- (5) use of combined plaster-ceramic molds;
- (6) heating the molds while casting;
- (7) blowing warm air into the molds after pouring out the excess slip;
- (8) pouring only sufficient slip for the body in the mold and rotating the mold.

Examples given for the casting of porcelain and fireclay show that the rate of body building and the crushing strength of the products can be increased by 30 to 40 per cent.

3. Bradshaw, W. G. and Matthews, C. O., "Properties of Refractory Materials: Collected Data and References," PB 171101, Second ed., third print (15 June 1960).

A comprehensive survey was made of the properties of materials melting above 2500° F to assist in the selection of materials for high-temperature applications.

The maximum recommended use temperatures (in a suitable medium) and the high-temperature oxidation characteristics of the carbides are given. Since the nitrides are subject to decomposition in the absence of an adequate nitrogen overpressure, the vapor pressures have been listed for the nitrides along with their high-temperature oxidation characteristics. For the borides, the oxidation characteristics and high-temperature stabilities are presented. For the oxides, whose behavior varies markedly in different environments, high-temperature stabilities are given for an oxidizing atmosphere, a reducing atmosphere and a vacuum. Also listed are the oxidation characteristics of the silicides and sulfides, the volatility of the sulfides, the high-temperature characteristics of mixed oxides and chromites, and the high-temperature properties of beryllides, aluminides, other intermetallics, and phosphides.

Thermal properties including the thermal shock resistance, thermal conductivity and thermal expansion are presented for carbides, oxides, nitrides, borides, sulfides and silicides. In the case of the oxides, the thermal conductivity is given for the dense material and for a material with some porosity. The data on the emittance of some of the materials are also presented.

Mechanical properties are listed for refractory carbides, oxide, nitrides, and silicides.

A number of pertinent figures are presented. However, the real value of the report lies in its tables which list the properties of materials at various temperature levels together with references. Most of the data on thermal shock resistance was extracted from Campbell, I. E., "High-Temperature Technology," John Wiley & Sons, New York (1956).

4. Goldsmith, Alexander, Waterman, T. E. and Hirschhorn, H. J., "Thermophysical Properties of Solid Materials," Five volumes, Macmillan Company, New York (1961), 4263 pg.

All original test data published from 1940 to 1957, inclusive, on the thermophysical properties of solids were collected, and the data are presented in five volumes: I. Elements, II. Alloys, III. Ceramics, IV. Intermetallics, Polymers, and Composites, V. Appendix. The materials covered in volumes III and IV include those that melt above 1000° F. Most of the data are presented in graphical form. Most probable values are presented for both the graphical data and the tabular data. Volume V serves as the material index for the first four volumes and includes the references and the author index.

5. Shaffer, F. T. B., "High-temperature Materials, No. 1 - Materials Index," Plenum Press, New York (1964).

Data on the properties of more than 520 different materials are presented. Data are presented in tabular form, and sometimes in equation form, for a wide range of temperatures. Borides, carbides, nitrides, oxides, and silicides are among the materials which are considered. The volume is well indexed and well documented.

6. Stutzman, R. H., Salvaggi, J. R. and Kirchner, H. P., "Summary Report on an Investigation of the Theoretical and Practical Aspects of the Thermal Expansion of Ceramic Materials, Volume one - Literature Survey," AD220685 (August 31, 1959).

A literature survey was conducted on the reversible thermal expansion of various materials, and 954 references are assembled in a bibliography. The results of thermal expansion measurements from 523 articles and reports are presented in tabular form. The materials considered include crystalline ceramics, glasses, cermets, intermetallic compounds, and ceramics combined with other types of materials. The data are listed in alphabetical order according to chemical composition, with only a few exceptions.

7. Wood, W. D., Deem, H. W. and Lucks, C. F., "Thermal Radiative Properties of Selected Materials," DMIC Report 177, Volume 1 and Volume 2 (November 15, 1962).

The first volume includes data on refractory metals and their alloys, superalloys, and titanium and its alloys, together with a brief discussion of the fundamentals of thermal radiation and the methods used to measure thermal radiative properties. The second volume includes radiative property data for ceramics, graphite, and coated materials for high temperature. Emittance data are presented in graphical form as a function of temperature and as a function of wavelength, and references to the source of the data are cited. The coverage is excellent with data on ceramics listed for carbides, nitrides, oxides, silicides and Pyroceram®.

The data on ceramics and graphites was published separately at an earlier date: *Ibid*, "The Emittance of Ceramics and Graphites," AD 274148, DMIC Memorandum 148 (March 28, 1962).

8. Astarita, G., "Contribution to the Study of Thermal Shock," Bulletin de la Société Francaise de Céramique, no. 41, 3-20 (1958).

PART ONE

The resistance of a given material to variations of temperature depends on the thermal and mechanical parameters relative to the material, on the geometric form and conditions of contact of the sample, and on the type of thermal phenomenon acting on the exterior.

The mechanical parameters include: the critical stress σ (resistance to tension or compression according to whether the thermal phenomenon is cooling or heating); Young's modulus E ; the Poisson coefficient μ ; the coefficient of linear expansion α ; and Weibull's constant m .

The thermal parameters include: the conductivity k ; the thermal diffusivity a ; and the specific heat c .

The geometric form of the test piece and conditions of contact can be characterized by a sufficient number of form coefficients and by a single linear dimension L ; the thickness of the piece in the direction perpendicular to the surface exposed to thermal shock is usually chosen. To characterize the external thermal effect, there are available a sufficient number of form factors, a characteristic time θ and two parameters: the maximum level of external temperature t'_{\max} and the surface heat transfer coefficient h . The influence of each of these parameters is not always the same, but depends on the value of the others.

Some predictions can be made concerning the relative influence of these parameters by using the principles of dimensional analysis. Dimensional analysis allows the independent variables to be reduced to six groups according to their dimensions:

$$\alpha, t'_{\max}, \sigma/E, m, \mu, \frac{a\theta}{L^2}, \frac{hL}{k}$$

Furthermore, the theory of elasticity shows that the stresses of thermal origin are always proportional to the product αE . Accordingly, the first two groups can be reduced to one, and only the following five variables remain:

$$M = \frac{\sigma}{\alpha E t'_{\max}}, \text{ resistance figure of merit}$$

$$F = \frac{a\theta}{L^2}, \text{ Fourier number}$$

$$N = \frac{hL}{k}, \text{ Nusselt number} \quad (65)$$

m , the Weibull constant

μ , the Poisson coefficient

Each time that the theory of maximum stress can be accepted as valid, dimensional analysis can be applied for determination of the degree of thermal shock which the material can withstand without shattering ($\sigma_{\max} = \sigma$). Otherwise, the limiting degree is determined by the condition that the "risk of rupture" of the effect considered is equal to the critical value of that effect.

The relative influence of the above variables, in (65), cannot be predicted a priori, but must be separately determined in each particular case.

To fix attention on the ratio h/k , the Nusselt number, implies formulating the problem as a function of parameters which are not proper to the material (h), therefore confirming the impossibility of a quantitative formula for the coefficient of resistance as a function of all parameters relative to the material and it alone.

Occasionally, the thermal variations of the parameters of the material can be important, and it is necessary to take them into account. Recourse should then be made to direct methods for calculating the distribution of stresses. When the temperature distribution is known, the stress distribution can be calculated by means of the theory of elasticity. Furthermore, the maximum stress can always be compared to the critical value relative to the temperature existing at the point and at the instant where this stress appears.

It is difficult to handle the variations of Young's modulus, but variations of the E modulus with temperature can be important. One cannot establish whether or not this is favorable. In order to furnish some qualitative indications of the importance of the E modulus, stress diagrams relative to two types of thermal cycles were produced on plane surfaces 11 cm thick by choosing average constant values for α and E and by taking into account their variation with temperature. The following table includes the data for the material and the thermal cycles considered. For test 1, the variation of α and E led to higher stress levels within the slab, while the variation led to lower stress levels for test 2.

Parameter	$32^{\circ} F$	$392^{\circ} F$	$752^{\circ} C$	$1112^{\circ} F$	$1472^{\circ} F$
k , BTU/ft \cdot $^{\circ} F$ \cdot hr	0.4	0.4	0.4	0.4	0.4
$10^4 \alpha$, ft^2/hr	1.07	1.07	1.07	1.07	1.07
σ , psi	1670	1270	1470	1700	2120

(Continued)

Parameter	<u>32° F</u>	<u>392° F</u>	<u>752° C</u>	<u>1112° F</u>	<u>1472° F</u>
$10^{-3}E$, psi	198	198	226	325	297
$10^6 \alpha_{avg}$, $^{\circ}F^{-1}$	-	3.0	3.1	3.3	2.7
m ,-----	9.4	10	9.4	9.4	9.4
Composition		SiO_2		69.21%	
		Al_2O_3		26.36	
		Fe_2O_3		3.25	
Loss to fire				0.70	

Thermal cycle: Thickness of wall 11 cm. Initial temperature distribution, linear, from 1832 to 68° F. Natural cooling in still air (test 1); forced cooling with air blast at 0.75 ft/sec (test 2).

Conclusions:

By means of analytical and graphical methods proposed by various authors, thermal phenomenon can, at least, be theoretically predicted. This prediction can be justified by the agreement of results of calculations and experiences demonstrated by recent studies. These prediction methods do not neglect the influence of the value of the surface heat transfer, the geometric form of the elements subjected to stress, the conditions of binding, the homogeneity of the material (the Weibull constant m), or variations of the parameters with temperature. It cannot be affirmed *a priori* if the latter influence is favorable or not to the material's resistance to stresses of thermal origin, but it is at least possible to have theoretical prediction in a given particular case.

PART TWO

MECHANICAL RESISTANCE OF PLANE SURFACES TO PROGRESSIVE PROCESSES OF HEATING AND COOLING

With regard to the coefficient of homogeneity, it is well to observe that its influence is negligible when its value exceeds 10, and the theory of maximum stress can be accepted as applicable. The author's research has been limited to materials with $m > 10$. In the case where this inequality does not hold, a higher safety factor would be adopted to take account of the degree of approximation introduced. However, recent studies have shown that even for

rare materials where $m < 10$, the theory of maximum stress gives sufficient predictions. The difference in experimental results does not exceed 10 to 20 per cent.

The following problem is dealt with in this note: given a plane surface of known depth and of known thermal and mechanical properties, the initial temperature distribution being constant or linearly variable in the direction of depth (thickness), determine the most severe heating (or cooling) conditions of the atmosphere in contact with one of the surfaces (the surface of highest temperature) which assure the resistance of the material to stresses which are set up during the transitory period.

The problem is particularly interesting in the case where the external temperature difference is greater than the minimum value for absolute safety, namely

$$t'_{\max} > \frac{\sigma}{\alpha E} ; \quad M > 1 \quad (66)$$

where t'_{\max} is the total temperature variation. The object of the theoretical and experimental study here is the determination of a law of general character, which furnishes the minimum period θ capable of assuring the mechanical resistance of a surface subjected to a progressive thermal shock for which $M > 1$.

Theoretical Study

For simplification, it is supposed that the Nusselt number is infinite. Hence, the predictions formulated theoretically would err in favor of safety. It is also supposed that the distributions of temperatures are independent of the thermal characteristics of the unexposed surface. The initial distribution of temperatures is considered uniform when heating is in question, and variable in thickness according to a linear law in the case of cooling. The external temperature is assumed to follow a linear law as a function of time.

The following relation is developed between M and F :

$$\frac{1}{pM} = 1 - 1.2 \sqrt{F} \left[2 + e^{-1.67/\sqrt{F}} \right] + 2.16F \left[1 - e^{-1.67/\sqrt{F}} \right] \quad (67)$$

where p is the safety factor. The relation shows that the resistance to a known shock will be all the better when the diffusivity α and the critical stress σ are larger, and when the coefficient of linear expansion α , the modulus of elasticity E , and the thicknesses L are smaller. However, for shocks of very short duration or truly instantaneous nature, the parameters α and L play no part. Furthermore, the preceding confirms the impossibility of characterizing materials in a general manner because of the influence of thermal parameters which depend on the type of shock considered.

Experimental Part

A series of experimental determinations were performed, and the results exactly confirmed the fundamental theoretical hypotheses. While the tests performed have been chiefly with cooling, some tests with heating have given results which agree with the theory. Most of the experimental work was performed on magnesia refractory bricks, but the results of other experimental work with silicious and silico-aluminous bricks were also examined. The criterion for failure was cracking at the surface of the bricks.

Conclusions

The relation developed represents a limiting condition: infinite Nusselt number. Insofar as this condition can be regarded as exact, the relation supplies exact predictions. Undoubtedly this limiting condition is not always verifiable in practice; however, in all cases this relation offers predictions relative to the most unfavorable case, and allows the severity of the thermal shock to be maintained within limits of absolute safety.

O. Bahn, Rolf and Pump, Karl, "Investigation of a Simple Measuring Procedure for The Determination of the Thermal Shock Resistance," Silikattechnik, 10, 190-2 (1959).

In many cases, the critical examination of the thermal shock resistance of ceramic materials exhibits considerable deficiencies because of the very different (and often inadequate) measuring methods which are used. As a result, these measuring methods are only comparable if similar samples are used. M. S. Tacvorian has found, however, that the appearance of cracks always precedes a visible destruction of a sample and that a reproducible and exact relationship exists between visible fracture and decrease of mechanical strength. The purpose of this research was to examine this dependency.

A number of cylindrical rods, 8 to 10 mm in diameter, of drawn sintered corundum were tested for bending strength ($\sigma_0 = 32,100$ psi) while others were submitted to five thermal shocks. After each shock five rods were selected and bending strengths (σ) were taken. For the bending strength an edge distance of 70 mm was used. The thermal shocking was accomplished by heating the rods in a small furnace at a rate of 5.4° F/min., allowing the rods to stabilize 30 min. at the final temperature of the furnace, and quenching the rods in water. The temperature change ΔT for the shocks were increased by constant intervals to establish the characteristic function $\frac{\sigma}{\sigma_0} = f(\Delta T)$.

Since the decay of the structure took place gradually, a precise determination of the thermal shock carrying capacity was not obtained. A threshold value of 160° F, however, was obtained for the material. Above the threshold disintegration becomes apparent because of a decrease in the mechanical strength.

Below the threshold no disintegration took place, regardless of the number of times it was shocked. It was, therefore, suggested that a characteristic function $\frac{C}{G_0} = f(\Delta T)$ and a threshold could be determined for any ceramic material and that a sample below its threshold could survive any number of thermal shocks, regardless of its shape.

In the experiment it was observed that samples of the drawn sintered corundum shocked beyond the 160° F threshold showed cracks at the surface, while the core was unaffected, but the samples still had a certain bending strength. For samples cycled five times, a plot of $\frac{C}{G_0}$ versus ΔT showed a minimum at a ΔT of approximately 300° F. The samples investigated in the minimum exhibited no external cracks, but were under a high tension (stress) caused by the thermocycling so that the bending strength was low. These stresses decreased after the surface cracked with increased shock, and the bending strength increased to a small extent.

It was of interest to what extent the shape of the sample would have on the results of this experiment. For this phase a special china for lab devices was assembled into (1) 10 mm (dia) cylindric rods, and (2) pipes with a 12 mm outside diameter and a 2 mm wall thickness. These samples were thermocycled in the same way as the previous samples. The results show that the thermal shock resistance of the two pieces was very similar.

In other experiments the occurrence of a maximum, in isolated cases also a minimum, preceding the threshold was found to be a characteristic for materials consisting of various components. No maximum was observed with one component material systems, such as Al_2O_3 or ZrO_2 regardless of the shape of the sample. Thus in multi-component systems, stresses due to different coefficients of thermal expansions of the various components must cause other stresses in the samples.

In experiments on a glazed china it was found that a well fitting glazing "sits" on a ceramic material with little tensile stress. One glazing, which "sat" on a ceramic under compressive stress, exhibited a rather high maximum $\frac{C}{G_0}$ versus ΔT before the threshold was reached.

Measurements were also carried out for the development of mixed ceramic materials. It was found that the thermal shock resistance of pure clay increased only a small amount with increasing chromium content (up to 30%), while the threshold increased slightly. The characteristic feature of the $\frac{C}{G_0}$ versus ΔT plots for mixed ceramics is that they do not decrease to zero right after the threshold, but remain constant within a relatively wide range.

In general, it was found in these experiments that scattering of the strength results appears to be the greatest at the threshold. This can be explained by the initiation of the structure disintegration in this range.

10. Berezhnoy, A. S., "Search for New Refractories," Ogneupory (Refractories, Soviet), no. 8, 341-47 (1963).

A survey is presented on statistical rules governing the relation between the melting point and physicochemical properties. The melting point decreases as the number of components involved in the crystal lattice increases. The refractoriness of a compound with two simple oxides is two orders of magnitude greater than the refractoriness of a compound with three components. Hence, new oxide refractories must, above all, be searched in binary oxide systems.

11. Blank, H., "Transmission Electron Microscopy of Single Crystals of Ceramic Materials," Berichte der Deutschen Keram Gesellschaft (Reports of the German Ceramics Society), 40, no. 2, 136-39 (1963).

The method of investigating lattice defects in crystals have been largely developed for metals and in most cases they are applicable to non-metals. Some results on irradiated and non-irradiated UO_2 crystals are reported. Using an electron beam, cracks can be produced in the specimens by thermal shocks and changes in the structure can be observed. In irradiated UO_2 the lattice defects caused by nuclear fission and the traces of fission atoms become observable.

12. Dawihl, W. and Dörre, E., "The Strength and The Deformation Properties of Sintered Alumina Bodies as a Function of Their Composition and Structure," Berichte der Deutschen Keramischen Gesellschaft (Reports of the German Ceramics Society), 41, no. 2, 85-97 (1964).

Sintered alumina bodies were investigated at room temperature, at 572° and at 1832° F for crushing strength, impact strength, shrinkage and hardness in two series: a) varying the MgO and SiO_2 content and keeping the firing conditions constant, and b) varying the firing conditions and keeping the composition constant. The crushing strength of sintered alumina containing up to 3.5% MgO or 6.5% SiO_2 comes up to that of $WC + 6\% Co$. The crushing strength is inversely proportional to the grain size above the critical size of 3-4 μ . Below this size, effects of porosity, etc. play the first part. The spinel which originates from the MgO addition forms agglomerates increasing in size with increasing MgO content without affecting the crushing strength.

13. Delrieux, J. and Rocco, D., "Reflections on the Fracture of Thermal Origin in Refractories Subjected to Service Conditions," Silicates industriels (Industrial Silicates, French) 28, no. 2, 59-70 (1963).

The fractures of thermal origin in refractories in service can take a variety of forms. Some can be explained in a simple way but for others the

absence of a mechanical explanation of the phenomenon has led to the belief that the influence of physicochemical processes, which change the properties of the material, had an over-riding influence. For the simple case of refractory bricks exposed to a furnace on one side, the direction of the thermal shock affects the crack formation--quenching acts more intensively than heating. In practice neither elastic nor plastic deformation occurs, but a series of intermediate states with various degrees of elastic and plastic properties. Hence, one must appreciate the complexity of the phenomenon and estimate the thermal shock resistance of refractories with great care.

14. Kukolev, G. V. and Nemets, I. I., "Up-to-date Conceptions on the Heat Resistance of Ceramic Refractory Materials and Means for Its Increase," Zhurnal vsesoyuznogo khimicheskogo obshehestva im. D. I. Mendeleyeva (Journal of the All-Union D. I. Mendeleyev Chemical Society, Soviet), 8, no. 2, 155-62 (1963).

Relevant equations are given for the maximum temperature difference that a material can withstand, and cases of quick and slow heat transfer, as well as the size factor, are discussed. For heterogeneous systems (refractories and ceramics), the maximum stresses, as well as the statistics, must be taken into consideration. Supplementary to the statistical theory by Weibull, not only the presence of the defects expressed by the homogeneity factor m but, also, their size and position in the material are decisive for the heat resistance. Existing test methods do not yet consider the change of a refractory during service. As a test for cermets, the change of the bending strength before and after the thermal shock is measured; for alumina-silicate refractories changes in the gas permeability and adhesion are determined before and after the thermal shock. One new method is the determination of the occurrence of cracks after thermal shock by measuring the change in the resonance frequency of the material or the ultrasonics propagation rate.

Means for increasing the heat resistance are mentioned, such as: reducing the coefficient of thermal expansion α ; modification of the coefficient of shear by microcrack structure; allowing mutual displacement of the grains (for example, by combining two or more phases); or by using porous or fibrous ceramics.

15. Lambert, R., "Influence of the Conditions of The Edge on The Thermal Shock of a Piece of Flat Glass," Verres Refractories, 14, no. 6, 333-39 (1960).

The manner of cutting and fabrication of a glass object can affect its permanence once it is in place. In effect it can produce momentary tensile stresses due to local heating which, acting on a point of low resistance, can produce breaking of the glass. The breaking depends not only on the magnitude of the stress, but also on the nature and on the orientation of the already existing weak points.

Heating is often local and protected edges, in particular, participate in different cycles of heating and cooling. In addition, local stresses can be generated and the extensions are especially dangerous on the edges of the volume which possess the imperceptible weak points due to handling and the method of making the edges.

In the extreme case, part of a glass surface is heated by radiation and a break occurs at the end of a certain time. The origin of the break is always located on the closest edge of the heating zone. The break comes from a spot less resistant and propagates to the heated zone. It can then penetrate into a part in compression where it expires, but if it goes out of this zone it becomes violent and spreads over the remaining volume.

If the guard, i.e., the distance between the heated zone and the edge of the volume, is decreased without changing the heat source, the time which elapses between the beginning of the heating and the break also decreases, and the break becomes less and less violent. If the distance between the heating source and the edge is decreased until they finally are in contact, tensile stresses do not rise as long as the heating period lasts, but a break can occur on cooling because the conditions of cooling are no longer the same between the edge and the interior of the volume. It has been found experimentally that the heating time needed to cause a break is a minimum for a guard of 10 to 15 mm, and experience has shown that changes in cutting and finishing techniques can result in a 70° to 150° F temperature difference at thermal shock failure for a piece of flat glass.

16. Lapoujade, Paulette, "General Conceptions Regarding Thermal Shock - Parts I and II," Silicates industriels, no. 22, 491-496, 578-582 (1958).

Two distinct phenomena in the evaluation of the resistance of products to sudden variations of temperature ought to be noticed: (1) the appearance of fissures at the moment when the resistance becomes insufficient to support the stresses imposed by the thermal shock, and (2) the propagation of these fissures which can lead to detachment of a part of the ceramic piece considered.

Some very detailed studies have been made, and are being made, on the nature of thermal stresses induced by thermal shock by basing everything on the determination of the maximum stress supportable by the sample before the appearance of a fissure. The most generally accepted conclusions are:

1. The resistance to shearing comes into play only slightly in a sample subjected to a thermal shock.
2. The maximum stress is not always produced at the surface but can be produced at a certain distance in the depth of the sample.

Often, however, these studies lead to the development of theoretical formulas which are only valuable under well defined conditions, and it is evident that

the formulas can only furnish an approximate idea of resistance to variations of temperatures in refractories and only relate to the appearance of fissures.

Even though the theoretical analysis of the phenomena have their faults, they can serve to improve the empirical experiments actually made. An empirical test that is carefully defined and conducted can give as much, if not more, information on the service life of a refractory product than a theoretical formula; since not only the appearance of the fissures and their propagation is followed, but the fashion in which the product accommodates the stresses is also taken into account.

Given all the imperfections of empirical tests and the difficulties of the application of theoretical formulas, there has been a several years' search to find indirect test methods for determining the resistance of ceramic products to thermal shocks. A number of researchers have studied the variation of the modulus of elasticity E as a function of thermal cycles undergone by the products, either by sonic methods, ultrasonic methods, or static methods. Others, owing to the difficulties of measuring E , have addressed themselves to resistance to torsion. The study of variations of the resistance to flexure as a function of amplitude of the thermal shock imposed has permitted Tacvorian, among others, to specify the "threshold" for thermal shock supportable by a given product.

Several researchers have tried to detect the onset of invisible fissures and relate it:

- with the limiting rate of heating, by sonic study of the variation of the modulus of elasticity, and
- with the number of thermal shock cycles endurable, for example in France by studying the variation of permeability after two thermal shock cycles, or by ultrasonic measurement of the variation in the modulus of elasticity.

Other researchers have taken for systematic study the rates of heating undergone by a piece, or a plate, placed in given conditions and have measured the time required for fissures to form.

And finally, research on structure is the last of the indirect methods to have appeared and possibly will be the most valuable since it attempts to determine what in the very structure of the product can account for the creation of thermal stresses and for the transmission of these stresses and the resulting fissures.

17. L'vov, S. N., Nemchenko, V. F., and Paderno, Yu. B., "Heat Conductivity of The Hexaborides of Alkaline-earth and Rare-earth Metals," Dokl. Akademii Nauk SSSR (Reports of the Academy of Sciences USSR), 149, no. 6, 1371-72 (1963).

Data are given for the heat conductivity of the hexaborides of Ca, Sr, Ba, Y, La, Ce, Pr, Nd, Sm, Eu, Gd, Tb, Th. In all cases, the heat conductivity is about three times higher than that of the corresponding metals.

18. Massimilla, L., and Bracale, S., "Investigations Concerning the Resistance of a Silica-Alumina Refractory to Rapid Cooling Tests," Giornata dei Refrattari, Milan, April 26, 1957.

In investigations concerning the resistance of a material to thermal shocks the two most common theories dealt with are: (1) the theory of maximum stress, and (2) Weibull's statistical theory.

For the determination of the actual temperature distribution in a refractory wall, it is sufficient to know: (1) the thermal cycle to which the wall will be subjected (2) the thermal and mechanical characteristics of the material from which the wall is constructed; i.e., thermal diffusivity and conductivity, coefficient of thermal expansion, the modulus of elasticity, and the effect of temperature change on each, and (3) the coefficients of external thermal transmission and the nature and characteristics of the external constraints. After the actual temperature distributions within a refractory and the breaking strengths (tensional and compressional) of the refractory are known, it is then possible to make predictions concerning the stability of the refractory to the stresses that take place in the structure after a designated thermal cycle.

A choice between the maximum stress theory and Weibull's statistical theory should be made by taking into account the value of the homogeneousness constant m for the refractory material from which the wall is made. If m is high, i.e., the material is very homogeneous, the theory of maximum stress will give adequate results. On the other hand, when a nonhomogeneous refractory material is used or when the wall is to be exposed to high rates of heating or cooling, the zone of high stresses is much smaller with respect to the whole volume and Weibull's statistical theory should be used. As a general rule, when working with materials with a high m , higher than 20 for sufficiently homogeneous materials, it is superfluous to use Weibull's statistical theory, but for materials with an m below 3 it becomes necessary to use Weibull's statistical theory even in the case of slow cooling. In the intermediate cases, i.e., when the homogeneousness constant for the refractory is between 3 and 20, it is impossible to know *a priori* on which of the two theories the investigations should be based. Nevertheless, even in these cases, Weibull's statistical theory has the most to offer because it takes the homogeneity characteristics of the material into consideration.

Experimental

Tables II and III give an insight into the various properties of the refractory materials considered. The breaking strengths were obtained by averaging the results of 20 to 25 breaking tests on a rectangular section (210 x 30 x 10 mm) of the refractory material to be shocked using 3 point loading with 200 mm between the two fixed knifes.

TABLE II
CHEMICAL COMPOSITION AND THERMAL AND MECHANICAL CHARACTERISTICS
OF THE SILICA-ALUMINA REFRACTORY UNDER EXPERIMENTATION

Chemical composition	SiO_2	69.21%
	Fe_2O_3	3.25% Loss on fire 0.7%
	Al_2O_3	26.36%
Thermal Conductivity	0.405	BTU/ft. ² °F·hr.
Specific heat	28.9	BTU/ft ³ ·°F
Thermal diffusivity	1.05×10^{-4}	ft ² /hr.
Linear thermal expansion	3.5×10^{-6}	per °F.

TABLE III
BREAKING TENSILE STRENGTH, MODULUS OF ELASTICITY AND
HOMOGENEUSNESS CONSTANT OF THE MATERIAL AT TEMPERATURES
BETWEEN 68° AND 1472° C

Temp. (°F)	Minimum breaking strength (psi)	Maximum breaking strength (psi)	Average breaking strength (psi)	Homogen- eouness constant (no dim.)	Modulus of elasticity (psi)
68	762	1510	1255	10.9	197,600
752	1105	1840	1465	9.4	221,600
1202	1520	2090	1685	9.4	326,000
1472	1520	3210	2115	9.4	292,800

The testing was done on panels cut from bricks so that the walls were 120 mm thick. These panels were slowly heated until both the oven and the panel were at the testing temperature and a nearly linear temperature distribution was established. All data concerning these tests are listed in Table IV. The value of the homogeneousness constant m of the material was close to 9 so it was not possible to state a priori whether the theory of maximum stresses or Weibull's theory should be used. Because of this uncertainty both theories were used so that the results could be compared. The temperature distribution in the wall and the tensions that take place in the refractory during the determined thermal cycle were calculated at time intervals of 0.58 seconds. In all calculations, m was assumed to have a constant value of 9.4.

It can be deduced from Table IV that, as a general rule, the theory of maximum stress is sufficient enough to make predictions on the resistance to rapid temperature variations of the refractory. In all the tests the refractory was fractured when the maximum generated stress was roughly close to the critical strength of the material. However, the comparison between the stresses generated in the wall and the critical strengths was uncertain in some tests where the maximum calculated stresses were sometimes 20 to 25% lower than the average breaking stresses and, yet, the wall was fractured. These uncertainties are caused by the disputable physical significance of the average breaking strengths and can be eliminated by using Weibull's statistical theory. The refractory wall is characterized by a fairly well defined breaking risk (close to 13).

19. Neshpor, V. S. and Ordanyan, S. S., "Shear Moduli of the Silicides of Some Transition Metals," Poroshkovaya metallurgiya (Powder Metallurgy, Soviet), no. 1 (19), 23-28, (1964).

The shear moduli of MoSi_2 , WSi_2 , ReSi_2 , Mo_3Si , Mo_5Si_3 , ReSi , Re_3Si , and MoGe_2 were studied experimentally. Data on the velocity of sound and the shear modulus were obtained for the first time. The covalent bonds between the silicon atoms in higher silicides were found to be predominant.

20. Neshpor, V. S. and Reznichenko, M. I., "Investigations of the Thermal Expansion of Some Silicides," Ogneupory (Refractories, Soviet), no. 3, 134-37 (1963).

On the basis of a empirical formula $\alpha = at^b$ (where a and b are constants, and t is the melting point), α was calculated for the silicides of T, V, Cr, Co, Ni, Fe, Zr, Nb, Ta, W, Re, La, Ba, Mg, and U and compared with data obtained experimentally. As a rule, the deviations vary between 5 and 10%, but sometimes they vary between as much as 20 and 40%.

TABLE IV
RESULTS OF THE TESTS AND CALCULATIONS

Test	Temp. Change (°F)	Type of Cooling	Maximum Tension Stress in Test (psi)	Maximum Breaking Risk in Test	Breaking Strength (psi)	Observations (Whether the Panel was Fractured or Not)

1	2160	air:0.72 ft/sec.	1400	518	1440	Yes
2	2160	calm air.	1330	473	1450	Yes
3	1980	air:0.72 ft/sec.	1330	470	1450	Yes
4	1890	air:6.98 ft/sec. water:11.7 lb/ft ² ·hr.	1830	5200	1480	Yes
5	1800	air:6.98 ft/sec. water:7.1 lb/ft ² ·hr.	1580	2300	1500	Yes
6	1800	air:6.98 ft/sec.	1480	1200	1480	Yes
7	1800	air:4.98 ft/sec.	1380	522	1480	Yes
8	1800	air:1.51 ft/sec.	1310	451	1440	Yes
9	1800	air:0.72 ft/sec.	1280	380	1430	Yes
10	1800	calm air	1270	318	1430	Yes

TABLE IV (Continued)
RESULTS OF THE TESTS AND CALCULATIONS

<u>Test</u>	<u>Temp. Change</u> (°F)	<u>Type of Cooling</u>	<u>Maximum * Tension Stress in Test</u> (psi)	<u>Maximum ** Breaking Risk in Test</u> (psi)	<u>Breaking *** Strength</u> (psi)	<u>Observations (Whether the Panel was fractured or not)</u>
11	1620	air: 6.98 ft/sec. water: 10.1 lb/ft ² ·hr.	1610	2810	1310	Yes
12	1620	air: 6.98 ft/sec.	1330	462	1440	Yes
13	1620	calm air	1170	120	1430	Yes
14	1440	air: 6.98 ft/sec.	1140	118	1510	Yes
15	1440	calm air	1030	43	1470	Yes
16	1260	air: 6.98 ft/sec. water: 10.1 lb/ft ² ·hr.	1230	213	1330	Yes
17	1260	air: 6.98 ft/sec.	920	14	1450	Yes
18	1260	calm air	850	6	1450	No
19	1080	air: 6.98 ft/sec. water: 37.9 lb/ft ² ·hr.	1000	35	1310	Yes

TABLE IV (Concluded)

RESULTS OF THE TESTS AND CALCULATIONS

<u>Test</u>	<u>Temp. Change (°F)</u>	<u>Type of Cooling</u>	<u>Maximum Tension Stress in Test (psi)</u>	<u>Maximum Breaking Risk in Test</u>	<u>Breaking Strength (psi)</u>	<u>Observations (Whether the Panel was broken, or not)</u>
20	1080	air:6.98 ft/sec. water:10.1 lb/ft ² .hr.	900	12	1,210	Yes
21	1080	air:6.98 ft/sec.	620	0.36	3,120	No

* These values have been found using procedures stated in La Metallurgia Italiana, XLVI, 225, 1954, by A. Giannone.

** These values are relative breaking risks.

*** These values were obtained by bending breaking tests. The temperature of these tests was the same as the temperature that existed at the moment when the maximum tension was generated at a certain point in the panel.

21. Poluboyarinov, D. N., Bashkatov, V. A., Serova, G. A., Golubeva, Ye. V. and Shlemin, A. V., "Test of High-refractory Insulating Materials in Lithium Vapor and in Vacuo at High Temperatures," Ogneupory (Refractories, Soviet), no. 2, 82-89 (1964).

The compounds ZrO_2 , $ZrSiO_4$, CaO , and MgO are unstable against thermal shock.

22. Robijn, P., "Measurement of the Mean Specific Heat of Refractory Material," Silicates industriels (Industrial Silicates, French) 28, no. 5, 247-53 (1963).

Changes of the specific heat can point to the structural changes, as, f. i., with zirconia fusion cast refractories for which the specific heat is variable due to different degrees of stabilization. For Al_2O_3 , MgO , and ZrO_2 , the thermal shock (2282/68° F) produced no change of the specific heat and thus no structural changes.

23. Rubin, G. A., "Thermal Shock Resistance of Ceramic Materials," Berichte der Deutschen Keram Gesellschaft (Reports of the German Ceramic Society) 40, no. 1, 13-15 (1963).

The temperature dependence of the thermal shock resistance of sintered alumina and beryllia was studied by use of literature values and recent measurements of the tensile strength, thermal conductivity, linear expansion coefficient, and the modulus of elasticity of these compounds. In the case of a moderate heat exchange rate on cooling, BeO is found to be far superior to Al_2O_3 because of its high thermal conductivity, and with a high heat exchange rate Al_2O_3 is more resistant than BeO because of its higher strength. When a sintered polycrystalline material with a porosity of 2-3% was exposed to a temperature gradient of about 440° F/inch per 0.1 sec., the maximum stress in the contour zone was found to be 20,600 psi for Al_2O_3 and 10,700 psi for BeO . Investigations with Al_2O_3 compositions have shown that a change in the modulus of elasticity due to a decrease in temperature is a useful measure for the thermal shock resistance of a material.

24. Schwiete, H. E., "Contribution To The Development of Methods for Testing Refractory Construction Materials for Thermal Shock Resistance," Transactions of the 8th Ceramic Congress, 1962, p 193.

The behavior of refractory construction materials to thermal shock is often of decisive importance for their use. The test processes in current use can be divided into two principal groups:

1. Technological investigations, and
2. Analytical processes.

The method most used in Germany for determining thermal shock resistance is the test according to DIN 1068 B. In this test the solid samples, 36 mm in diameter and 60 mm long, are heated to a temperature of 1742° F and quenched for 5 minutes in running water at 50-68° F.

In Austria it is felt that the results of thermal shocking basic ceramics in water can distort the results because of hydration. So ceramics are heated for 50 minutes at 1742° F and cooled by laying them on an iron plate and blowing them with compressed air for 10 minutes. After a fixed number of quenches, if the ceramics have not been previously broken, they are evaluated according to their appearance. To supplement these results, the loss in bending strength can be ascertained.

Kronpicky, in modification of DIN 1068 A, has developed a test procedure in which the ceramics to be studied are loaded into the furnace so that 1/3 projects into the furnace, 1/3 is cooled by the outside air, and the middle is surrounded by the furnace lining. In this test procedure the ceramics are turned after the front end has reached test temperature. In addition, there are other test methods in use in other countries.

On the basis of long experience it can now be stated, especially in the case of DIN 1068, that,

1. The experimental results are affected by subjective influences,
2. The test does not correspond, in severity, to service stresses or other stresses because of the prescribed maximum temperature, and
3. The test does not differentiate between various types of ceramics and does not consider the mineral structure.

Because of these deficiencies, it is sometimes preferable to calculate the thermal shock resistance from measured physical quantities. However, these computed results have not been too successful in practice.

In order to obtain reproducible results on the thermal shock behavior of refractory materials, the customary water quench should be replaced by a less drastic cooling method and a standard ceramic should be used as the test body.

The Aachen method best approaches these "ideals." With this method ceramics are placed in a gas-heated furnace at temperatures of 1742°, 1832°, 2012°, or 2192° F. Quartz rich materials are preheated in a special furnace in the region of the quartz transformation. The ceramics are then held 40 minutes at the investigation temperature, taken from the furnace, cooled on a water cooled copper plate to 392° F for one hour, and returned to the

furnace and heated again. As a criterion for thermal shock resistance a decrease of bending strength is recorded after a fixed number of quenches.

A number of ceramics were tested for specific weight, water uptake, porosity, bending strength, and cold compressive strength both before and after thermal shock testing. Good agreement between the Aachen method and the results of Konipicky was established. In particular, the results show that the specific weight is somewhat decreased by the varying shock while the values for water uptake and porosity increase; however, the variation of these data is small when compared to the strength change.

In other experiments ceramics were quenched according to the Aachen method. The cooling time from 1742° F to room temperature took 2 hours on a cool plate and 12 hours in air. The ceramics were tested, both before and after thermal shock tests, by sonic methods. The following types of ceramics were investigated:

1. Hard fire clay AI
2. Dry pressed fire clay ceramics, grades AI, AII, AIII
3. Plastically formed fire clay ceramics, grades AI, AII, AIII

In all cases investigated, a good parallelism existed between the decline of frequency and the decline of bending strength, and in all cases a strong decline of the natural frequency was observed after the first thermal cycle. It was concluded that the variation of natural frequency of the investigated refractory ceramics can be taken as a criterion for evaluation of thermal shock resistance. It would be ideal if the natural frequency of these materials in their new condition could be taken as the criterion for good or poor thermal shock resistance. It would then be possible to test ceramics nondestructively and afterwards use them for construction. However, given the present state of these investigations and the results up till now, this appears as a distant future possibility.

25. Sieder, N., "Physical Properties of Quartz Glass and Quartz Ware," Silikattechnik (Technology of Silicates, Eastern Germany), 15, no. 4, 116-19 (1964).

Quartzglass (I) was melted from pure mountain crystal, quartzware (II) from pure quartz sand. For I, the following mechanical characteristics were found: crushing strength 92,000 psi, tensile strength 8500 psi, bending strength 14,000 psi, impact strength 15 psi. The values for II are only 1/2-1/3 of the values for I. The thermal expansion coefficient of I is 3×10^{-7} at 68° F and 6×10^{-7} at 2192° F. From this follows a high thermal shock resistance: samples with a wall thickness of up to 3 mm stand thermal shocks of 1832° F/air. Slowly cooling to 350-450° F causes the $\alpha \rightarrow \beta$ cristobalite transformation, a decrease of the volume, and the destruction of the sample.

26. Solomin, N. V., "Thermomechanical Stress in Joints Between Glass, Ceramics, Metals, and Other Materials," Steklo i Keramika (Glass & Ceramics, Soviet), no. 8, 14-15 (1962).

Formulas are derived for the tangential stress between two thin coaxial cylinders having different thermal expansion coefficients. It was found that the tangential stresses do not depend on the radius.

27. Spath, W., "Thermal Shock Resistance of Refractories. III," Radex-Berichte (Radex Reports, Austria), no. 5, 221-30 (1962).

The reciprocal skeleton stresses occurring in refractory materials are compared with phenomena observed in prestressed glass and on germanium single crystals. The use of the polarizing microscope and the determination of dislocations promise further progress with regard to the elucidation of the microstability during stresses caused by temperature changes. However, phenomena caused by these stresses can only be elucidated by a very close imitation of the conditions met in practice.

28. Spath, W., "Statistics of Internal Processes in Solids," Radex-Berichte (Radex Reports, Austria), no. 3, 462-70 (1963).

The agglomerate of a solid body is considered as a statistic collection of numerous elementary ranges, the behavior of which under any influences follows statistic principles. This is set forth on the example of the progressive damage of a solid body under alternative mechanical stressing, and conclusions are drawn regarding the deterioration of refractory materials under alternative thermal stressing.

29. Spath, W., "On The Resistance of Refractory Materials To Thermal Shock," Radex-Rundschau, no. 5, 673-88 (1961).

Considerations regarding thermal shock resistance, as a rule, proceed from the statement that: due to temperature differences between the individual parts of a ceramic piece, perhaps between its surface and its core, opposing mechanical stresses are produced which lead to formation of cracks and ultimately to spalling. The complicated process of crack formation and spalling is influenced by the elasticity, thermal expansion, tensile strength, thermal conductivity, temperature distribution in the ceramic and, above all, the structure itself. It is well known that a method has been long sought to bring these physical quantities into formal relationships in order to determine the thermal shock resistance mathematically. However, caution must be used to avoid attributing too much importance to relationships characterized by such formulas for quantitative purposes. These relationships are set up under

the assumption that a homogeneous body is shocked, but it must be remembered that refractory ceramics are not homogeneous because of the distribution of crystals and the pore structure.

A refractory material can be conceived as a statistical collection of numerous elementary regions in which portions with entirely different mechanical and thermal properties adjoin. Each of these elementary regions represent a "compound solid." Because of dissimilar coefficients of expansion of the components mutually bound in the most varied fashions, microscopically distributed stresses arise between these various structural constituents of the material. A characteristic of these stresses is that they are operative when the temperature of the entire solid under investigation is completely uniform and depend, to a large extent, on the temperature at hand. With varying temperatures the entire structure consequently must "breathe" and very high loads can arise from the stresses so that local breaks can occur in the structure. These microscopic stresses caused by dissimilar coefficients of expansion cannot be relieved by annealing. By sufficiently strong heating these stresses can be made to disappear, but they must reappear upon subsequent cooling.

It can be concluded from the foregoing considerations that with cyclic heating of a refractory ceramic defects appear which depend on two entirely different processes which must be rigorously differentiated. Upon heating different temperatures occur in the individual zones and cause opposing stresses in these zones. The capacity for resistance to these stresses upon cyclic repetition of the heating will be called "macroresistance to thermal shock."

However, a second cause of the defects which occur is to be differentiated from this. Opposing stresses exist between the different structural constituents and therefore also between crystal grain and cohesive phase because of the unequal coefficients of expansion of these structural constituents. These "microstresses" vary with the temperature so that very finely distributed forces of varying direction appear as a function of the instantaneous temperature. The resistance of a refractory material to this "breathing" of the entire structure will be called "microresistance to thermal shock."

Obviously, a certain interaction can exist between the two effects, and since the effects obey entirely different laws, very different types of phenomena are to be expected from the interaction. Delay phenomena of a fracture with cooling can be explained by the course of microstresses. With cooling the microstresses usually increase. When a structure is suddenly quenched, the microstresses, which are still small, suddenly begin to grow steeply. Therefore, a certain time can vanish before the total intrinsic stress reaches a maximum and the strength of the material is exceeded.

30. Spath, W., "The Thermal Shock Resistance of Refractory Materials," Radex-Rundschau, no. 13, 3-13 (1962).

1. S. S. Manson ("Behavior of Materials Under Conditions of Thermal Stress," NACA Report 1170 [1954]) heated geometrically similar samples of steatite to a definite temperature and then quenched them, either in water or in air. As an index of effectiveness, the temperature difference between the hot solid and the cooling medium, which leads directly to a breaking of the solid to be studied in a single thermoshock, was used.

When a graph of the temperature difference versus the reciprocal of the sample diameter was plotted, a straight line was obtained not only for quenching in water but in air also. The line for air quenching lies noticeably higher and both lines intercept the ordinate at a critical temperature of 250° F.

2. F. J. Bradshaw ("The Improvement of Ceramics for Use in Heat Engines," Tech. Note MET III, British RAE [Oct. 1949]) investigated the behavior of samples of beryllium oxide and aluminum oxide with mild air quenching and more abrupt quenching in water. In this case the particular critical temperature at which the sample cracked with a single shock was determined.

With air quenching, the beryllium oxide samples resisted up to a temperature of 1418° F and the aluminum oxide samples up to a temperature of 1053° F. Therefore, for this test, the beryllium oxide was rated much higher. When water quenching was used the corresponding temperatures were 797° F for beryllium oxide and 979° F for aluminum oxide. The classification for abrupt quenching was thus inverted.

3. During German experiments on turbine blades in 1938, which are described by Manson, experimental pieces were heated for one minute in a gas flame and then cooled for three minutes in air. Two maximum temperatures were chosen; first, the heating was chosen in the region between 1200° F and 1290° F; and in a second series of experiments the maximum temperature was raised to 1530° - 1650° F. It was shown that a material which was regarded as the best with the high heating behaved the poorest at the lower temperature.

It should be mentioned with regard to this series of experiments that experiments comparing thermal shock resistance to breaking strength at room temperature gave no correlation. The same holds for the creep properties at 1328° F. Two materials with about a 23 per cent difference in breaking strength possessed the identical thermal shock resistance. Two materials with practically the same creep properties withstood the lowest and the highest number of thermal shocks.

The author shows that the apparent contradictions listed in the three examples above can be explained qualitatively by the interactions of different types of stresses (micro- and macro-stresses) and the damages caused by them. The author then points out that a conclusion for carrying out thermal shock investigations ought to be established by practical experiences as well as by theoretical considerations. If a test piece of definite form is studied in the usual way for determining thermal shock resistance of a material, within a definite temperature interval and with a definite velocity sequence of temperature change, then only one particular case is singled out from the

abundance of combination possibilities. Such a "one-point" measurement cannot characterize a fixed material reliability and completely, nor classify its worth fairly in comparison to other materials. Under experimental conditions, other indexes are to be expected whereby two materials can be classified exactly the inverse. This is true for changes of geometric form of the test piece, with changes of extent and position of the temperature interval of the thermal shock, and also with changes of velocity sequence. Measurements in which more severe experimental conditions are chosen for short cut purposes, as are expected in more recent work, will usually not be able to yield any valuation related to practice. A material established as good by means of a test can prove poorer in practice than a second material which was classified poor by the same test. There also exists the opposite possibility, namely that a material classified as poor behaves better than expected in practice.

31. Troshchenko, V. T., "The Effect of the Loading Rate on the Strength Characteristics of a Number of Cermets," Poroshkovaya metallurgiya (Powder Metallurgy, Soviet), no. 1 (13), 26-32 (1963).

The materials investigated were: 75% Cr_3C_2 + 25% Ni; 65.83% SiC + 25.13% C_{free} + 9.04% Si free, and iron base cermets with 15% and 34% porosity. The effect of the loading rate V on the strength of these materials was studied in the range between 1.4 and 1.4×10^6 psi/sec. With increasing loading rate, the strength characteristics of the investigated cermets grew by 10-20%. The following relationships were found: $\sigma = 80,500 + 1.36 \log V$ for Cr_3C_2 base material; $\sigma = 19,500 + 0.85 \log V$ for SiC base material; $\sigma = 28,000 + 0.39 \log V$ for iron with 15% porosity, and $\sigma = 8800 + 0.78 \log V$ for iron with 34% porosity.

32. Vaysfel'd, N. M., Gorbachev, A. A. and Yusim, L. M., "Crystallization of Light-sensitive Glasses in Dependence on the Isolation of the Crystallization Centers," Dokl. Akademii nauk SSSR (Reports of the Academy of Sciences USSR), 152, no. 4, 901-04 (1963).

The following results were obtained from electron microscope investigations of $\text{LiO}_2\text{-Al}_2\text{O}_3\text{-SiO}_2$ glass with colloidal Ag particles: Slow heating (7° F/min up to 1382° F) gives a non-uniform crystal structure. Thermal shock (inserting of the specimen in the furnace previously heated to 1382° F) gives a dense fine-crystalline structure due to the formation of numerous crystallization centers whose number increases when thermal shock is repeated.

33. Verworner, O., "The Importance of Mineralogy in the Refractories Industry," Silikattechnik (Technology of Silicates, Eastern Germany), 14 no. 7, 213-16 (1963).

The author points out that the mineralogical-petrographic investigation permits clarification of the different behavior of refractories and their resistivity against thermal shock.

34. Gugel, E., "High-Melting Materials and Their Application For Refractory Purposes," Ber. Seut. Keram. Ges., 40, no. 9, 533-43 (1963).

The demand for refractory materials is steadily increasing, especially where qualitative requirements are foremost. For a long time, and especially during the last twenty or thirty years, new materials have been sought and known high melting materials have been tested for their applicability for refractory purposes. This development has been caused, on one hand, by the increase in temperature of technical processes and, on the other hand, by the demand for heat resisting construction parts in such new fields as rocket and space technology and reactor technology. All other technical fields which have a demand for refractory materials profit from the results of this research.

This paper gives a survey of the production of refractory materials already in use and of potentially applicable high-melting materials. It deals, at first, with the properties of basic materials because these determine the possibility of application. The production is slightly touched upon in its principal possibilities, and applications are given in typical cases for the very modern materials.

Materials considered are: metals, carbon, borides, carbides, nitrides, oxides, silicides, intermetallic compounds, phosphides, sulfides, fluorides, boride-metal compacts, carbide-metal compacts, nitride-metal compacts, oxide-metal compacts, metal-free compacts, and multicomponent compacts.

35. Paquin, Pol, "Trends of the Evolution of Ceramic Products," Suppl. Bull. Soc. Fr. de Ceram. 57 (October-December 1962).

A bibliography, 200 references, is established from books and articles published from 1959 to 1962 in the field of material science. The rapid development of ceramic products is examined, and attention is given to applications in the nuclear, aerospace, and electronics fields and to the material requirements for these applications. Considered are the monoxides, mixed oxides, carbides, nitrides, silicates, borides, sulphides, fluorides, graphites, cermets, mineral polymers, ceramic whiskers, composite materials, and coatings.

36. Arabey, B. G., Shtrom, Ye. N., and Lapitskiy, Yu. A., "Features of the Technology of Manufacturing Compact Parts and the Mechanical Properties of Some Hexaborides of Rare Earth Metals," Poroshkovaya metallurgiya (Powder Metallurgy, Soviet), no. 5 (23), 65-70 (1964).

The authors studied the regularities of hot pressing and the mechanical properties of hexaborides of La, Sm, Eu, and Dy. It is shown that compact parts with a density close to the theoretical, made of LaB_6 , SmB_6 , EuB_6 , and DyB_6 , may be obtained by hot pressing at 3480° to 3720° F.

The hexaborides of the TR elements have a high brittleness.

37. Burykina, A. L., and Yevtushok, T. M., "Investigation of Contact Interaction of Metal-like Carbides with Graphite at High Temperatures in Vacuo," Poroshkovaya metallurgiya (Powder Metallurgy, Soviet), no. 2 (20), 19-21 (1964).

The authors established that carbides of Ti, Zr, Hf, Nb, Ta, Mo, and W do not interact with graphite in vacuo at temperatures up to 3990° F during 10 hours.

38. Fesenko, V. V., and Bolgar, A. S., "Evaporation Rate and Vapor Pressure of Carbides, Silicides, Nitrides, and Borides," Poroshkovaya metallurgiya (Powder Metallurgy, Soviet) no. 1 (13), 17-25 (1963).

A review is given on literature data as to the evaporation rate and the vapor pressure P of carbides, silicides, nitrides, and borides of transition metals. Own investigations were carried out with TiC , TiB_2 , and LaB_6 at temperatures up to 4150° F. The refractory compounds dissociate in vacuo, and the vapor pressure is determined both by the vapor pressure of the metal and that of the metalloid. The evaporation rate of refractory compounds generally increases, for the same metals, according to the series: carbides < borides < silicides < nitrides. The partial pressures for TiB_2 at 2193° K are: $P_{\text{Ti}} = 1.921 \cdot 10^{-7}$ at, $P_{\text{B}} = 1.828 \cdot 10^{-7}$ at; and for LaB_6 : $P_{\text{La}} = 9.78 \cdot 10^{-7}$ at, $P_{\text{B}} = 16.3 \cdot 10^{-7}$ at.

39. Perex y Jorbe, M.; Tilloca, G.; and Collongues, T., "Structure and Properties of Strontium Zirconate," International Symposium on Magnetohydrodynamic Electrical Power Generation, Paper No. 78, Paris, France, July 6-11 (1964).

The equilibrium diagram ZrO_2 - SrO was investigated. The material SrZrO_3 is of interest as an ultra-refractory material because of its high melting point. Its melting point (approximately 5070° F) is higher than that of CaZrO_3 and BaZrO_3 . If the SrO content exceeds the stoichiometric ratio, the stability of SrZrO_3 is impaired. In addition, any contact between SrZrO_3 and alumina must be avoided.

40. Rakovskiy, V. S., "The Strength of Cermets," Poroshkovaya metallurgiya (Powder Metallurgy, Soviet), no. 5, (11), 45-50 (1962).

The results of mechanical tests obtained on the cermets TiC - Co, TiC-Ni, and TiC-Mo, close by their nature to WC-Co, at temperatures of 68° and 2192° F confirm that "refractory compounds - metal alloys" are brittle within a wide range of changes in bond and temperature. It is shown that "skeletal structure" of the material of SiC - C type secures a greater strength (7100 to 8500 psi at 2192° F) than the structure of "scattered type" (3500 to 4200 psi).

41. Ryshkewitch, E., "Oxide-Metal Compound Cermets," Plansee Seminar on Powder Metallurgy, Preprint Paper No. 34 (June 1964).

The most promising way to expand the applicability of available materials is to combine two or more appropriate constituents to new composites. National Beryllia Corporation (USA) developed several methods of blend-uniting and joining such dissimilar construction materials as beryllia (or other refractory) with tungsten (or some other refractory) metal or carbide to produce compound bodies of uniform of gradient composition, including pieces consisting of pure sintered beryllia at the one end and pure sintered tungsten on the other. Nozzles of rocket engines, nose cones of extro-atmosphere reentry missiles and other responsible construction parts of low specific weight and high thermal and mechanical stability can successfully be made from such composites. The problem of incorporating beryllium metal powder into the sintered beryllia matrix was solved by a method of programmed hot-pressing, with the results that gradient or uniform BeO-Be compound ceramics were produced, containing up to 50 volume per cent Be metal. At temperatures surpassing 2700° F porous ceramics lose their heat insulation properties and become increasingly good heat conductors. Barriers reflecting and dissipating photons were introduced into porous ceramics. To this effect, to zirconia foam of a 80 volume per cent porosity tungsten flakes, 20-40 μ in diameter, and tungsten-coated hollow micro-spheres or zirconia about 200 μ in diameter were introduced in amount 0.3 up to 1 volume per cent of the foam. Porous zirconia with barriers transfers at 4350° F only 1/4 of the heat transferred by the same body without barriers.

42. Yerouchalmi, D., "Materials and Structures for the MHD Conversion in Open Cycles," International Symposium on Magnethydrodynamic Electric Power Generation, Paper No. 75, Paris, France, July 6-11 (1964).

The dependence of electrical conductivity (permissible ~ 3 ohm/ft) on temperature shows that MgO cannot be used beyond temperatures of 2550° to 2900° F, whereas SrZrO₃ can be used even at 3350° to 3600° F. The compatibility of insulating ceramics with conducting materials was also tested and it was found that MgO reacts with ZrO₂, TiB₂, and TiC. A possible solution to this problem is that an inner layer which is compatible with both materials could be used, such as CeO₂.

43. Antonova, N. D., Kalinina, A. A. and Kudryavtsev, V. I., "Obtaining Materials on a Silicon Carbide Basis with Additions of Boron and Aluminum, and Some of their Properties," Poroshkovaya metallurgiya (Powder Metallurgy, Soviet), 12, no. 6, 54-60 (1962).

Silicon carbide with additions of 1 to 5% by weight B, or 5 to 10% by weight Al was pressed at 6360 psi and heated to 3810° to 3960° F. The crushing strength increased from 21,000 psi for 1% B to 100,000 psi for 5% B, and dropped from 75,000 psi for 5% Al to 28,000 psi for 10% Al. Increasing Al content reduces the refractoriness owing to easier oxidizability. Compositions with 3 to 5% Al withstood more than 100 (2192° F to oil) thermal shocks.

44. Budnikov, P. P. and Cherepanov, A. M., "Some Zirconium Compounds and the Fields of Their Application," Zhurnal vsesoyuznogo khimicheskogo obshchestva im. D. I. Mendeleyeva (Journal of the All-Union D. I. Mendeleyeva Chemical Society, Soviet) 8, no. 2, 141-48 (1963).

A Survey is given on the use of ZrO_2 and $ZrSiO_4$ as refractories. Mentioned is the use of ZrO_2 with addition of Ti, Zr, Cr, Mo, W, V, or Nb in aeronautics. Literature data are given for crushing strength, linear thermal expansion coefficient, elasticity modulus, specific gravity, and heat conductivity. The refractory from fused cast ZrO_2 + 30% monoclinic ZrO_2 withstands 150 thermal shocks and is used for steel casting, for crucibles for Pt or Ir melting and for quartz melting.

45. Guzman, I. Ya., Kosmissarova, N. M., Krutikova, I. M. and Stepanov, M. A., "Sintering and Certain Properties of CaF_2 Ceramics," Ogneupory (Refractories, Soviet), no. 4, 182-85 (1964).

Pure and commercial CaF_2 powder of varying grain size was sintered at 1560° to 2370° F. Sintered commercial CaF_2 had a crushing strength of 34,000 to 42,000 psi and a bending strength of 7000 to 8500 psi, whereas ceramics from pure CaF_2 reached only 14,000 to 16,000 psi and 4200 to 5000 psi, respectively. The small heat shock resistance of CaF_2 is due to the high thermal expansion coefficient ($\sim 14 \times 10^{-6}/^{\circ}F$) and to the low heat conductivity of the material. Coarse grained CaF_2 ceramics, however, stood twenty thermal shocks (1472° F to air).

46. Guzman, I. Ya., and Poluboyarinov, D. N., "Some Properties of Porous Ceramics Prepared From Beryllium Oxide," Ogneupory (Refractories, Soviet), no. 10, 457-62 (1962).

BeO was foamed with a colophony-glue foamer then fired at 3092° F. The thermal conductivity was found to be 1.5 BTU/ft·hr·°F at 2550° F, the specific density 0.65 (~ 78% porosity), the softening point was higher than 3270° F, and the material had a crushing strength of 16,200 psi.

47. Kukolev, G. V. and Nemets, I. I., "Introduction of Organic Liquids into Fireclay Products for the Purpose of Controlling the Structure and Improving Their Thermal Stability," Ogneupory (Refractories, Soviet), no. 2, 85-92 (1963).

The addition of a water-repellent liquid to fine grained fireclay before the addition of the binder causes the formation of microcracks on the grain-binder interface and increases the thermal shock stability ($2372^{\circ}\text{ F} \rightarrow$ water). The optimum addition is 10%, the product resists 4 thermal shocks instead of only 2 without an addition. However, the addition of the water-repellent liquid to the binder causes the formation of pores in the binder and lowers the thermal stability.

48. Kutateladze, K. S. and Zedginidze, Ye. N., "The Problem of Nitriding Kaolin," Zhurnal prikladnoy khimii (Journal of Applied Chemistry, Soviet) 36, no. 2, 283-87 (1963).

Investigated was the feasibility of obtaining nitride refractories by nitriding kaolin in the presence of aluminum powder: $3(\text{Al}_2\text{O}_3 \cdot 2\text{SiO}_2 \cdot 2\text{H}_2\text{O}) + 8\text{Al} \rightarrow 7\text{Al}_2\text{O}_3 + 6\text{Si} + 6\text{H}_2\text{O} + \text{heat}$. The Si is bonded to Si_3N_4 in nitrogen atmosphere at 2552° F (4 hours firing). The refractory obtained is composed of Al_2O_3 and Si_3N_4 , it does not show shrinkage, it has a compression strength equal to 5000 psi, and a refractoriness up to 3450° F . The specimens are not destroyed after 20 thermal shocks $1562^{\circ}\text{ F}/\text{water}$ or $2192^{\circ}\text{ F}/\text{air}$ and stand 40 shocks 2912° F (25 sec) to water. The material is stable against molten metals and is obtainable from an inexpensive raw material.

49. Lukin, Ye. S. and Poluboyarinov, D. N., "Some Thermochemical Properties of Ceramics from Pure Oxides," Ogneupory (Refractories, Soviet), no. 7, 318-23 (1963).

The following ceramics were investigated: pure Al_2O_3 , $\text{Al}_2\text{O}_3 + 1\%$ TiO_2 , $\text{Al}_2\text{O}_3 + 5\%$ ZrO_2 , $\text{Al}_2\text{O}_3 + 1\%$ MgO , $\text{Al}_2\text{O}_3 + 1\%$ $\text{TiO}_2 + 5\%$ ZrO_2 , $\text{ZrO}_2 + 8$ to 12% CaO or MgO , pure MgO , and BeO . The softening point of the ceramics based on Al_2O_3 lies between 3380° F and 3510° F . MgO and BeO have a higher softening point but are volatile in vacuo. Zirconia stabilized with MgO has a bending strength 31,000 psi after thermal shock (2372° F to air on 1562° F to water). At high temperatures MgO and BeO have a higher crushing strength than the other oxides (4800 to 5100 psi at 3270° F).

50. Margulis, O. M., and Stovbur, A. V., "The Stability of Oxide Products," Ogneupory (Refractories, Soviet), no. 5, 206-09 (1964).

The stability of specimens of MgO or of ZrO_2 stabilized with 8% CaO and with the addition of monoclinic ZrO_2 was investigated by repeated rapid heating

and quenching. At 3270° F, MgO and ZrC₂ products were found to be compatible. The thermal shock stability for MgO was found to be 3 at a temperature drop 3452° F to 752° F, 120 at 3452° F to 1832° F, and 400 at 3452° F to 2732° F, and the thermal shock stability of ZrO₂ was found to be 1 to 2 at a temperature drop 3452° F to 752° F, and 30 at 3452° F to 2732° F. Monoclinic ZrO₂ is regenerated because of the decomposition of the solid CaO-ZrO₂ solution during thermal shock cycles.

51. Margulis, O. M., Usatikov, I. F. and Kamenetskiy, A. B., "Large Size Zirconia Products with Increased Thermal Stability," Ogneupory (Refractories, Soviet), no. 2, 63-67 (1964).

The following results were obtained from experiments made at the pilot plant level: ZrO₂ + 5% CaO fired at 2870° to 2950° C withstood only one thermal shock (2372° to 68° F). An addition of 15% monoclinic ZrO₂ and firing at 3182° F gave an average thermal stability of 3.5 to 9.5 thermal shocks (2912° to 68° F). Large sized products which were manufactured by the improved method stood 15 (2372° to 68° F) and 3 (2912° to 68° F) thermal shocks.

52. Poluboyarinov, D. N., Kalliga, G. P. and Lyutsareva, L. A., "Problems of Stabilization and Sintering of Highly Pure Zirconia," Ogneupory (Refractory, Soviet) no. 4, 175-79 (1963).

Zirconia, 99.5%, was sintered with additions of 4 to 15 mol % CaO or MgO. Oxidative firing at 3110° F for 5 hours resulted in total sintering with 10% stabilizer and gave a bending strength of 21,600 psi and 19,600 psi after thermal shock (2372° F to air). Higher stabilizer content decreases the bending strength. A 10% addition of stabilizer causes a low density (325 lb/ft³ with CaO, 330 lb/ft³ with MgO). Firing at 3990° F has no effect on the density. Higher density can be obtained by (a) a 10% addition of a Ca compound with another anion (333 lb/ft³ with CaF₂, bending strength 27,700 psi, but only 13,600 psi after thermal shock) or (b) preliminarily firing of the initial ZrO₂ (giving similar values).

53. Rummel, W., "Materials For MHD Ducts," International Symposium on Magnetohydrodynamic Electrical Power Generation, Paper No. 73, Paris, France, July 6-11 (1964).

The possibility of using various ceramics as insulators at a plasma temperature range of 4040° F to 4940° F was studied. ZrB₂ and ZrN alone or with the addition of ZrO₂, CaO, or SiC for improving the oxide skin proved to be stable in 10 minute tests. In the case of ZrO₂, the oxide skin was destroyed on cooling; this destruction is due to the transformation of the tetragonal modification into the trigonal modification at 1830° to 2010° C.

A $\frac{5}{4}$ addition of CaO has, however, a stabilizing effect. Furthermore, quartz which forms from added SiC or silicides can act as a stabilizer. Other material combinations which proved to be stable were: 90% ZrB₂ + 10% SiC, 90% ZrN + 10% SiC, and 90% ZrB₂ + 10% MoSiO₂. A difficulty was encountered in that the seeding material used (K₂O) destroys any layer which contains SiO₂.

54. Sukachev, V., "Experiments on the Use of Lithium Carbonate in Ceramics," Sprechsaal für Keramik, Glas und Email (Consultations on Ceramics, Glass, and Enamel, German) 97, no. 13, 387-88 (1964).

Although favorable results have been obtained in preliminary experiments on the working of bodies with additions of 0.1 to 0.2% Li₂CO₃, difficulties occurred on an industrial scale in the drying process. The cast articles had a low thermal shock resistance which was caused by the crystallization of lithium aluminosilicates in the glass phase. The resultant crystals had a negative expansion coefficient while the coefficient of expansion of the glass phase was positive, and large internal stresses were developed. The difficulties were overcome by rapid cooling (572° F/hr) to 2012° F and introducing the lithium as a Li-quartz frit (10% Li₂CO₃ + quartz fired at 2282° F) which favored mullite crystallization and lowered the firing temperature. The resultant products obtained were resistant against 4 to 5 thermal shocks from 203° F to 68° C water.

55. Vlasov, A. S. and Poluboyarinov, D. N., "Utilization of the Exothermal Reaction for the Preparation of Cermets Based on Chromium and Alumina," Ogneupory (Refractories, Soviet), no. 5, 232-34 (1963).

The exothermic reaction Cr₂O₃ + Al \rightarrow 2Cr + Al₂O₃ is used for the preparation of cermet. If a cermet incorporating 70% corundum is desired, the necessary amount of Al₂O₃ can be added either before or after the reaction. The product is then ground and fired at 3130° F for one hour in a helium atmosphere. The resulting product has a higher specific density (4.87 to 5.17), crushing strength (201,000 to 205,000 psi as compared with 170,000 psi), and bending strength (40,000 psi as compared with 30,000 psi) than a similar cermet made by mixing chromium and corundum. The thermal shock resistance is smaller (45% residual strength compared with 60% on the non-thermite cermet in the case of thermal shocking from 1562° F to water).

56. Washburn, M. E., "A Silicon Carbide Refractory Bonded with Silicon Oxynitride," Keramische Zeitschrift (Ceramics Journal, German), 15, no. 4, 203-05, no. 5, 273 (1963).

Silicon oxynitride and silicon nitride act differently as bonds for SiC. The oxynitride is more adherent to the SiC than the nitride. The oxynitride

combines this better coherence with good oxidation resistance and good thermal shock resistance. With the combination of unique characteristics, silicon carbide products bonded with silicon oxynitride have shown advantage over SiC products when used in structural and corrosive environments. Oxynitride-bonded SiC is a general purpose SiC refractory and its use eliminates the necessity of choosing a specific bond for a specific application. SiC bonded with nitride withstands 16 thermal shocks (2192° F/air stream) with a rapid decrease of the modulus of elasticity setting in, while SiC with oxynitride bond shows no break in the continuity of the modulus of elasticity after 40 thermal shock cycles. For oxynitride bond, the modulus of rupture after 20 cycles lies at 3000 psi, for nitride bond at 2000 psi, and for silicate bond at 280 psi.

APPENDIX II

AN EXAMPLE OF A THERMO-STRUCTURAL ANALYSIS

171
PRECEDING PAGE BLANK

THERMO-STRUCTURAL ANALYSIS FOR RADOMES

Introduction

To provide an example of a thermal and mechanical analysis for a ceramic component used in an aerospace application the structural analysis for a missile radome is considered. The following problem is dealt with: for a given mission profile, determine the response of a typical ceramic radome. The problem is solved in four steps.

The first step in the solution of the problem is to determine the value of the recovery boundary-layer temperature and the value of the surface heat-transfer coefficient for the radome as a function of time. The second step is to determine the temperature distribution in the radome as a function of time. The third step is to compute the thermal stresses caused by the temperature gradients in the radome. In the fourth and final step the stresses resulting from the attachment of the radome are considered.

Aerodynamic Heating

Before the heat transfer rates to a radome can be predicted, the pressure distribution over the radome surface must be determined. One semi-empirical method for estimating pressures which has been favored because of its simplicity and its degree of success under various conditions can be expressed in the form (Ref. 198):

$$(P_{\delta} - P_{\infty}) / (P_{\delta_s} - P_{\infty}) = \sin^2 \gamma \quad (68)$$

where

P_{δ} = local pressure

P_{∞} = undisturbed ambient pressure

P_{δ_s} = stagnation pressure behind the normal shock wave

γ = angle between the stream and the tangent to the surface

Equation 68 will generally suffice for the evaluation of structural loads. However, in many cases the pressure distribution over a radome must be known with greater accuracy for the determination of heat transfer rates. This is particularly true in the stagnation regime of a blunt body (Ref. 198). Fortunately, relatively precise methods have recently become available for such calculations. Kennealy (Ref. 198), for example, has presented methods

for calculating the pressure distributions of various nose shapes at zero angle of attack or for small angles of attack in the range of Mach numbers 0.9 to 7.0.

Once the pressure distribution over a radome (or other body) is known, the inviscid velocity distribution can generally be computed from well known relations of fluid mechanics.

A number of researchers have dealt with the problem of aerodynamic heating associated with high-speed flight vehicles, and aerodynamic heat fluxes on non-ablating bodies of simple shapes can be readily calculated from information which is available in the literature. Some of the basic relationships which have been found to give reasonable estimates of aerodynamic heating rates have been summarized by Eliason and Zellner (Ref. 199).

With the altitude and velocity of the vehicle specified as a function of time and a knowledge of the atmospheric properties, the following calculations can be made:

$$t_r = \left[1 + (P_r)^n \frac{\gamma - 1}{2} M_\delta^2 \right] t_\delta \quad (69)$$

where:

t_r = the recovery boundary-layer temperature

$P_r = \frac{C_p \bar{u}}{k}$ = the Prandtl number

$n = \begin{cases} 1/2 & \text{for laminar flow} \\ 1/3 & \text{for turbulent flow} \end{cases}$

$\gamma = \frac{C_p}{C_v}$ = the ratio of specific heats

M_δ = the local stream Mach number

t_δ = the local stream temperature

C_p = the specific heat at constant pressure

C_v = the specific heat at constant volume

$\bar{\mu}$ = the viscosity

k = the thermal conductivity

The transition between laminar and turbulent flow is associated with a Reynolds number R_e on the order of 10^6 for a flat plate and 2×10^6 for a cone.

$$R_e = \frac{\rho u x}{\bar{\mu}}$$

where:

ρ = the local density

u = the local velocity

x = the distance from the stagnation point measured along the surface of the radome

For laminar flow over the surface of a blunt body (Ref. 200):

$$h = \frac{0.763}{P_r^{0.6}} \cdot \left(\frac{x}{D} \right) \cdot \left(\frac{BD}{u_\infty} \right)^{1/2} \left(\frac{\bar{\mu}_\infty}{\rho_\infty u_\infty D} \right)^{1/2} \left(\frac{\rho_\delta}{\rho_\infty} \right)^{1/2} \left(\frac{\bar{\mu}_\delta}{\bar{\mu}_\infty} \right)^{1/2} \rho_\infty u_\infty c_p \quad (70)$$

where:

h = surface heat-transfer coefficient

D = diameter of spherical nose

$$B = \frac{u_\delta}{D} \left(\frac{8 \left[(\gamma - 1) M_\delta^2 + 2 \right]}{(\gamma + 1) M_\delta^2} \cdot \left[1 + \frac{\gamma - 1}{2} \cdot \frac{(\gamma - 1) M_\delta^2 + 2}{2 \gamma M_\delta^2 - (\gamma - 1)} \right]^{1 - \frac{1}{\gamma - 1}} \right)^{1/2} \quad (71)$$

The subscript ∞ refers to conditions in undisturbed flow, and the subscript δ refers to local conditions at the outer edge of the boundary layer. The functional value $f(\frac{x}{D})$ is given approximately by (Ref. 201):

$$f(\frac{x}{D}) = 0.765 + 0.235 \cos 2.6 (\frac{x}{D}) \quad (72)$$

Equation 70 holds until the asymptotic value of h is reached (Ref. 199):

$$h = \frac{0.332}{P_r^{2/3}} \rho_\delta \mu_\delta C_p \quad (73)$$

for a flat plate, and

$$h = \frac{0.323 \sqrt{3}}{P_r^{2/3}} \rho_\delta \mu_\delta C_p \quad (74)$$

for a cone.

For turbulent flow over the surface of a blunt body the corresponding equation is (Ref. 200):

$$h = \frac{0.042}{P_r^{-2/3}} \left(\frac{BD}{u_\infty} \right)^{4/5} \left(\frac{\bar{\mu}_\infty}{\rho_\infty u_\infty D} \right)^{1/5} \left(\frac{\rho_\delta}{\rho_\infty} \right)^{4/5} \left(\frac{\bar{\mu}_\delta}{\bar{\mu}_\infty} \right)^{1/5} \left(\frac{x}{D} \right)^{3/5} \rho_\infty u_\infty C_p \quad (75)$$

until the asymptotic value of h is reached:

$$h = \frac{0.030}{P_r^{2/3} \text{Re}_\delta^{1/5}} \rho_\delta \mu_\delta C_p \quad (76)$$

for a flat plate, and the asymptotic value for a cone in axial flow will equal that for a flat plate for the same local Mach number and wall-to-local-free-stream temperature ratio if the calculation on the plate is made using a Reynolds number of one-half that on the cone.

The ratios ρ_δ/ρ_∞ and $\bar{\mu}_\delta/\bar{\mu}_\infty$, as well as B and T_r , are evaluated by computing the pressure ratio from Newtonian theory and isentropic expansion from the stagnation point.

Once the recovery boundary-layer temperature and the surface heat-transfer coefficient have been determined as a function of time, the net heat flux on the surface of the radome can be expressed in terms of the temperature of the radome surface on the basis of an overall heat balance. For a given point on the radome surface:

$$q = h (t_r - t_s) - \epsilon \bar{\sigma} t_s^4 \quad (77)$$

where:

q = net heat flux to the radome

t_s = surface temperature of the radome

ϵ = emittance at the surface

$\bar{\sigma}$ = Stephan's radiation constant

Temperature Distribution in the Radome

In the general case, the temperature distribution in a body is computed using an incremental analysis and finite difference equations. An advantage of the approach is that it takes into account the temperature dependence of the pertinent material properties. In addition, the use of an incremental analysis eliminates the shape of the body as a critical parameter in the analysis.

In an incremental analysis using finite difference techniques, the body is partitioned into an integral number n of volumetric elements. Within each volume element one station (point) is selected as a reference point for that element. For example, the i^{th} element, which would have volume V_i , would contain a characteristic point (x_i, y_i, z_i) , if Cartesian coördinates were employed. The temperature at the point (x_i, y_i, z_i) at a given time θ_j would be designated $t_i(\theta_j)$. For an element exposed directly to the environment, a point on the surface of the body would in general be selected for the reference point.

The temperature profile in the body is computed on the basis of approximate heat balances taken over the individual elements. For example, for the time interval $\Delta\theta_j = \theta_j - \theta_{j-1}$:

$$Q_i(\theta_j) + \sum_p k \left[t_i(\theta_{j-1}) \right] \cdot A_{pj} \frac{t_p(\theta_{j-1}) - t_i(\theta_{j-1})}{\sqrt{(x_p - x_i)^2 + (y_p - y_i)^2 + (z_p - z_i)^2}} = \\ v_i \cdot \rho \left[t_i(\theta_{j-1}) \right] \cdot c \left[t_i(\theta_{j-1}) \right] \cdot \{ t_i(\theta_j) - t_i(\theta_{j-1}) \} \quad (78)$$

where the sum is taken over the collection $\{p: v_p \text{ is adjacent to } v_i\}$. Generally, equation (1) can be simplified to a large extent by careful selection of the partitions (v_1, v_2, \dots, v_n) and careful placement of the stations (x_i, y_i, z_i) , $i = 1, 2, \dots, n$. For a specific example the reader may refer to Reference 199.

The thermal conductivity k , the density ρ , and the specific heat c of the material used in equation (78) are those associated with the temperature in the i^{th} element at a time θ_{j-1} previous to the time θ_j . A_{pj} is the area common to the i^{th} and p^{th} elements projected into a plane normal to the vector $(x_p - x_i, y_p - y_i, z_p - z_i)$. $Q_i(\theta_j)$ is the net heat flow to the i^{th} elements from the environment (during the period $\theta_j - \theta_{j-1}$) and pertains only to those elements exposed directly to the environment, in which case:

$$Q_i(\theta_j) = s_i \cdot q_i(\theta_j) \cdot (\theta_j - \theta_{j-1}) \quad (79)$$

where s_i is the surface area of the i^{th} element exposed to the environment, and $q_i(\theta_j)$ is the net heat flux to the surface s_i at time θ_j as given by Equation 77.

The temperature distribution within the body is established according to the following scheme:

1. At time $\theta_0 = 0$, the temperature distribution is known, and $t_i(\theta_0)$ is taken as the temperature at the point (x_i, y_i, z_i) at time θ_0 for $i = 1, 2, \dots, n$.
2. A finite time $\Delta\theta_1 = \theta_1 - \theta_0$ is assumed to have elapsed, and equation (1) is used to compute $t_i(\theta_1)$ for $i = 1, 2, \dots, n$.
3. Continuing in this fashion, $t_i(\theta_j)$ is determined for $i = 1, 2, \dots, n$, for $j = 2, 3, \dots, m$, where θ_m is the total time of exposure.

4. The above procedure is continued using finer partitions (V_1, V_2, \dots, V_n) and $(\theta_0, \theta_1, \dots, \theta_m)$ until the temperature distribution is obtained to a reasonable degree of precision in the sense of a limit.

Stresses Caused by Temperature Gradients in the Radome

Once the temperature distribution has been established, the stress field can be predicted. This can also be accomplished using an incremental analysis and finite difference equations on small volume elements if the elements are "idealized." Again this eliminates the shape of the body as a critical parameter in the analysis. In the case of a radome, the stress analysis is generally based on known solutions for simple shapes such as a cylinder, sphere, and cone.

Loyet and Levitan (Ref. 177) have presented equations defining the thermal stress components for hollow spheres and cylinders. The equations were developed using the three-dimension theory of elasticity under the assumptions

1. infinitesimal deformations
2. strains proportional to stresses
3. an isotropic material
4. negligible axial and circumferential temperature gradients

For a right circular cylindrical shell free at both ends and subjected to a radial temperature gradient:

$$\sigma_r(r) = \frac{1}{r^2} \left[\frac{r^2 - a^2}{b^2 - a^2} \int_a^b \frac{\alpha E}{1 - \mu} t(r) dr - \int_a^r \frac{\alpha E}{1 - \mu} t(r) dr \right]$$

$$\sigma_\theta(r) = \frac{1}{r^2} \left[\frac{r^2 + a^2}{b^2 + a^2} \int_a^b \frac{\alpha E}{1 - \mu} t(r) dr + \int_a^r \frac{\alpha E}{1 - \mu} t(r) dr \right] - \left(\frac{\alpha E}{1 - \mu} t \right)_r \quad (81)$$

$$\sigma_z(r) = \frac{2}{b^2 - a^2} \int_a^b \frac{\alpha E}{1 - \mu} t(r) dr - \left(\frac{\alpha E}{1 - \mu} t \right)_r \quad (82)$$

where: σ_r , σ_θ , σ_z = normal stress components in cylindrical coördinates
 r , θ , z

E = modulus of elasticity

μ = Poisson's ratio

α = linear coefficient of expansion, a function of
temperature

t = temperature

a , b = inner and outer radius, respectively

For a thick, hollow sphere subjected to a radial temperature gradient:

$$\sigma_r(\rho) = \frac{\rho^3 - a^3}{(b^3 - a^3)} \frac{2}{\rho^3} \int_a^b \frac{\alpha E}{1-\mu} t(\rho) d\rho - \frac{2}{\rho^3} \int_a^b \frac{\alpha E}{1-\mu} t^2(\rho) d\rho \quad (83)$$

$$\sigma_\theta(\rho) = \sigma_\phi(\rho) = \frac{2\rho^3 - a^3}{(b^3 - a^3)} \frac{1}{\rho^3} \int_a^b \frac{\alpha E}{1-\mu} t^2(\rho) d\rho + \frac{1}{\rho^3} \int_a^b \frac{\alpha E}{1-\mu} t^2(\rho) d\rho - \left(\frac{\alpha E}{1-\mu} t \right)_\rho \quad (84)$$

where σ_r , σ_θ , σ_ϕ are the normal stress components in spherical coördinates
 ρ , θ , ϕ , and the other symbols are as previously defined.

The analysis of various ceramic radomes has shown that the limiting stresses in a radome design are the σ_θ and σ_z components or the σ_θ and σ_ϕ components, and these stresses become a maximum at the inner or outer surface of a radome (Ref. 177). Since the rate of acceleration for a missile is usually much greater than the rate of deceleration, peak stresses generally occur during acceleration and the maximum tensile stresses appear on the inner surface of the radome. Since ceramic materials are about an order of magnitude stronger in compression than in tension, the limiting stress is the tensile stress occurring at the inner surface.

Loyet and Leviton have attempted to correlate thermal shock test results with calculated predictions based on the thermal stress analysis of the hollow spherical section for a radome tip and based on the thermal stress analysis of the cylinder for radome sections where the wall thickness was small compared with the inner radius. Reasonable results were obtained for an alumina radome.

Attachment

In addition to the stresses from the aerodynamic forces and from the temperature gradients in the radome, there will be stresses caused by the attachment. In the vicinity of the attachment, the recovery temperature will be the same for both the radome and vehicle wall, but generally the thermal expansion of the two structures will differ. The average temperatures of the structures will differ (because of the dissimilar material properties), and the thermal expansion coefficients will differ.

For the case where the design is based on an absence of stresses introduced by a mismatch in the slopes of the mating sections (that is, in the case of a pin-jointed boundary condition), the following analysis can be made (Ref. 199):

$$M = \frac{1}{\lambda_r} V_o d^{-\lambda_r} r^z \sin \lambda_r z \quad (85)$$

where:

M = bending moment in the radome

$$V_o = 2 r_a (\alpha_r t_r - \alpha_m t_m) \cdot \frac{1}{\frac{1}{D_r \lambda_r} + \frac{1}{D_m \lambda_m}} \quad (86)$$

$$\bar{D} = \frac{z E a^3}{3(1-\mu^2)} \quad (87)$$

$$\lambda = \left[\frac{3(1-\mu^2)}{4 r_a^2 a^2} \right]^{1/4} \quad (88)$$

r_a = middle radius of radome at the region of attachment

α = linear thermal expansion coefficient

t = average temperature at the attachment

z = distance from attachment measured in the direction of the axis of the radome

E = modulus of elasticity

a = half wall thickness of radome

ν = Poisson's ratio

The subscript r refers to the radome, and the subscript m refers to the vehicle structure (metal).

Examples

To exemplify the magnitude of the thermal stresses imposed on ceramic radomes flown at supersonic and hypersonic speeds, Loyet and Levitan (Ref. 177) considered the two mission profiles shown in Figure 10 and an ogival X-band radome having a 1.5-inch spherical tip radius and a fineness ratio of 2.0. For a Pyroceram® radome launched at 70° F on the trajectory shown in Figure 10-A, a thermal analysis produced the temperature profiles shown in Figure 11 for the tip of the radome. A thermal stress analysis based on Equation 81 produced the thermal stresses shown in Figure 12. The maximum tensile stress on the inner surface of the radome was estimated to be 14,500 psi - well within the safe operating limits of the Pyroceram® at the temperatures encountered. For an alumina AD-99 radome launched on the trajectory shown in Figure 10-B, the analysis produced the temperature gradients shown in Figure 13 and the thermal stresses shown in Figure 14 for the tip of the radome. The maximum tensile stress on the inner surface of the radome was estimated to be 40,750 psi. The alumina radome would fail after approximately 6-1/2 seconds since the tensile strength of the alumina at the temperatures encountered is about 27,000 psi.

For an example of an analysis made for the attachment of a radome, the reader may refer to Reference 198.

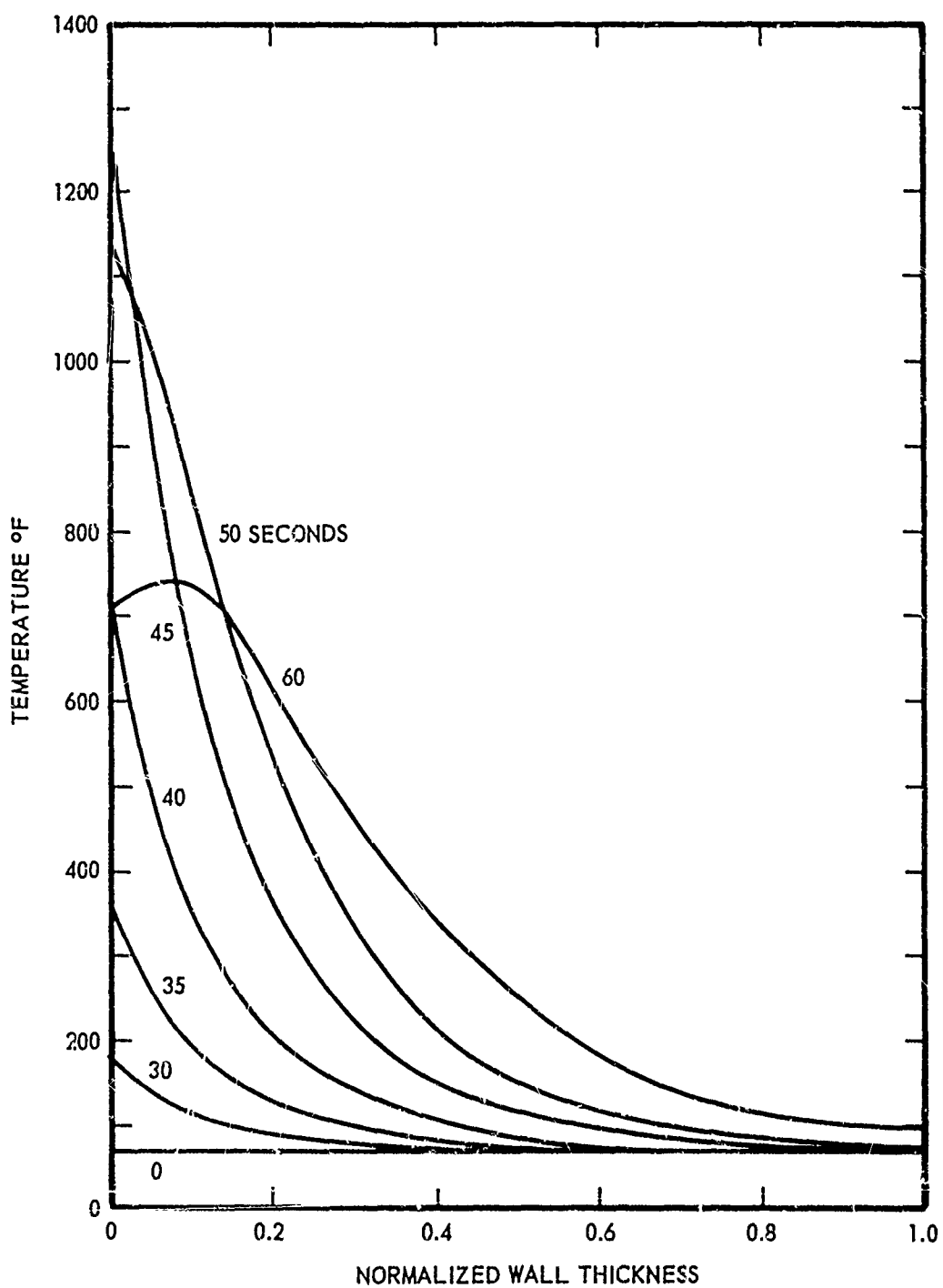


Figure 10. Theoretical Mach Number Histories Used in Thermal Stress Analysis.

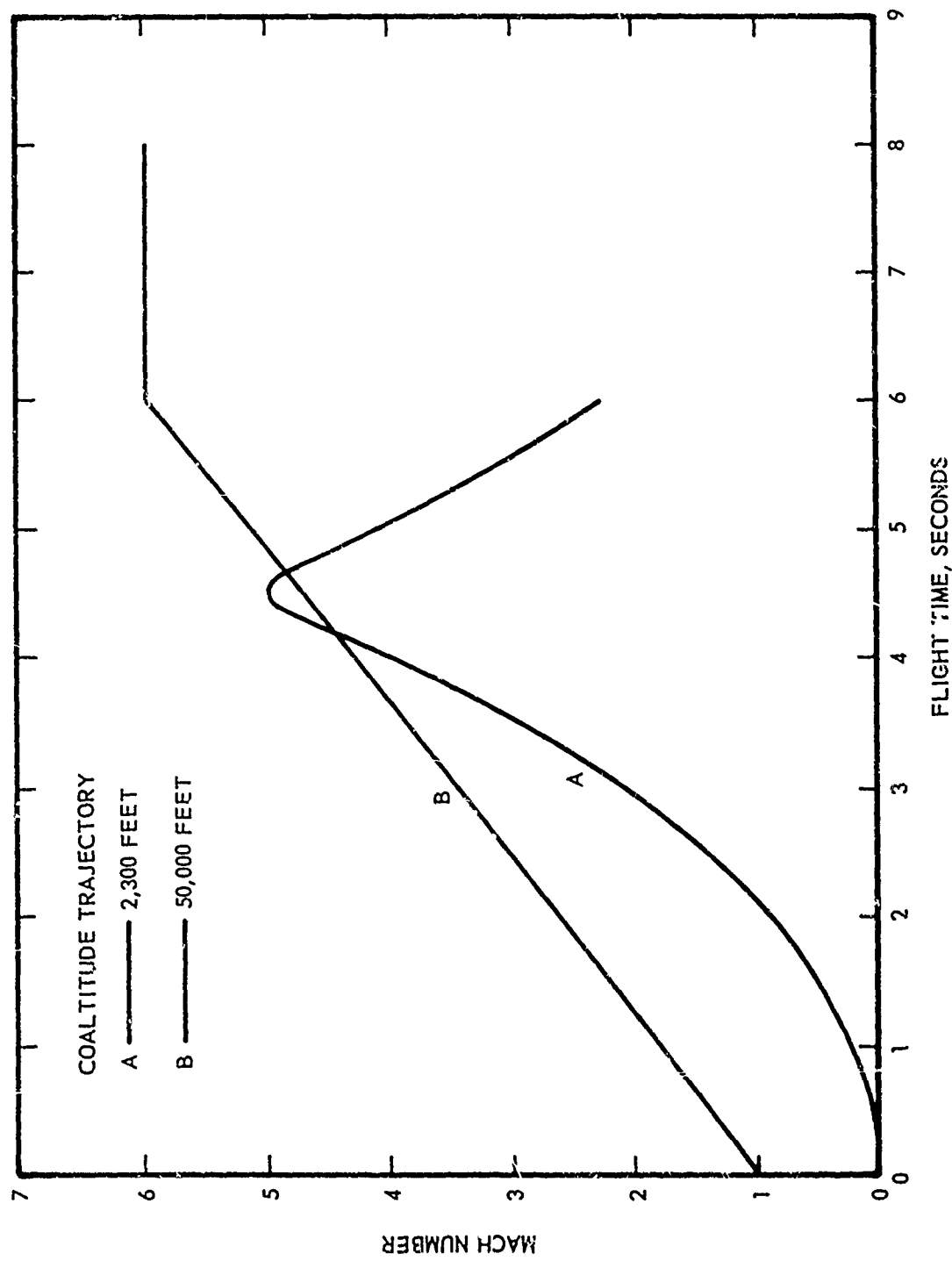


Figure 11. Temperature Gradients at Stagnation Point For Pyroceram® Radome.

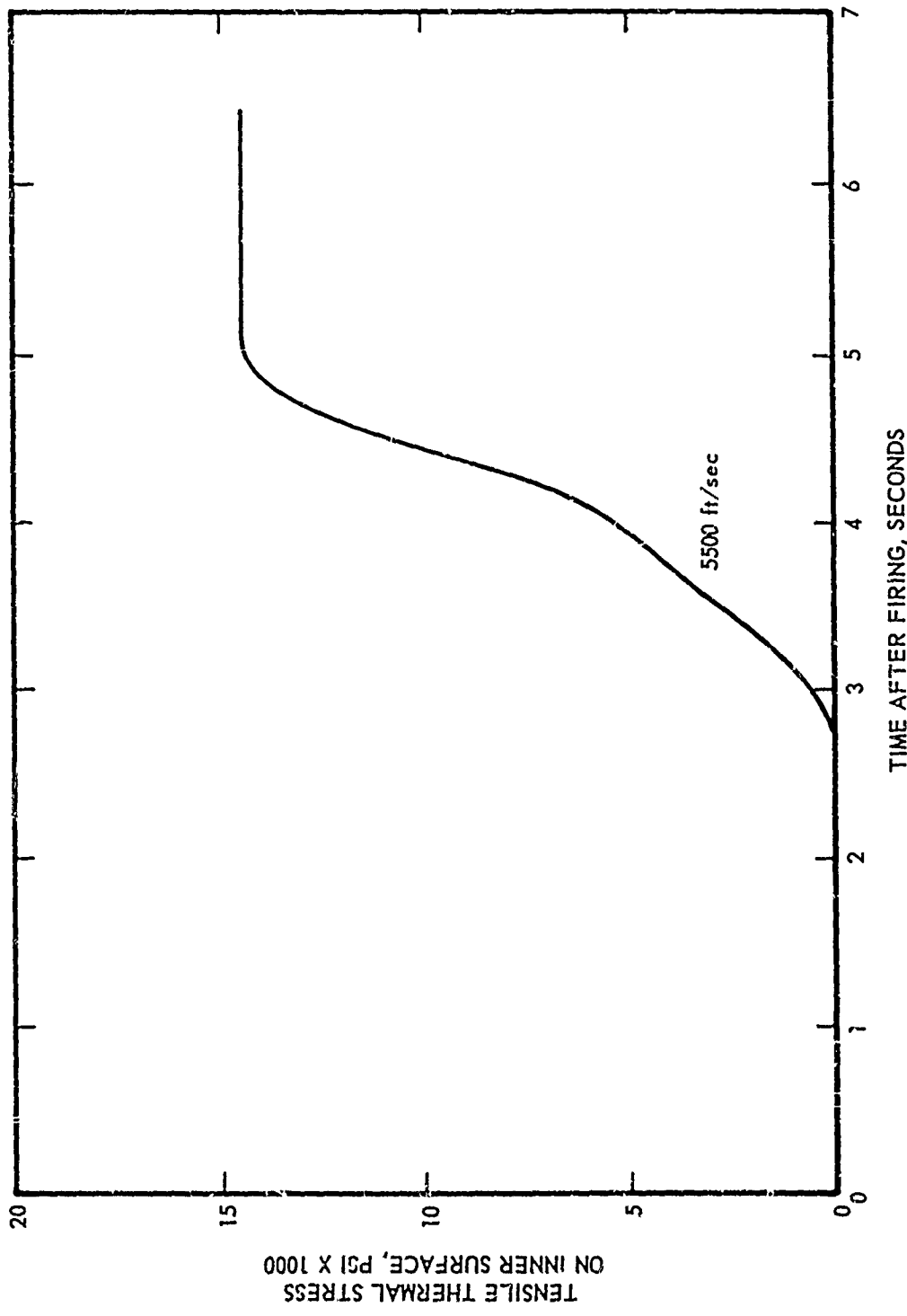


Figure 12. Tensile Thermal Stress at Stagnation Point Versus Flight Time for Pyroceram® Radome.

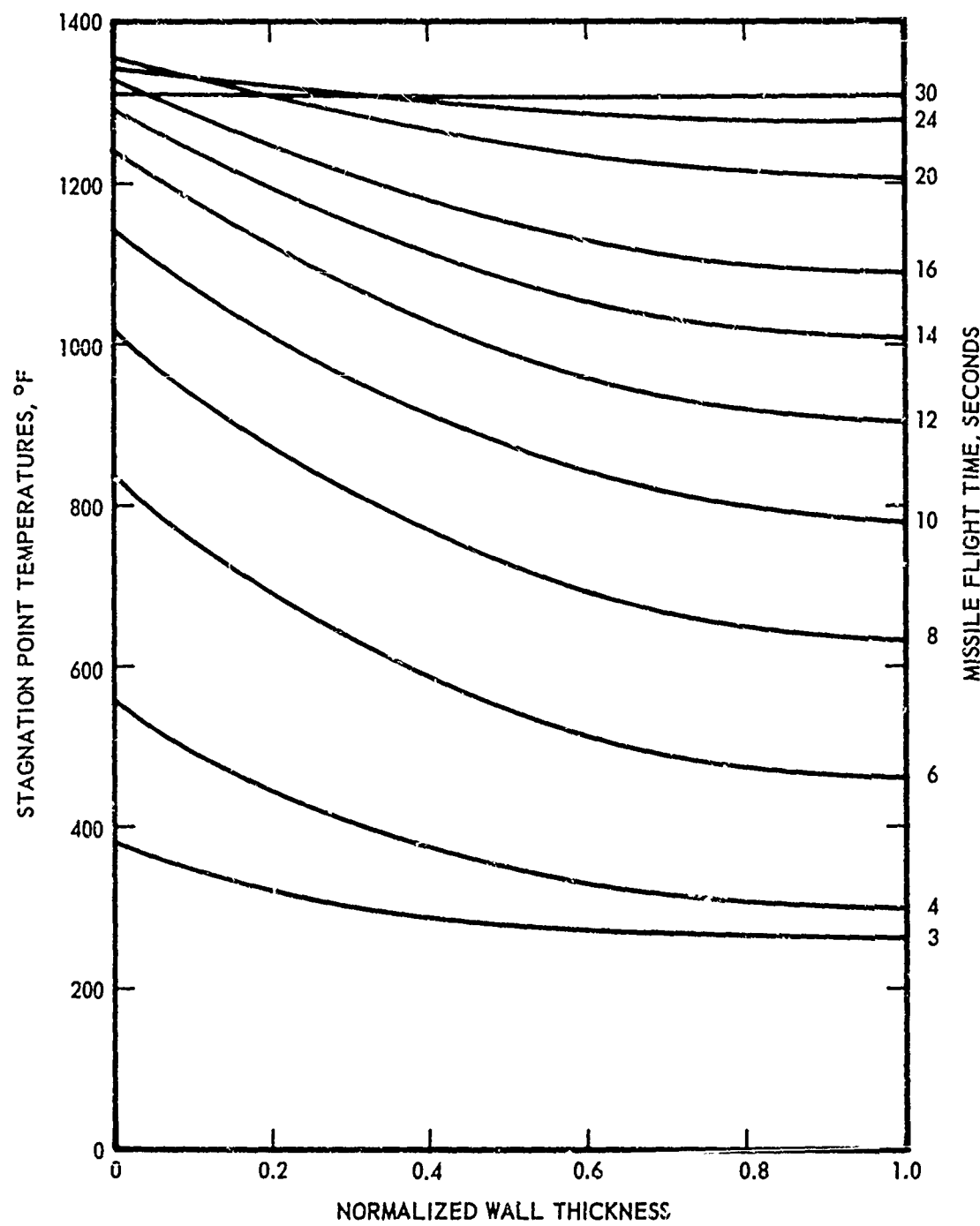


Figure 13. Temperature Gradients at Stagnation Point for Alumina Radome.

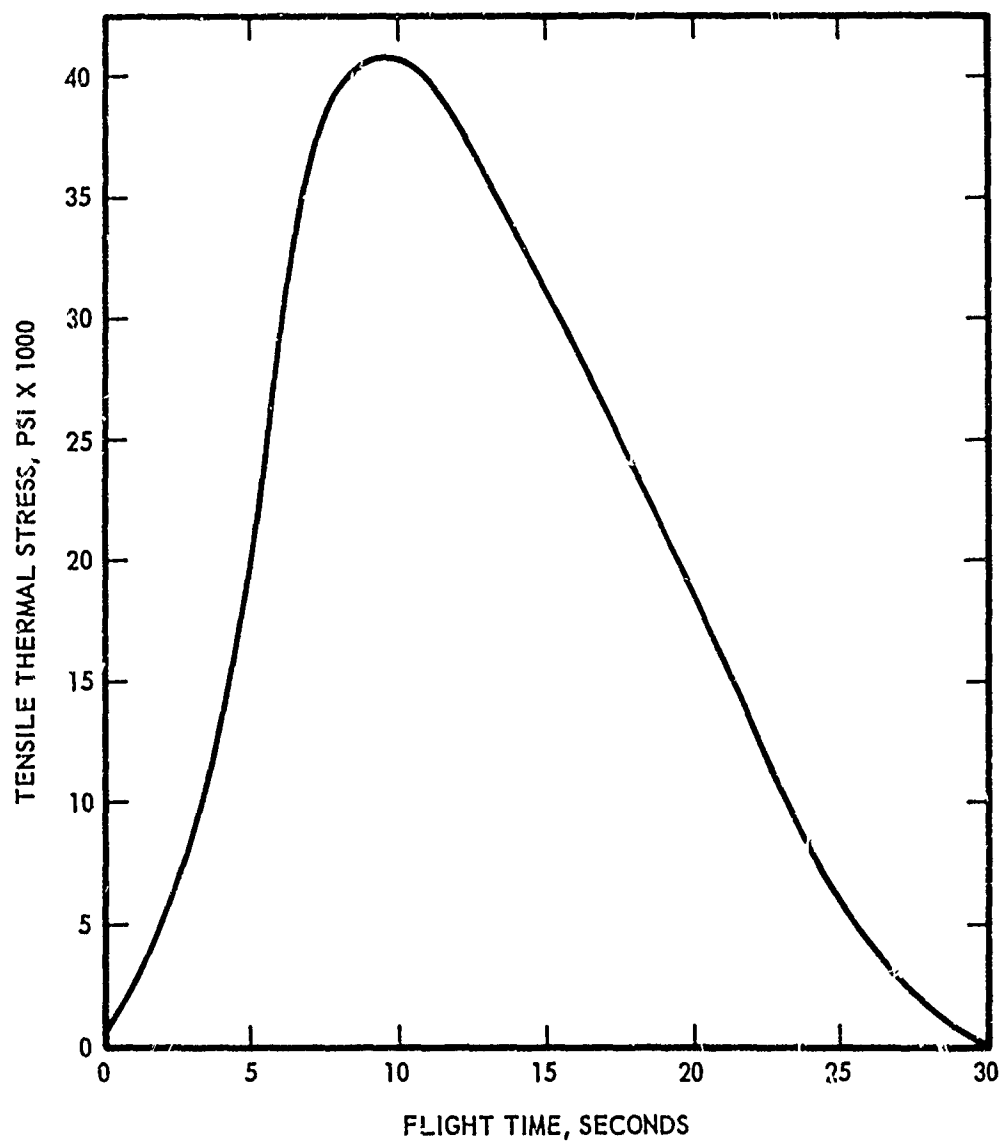


Figure 14. Tensile Thermal Stress at Stagnation Point Versus Flight Time for Alumina Radome.

Discussion

The thermo-structural analysis for a ceramic component to be used in an aerospace application will, in general, be accomplished in four steps. The rate of heat transfer to or from the component must be calculated, the temperature distributions in the component must be determined, the thermal stresses caused by the temperature gradients in the component must be computed, and the influence of the attachment must be assessed.

The heat fluxes on non-ablating bodies of simple shapes can be readily calculated from information which is available in the literature. Methods also exist for the prediction of heat fluxes on arbitrary shapes. The calculation of the heat transfer with laminar flow is considered quite reliable because the basic relations are amenable to mathematical solution. In the case of turbulent flow, the phenomenon is not well understood, and the calculation of heat transfer rates is less reliable. The calculation of the rate of heat transfer in the transition range is the least reliable of all because little is known about the phenomenon or its location (Ref. 198, 200).

With the aid of an incremental analysis and finite difference equations, the temperature distributions in essentially any ceramic shape can be reliably established once the heat transfer rates have been determined. The calculations require a complete knowledge of the thermal properties of the ceramic, but the analysis can usually be made without regard to the stress fields in the component. This follows because the deformations in a ceramic component will generally be very small. The stress fields in the component can also be reliably estimated using an incremental analysis if the component can be partitioned into "idealized" elements for which exact relations are known.

In the case of a radome, the thermo-structural analysis is usually based on known solutions for cylinders, spheres, cones, and plates. The analyses have shown that three regions of a radome are thermally critical: the forward tip where high local heat transfer rates are encountered, the transition region where complete turbulent flow first occurs, and the region of attachment. The temperature is, in general, expected to take on an absolute maximum value at the stagnation point and a relative maximum value at the transition point, but the (absolute) maximum tensile stress in the radome may occur at the stagnation point, at the transition point, or in the region of the attachment. Other indications are that the maximum thermal gradient will occur through the radome wall and that the axial and circumferential thermal gradients will be negligible (Ref. 177, 179). For most ceramic materials, it is also indicated that the stresses induced by thermal gradients through a radome wall will exceed by at least an order of magnitude the stresses due to aerodynamic pressure distributions. A notable exception to the rule of critical stresses induced by thermal gradients is fused silica whose thermal expansion coefficient is only about $3 \times 10^{-7}/^{\circ}\text{F}$.

Unclassified

Security Classification

DOCUMENT CONTROL DATA - R&D

(Security classification of title, body of abstract and indexing annotation must be entered when the overall report is classified)

1. ORIGINATING ACTIVITY (Corporate author) Engineering Experiment Station Georgia Institute of Technology Atlanta, Georgia		2a. REPORT SECURITY CLASSIFICATION Unclassified
3. REPORT TITLE AEROSPACE CERAMICS - CHARACTERISTICS AND DESIGN PRINCIPLES		2b. GROUP
4. DESCRIPTIVE NOTES (Type of report and inclusive dates) Final Report January 1964 - April 1965		
5. AUTHOR(S) (Last name, first name, initial) Boland, Paul and Walton, Jesse D., Jr.		
6. REPORT DATE June 1965	7a. TOTAL NO. OF PAGES 187	7b. NO. OF REFS 201
8a. CONTRACT OR GRANT NO. AF 33(615)-1308	9a. ORIGINATOR'S REPORT NUMBER(S) A-749 Final Report	
b. PROJECT NO. 7381	9b. OTHER REPORT NO(S) (Any other numbers that may be assigned this report) AFML-TR-65-171	
c. Task No. 738105	d.	
10. AVAILABILITY/LIMITATION NOTICES Qualified requesters may obtain copies of this report from the DDC. Distribution restricted in accordance with U. S. Export Control Act of 1949 (63 STAT.7), as amended (50 U.S.C. App. 2020.2031), as implemented by AFR 400-10.		
11. SUPPLEMENTARY NOTES	12. SPONSORING MILITARY ACTIVITY United States Air Force Materials Application Division Wright-Patterson Air Force Base, Ohio	
13. ABSTRACT <p>The purpose of this research was to compile into a single volume present knowledge which will be useful to a designer applying ceramic materials in aerospace structural applications. All efforts were directed toward the collection of information to acquaint designers with the properties, fundamental principles, characteristics, limitations, utilization and performance of high-temperature, load-bearing ceramic products and with the characteristics, limitations and utilization of ceramic processes. The information provided in this manual was obtained by means of intensive literature surveys and through contacts with various government agencies, industrial concerns, and academic institutions. The case-history approach was used for the compilation of information on the behavior of ceramic products and material systems subjected to thermal loads to provide the background for a possible correlation between known thermal shock theories and brittle materials behavior.</p>		

DD FORM 1 JAN 64 1473

Unclassified

Security Classification

Unclassified

Security Classification

14. KEY WORDS	LINK A		LINK B		LINK C	
	ROLE	WT	ROLE	WT	ROLE	WT
High Temperature Structural Materials Borides Carbides Composites Intermetallic Compounds Nitrides Oxides High Temperature Structural Components Characteristics Design Properties Mechanical Physical Thermal Ceramic Forming Processes						
INSTRUCTIONS						
1. ORIGINATING ACTIVITY: Enter the name and address of the contractor, subcontractor, grantee, Department of Defense activity or other organization (corporate author) issuing the report.	imposed by security classification, using standard statements such as:					
2a. REPORT SECURITY CLASSIFICATION: Enter the overall security classification of the report. Indicate whether "Restricted Data" is included. Marking is to be in accordance with appropriate security regulations.	(1) "Qualified requesters may obtain copies of this report from DDC."					
2b. GROUP: Automatic downgrading is specified in DoD Directive 5200.10 and Armed Forces Industrial Manual. Enter the group number. Also, when applicable, show that optional markings have been used for Group 3 and Group 4 as authorized.	(2) "Foreign announcement and dissemination of this report by DDC is not authorized."					
3. REPORT TITLE: Enter the complete report title in all capital letters. Titles in all cases should be unclassified. If a meaningful title cannot be selected without classification, show title classification in all capitals in parenthesis immediately following the title.	(3) "U. S. Government agencies may obtain copies of this report directly from DDC. Other qualified DDC users shall request through _____."					
4. DESCRIPTIVE NOTES: If appropriate, enter the type of report, e.g., interim, progress, summary, annual, or final. Give the inclusive dates when a specific reporting period is covered.	(4) "U. S. military agencies may obtain copies of this report directly from DDC. Other qualified users shall request through _____."					
5. AUTHOR(S): Enter the name(s) of author(s) as shown on or in the report. Enter last name, first name, middle initial. If military, show rank and branch of service. The name of the principal author is an absolute minimum requirement.	(5) "All distribution of this report is controlled. Qualified DDC users shall request through _____."					
6. REPORT DATE: Enter the date of the report as day, month, year, or month, year. If more than one date appears on the report, use date of publication.	If the report has been furnished to the Office of Technical Services, Department of Commerce, for sale to the public, indicate this fact and enter the price, if known.					
7a. TOTAL NUMBER OF PAGES: The total page count should follow normal pagination procedures, i.e., enter the number of pages containing information.	11. SUPPLEMENTARY NOTES: Use for additional explanatory notes.					
7b. NUMBER OF REFERENCES: Enter the total number of references cited in the report.	12. SPONSORING MILITARY ACTIVITY: Enter the name of the departmental project office or laboratory sponsoring (paying for) the research and development. Include address.					
8a. CONTRACT OR GRANT NUMBER: If appropriate, enter the applicable number of the contract or grant under which the report was written.	13. ABSTRACT: Enter an abstract giving a brief and factual summary of the document indicative of the report, even though it may also appear elsewhere in the body of the technical report. If additional space is required, a continuation sheet shall be attached.					
8b, 8c, & 8d. PROJECT NUMBER: Enter the appropriate military department identification, such as project number, subproject number, system numbers, task number, etc.	It is highly desirable that the abstract of classified reports be unclassified. Each paragraph of the abstract shall end with an indication of the military security classification of the information in the paragraph, represented as (RS), (S), (C), or (U).					
9a. ORIGINATOR'S REPORT NUMBER(S): Enter the official report number by which the document will be identified and controlled by the originating activity. This number must be unique to this report.	There is no limitation on the length of the abstract. However, the suggested length is from 150 to 225 words.					
9b. OTHER REPORT NUMBER(S): If the report has been assigned any other report numbers (either by the originator or by the sponsor), also enter this number(s).	14. KEY WORDS: Key words are technically meaningful terms or short phrases that characterize a report and may be used as index entries for cataloging the report. Key words must be selected so that no security classification is required. Identifiers, such as equipment model designation, trade name, military project code name, geographic location, may be used as key words but will be followed by an indication of technical context. The assignment of links, roles, and weights is optional.					
10. AVAILABILITY/LIMITATION NOTICE: Enter any limitations on further dissemination of the report, other than those						

DD FORM 1 JAN 64 1473 (BACK)

Unclassified

Security Classification